Structural (Mis)behaviour In Selected Heteroboranes

Thomas David McGrath

Thesis Presented for the Degree of Doctor of Philosophy
University Of Edinburgh
1994

For Jill, for my family,

and in memory of Julie Rose

The years of anxious searching in the dark, with their intense longing, their alternations of confidence and exhaustion, and the final emergence into the light - only those who have themselves experienced it can understand that.
....One thing I have learned in a long life: that all our science, measured against reality, is primitive and childlike - and yet it is the most precious thing we have.

Albert Einstein

Acknowledgements

I would like to thank my supervisor, Dr. Alan Welch, for his advice, help and enthusiasm over the past four years. Grateful acknowledgement is also made to Dr. Kerry Adams for his tolerance and assistance during our joint efforts reported in the latter half of Chapter 4.

Thanks must also be given to my colleagues Dr. Gwenda Kyd, Rhodri Thomas and Lockhart Horsburgh, for their many helpful discussions and comments, without which this Thesis might have been finished much sooner. Above all I must thank Jill Cowie for everything, and Professor Vasili Sukhan for being a source of constant inspiration.

I also thank the departmental n.m.r. and microanalysis services - particularly John Millar and Lorna Eades - for spectra and analyses.

Finally, I wish to thank the S.E.R.C. and the University of Edinburgh for financial support.

Abstract

This *Thesis* deals with some aspects of the unusual structural behaviour observed in certain polyhedral heteroboranes.

Chapter 1 begins with an overview of the recent development of polyhedral boron hydride chemistry, and an illustration of the present scope and utility of the field. Some appropriate aspects of the nomenclature of these species are then presented, followed by a brief survey of electron counting rules and bonding approaches. The preparative chemistry of carbaboranes is introduced, and features of the structural behaviour of *C*-phenyl carbaboranes are discussed in particular; a short illustrative review of some chemistry (primarily synthesis) of other heteroboranes then ensues. Thereafter, there is a discussion of boron clusters containing metal vertices. The Chapter then proceeds to a consideration of a number of aspects of heteroborane structural behaviour - namely cluster distortion, isomerisation and anomalous geometries - and concludes with an indication of the scope of work discussed in the next Chapters.

In **Chapter 2** are presented the syntheses and characterisation of the species 1-Ph-2-R-1,2-*closo*-$C_2B_{10}H_{10}$ (R = Me, **1**; Br, **2**; Me_3Si, **3**; $^tBuMe_2Si$, **4**; $^iPr_3Si$, **5**); compounds **1** to **4** were the subject of single crystal *X*-ray diffraction studies. An increasing steric interaction between the C_{cage}-bound substituents is apparent, and gives rise to mutual *bending back* of the pendant groups in addition to forcing a progressive elongation of the C_{cage}—C_{cage} connectivity. Internal distortions of the somewhat flexible trialkylsilyl substituents further relieve the intramolecular crowding. The sterically-induced distortions of the carbaborane polyhedron are analysed in detail, and evidence is presented which discounts movement along a *diamond—square—diamond* pathway; instead, the results show that *rotation* of a C_{cage}—B(3 *or* 6) edge occurs, by *pivoting* of the appropriate triangular face.

Chapter 3 discusses the formation of the sterically demanding ligand [7-Ph-8-Me-7,8-*nido*-$C_2B_9H_9]^{2-}$, **8**, derived from **1**, characterisation of its protonated relative $\mathbf{8}H^+$, and the formation and characterisation of *bis*(phosphine)-

platinum complexes of **8**. Specifically, the compounds 3,3-$(R_3P)_2$-1-Ph-2-Me-3,1,2-$PtC_2B_9H_9$ (R_3 = Me_2Ph, **10**; R = Et, **11**; Ph, **12**; *p*-tol, **13**) were prepared; **11** and two crystalline forms of **12** were subjected to *X*-ray diffraction analysis. Most significantly, the influence of steric crowding is reflected in substantially enhanced lateral slippage (Δ); in **11** Δ = 0.74Å, whilst in **12** Δ = 0.94 and 0.91Å (*c.f. ca.* 0.4Å in less crowded analogues).

Chapter 4 deals with two systems of 11-vertex heterometallaboranes which display apparent structural anomaly, the structures of which are analysed by the technique of *r.m.s. misfit* calculations. First, the apparent structural irregularity found in a pair of (*closo* and *nido*) dicarbaplatinaboranes is resolved by these calculations, and a distorted *closo* structure is proposed. Next, the anomalous behaviour of a number of rhodathiaboranes, upon analysis, is shown to be genuine; however, closer inspection of the metal atom environment leads to the proposal of two long-range, agostic-type Rh⟋—H—C interactions which afford the rhodium vertex an additional electron pair. As part of an endeavour deliberately to synthesise "non-anomalous" analogues of these species, the preparation of the related (also structurally anomalous) compound 8-(dppe)-8,7-$RhSB_9H_{10}$, **18**, is presented; whilst the formation and characterisation in related experiments of a novel *dirhoda*thiaborane, 2,3-$(CO)_2$-$\mu_{2,3}$-CO-7-Cl-2,3-$(PPh_3)_2$-2,3,1-$Rh_2SB_9H_8$, **19**, is also reported.

In **Chapter 5** are detailed the experimental methods employed in the synthesis, characterisation and single crystal *X*-ray diffraction structural studies of compounds discussed in the three preceding Chapters. Tables of fractional coordinates, and anisotropic thermal parameters for non-H atoms, derived from crystallographic studies are also included. Finally, the coordinates of both (idealised) model compounds and the heterometallaborane species analysed by the *r.m.s. misfit* technique are tabulated.

Abbreviations

BTMA	benzyltrimethylammonium
^{t}Bu	*tert*-butyl
cod	*cyclo*octa-1,5-diene
p-cym	*para*-cymene
dmpe	*bis*(dimethylphosphino)ethane
dppe	*bis*(diphenylphosphino)ethane
dppm	*bis*(diphenylphosphino)methane
D.S.D.	diamond-square-diamond
E.H.M.O.	Extended Hückel Molecular Orbital
Et	ethyl
g.s.d.	ground state destabilisation
HOMO	highest occupied molecular orbital
I.R.	infrared
LUMO	lowest unoccupied molecular orbital
Me	methyl
n.m.r.	nuclear magnetic resonance
OMO	occupied molecular orbital
Ph	phenyl
pip	piperidine
p.p.m.	parts per million
^{i}Pr	*iso*-propyl
r.m.s.	root mean square
t.l.c.	thin layer chromatography
p-tol	*para*-tolyl
UMO	unoccupied molecular orbital

Abbreviations for Specific Compounds

1-Ph-2-Me-1,2-*closo*-$C_2B_{10}H_{10}$	**1**
1-Ph-2-Br-1,2-*closo*-$C_2B_{10}H_{10}$	**2**
1-Ph-2-Me_3Si-1,2-*closo*-$C_2B_{10}H_{10}$	**3**
1-Ph-2-^{t}BuMe$_2$Si-1,2-*closo*-$C_2B_{10}H_{10}$	**4**
1-Ph-2-^{i}Pr$_3$Si-1,2-*closo*-$C_2B_{10}H_{10}$	**5**
1-^{t}Bu-1,2-*closo*-$C_2B_{10}H_{11}$	**6**
1-^{t}Bu-2-Br-1,2-*closo*-$C_2B_{10}H_{10}$	**7**
[7-Ph-8-Me-7,8-*nido*-$C_2B_9H_9$]$^{2-}$	**8**
[7-Ph-7,8-*nido*-$C_2B_9H_{10}$]$^{2-}$	**9**
1-Ph-2-Me-3,3-(Me$_2$PhP)$_2$-3,1,2-$PtC_2B_9H_9$	**10**
1-Ph-2-Me-3,3-(Et_3P)$_2$-3,1,2-$PtC_2B_9H_9$	**11**
1-Ph-2-Me-3,3-(Ph_3P)$_2$-3,1,2-$PtC_2B_9H_9$	**12**
1-Ph-2-Me-3,3-(*p*-tol$_3$P)$_2$-3,1,2-$PtC_2B_9H_9$	**13**
9-H-9,9-(Et_3P)$_2$-$\mu_{10,11}$-H-9,7,8-$PtC_2B_8H_{10}$	**14**
9-H-9,10-(Et_3P)$_2$-9,7,8-$PtC_2B_8H_9$	**15**
8,8-(Ph_3P)$_2$-$\mu_{9,10}$-H-8,7-$RhSB_9H_9$	**16**
9-OEt-8,8-(Ph_3P)$_2$-$\mu_{9,10}$-H-8,7-$RhSB_9H_8$	**16A**
8,8,8-(Me$_2$PhP)$_3$-$\mu_{9,10}$-H-8,7-$RhSB_9H_9$	**17**
8,8-(Ph_3P)$_2$-$\mu_{8,9}$-S_2CH-$\mu_{9,10}$-H-8,7-$RhSB_9H_8$	**17A**
8-(dppe)-$\mu_{9,10}$-H-8,7-$RhSB_9H_9$	**18**
cis-2,3-(CO)$_2$-$\mu_{2,3}$-CO-7-Cl-2,3-(PPh$_3$)$_2$-2,3,1-*closo*-$Rh_2SB_9H_8$	**19**
cis-2,3-(CO)$_2$-$\mu_{2,3}$-CO-2,3-(PPh$_3$)$_2$-2,3,1-*closo*-$Rh_2SB_9H_9$	**19A**
trans(?)-2,3-(CO)$_2$-$\mu_{2,3}$-CO-2,3-(PPh$_3$)$_2$-2,3,1-*closo*-$Rh_2SB_9H_9$	**19B**

In addition, the following compound abbreviations were employed in specific Chapters:

Chapter 2

1-Ph-1,2-*closo*-$C_2B_{10}H_{11}$*	**A**
1,2-Ph_2-1,2-*closo*-$C_2B_{10}H_{10}$†("*B*", "*A*")	**B, C**
1-Ph-2-[4'-Br-C_6F_4]-1,2-*closo*-$C_2B_{10}H_{10}$† ("*B*", "*A*")	**D, E**
1-^{t}Bu-2-[4'-Br-C_6F_4]-1,2-*closo*-$C_2B_{10}H_{10}$	**F**
1,2-{-S-CH_2CH_2-O-CH_2CH_2-S-}-1,2-*closo*-$C_2B_{10}H_{10}$	**G,**
1,2-{-S-(-CH_2CH_2-O-)$_2$-CH_2CH_2-S-}-1,2-*closo*-$C_2B_{10}H_{10}$† ("*50*", "*0*")	**H, J**

Chapter 3

3,3-$(Et_3P)_2$-3,1,2-$PtC_2B_9H_{11}$	**A**
3-(dppe)-3,1,2-$PtC_2B_9H_{11}$	**B**
1-Ph-3,3-{Me_2PhP}$_2$-3,1,2-$PtC_2B_9H_{10}$	**C**
1-(CH_2OCH_3)-3,3-{Me_2PhP}$_2$-3,1,2-$PtC_2B_9H_{10}$† ("*A*", "*B*")	**D, E**

Chapter 4

nido-[$B_{11}H_{14}$]-	**A**
nido-8-Ph_3P-7-$CB_{10}H_{12}$	**B**
nido-[7,8-$C_2B_9H_{12}$]-	**C**
nido-$B_{10}H_{14}$	**D**
closo-[2-$(Me_3Si)_2$CH-2-$CB_{10}H_{10}$]-	**E**

* crystallographically ordered molecule

† crystallographically independent molecules (respective labels)

Contents

Chapter 1

Background

Introduction

> "... *it is steadily becoming more and more evident that the hydrides of boron may have special significance in the development of our general ideas on valency and chemical linkage*"
>
> Alfred Stock, 1932

The seminal work of Alfred Stock **[1]**, who pioneered the chemistry of the boron hydrides over a twenty year period in the early part of the twentieth century, is the foundation for a now extensive field of modern chemistry. Stock not only synthesised, characterised, and studied the reaction chemistry of six binary boranes - B_2H_6, B_4H_{10}, B_5H_9, B_5H_{11}, B_6H_{10} and $B_{10}H_{14}$ - and was able to recognise rudimentary patterns in their molecular formulae but, in the course of his work, also developed the high vacuum techniques necessary to study these highly reactive materials.

From the outset, the established formulae of these boranes could not easily be rationalised in terms of existing ideas of structure and bonding. Thus, although diborane B_2H_6 has the same stoichiometry as its hydrocarbon *analogue* C_2H_6, the boron compound has insufficient valence electrons available to form the required number of conventional two-centre, two-electron bonds. Since this is an apparent consequence of the boron atom having one less electron than carbon, the term "electron deficient" has often been applied - albeit somewhat inaccurately - to the family of boron hydride cluster compounds. The later concept, due to Longuet-Higgins, of *three*-centre, two-electron bonding **[2]** elegantly resolves this dilemma, and suggests the bridged "dimeric" structure of B_2H_6 shown in figure 1.1 which has been confirmed by both electron **[3]** and *X*-ray diffraction studies **[4]**.

The four terminal B-H bonds in diborane are considered to be of the conventional two-centre, electron pair type, whereas each of the two B-H-B bridges are believed only to involve *two* electrons in bonding the *three* centres.

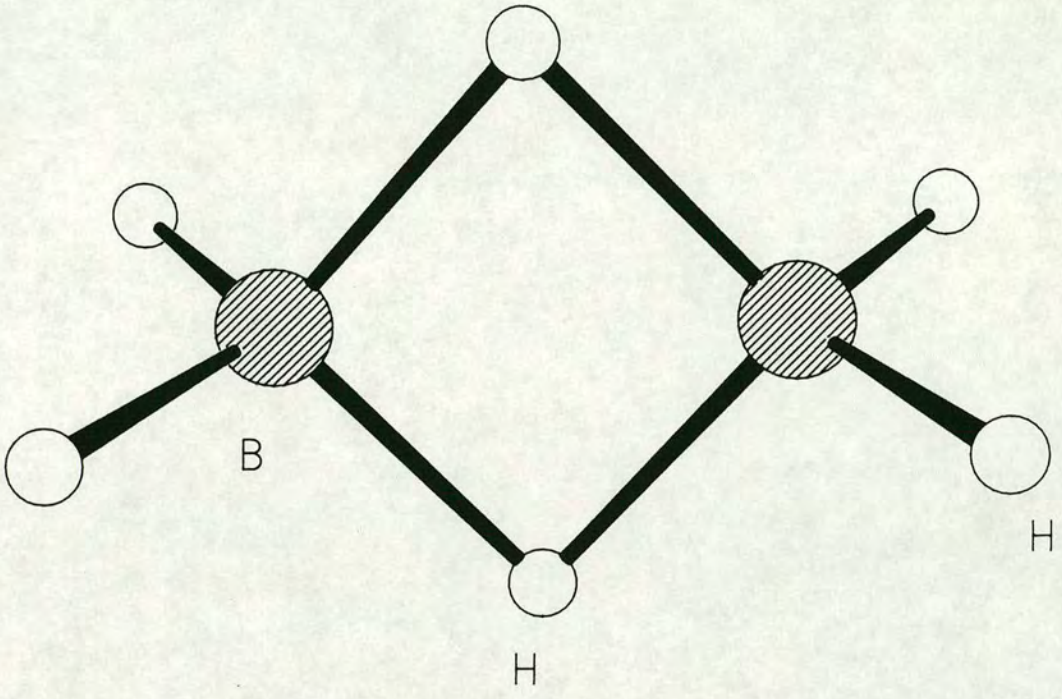

Figure 1.1 The structure of diborane, B_2H_6, by an electron diffraction study

This principle of three-centre, two electron bonds may be generalised from three-centre to multicentre bonding and can be directly linked to now-accepted rules (discussed in more detail below) relating electron count to the cluster geometries observed for the higher boranes.

From Stock's starting point of six boranes, the field has expanded enormously and there are now literally thousands of known boron hydride derivatives which incorporate elements from almost all parts of the Periodic

Table. These range from simple carbaborane relatives of Stock's original binary boranes - such as $C_2B_3H_7$ **[5]** (figure 1.2), an analogue of B_5H_9 - to large heterometallaboranes - for example, $[(C_6H_6)RuB_{10}H_{10}NR]$ **[6]** (figure 1.3) - and species such as $[Cu_3(\mu\text{-}H)_3\{C_2B_9H_9\}_3\{4\text{-}(C_5H_4N)CO_2CH_3\}_3]$ **[7]** (figure 1.4) containing multiple metal atoms, which can incorporate considerable functionality and flexibility.

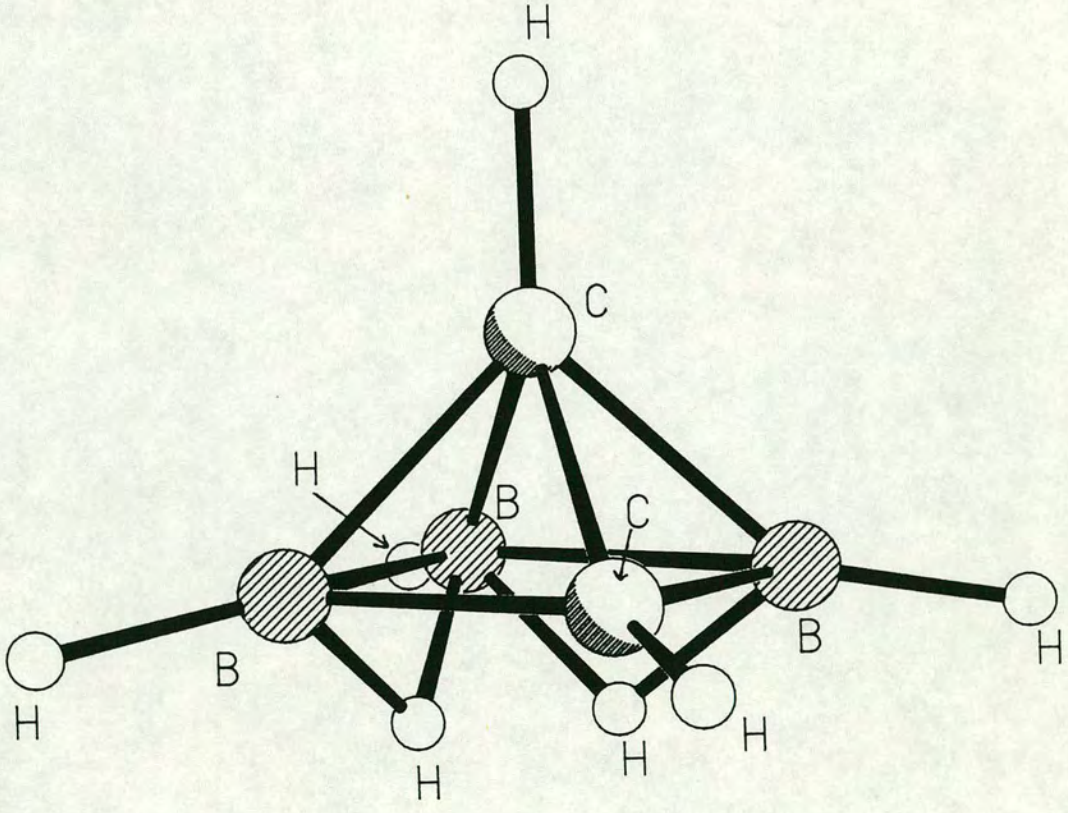

Figure 1.2 $C_2B_3H_7$

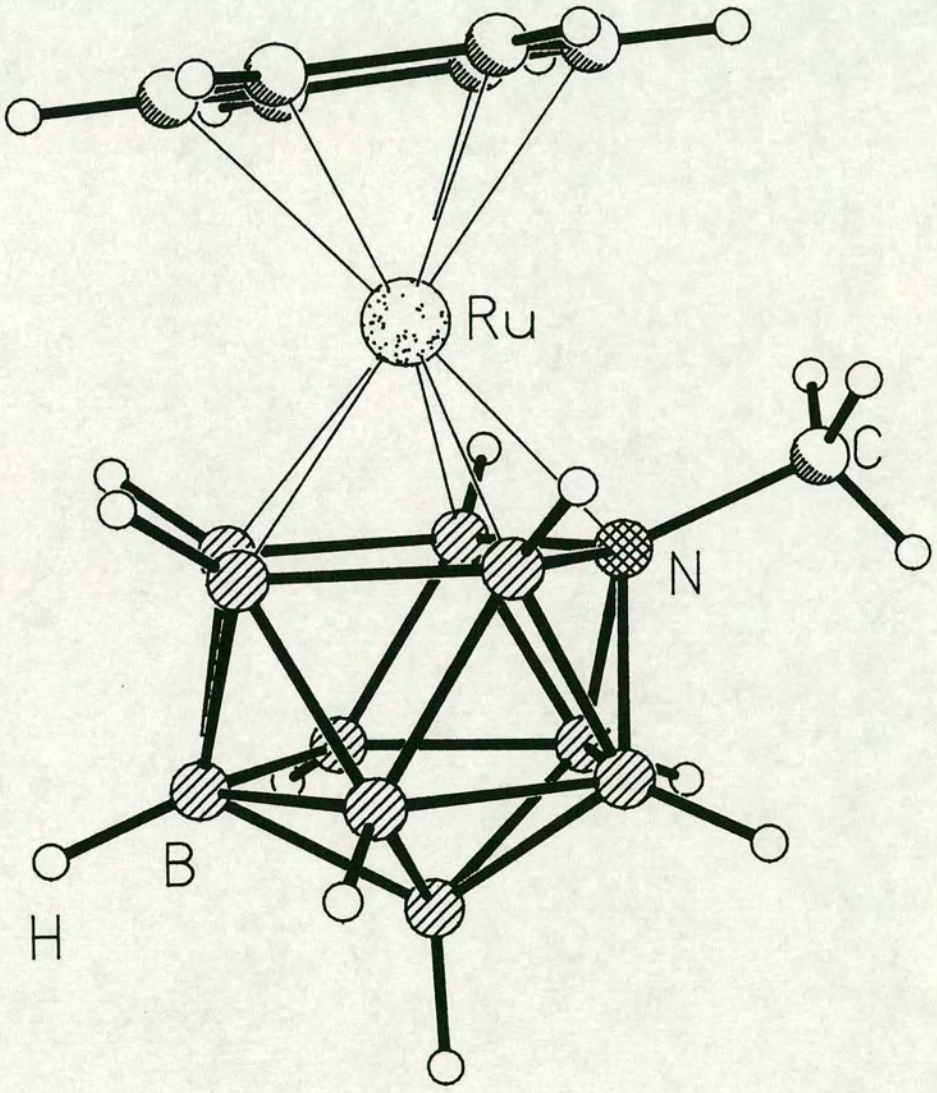

Figure 1.3 Representation of [(C_6H_6)Ru$B_{10}H_{10}$NR]

Figure 1.4 The "pinwheel" cluster $[Cu_3(\mu\text{-}H)_3\{C_2B_9H_9\}_3\{4\text{-}(C_5H_4N)CO_2CH_3\}_3]$

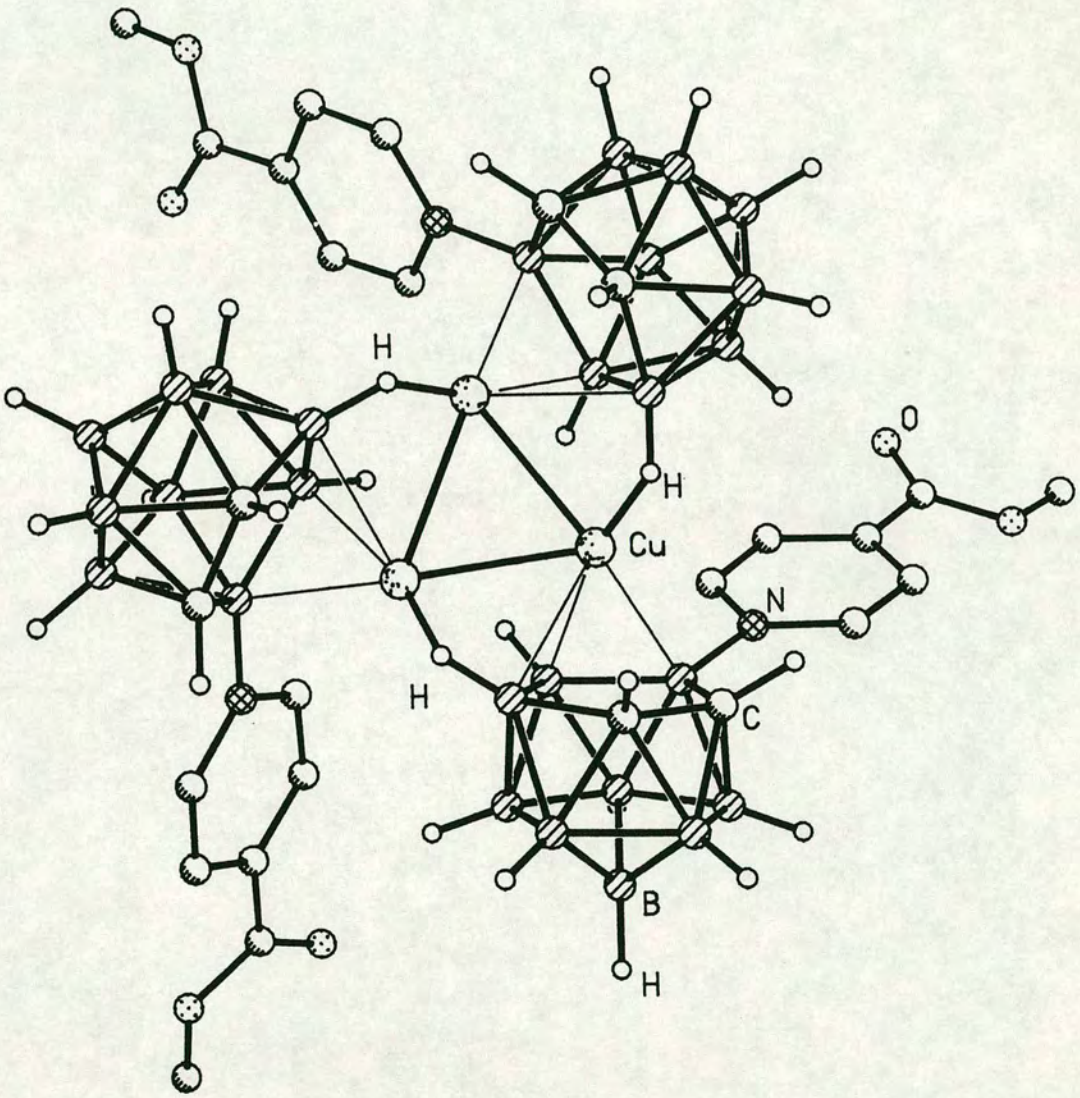

Much of the interest in research into boron hydride cluster chemistry - which contributed significantly to the growth of this field - was related to the potential use of these materials as rocket fuels. However, in addition to the intense academic interest in the unique bonding and structural behaviour of boron cluster compounds, there are a considerable number of other, very diverse areas where these species find application **[8]**.

A major area of current effort **[9]** lies in the search for polyboron species suitable for use in Boron Neutron Capture Therapy for the treatment of certain severe brain tumours **[10]**. In this, boron compounds are localised at or (ideally) within the tumour and then bombarded with thermal neutrons. The resulting nuclear reaction between neutron and ^{10}B nucleus (only)

$$^{10}B + {}^{1}n \longrightarrow {}^{4}He + {}^{7}Li + \textit{energy}$$

releases energetic particles, thereby effectively delivering a dose of lethal radiation to adjacent (tumour) cells. Boron hydride cluster compounds are, therefore, potentially well-suited to providing a relatively high concentration of boron atoms in the vicinity of a tumour: the thio derivative $[B_{12}H_{11}SH]^{2-}$ ("BSH") has been used with some success in this area.

Polymers incorporating boron cluster units have been prepared. In particular, siloxane polymers such as

$$-[-SiMe_2-CB_{10}H_{10}C-SiMe_2-O-SiMe_2-O-SiMe_2-O-]_n-$$

have been found to possess unusually high air and thermal stabilities **[11]**. In addition, polymer materials containing polyhedral borane subunits have been successfully converted to boron-based ceramics **[12]**.

The system $(PPh_3)_2(H)RhC_2B_9H_9RR'$ (R, R' = H, alkyl, aryl) has been examined **[13]** as a homogeneous catalyst precursor. Several such species exist in two, readily-interconverting tautomeric forms (figure 1.5) in which the {Rh} fragment occupies, respectively, *closo* and *exo-nido* positions.

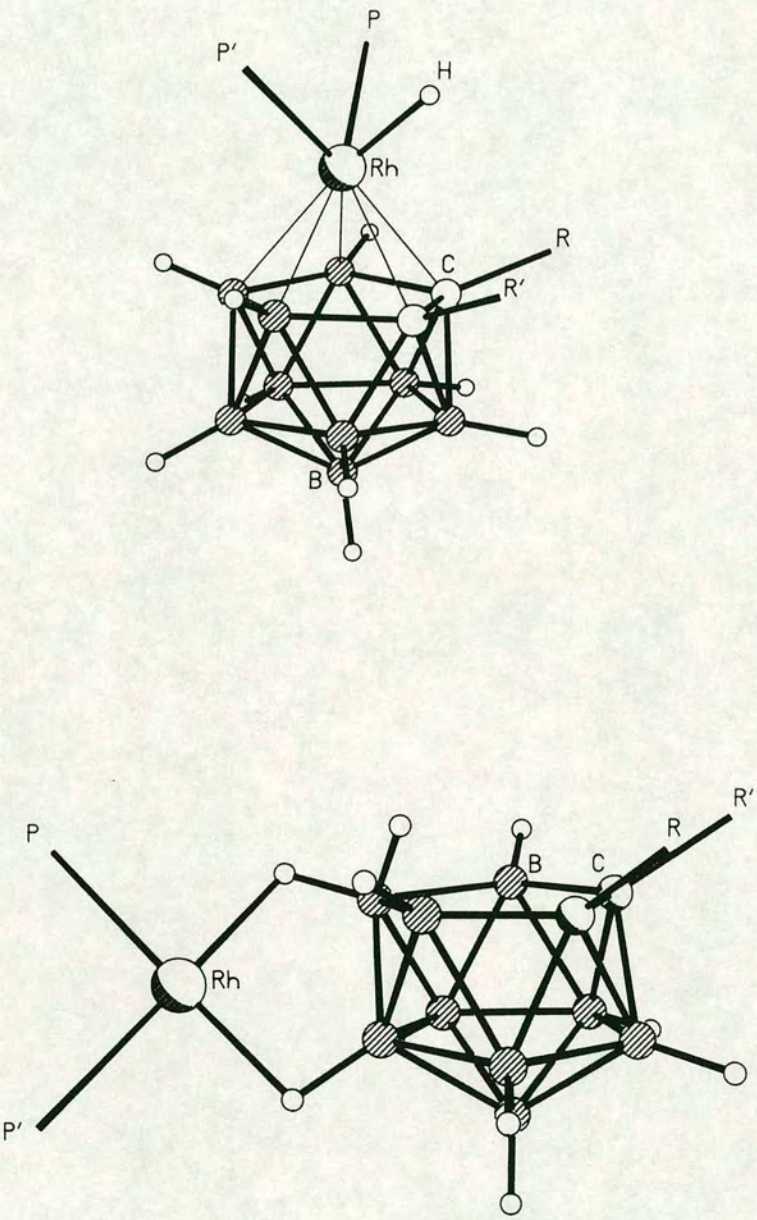

Figure 1.5 The two tautomers of $(PPh_3)_2(H)RhC_2B_9H_9RR'$

These have been shown to act as catalysts for, for example, the hydrogenation and isomerisation of terminal alkenes **[13(a), 13(e)]**.

The remainder of this introductory chapter is devoted to a consideration of some of the concepts of nomenclature and bonding which underpin any discussion of the behaviour of boron hydrides and their derivatives. There then follows a brief summary of some relevant examples of the preparative and reaction chemistry of carbaboranes, some heteroboranes, and their metal complexes. Finally, there is a short examination of some modes by which these species can *"misbehave"* and how this can be probed and quantified.

Polyhedral Shapes, Nomenclature and Numbering

Historically, the advent of powerful structural techniques such as diffraction methods allowed elucidation of the geometries adopted by boron cluster compounds and their derivatives. Such studies revealed these species to have geometries based on polyhedra with triangular faces. As more results were available, it became clear that patterns of structure existed within this broad family of deltahedra: observed partially *open* geometries could be formally derived from related, more *closed* polyhedra by removal of a vertex. Ultimately a whole series of such relationships could be predicted, based on "closed" parent clusters with varying numbers of vertices.

Those polyhedral cages having a fully "closed" geometry (that is, having all faces triangulated) have been termed ***closo***; the related species derived by removal of one vertex is designated ***nido*** (*nest-like*); loss of a further vertex yields an ***arachno*** (*web-like*) structure; and so on.

In the absence of heteroatoms, cage numbering proceeds thus: For *closo* species, an apex is chosen and labelled 1; numbering proceeds in a "corkscrew" fashion around "belts" of atoms: on crossing from one belt to another, a connectivity must be crossed also. In *nido* species, the atom opposite the open face is assigned as 1, and the remaining atoms are labelled as before. The numbering of heteroboranes is chosen such that - subject to the rules outlined above - heteroatoms have as low a number as possible; in this, carbon atoms have preference over other heteroatoms, which in turn have preference over metal atoms.

Exopolyhedral substituents and ligands adopt the number of the cluster atom to which they are bound.

The numbering of the *closo* icosahedral carbaborane $C_2B_{10}H_{12}$ and the related *nido* carbaborane $[C_2B_9H_{12}]^-$ are illustrated in figure 1.6.

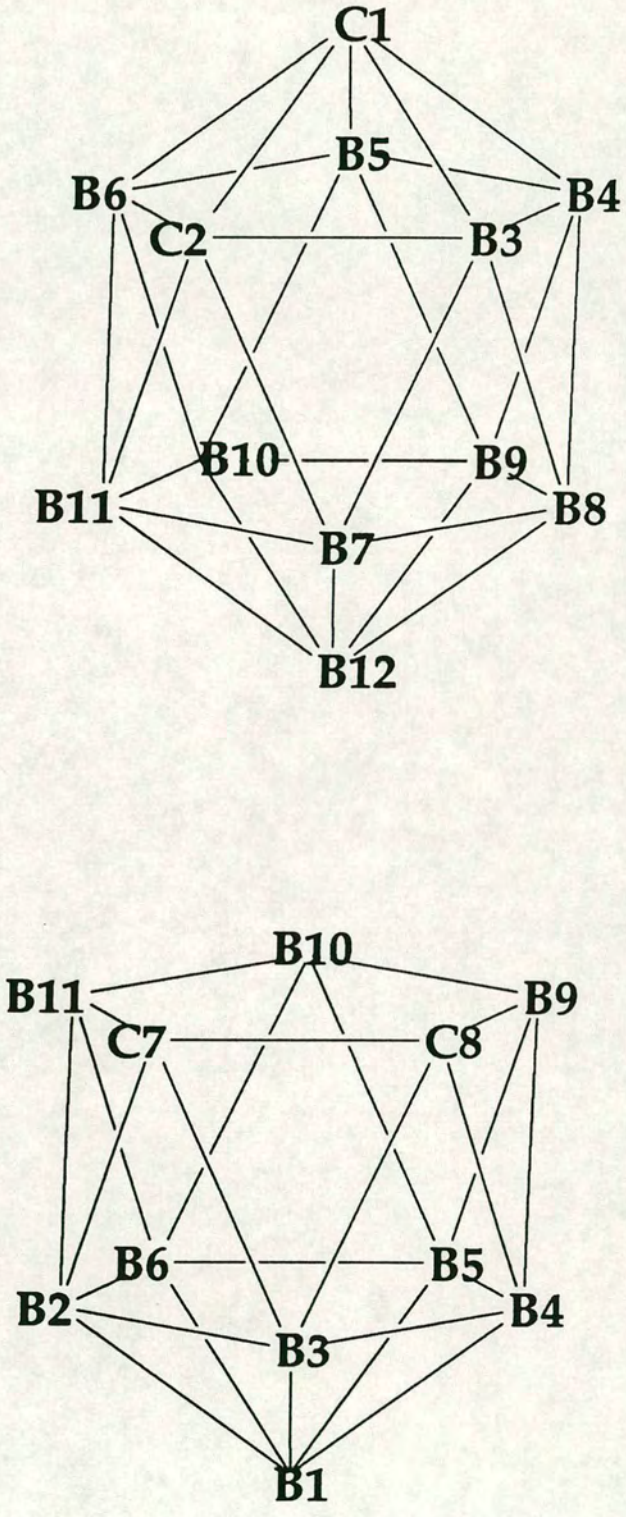

Figure 1.6 Numbering of *closo*-$C_2B_{10}H_{12}$ and *nido*-$[C_2B_9H_{12}]^-$ (H atoms omitted)

Electron Counting and Bonding

It has been seen that the somewhat limited conventional description of the covalent bond cannot adequately account for the bonding observed in boron cluster compounds. Rationalisation of the unprecedented structures adopted by the polyboron hydrides and their derivatives is, in several ways, closely linked to the development of many current principles which may be applied to inorganic, organometallic and cluster bonding and structural chemistry.

Longuet-Higgins' concept of the three-centre, two-electron bond was the first successful attempt to satisfactorily explain the bonding in boranes. In generalising this principle from three-centre to multicentre bonding Longuet-Higgins investigated the electronic structures of polyhedra of boron atoms, and made the brilliant prediction of unprecedented stable polyhedral dianions including the icosahedral cluster $[B_{12}H_{12}]^{2-}$ **[14]**. Such species were not discovered experimentally until five years later **[15]**.

In forming deltahedra, each constituent {BH} fragment maximises the number of nearest neighbour B···B contacts and more effective delocalisation of the electrons donated by each vertex is thereby ensured. This may be viewed as a process attempting to relieve the notional "electron deficiency" of each isolated vertex. The highly delocalised bonding within boron polyhedra clearly renders appropriate a description in terms of truly *molecular* orbitals. A simple qualitative molecular orbital picture of a {BH} fragment is shown in figure 1.7 below. The B atom contributes 4 orbitals (*2s* and three *2p*) containing a total of three electrons; the H atom contributes a single *1s* orbital containing one electron. An outward-pointing boron based *sp* hybrid overlaps with the H *1s* to form a conventional exopolyhedral B-H bond. The other "radial" *sp* hybrid and the two "tangential" boron *p* orbitals, containing the two remaining electrons, are then available for cluster bonding. Thus, each {BH} vertex is a 3-orbital, 2-electron donor for polyhedral bonding. These three orbitals might contribute to binding a bridging H atom (that is, a three-centre B-H-B bond), an *endo*-polyhedral H atom (an inward-pointing H, located on the surface defined by the boron atoms), or to bonding to adjacent boron atoms.

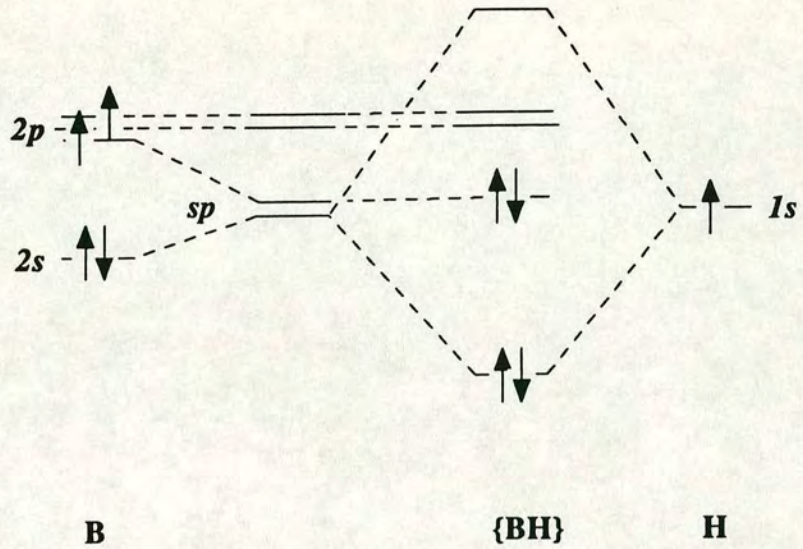

Figure 1.7 A qualitative molecular orbital diagram for a {BH} fragment

A systematic procedure for describing bonding in these species was developed by W. N. Lipscomb **[16]**. This took the form of a topological approach and describes numbers of orbitals, electrons, and B and H atoms in terms of s, t, y and x values. Thus, in a simple binary borane B_pH_{p+q}, ignoring the terminal B-H bonding, there are:

s	3-centre B-H-B bridges
x	*endo* B-H groups
t	3-centre B-B-B bonds
y	2-centre B-B bonds.

It may be shown* that

$$q = s + x$$
$$p = s + t$$
$$p = t + y + q/2.$$

* Each of the p B vertices bears one terminal (exopolyhedral) H atom, so that clearly $q = s + x$. Since each B atom supplies 3 orbitals but only 2 electrons, the discrepancy must be made up by three centre bonds: one of these is required per B atom; hence $p = s + t$. Finally, the p electron pairs donated by the {BH} vertices are used up as 3-centre B-B-B and 2-centre B-B bonds, and in supplying one electron to bind each extra *endo*-H atom; thus (remembering $q = s + x$), $p = t + y + q/2$.

A more general form of these equations for a borane $[B_pH_{p+q}]^c$ bearing a charge c affords "rules" by which *styx* values may be calculated, and hence known species' structures may be rationalised and new compounds predicted.

R. E. Williams **[17, 18]** first recognised structural patterns in polyhedral boranes and their isoelectronic carbaborane analogues. He noted the existence of three series of boranes, namely *closo*-$[B_xH_x]^{2-}$, *nido*-B_xH_{x+4} and *arachno*-B_xH_{x+6}, each group having a different common structural motif. (The latter two of these series had crudely been noticed by Stock earlier.) In principle, a parent *n*-vertex *closo*-$[B_nH_n]^{2-}$ compound can, formally, by removal of a $\{BH\}^{2+}$ vertex followed by appropriate protonation, form the geometrically-related *nido*-$B_{(n-1)}H_{(n-1)+4}$ species: the two structures are essentially similar save for the "missing" vertex in the latter case. The electron pair left behind by the "lost" vertex is retained for skeletal bonding, and addition of protons clearly does not affect the cluster electron count; hence the two clusters related in this way have the same number of framework electron pairs.

A series of such relationships is possible **[19, 20]**; some of these are illustrated in figure 1.8. The horizontal rows contain species with the same numbers of vertices; whilst the diagonal rows may be seen to have geometrically-related structures: for example, the *closo*-12-vertex, *nido*-11-vertex and *arachno*-10-vertex members all have the same icosahedral parent architecture. More importantly, these three also have the same number of cluster bonding electrons. Conversely, the formal addition of an electron pair to a *closo*-11-vertex species yields a *nido*-11-vertex cluster whose geometry is derived from a closed 12-vertex parent.

Figure 1.8 Structural interrelationships in *closo*, *nido* and *arachno* polyhedra

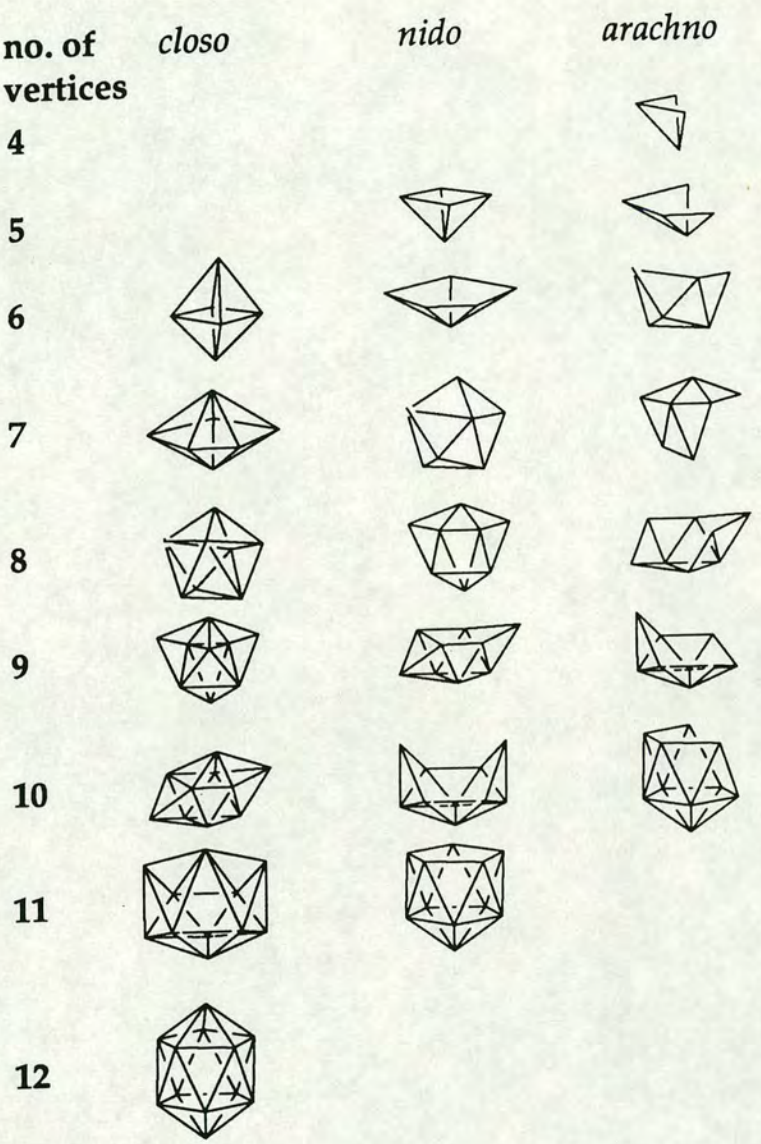

The above observations constitute, in part, the basis of **Wade's Rules**, by which the relationship between geometry and skeletal electron count may be very simply expressed **[21, 22]**. Early rudimentary molecular orbital calculations on closed cage species such as $[B_{12}H_{12}]^{2-}$ **[14]** established that a closed *n*-vertex molecule has $(2n+1)$ bonding molecular orbitals separated by a substantial energy gap from antibonding orbitals. These bonding orbitals consist of *n* essentially localised exopolyhedral B-H bonds plus $(n+1)$ skeletal bonding orbitals. Therefore, in the case of the *closo*-borane $[B_{12}H_{12}]^{2-}$, there are 13 framework orbitals for which 13 cluster electron pairs are required; the same applies to the structurally-related *nido*-$[B_{11}H_{14}]^{-}$ ion; and so on.

In general, Wade's rules may be summarised for an *n*-vertex system as:-

number of cluster bonding electron pairs	**geometry**
$n + 1$	*closo*
$n + 2$	*nido*
$n + 3$	*arachno*
$n + 4$	*hypho*

and so on. Comparison of the number of vertices present with the number of polyhedral electron pairs allows prediction of structure.

A simple example is the binary borane anion $[B_{10}H_{13}]^-$, figure 1.9.
In this there are

10 {BH} vertices	= 10 x 2	= 20 electrons
3 bridging H atoms	= 3 x 1	= 3 "
1 negative charge		= 1 "
		24 electrons = 12 electron pairs

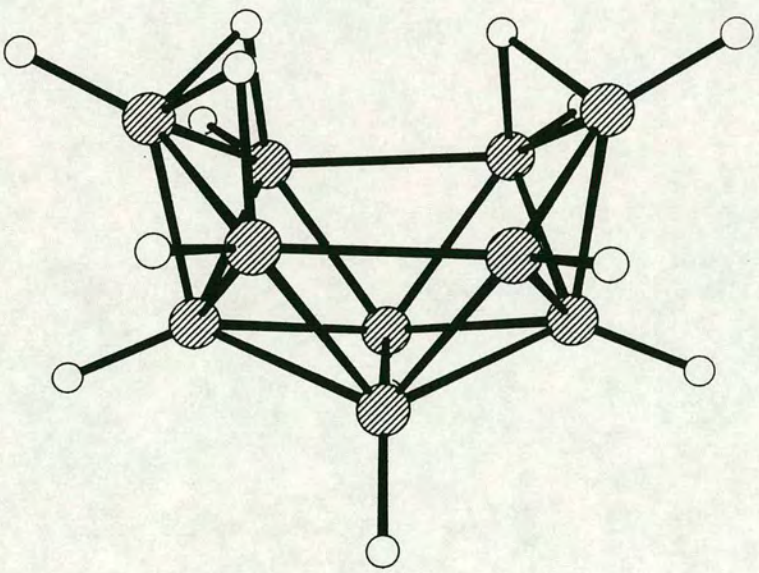

Figure 1.9 Structure of $[B_{10}H_{13}]^-$

n = 10 vertices are present, and there are 12 = (n + 2) cluster electron pairs; therefore the structure is predicted to be *nido*, as observed **[23]**.

Replacement of a {BH} by a {CH} vertex results in a 3-orbital, 3-electron donor. In general, for a main group atom of valence v bearing an exopolyhedral substituent donating x electrons, the number of electrons (e) available for cluster bonding is

$$e = v + x - 2$$

(since 2 electrons are required for the vertex-substituent bond, or a lone pair). For a transition metal vertex, 9 valence orbitals are present. In the case of an octahedral metal fragment, 6 of these are involved in binding ligands or are non-bonding; these are normally filled, rendering 12 electrons unavailable for bonding the cluster framework. Hence, a metal fragment donates

$$e = v + x - 12$$

electrons. A further example, namely 4-SMe_2-3,3,3-$(CO)_3$-3,1,2-$MnC_2B_9H_{10}$, figure 1.10, illustrates these latter points.

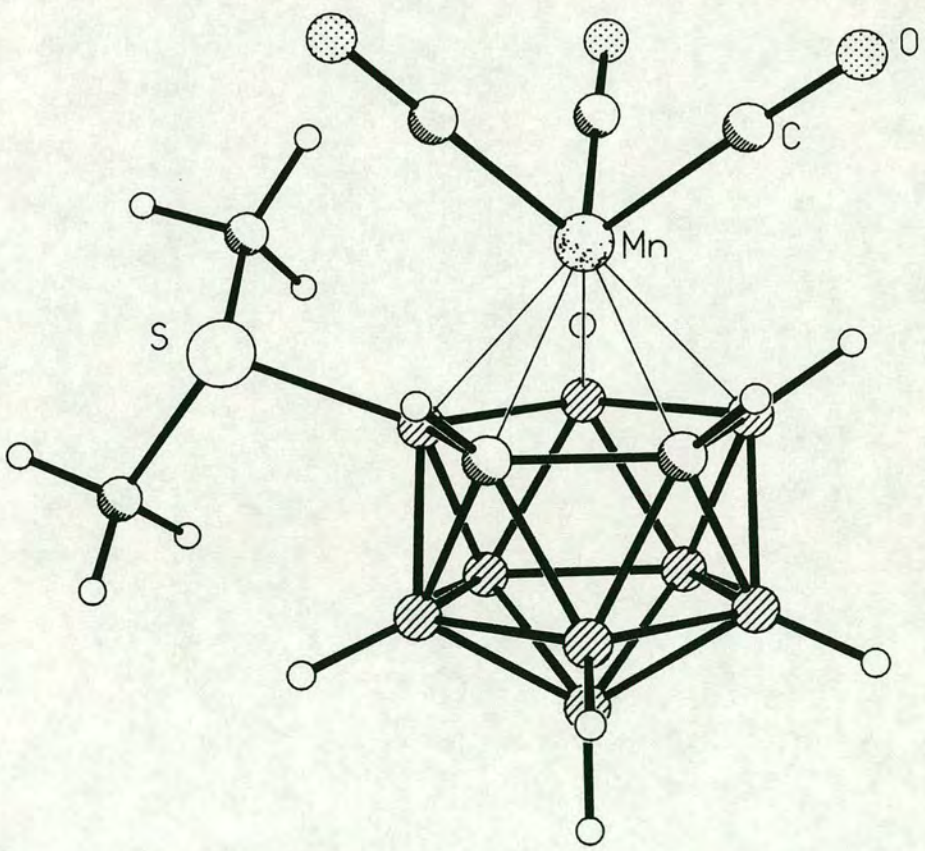

Figure 1.10 Structure of 4-SMe_2-3,3,3-$(CO)_3$-3,1,2-$MnC_2B_9H_{10}$

In this there are:

{$Mn(CO)_3$}	= 7 + (3 x 2) - 12	= 1
2x{CH}	= 2 x (4 + 1 - 2)	= 6
8x{BH}	= 8 x (3 + 1 - 2)	=16
{B-SMe_2}	= 3 + 2 - 1	= 3
		26 electrons = 13 pairs

Thus, the 12-vertex species is predicted to be *closo*, as observed **[24]**.

These principles, in a more general form, may be applied to other cluster systems; this *Polyhedral Skeletal Electron Pair* approach **[25]** has been extended to metal clusters and condensed polyhedra. Not all polyhedral borane derivatives obey these electron counting rules; some of these anomalies are considered later in this *Introduction*, and in Chapter 4.

Carbaboranes

The carbaborane analogues of the simple binary boron hydrides are formally derived from their parents by replacement of a {BH} vertex by {CH}. These new (often neutral) species are generally more stable than their (often anionic) borane relatives: for example, the higher carbaboranes such as $C_2B_{10}H_{12}$ - and their derivatives - show considerable air and moisture stability. A number of articles reviewing carbaborane chemistry have been published **[26 - 30]**.

Synthetic routes to carbaboranes depend almost exclusively on the introduction of carbon atoms into an already-formed boron cluster. A very widely-used preparative route is the direct interaction of an acetylene and a polyborane. Both small and large carbaboranes may be formed by this procedure, and it has proved possible to form *C*-substituted products *via* the use of a suitable substituted acetylene. For example, a mixture of the *closo* carbaboranes 1,6-$C_2B_4H_6$, 2,4-$C_2B_5H_7$ and 1,5-$C_2B_3H_5$ are formed in the direct reaction of *nido*-B_5H_9 with acetylene at 500-600°C in a continuous flow system **[31]**.

Of particular relevance to this work are "*ortho*-carborane" (*closo*-1,2-$C_2B_{10}H_{12}$), and a large number of its *C*-substituted derivatives, which have been synthesised by the reaction of *nido*-$B_{10}H_{14}$ with the appropriate acetylene in the presence of a Lewis base **L** such as acetonitrile, dimethyl sulphide or *N,N*-dimethylaniline **[32 - 36]**. Initially, $B_{10}H_{14}$ reacts with Lewis base to form an *arachno* adduct:

$$\textit{nido}\text{-}B_{10}H_{14} + 2L \longrightarrow \textit{arachno}\text{-}B_{10}H_{12}L_2 + H_2.$$

(The two molecules **L** each provide an electron pair, whilst two cluster electrons are lost to the evolved H_2; hence there is a net gain of two cluster electrons and the 10-vertex cage is converted from a *nido* to an *arachno* geometry.) An acetylene molecule then inserts into the *bis*(Lewis base) species

$$\textit{arachno}\text{-}B_{10}H_{12}L_2 + RC{\equiv}CR' \longrightarrow 1,2\text{-}R,R'\text{-}\textit{closo}\text{-}1,2\text{-}C_2B_{10}H_{10} + 2L + H_2$$

(where R and R' may be H, alkyl, aryl, haloalkyl, etc.) to yield the *closo* carbaborane product.

This route, however, is limited to those acetylenes which are available, and even then may proceed only in poor yield. More importantly, substituents R and R' must be compatible with the nucleophilic nature of the reactants; hence, acetylenes incorporating groups such as -COOH, -$SiMe_3$ and -C_6F_5 do not give the expected corresponding *closo* carbaborane. For example, the reaction of $B_{10}H_{14}$ with $Me_3SiC{\equiv}CSiMe_3$ (and with L = Me_2S) **[37]** results in the formation of two unexpected products including the *11-vertex* monocarbon carbaborane *nido*-9-Me_2S-7-[$(Me_3Si)_2CH$]-$CB_{10}H_{11}$ (figure 1.11).

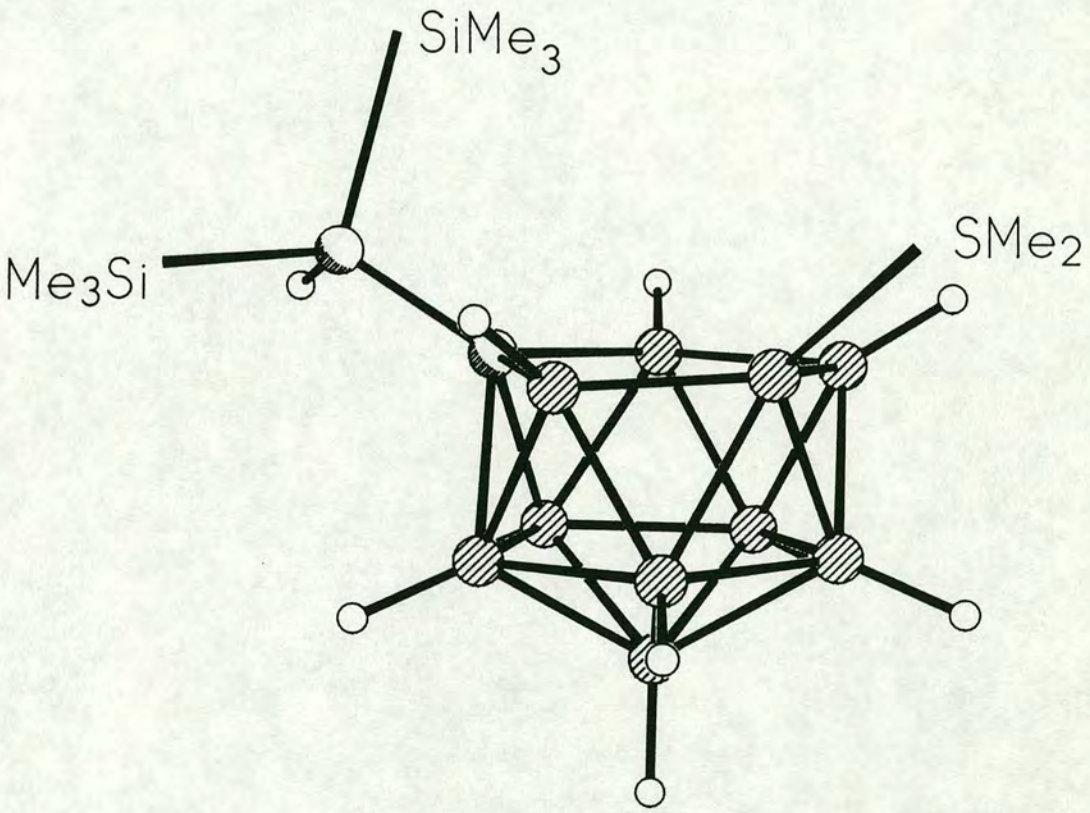

Figure 1.11 Representation of 9-Me_2S-7-[$(Me_3Si)_2CH$]-$CB_{10}H_{11}$ (μ-H not shown)

An important alternative means of carbaborane functionalisation utilises the weakly acidic nature of the H atoms attached to the C atoms of the carbaborane cage. Treatment with alkyl lithium deprotonates at this position, forming the *lithium salt* of the cage. The salt reacts with a variety of substrates which include dihalogens **[38]**, trialkylsilyl halides **[39]** and perhalobenzenes **[40, 41]** to yield an extensive range of *C*-substituted products.

Some of these are illustrated in the scheme below:

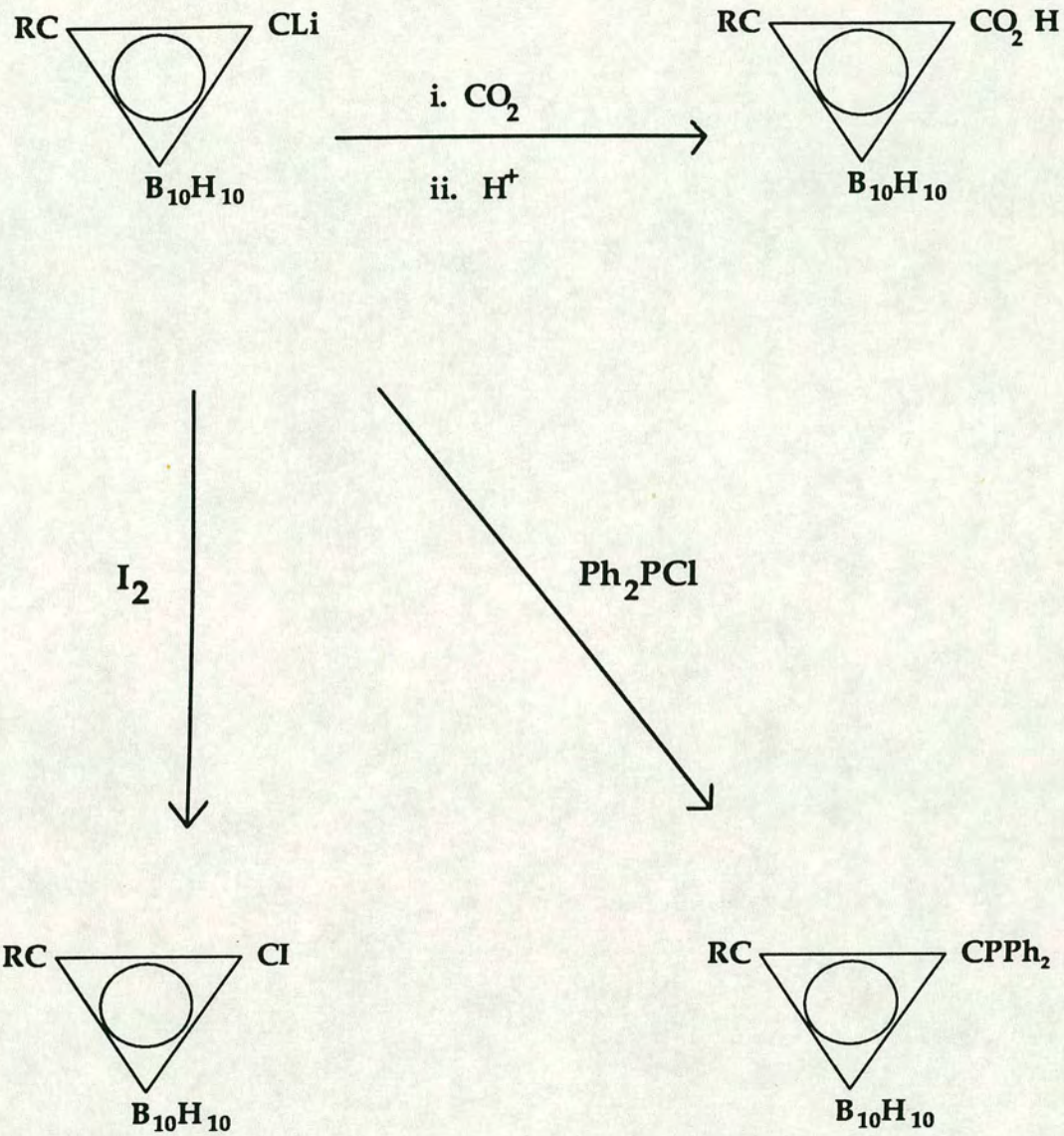

[It may be noted, in addition, that these lithium salts are also useful precursors to a variety of C-σ-bound metal complexes of carbaboranes **[42, 43]**.]

The utility of the above synthetic strategy is limited by a number of factors. Principal of these is the possibility of mixtures of un-, mono- and di-substituted products when attempting to functionalise *ortho*-carbaborane by this method. This arises from the establishment of the following equilibrium:

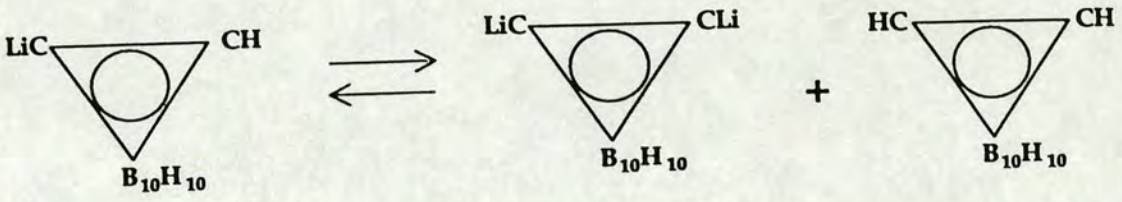

Clearly a carbaborane already bearing a single *C*-substituent does not suffer this problem. Indeed, a "protecting group" methodology for the formation of monosubstituted *ortho*-carbaborane has recently been developed **[44, 45]** to overcome this difficulty.

A second limitation of the synthetic use of carbaborane-lithium salts is the basic nature of the carbaborane anion: the substrate may suffer deprotonation, rather than the desired elimination of lithium halide.

A further technique relies upon the interaction of the lithio-carbaborane with copper (I) iodide in the presence of pyridine to form a *C*-Cu derivative **[46, 47]**. These species have proved useful in the synthesis of certain *C*-aryl carbaboranes which were not otherwise accessible **[47]**. However, it was also found that the reagent was reactive only towards some aryl halides. (This concurs with the author's own experience.)

Other, less widely used, reagents for carbaborane *C*-functionalisation include the *C*-MgBr Grignard-type species, and lanthanide halide complexes *C*-LnI **[48]**, which may themselves be formed from a *C*-Li precursor.

All of the carbaboranes discussed in Chapter 2 of this work were prepared either by direct insertion of an acetylene into $B_{10}H_{14}$, or by treatment of the *C*-lithium salt of an appropriate carbaborane with a suitable halo-substrate.

Although carbaboranes show considerable resistance to acid attack, they undergo relatively facile base degradation. In the case of icosahedral carbaboranes of the type 1,2-R,R'-*closo*-1,2-$C_2B_{10}H_{10}$, the higher electronegativity of carbon relative to boron results in those two boron atoms [B(3) and B(6)] adjacent to the cage carbon atoms being relatively attractive to nucleophiles. Treatment of the cluster with alcoholic base **[49, 50]** or, less commonly, with other bases such as amines **[51]**, results in a deboronation reaction. The (*closo*) cage is effectively "decapitated" to yield the corresponding (*nido*) open species. Such a pair of precursor and deboronated product have already been seen in figure 1.6. It is clearly desirable that cage-bound substituents should survive the deboronation conditions and there is, therefore, some limitation to the range of substituted parent carbaboranes which may be modified by this method.

The very wide synthetic usefulness of these decapitated carbaboranes for the formation of metal complexes will be discussed in more detail in a later section of this chapter. However, it appropriate at this point to touch briefly on their utility in the preparation of *B*-substituted carbaboranes. A simple example is the reaction between dianionic *nido*-$[C_2B_9H_{11}]^{2-}$ (as the salt of a suitable halophilic cation such as K^+) and $PhBCl_2$ to yield the corresponding *closo*-*B*-Ph-$C_2B_{10}H_{11}$ **[52]**.

C-Phenyl Carbaboranes

The class of icosahedral *closo*-dicarbaboranes bearing C-phenyl substituents is of particular relevance to this work. In addition to the parent compounds 1-Ph-*closo*-1,2-$C_2B_{10}H_{11}$ and 1,2-Ph_2-*closo*-1,2-$C_2B_{10}H_{10}$, which were among the first of the *closo*-dicarbadodecaboranes to be reported **[33, 34]**, many 2-substituted derivatives of the former parent are known.

Structural determinations have been performed upon the two parent carbaboranes. 1-Ph-*closo*-1,2-$C_2B_{10}H_{11}$ **[53]** crystallises with two independent molecules per asymmetric unit. One of these molecules is disordered: the position of the {CH} vertex could not be determined; instead, it is "averaged" over those five vertices adjacent to the vertex bearing the phenyl substituent. A view of the second, ordered molecule is shown in figure 1.12.

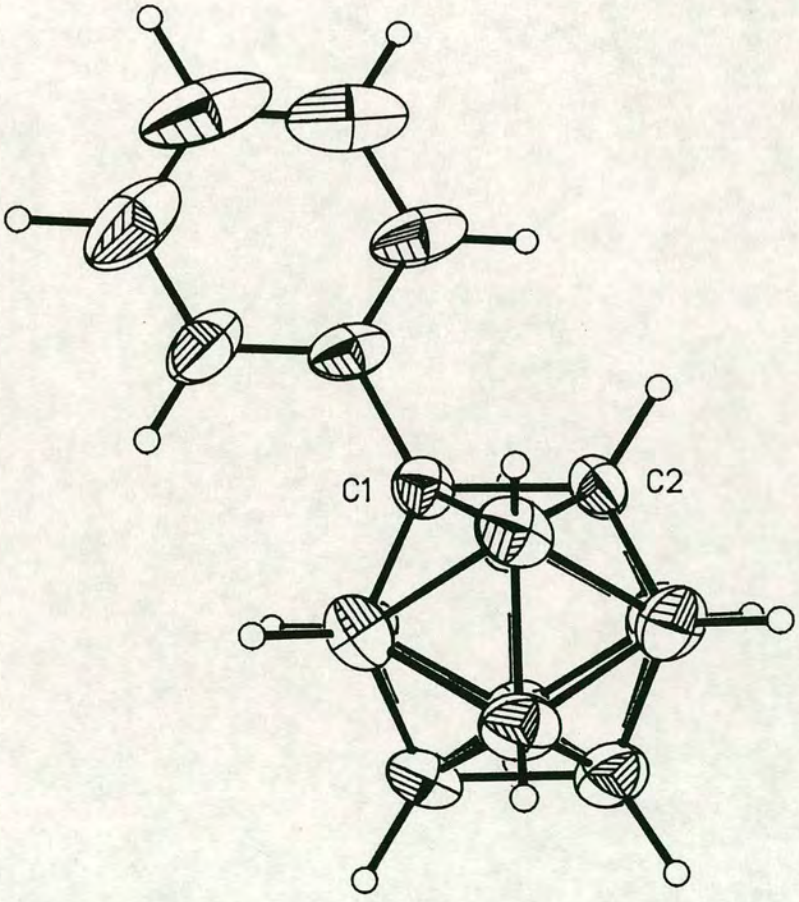

Figure 1.12 View of the crystallographically ordered molecule of 1-Ph-1,2-*closo*-$C_2B_{10}H_{11}$

Diphenylcarbaborane, 1,2-Ph_2-1,2-*closo*-$C_2B_{10}H_{10}$, also crystallises with two independent molecules in the asymmetric fraction of the unit cell **[54]**. Both molecules are ordered; a view of one is shown in figure 1.13 below.

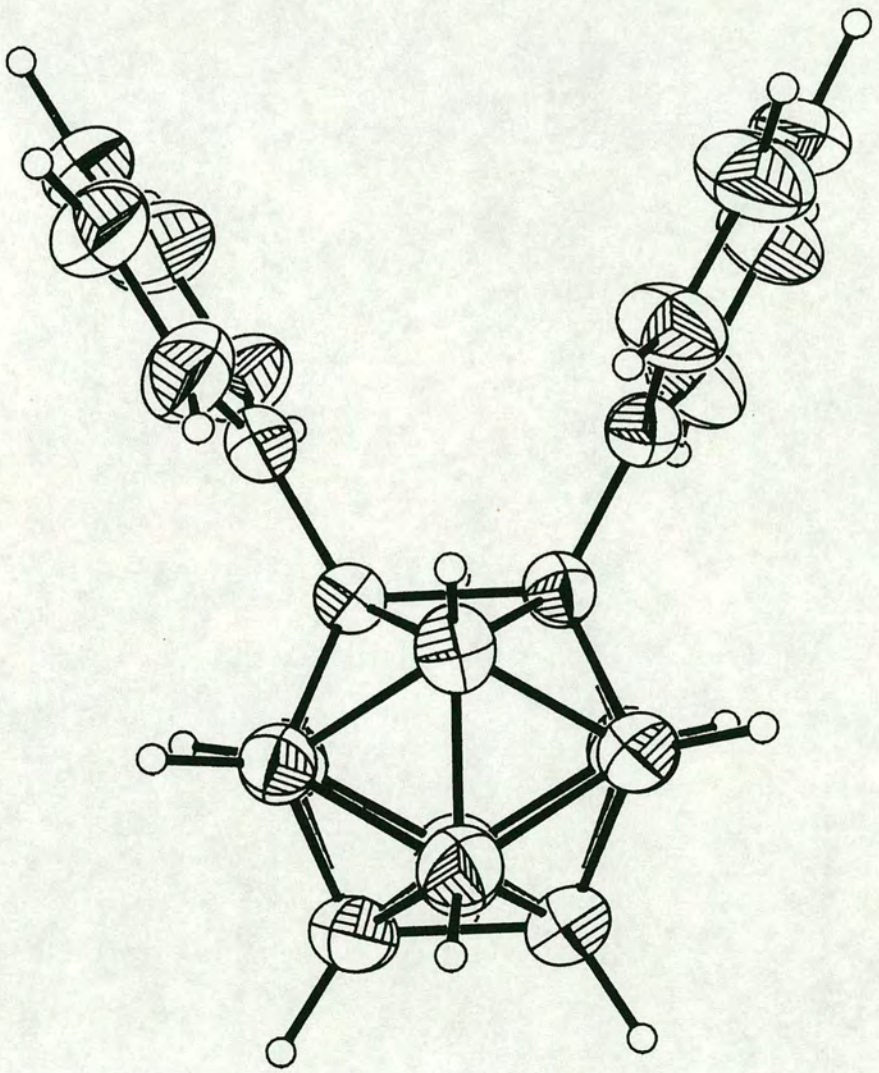

Figure 1.13 View of one of the crystallographically independent molecules of 1,2-Ph_2-1,2-*closo*-$C_2B_{10}H_{10}$

The anisotropic steric requirement of the phenyl ring (illustrated in figure 1.14 below) is an important consideration in the structural chemistry of this family of compounds - and, indeed, of their metal derivatives.

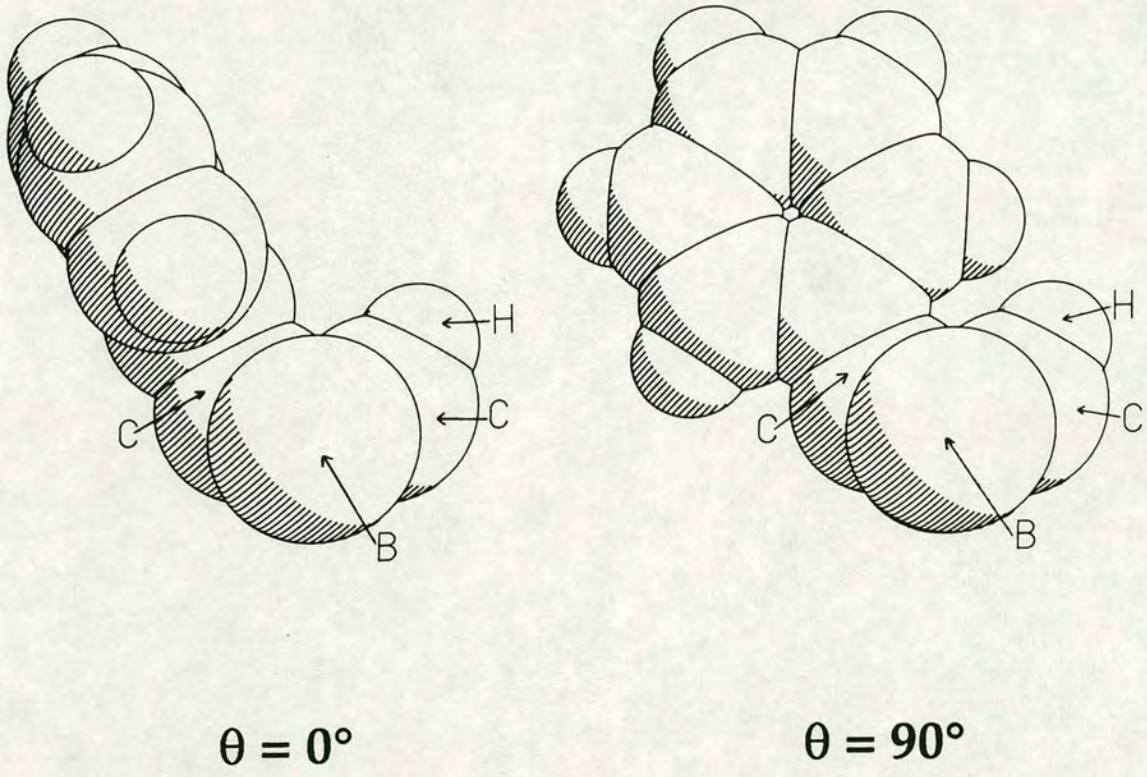

Figure 1.14 Two "space-filling" views of a phenyl ring

The conformation of a cage-bound phenyl group relative to the carbaborane polyhedron - and the C_{cage}-C_{cage} connectivity in particular - may be conveniently described in terms of an angle θ **[54]**. θ was defined as "*the average difference between 90° and the moduli of the* C_{cage}-C_{cage}-C-C *torsion angles*"; this is re-expressed herein and elsewhere **[55]** as the modulus of the average of the two C_{cage}-C_{cage}-$C_{phenyl(\alpha)}$-$C_{phenyl(\beta)}$ torsion angles. Extended Hückel molecular orbital calculations on idealised models of 1,2-*closo*-$C_2B_{10}H_{12}$ and its 1-Ph- and 1,2-Ph_2- derivatives have established an *electronic factor* and a

preferred phenyl ring conformation of $\theta = 90°$ **[54]**. This is a small, but definite and potentially significant, effect and it may be that conjugation between the aryl π system and cage carbon-based π orbitals is desirable and maximised when the two C_{cage} atoms and the phenyl ring are coplanar. Thus, when $\theta = 90°$, the $C_{cage}\cdots C_{cage}$ connectivity is predicted to be shorter than when $\theta = 0°$ (and likewise for the C_{cage}—C_{phenyl} bond).

Ab initio calculations **[53]** have confirmed this preference for large θ values, with the position of minimum energy at around $\theta = 65°$. Intramolecular crowding is thought to occur between the β-H atom of the phenyl ring and the adjacent B- and C_{cage}-bound H atoms when θ is increased further, thereby limiting the freedom of orientation of the phenyl moiety.

The crystallographically-ordered molecule of phenylcarbaborane has $\theta = 68.8°$, close to the "desired" value, and the $C_{cage}\cdots C_{cage}$ separation is 1.646(8)Å. (Packing effects in the crystal lattice are believed to hinder achievement of a more ideal phenyl ring orientation.) In the two crystallographically independent molecules of diphenylcarbaborane, steric congestion between the two adjacent aryl substituents severely limits twisting of the pendant groups and θ values closer to zero are measured: for the two independent molecules the average θ values are 2.4° and 8.6°, with correspondingly long $C_{cage}\cdots C_{cage}$ distances of 1.733(4) and 1.720(4)Å respectively.

The presence of C_{cage}-bound phenyl group has been found to produce a variety of unusual structural behaviour in the metal derivatives of the two above parent carbaboranes: several examples of these phenomena will be discussed later in this introductory Chapter.

Other Heteroboranes

The majority of the family of heteroboranes is made up by the carbaboranes. However, there do exist a significant number of boron clusters containing other heteroatoms, and study of their chemistry continues to enjoy current interest **[56]**. As with their carbaborane relatives, synthesis of these species relies almost exclusively on incorporation of the heteroatom(s) into a preformed boron cluster.

A considerable number of heterocarbaboranes are known, and their chemistry has been reviewed elsewhere **[57, 58]**: these include compounds which are, formally, carbaborane complexes of main group metals and metalloids. Other classes of heteroboranes are less well studied; and their syntheses are often not general.

Several heteroatom analogues of the icosahedral (*ortho-*) carbaboranes have been prepared. Among these is the diphosphaborane *closo*-1,2-$P_2B_{10}H_{10}$ **[59]**, and the corresponding diarsa- **[60]** and distiba- **[61]** derivatives, which are prepared by the interaction of decaborane $B_{10}H_{14}$ with the appropriate MCl_3 species in the presence of base and a reducing agent. A recent contribution reports the "*serendipitous preparation*" of the disilaborane 1,2-Me_2-*closo*-1,2-$Si_2B_{10}H_{10}$ **[62]**, which is isolated in significant yield from the reaction of $Me(H)Si(NMe_2)_2$ with decaborane. Some current interest focusses upon the synthesis, and derivative formation, of the icosahedral azaborane $NB_{11}H_{12}$ **[6, 63]**.

Of relevance to some of the work discussed herein are the 10- **[64, 65]** and 11-vertex **[65]** thiaboranes. (Related selena- and tellura- species are also known **[66]**.) In particular, the monoanionic thiaborane *arachno*-[6-SB_9H_{12}]$^{2-}$ is formed by the reaction of concentrated polysulphide with decaborane. This ion has been structurally characterised as the caesium salt **[67]**. The *arachno* cluster may be successively closed by first mild oxidation (I_2) to yield *nido*-6-SB_9H_{11}; then by pyrolytic disproportionation to the *closo*-1-SB_9H_9 species.

Metal Complexes of Boron Clusters

By far the largest group of derivatives of the polyhedral boranes is that in which a boron vertex (or, rather less commonly, vertices) is replaced by a metal-ligand group. A wide variety of species are potentially accessible *via* incorporation of one or more of the vast available range of metal fragments into the polyhedral (hetero)borane framework, and an additional diversity of structure is made possible by the flexibility (in numbers of electrons and orbitals available for contribution to cluster bonding) between different metal fragments. The synthesis and chemistry of these species has been extensively reviewed elsewhere [for example, **68 - 71**].

As is the case with their non-metal-containing relatives, metalla(hetero)boranes are prepared principally by the interaction of a preformed boron cluster and a metal fragment (both as appropriate derivatives). One major general route to metal derivatives of the (hetero)boranes is by polyhedral expansion, in which a metal is inserted directly into a boron cluster. For example, the reaction of $[(Et_3P)_3Pt]$ with the eleven vertex carbaborane *closo*-$Me_2C_2B_9H_9$ yields the twelve-vertex *closo* product $[(Et_3P)_2Pt\{Me_2C_2B_9H_9\}]$ **[72]**. Formally, this may be viewed as oxidative insertion of the metal centre: 2 electrons are donated to the cluster framework orbitals, so that the *closo*-carbaborane "opens" to accept and covalently bond the platinum fragment, as illustrated below (figure 1.15). Likewise, the {(toluene)Fe} fragment produced by thermal generation of iron atoms in the presence of toluene readily inserts into the thiaborane *nido*-SB_9H_{11} to yield the product *nido*-$[(toluene)FeSB_9H_{11}]$ **[73]**.

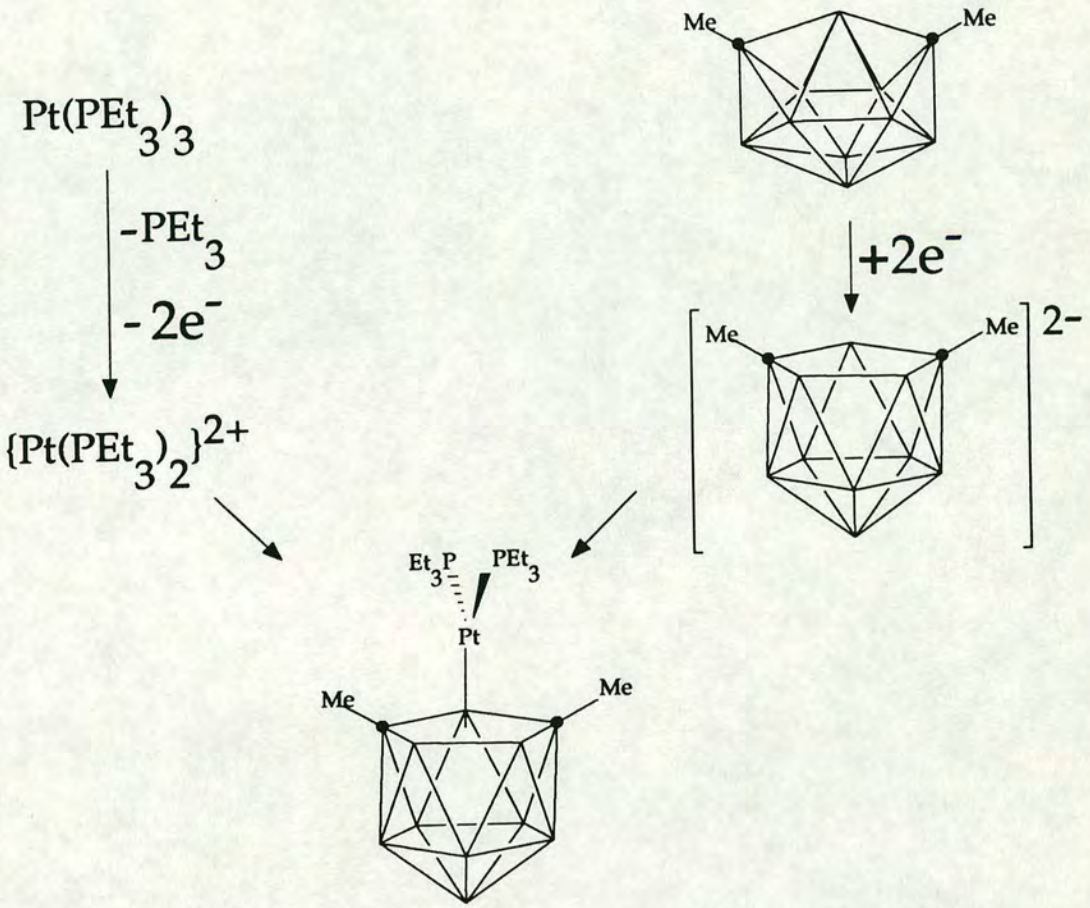

Figure 1.15 Representation of reaction between $\{(Et_3P)_3Pt\}$ and $Me_2C_2B_9H_9$

An important alternative route leading to metalla(hetero)boranes, of particular relevance to this work, is combination of the metal fragment with an 'already-opened' cage: no change in metal oxidation state occurs but, rather, the metal moiety takes up one of the vacant vertices of the heteroborane polyhedron. More specifically, the *nido*-carbaborane dianion $[\eta\text{–}C_2B_9H_{11}]^{2-}$ formed by decapitation of *ortho*carbaborane (or likewise its *C*-substituted derivatives) - as discussed earlier - constitutes a representative of an important class of carbaborane which may act as a ligand towards metal centres. The bonding capabilities of the ligand towards transition metal fragments have been recognised **[74]** as very similar to those of the ubiquitous $[\eta\text{–}C_5H_5]^-$ ligand in that both have similar frontier orbitals, figure 1.16 below; and both present a pentagonal coordinating face and behave as 6 π-electron, η^5-ligands to metal centres.

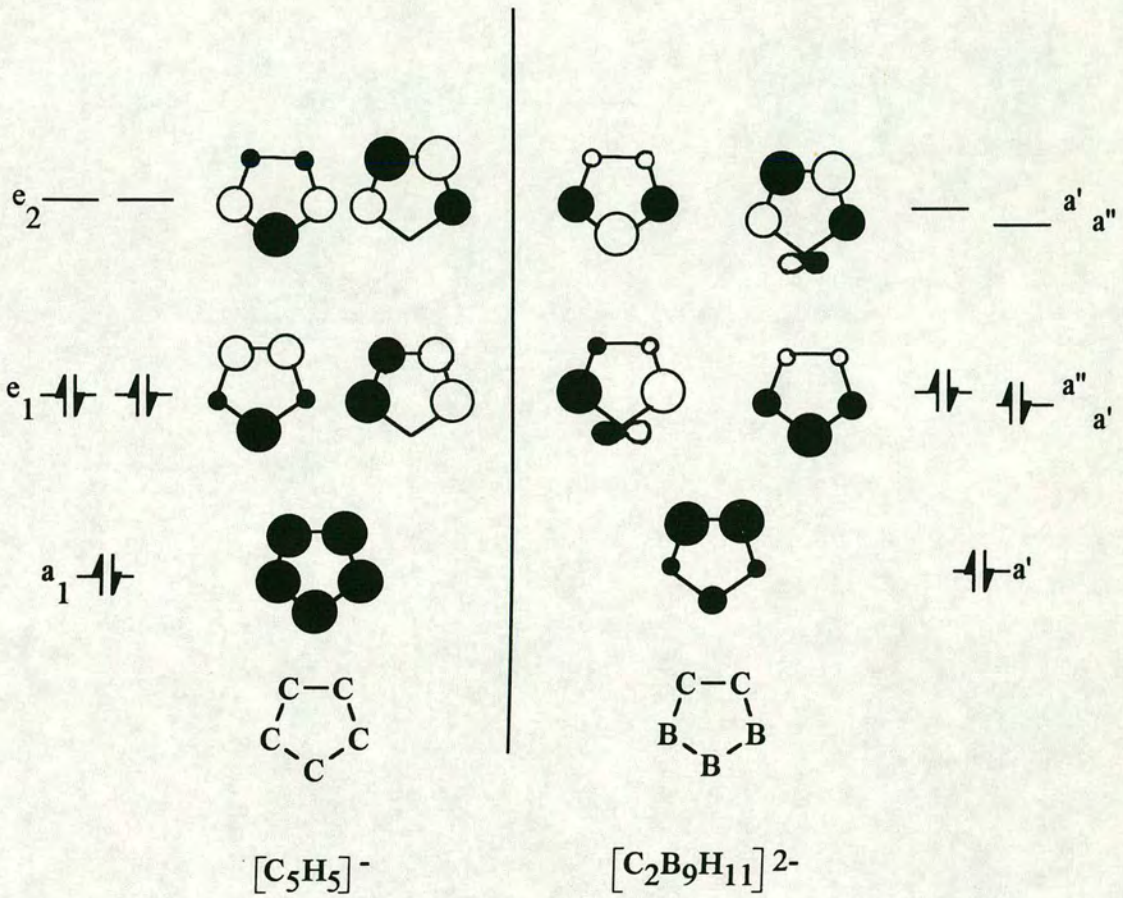

Figure 1.16 The π frontier orbitals of [η–C_5H_5]$^-$ and [η–$C_2B_9H_{11}$]$^{2-}$ ligands

[The lower symmetry of the carbaborane ligand results in a lifting of the degeneracy of the orbitals equivalent to the *e* pairs in the simple hydrocarbon ligand; a rather similar set of carbaborane π frontier orbitals is obtained when the symmetry is lowered further by *C*-substitution. The non-degenerate orbital pairs are, however, still close in energy and exhibit similar nodal properties to the corresponding {C_5H_5} orbitals.]

In a typical synthetic procedure, an icosahedral carbaborane $RR'C_2B_{10}H_{10}$ (R, R' = H, alkyl, aryl) is deboronated using alcoholic potassium hydroxide to form the dipotassium salt of the carbaborane dianion $K_2[RR'C_2B_9H_9]$; precipitation of this from aqueous solution as the dithallium salt $Tl[(Tl)RR'C_2B_9H_9]$* **[76]** yields a useful carbaborane precursor reagent. Treatment of this with a metal fragment halide salt results in elimination of thallium halide (which serves as a driving force) and the corresponding carbametallaborane is produced. The carbaplatinaborane described above (in figure 1.15, for example) could, in principle, equally well be formed *via* reaction of $[(Et_3P)_2PtCl_2]$ and dithallium [7,9-Me_2-7,9-*nido*-$C_2B_9H_9$]. Other salts of carbaborane ligands may be utilised generally in a similar fashion; in addition, salts of other heteroboranes may be employed in an analogous manner to obtain the corresponding heterometallaborane species.

Twelve-vertex carbametallaborane derivatives of *ortho*-carbaborane prepared as described above show deviation from ideal icosahedral symmetry as a consequence of the presence of various vertex atom types and substituents. Furthermore, the non-ideal geometries adopted by these species have been observed to show general distortions which may be resolved into a number of components, so that meaningful parameters relating to the distortions may be calculated and compared **[77]**. Several aspects of this deformation are illustrated in figure 1.17. [Note that in this figure the labelled atoms correspond to a 3,1,2-*closo*-MC_2B_9 numbering scheme: that is, ***1*** and **2** are C atoms whilst the metal atom (♦) would be labelled *3*.]

* One of the thallium ions is genuinely, although somewhat weakly, η^5-coordinated to the cage face **[75]**, whilst the other is a true counterion.

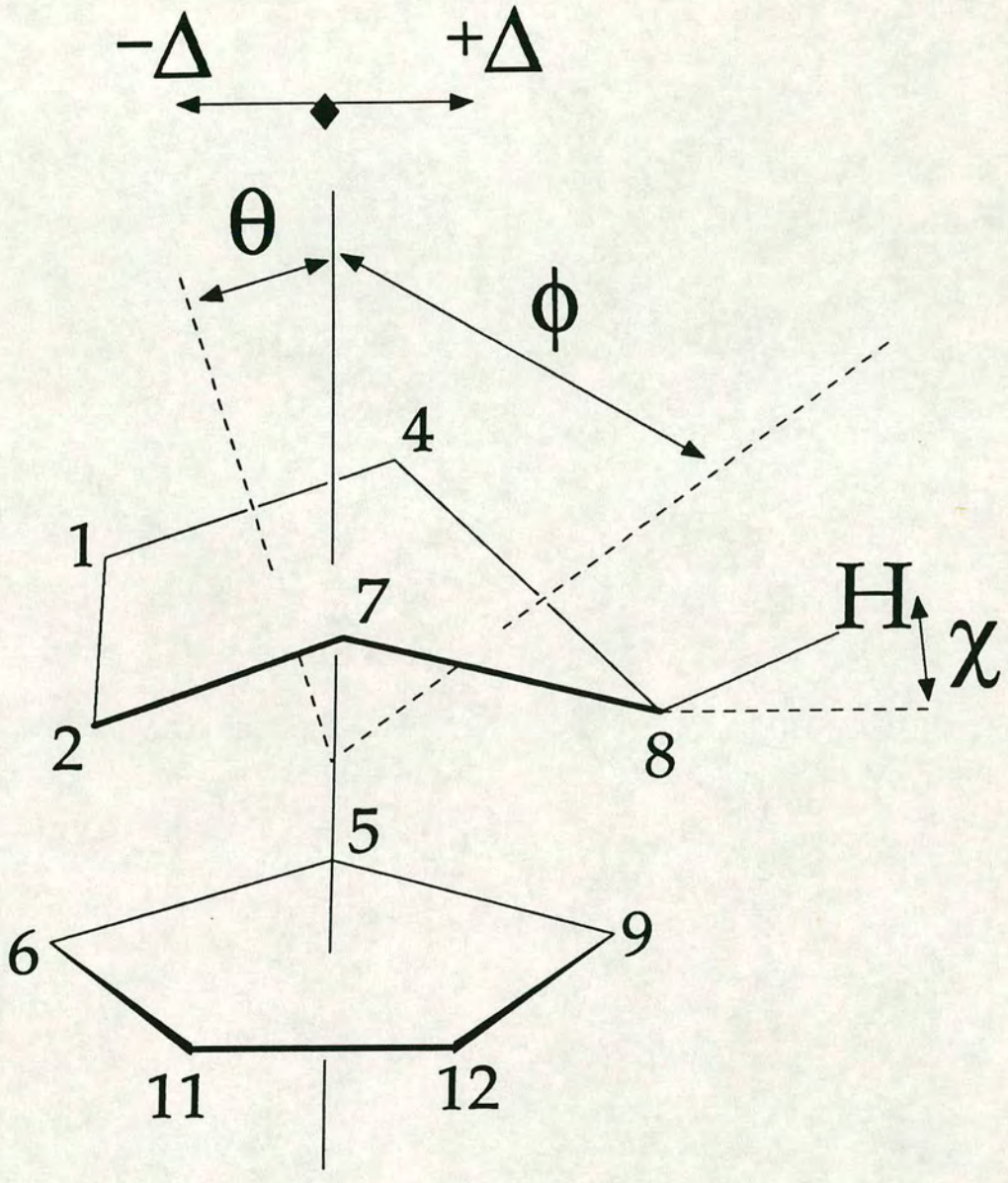

Figure 1.17 "Slipping" and "folding" distortions in 12-vertex carbametallaboranes

The lower B_5 pentagonal belt - that is, B(5)B(6)B(11)B(12)B(9) - is essentially planar, so that the various components of the polyhedral distortion may be defined with reference to a plane through these five boron atoms. The simplest deformation of the MC_2B_9 polyhedron is a movement of the upper C(1)C(2)B(7)B(8)B(4) pentagonal face relative to the lower belt, and is measured by the relative lateral displacements of the two centroids.

Slippage of the metal fragment is arguably the main distortion from regular geometry observed in these species. This occurs as a consequence of the frontier orbital characteristics of a given metal fragment; the metal vertex may not bond symmetrically to all five facial atoms of the carbaborane ligand. Thus, whereas a moiety such as {(arene)Ru} tends to lie over the centre of the ligating face; a {(phosphine)$_2$Pt} fragment has frontier orbitals which overlap preferentially with those cage frontier orbitals localised on boron, and the metal "slips" towards the 'rear' [*i.e.*, B(8)] of the open face. This situation is described by the slippage parameter Δ, with positive values of Δ indicating lateral movement towards B(8) and negative values corresponding to movement towards the C(1)—C(2) connectivity.

Some *folding* of the upper C_2B_3 face [about the B(4)···B(7) vector] is also generally observed, and is quantified as the angles θ and ϕ. This is thought to be associated with the slipping process and is generally more severe in cases where large slippages of the metal fragment have occurred.

One further quantity is useful in discussing these distortions, namely the substituent elevation parameter χ, which describes the angle between the (cage atom)—(substituent) bond and the plane to which the pendant group is bonded. For the purpose of this calculation it must be borne in mind that the C_2B_3 face is liable to folding and, therefore, the substituents bound to atoms C(1), C(2), B(4) and B(7) are inclined relative to the plane through these four atoms; and so on. In a regular icosahedron, substituents are elevated at an angle of 26.6° and deviations from this may be significant. (Note, however, that terminal H atoms bound directly to the cage are frequently placed in calculated, fixed positions and their χ value is consequently not a valuable measurement.)

Metal Complexes of *C*-Phenyl Carbaboranes

A number of metal derivatives of *C*-phenyl-substituted carbaboranes have been prepared, principally by the author's co-workers, and show a variety of unusual structural behaviour which is directly attributable to the steric influence of the pendant phenyl group(s). Certain *C*-aryl carbarhodaboranes display *closo/exonido* tautomerism, and potential catalytic activity; this has been referred to earlier in this Chapter. The novel distorted geometries adopted by cyclopentadienyl-rhodium and arene-ruthenium complexes of diphenylcarbaborane, and the facile isomerisation of *C*-phenyl carbaplatinaboranes, will be discussed in some detail in the following section; a few other examples from this system of the influence of sterics upon structure are worthy of note here.

The compound [10-*endo*-Ph_3PHg-7,8-Ph_2-7,8-$C_2B_9H_9$], in which the {Ph_3PHg} fragment is essentially σ-bound to the unique boron atom of the ligating carbaborane face, has been prepared and structurally characterised **[78]**. In contrast to the non-phenyl-substituted species **[79]**, in which Δ is 0.92Å, the former compound shows Δ = 1.10Å: this increased slippage appears to arise from intramolecular crowding between the cage substituents and the large mercury-bound phosphine.

(1,5-cyclooctadiene)-Pd and -Pt complexes of phenylcarbaboranes **[80]** similarly show enhanced metal slippage (Δ), and deformations of both the cage and the metal-ligand coordination. The diphenylcarbaborane derivatives rearrange to the corresponding *C*-separated 3,1,11-MC_2B_9 isomers; the Pt species does so spontaneously, whereas the Pd compound requires some thermal (110°C) encouragement.

In the *C,C'*-diphenyl analogue **[81]** of [{Ph_3PCu}$_2C_2B_9H_{11}$] **[7]**, the congestion which results from the presence of the cage-bound phenyl groups causes a disruption of the {Cu_2} unit: in the uncrowded parent, there is a copper-copper bond; whereas here the two copper atoms are over 4Å apart.

Finally, the potentially equally severe (*C*-phenyl)···(phosphine) steric interaction in [{$(Ph_3P)_2(Cl)Ru$}$C_2B_9H_{10}Ph_2$] **[82]** results in *vertex extrusion* such that the metal fragment is located exclusively in an *exo-nido* position. (In less crowded analogues **[83]**, some tautomerism of the kind observed in the carbarhodaboranes mentioned above is thought to occur.)

Aspects of Heteroborane Structural Behaviour

The principal theme of this thesis concerns the (unusual) structural behaviour of several groups of heteroboranes, and the analysis of this. It is of importance, therefore, firstly to consider some appropriate examples of structural misbehaviour and briefly to discuss some means by which this has been monitored.

In the previous section, a number of the ways in which factors such as varying metal fragment or the presence of steric crowding can produce structural perturbations in heteroboranes were introduced; the presence of asymmetry in borane polyhedra arising from vertex substitution or from exopolyhedral substituents results in distortions from idealised geometry such as "slipping" and "folding". There are, however, a number of examples of more serious, gross structural deformation, which are the subject of this section. (In particular, those distortions which arise in *C*-phenyl substituted species are of relevance to much of the present work.)

The first of these, 'straightforward' cluster distortion, is very often attributable to steric interactions - although electronic factors can often be equally significant. Polyhedral isomerisation, the second category of deformation here, may be viewed simplistically as an extreme form of distortion in which the deformed structure becomes untenable and isomerisation to a more stable form occurs. In a number of the examples discussed, this phenomenon may again be linked to steric or electronic factors. Thirdly, there are a number of boron cluster compounds whose structures are "anomalous" in terms of the accepted electron counting (Wade's) rules which have otherwise proved generally useful in considering the geometries adopted by these species.

A brief discussion of some methods for monitoring variations in cluster geometry then follows.

Cluster Deformation

In its simplest form, geometrical distortion of the polyhedron may be limited primarily to an elongation of a certain bond (or bonds). In the case of the present work (specifically in Chapters 2 and 3), the effect of crowding in 12-vertex dicarba(metalla)boranes is of interest. Changes in the C(1)-C(2) distance here constitute a convenient indicator of overall structural variation, since it is in this vicinity that bulky exopolyhedral groups are generally introduced; this is examined in some detail in Chapter 2. There are, however, several examples of 1,2-dicarbadodecaboranes in which the C_{cage}—C_{cage} connectivity is substantially elongated despite the absence of a steric factor which might account for this.

The first of these is the *C*-oxo species $[1\text{-}O\text{-}2\text{-}Ph\text{-}1,2\text{-}C_2B_{10}H_{10}]^-$, in which the C_{cage}—C_{cage} distance is 2.001(3)Å **[84]**. Here the {CO} unit may be considered to η^5-coordinate to the open face of the residual *nido*-$\{PhCB_{10}\}$ cage. Molecular orbital calculations reveal the cluster deformation to be electronic in origin: overlap between the frontier orbitals of the two above residues is made more favourable by the {CO} unit slipping away from the C(2) atom of the "ligating" carbaborane face.

A second group of icosahedral dicarbaboranes with long C_{cage}—C_{cage} separations have in common that this C—C connectivity is incorporated into an exopolyhedral macrocycle, such as in the species illustrated in figure 1.18 below. Two such carbaborane-macrocycles have been the subject of solid-state structural determinations. In the compound where the C_{cage}---C_{cage} linkage is $\{—S—CH_2CH_2—O—CH_2CH_2—S—\}$ **[85** and figure 1.18**]**, the C(1)-C(2) distance is 1.816(6)Å; whilst in the related species in which the linking group is $\{—S—(CH_2CH_2—O)_2—CH_2CH_2—S—\}$ **[86]** two crystallographically-independent molecules occur with C(1)-C(2) separations of 1.858(5) and 1.826(5)Å respectively.

Repulsions between the lone electron pairs on each sulphur atom, which are directed somewhat towards each other, are thought to be the main cause of the lengthening of the C(1)—C(2) connectivity in species of this type.

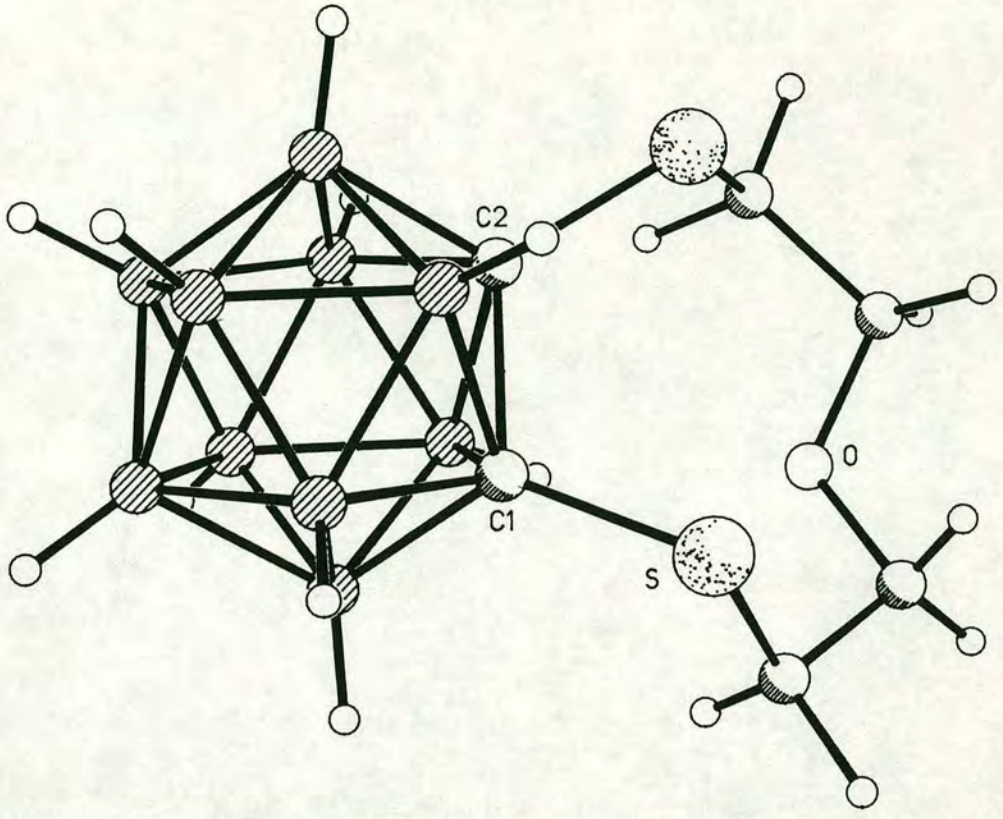

Figure 1.18 A 1,2-dicarbaborane bearing an exopolyhedral macrocycle

Rather more severe polyhedral distortions are found in several members of the series of carbametallaboranes [(arene)M{$C_2B_9H_9RR'$}], (where M = Ru, R/R' = H/Ph, Me/Ph, Ph/Ph; and M = Rh/Ir, R/R' = Ph/Ph) **[87 - 89]**. As the steric bulk of the groups bound to the C_{cage} atoms increases it is found that the C(1)···C(2) distance increases from (for example) 1.656(6)Å in [(mesitylene)Ru{$C_2B_9H_{10}Ph$}], to 1.754(11)Å in [(*p*-cymene)Ru{$C_2B_9H_9MePh$}], and in the diphenyl-substituted species such as [(C_5Me_5)Rh{$C_2B_9H_9Ph_2$}] the C(1)···C(2) connectivity is broken, being typically 2.51(3)Å. An example of these latter compounds, whose geometries have been termed *pseudocloso*, is illustrated in figure 1.19 below: it is interesting to note in addition that there is a concomitant shortening of the M(3)···B(6) vector, similar to a localised diamond→square transformation in the faces defined by C(1)M(3)C(2)B(6).

It seems certain that the {(arene)M} moiety forces severe intramolecular repulsions between the C_{cage}-bound phenyl groups; as they twist away from a more "comfortable" situation (with θ close to zero) to accommodate the metal-ligand set, repulsions force the two cage carbon atoms to separate.

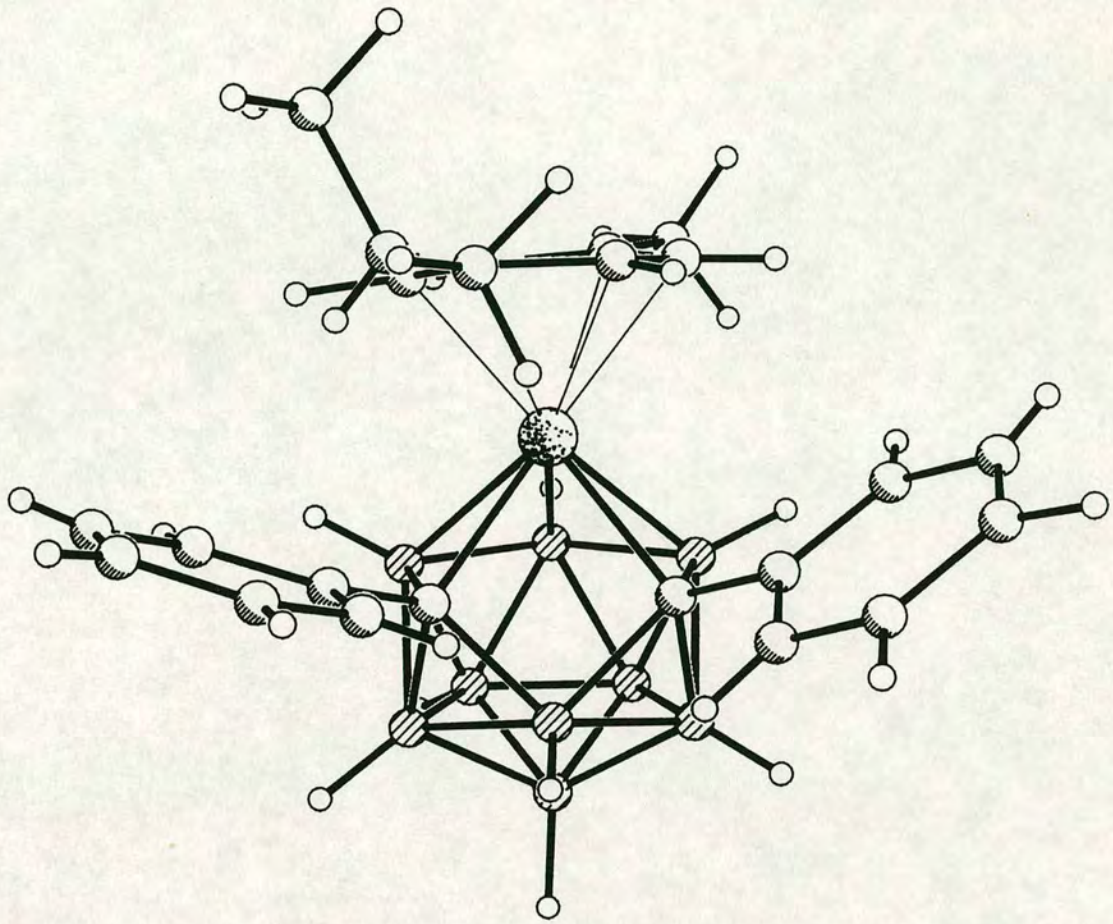

Figure 1.19 Structure of 1,2-Ph_2-3-*p*-cym-3,1,2-$RuC_2B_9H_9$

The above sterically-induced deformation was noted to be accompanied by a gradual loss of cluster electron density, evidenced by a downfield movement in the average ^{11}B chemical shifts. This is consistent with a partial transition from a *closo* geometry towards a *hypercloso* one **[90]**; such species have been shown to have *n* skeletal electron pairs rather than the (*n* + 1) possessed by a conventional *closo* cluster. Indeed, continuation along this pathway of C(1)···C(2) lengthening and M(3)···B(6) shortening until a M(3)—B(6) bond is established results in a true *hypercloso* species. Complexes of this latter type have been prepared by Stone and coworkers and do indeed show structures with a M—B(6) bond and C(1)···C(2) separations of 2.881(24) **[91]** and 2.917(9)Å **[92]**.

Polyhedral Isomerisation

Skeletal rearrangements are well known in carbaborane polyhedra and their derivatives, and are generally characterised by separation of the C_{cage} atoms. In the case of the icosahedral dicarbaboranes, three positional isomers are possible in which the carbon atoms are in the 1,2- ("*ortho*"), 1,7- ("*meta*"), or 1,12- ("*para*") positions. The presence of cage substituents, or of a further heteroatom such as a metal vertex, gives rise to many more possible isomers.

Polyhedral rearrangements involving species of this type were first demonstrated in the thermal conversion of *ortho*- to *meta*-carbaborane **[93]**, which occurs at around 450°C; further rearrangement to the most stable of the three isomers, *para*-carbaborane, occurs above 600°C **[94]** with some decomposition. These two processes are shown below (figure 1.20).

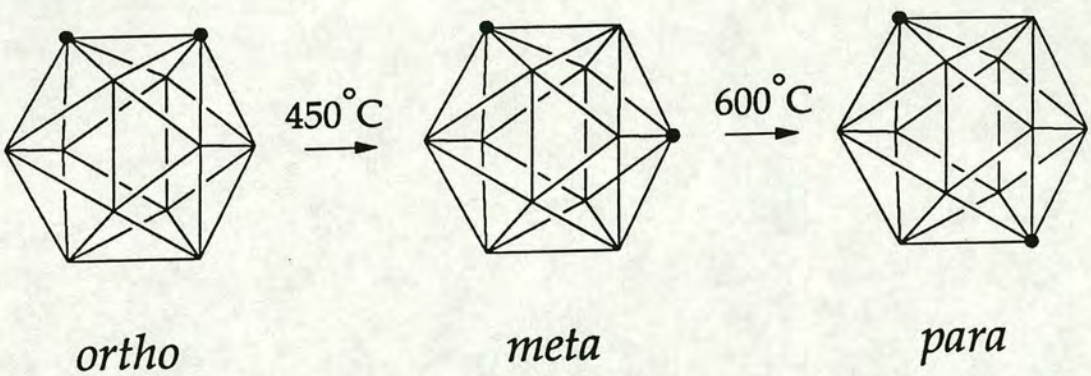

Figure 1.20 The *ortho* ⟶ *meta* ⟶ *para* -carbaborane isomerisation

The temperature at which this process occurs may be lowered by the introduction of bulky groups bound to the two adjacent C_{cage} atoms - the steric interaction presumably has some destabilising effect; hence, for example, the *C,C'*-(dimethylsilyl)$_2$- **[95]** and *C,C'*-(trimethylsilyl)$_2$- **[96]** derivatives of *ortho*-(1,2-)carbaborane rearrange to their 1,7- counterparts at around only 300°C.

Metal derivatives likewise undergo structural reorganisations of this type, and show similarity in terms of a reduction in isomerisation temperature, produced by steric effects. Thus, whereas $[Ni(C_2B_9H_{11})_2]$ requires temperatures of up to 400°C (in the vapour phase) to produce rearrangement, the *C,C'*-dimethyl-substituted species displays considerably more facile thermal isomerisation **[97]**.

A rearrangement process which is extraordinarily facile and - perhaps even more remarkably - is reversible, has been demonstrated by Stone and coworkers **[98]**. The process is summarised in essence in the figure (1.21) below.

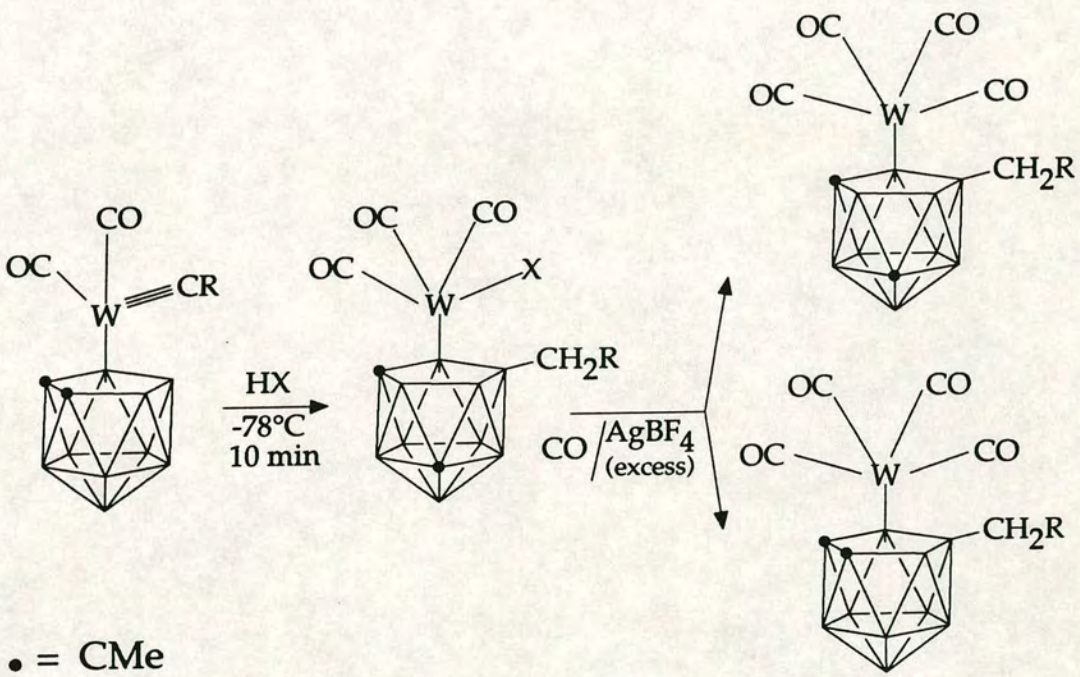

Figure 1.21 A facile, reversible isomerisation in a system of dicarbawolfraboranes

Low temperature rearrangements have also been observed in *bis*(phosphine)-platinum complexes of phenyl carbaboranes **[99]**, which are of some relevance to the present work. In this system, a steric factor has been invoked to account for the relatively facile nature of the isomerisation process. The mono-C_{cage}-phenyl compounds 1-Ph-3,3-$(R_3P)_2$-3,1,2-$PtC_2B_9H_{10}$ undergo rearrangement upon heating to only 55°C to yield two further, isomeric products (figure 1.22).

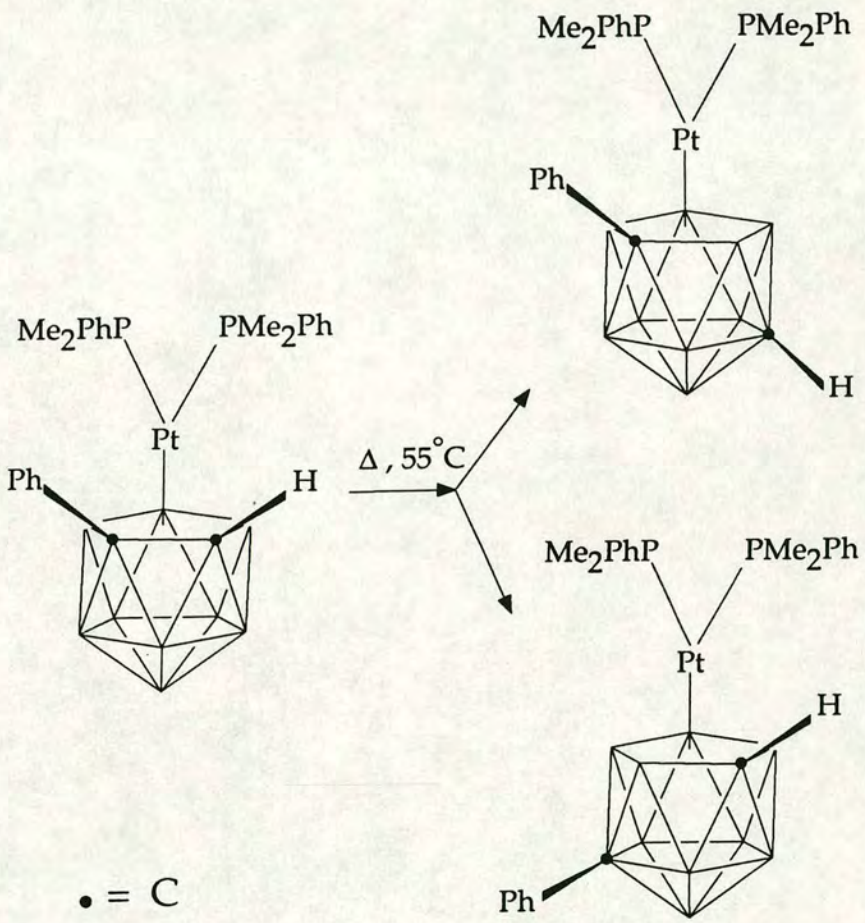

Figure 1.22 Isomerisation of 1-Ph-3,3-$(Me_2PhP)_2$-3,1,2-$PtC_2B_9H_{10}$

The first of these, the "11-Ph" isomer - that is, that where the {C-Ph} vertex has migrated - is the one which might be expected on the basis of steric arguments. However, the second product, where the {C-H} vertex has moved, is apparently as crowded as the parent and yet is stable under the thermolysis conditions. [With the corresponding *C,C'*-diphenylcarbaborane derivatives, the only isolable products are the analogous, isomerised {1,11-Ph_2-3,1,11-PtC_2B_9} species.]

The relative ease with which isomerisation occurs in the above diphenylcarbaborane derivatives is attributed to relief of steric congestion; whereas in the derivatives of phenylcarbaborane it is believed that *ground state destabilisation* facilitates the structural reorganisation. It has been shown **[77(b)]** that the preferred orientation of a {P_2Pt} fragment over a (C-adjacent) C_2B_3 face is as shown in figure 1.23(a); whereas the observed conformation in the above parent 3,1,2-PtC_2B_9 species is rotated by some 36° from this position, figure 1.23(b), as a consequence of accommodating the C_{cage}-bound phenyl group.

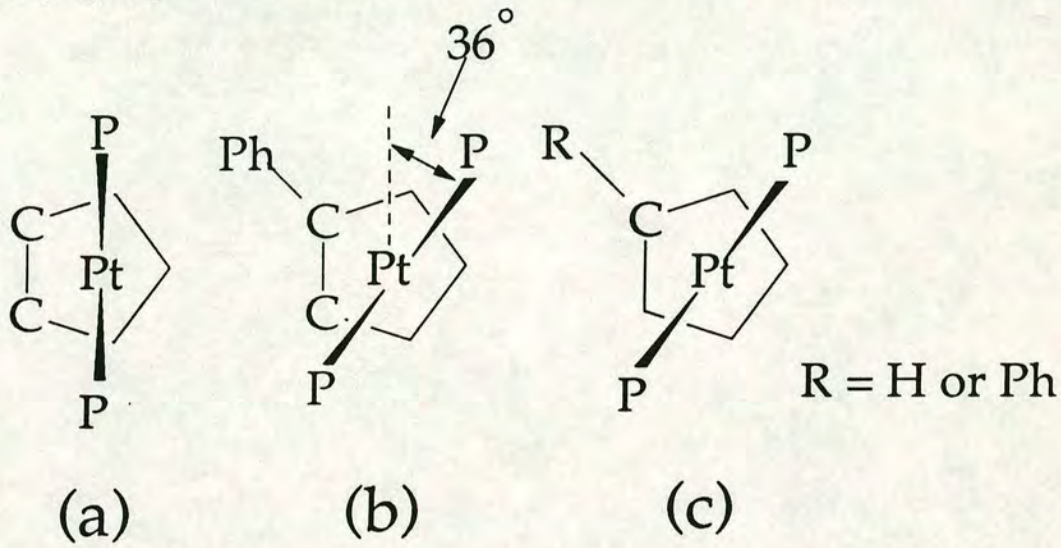

Figure 1.23 Orientation of {P_2Pt} fragments over ligating carbaborane faces

This displacement from a ground state energy greatly reduces the activation barrier to carbon-separation isomerisation. The observed conformation of the {P_2Pt} unit over the CB_4 face [figure 1.23(c)] in the product coincides with electronically-preferred situation, so that the two isomeric products are stable towards further rearrangement.

In this system, as in others where rearrangement processes occur, the mechanisms by which this takes place are the subject of considerable speculation and debate. Both experimental and theoretical probes of possible mechanisms have been made.*

* Where theoretical considerations are concerned, a note of caution may be struck; a number of proposed mechanisms have been somewhat discounted on the grounds that - in the rather idealised models considered - they are symmetry-forbidden; whereas in compounds such as the C-phenyl carbaplatinaboranes above (which have *much lower molecular symmetry*), such arguments must carry considerably less weight.

A *diamond-square-diamond* (D.S.D.) mechanism was first proposed by Lipscomb **[100]**, who successfully accounted for the isomerisation of *ortho-* to *meta*-carbaborane. The process, illustrated schematically in figure 1.24, involves six, concerted bond extensions (for example, C(1)—C(2) elongation) to yield a cubeoctahedral intermediate, followed by a further six, concerted motions which collapse the square faces of the intermediate (for example, B(3)—B(6) bond established). Antipodal relationships are maintained throughout.

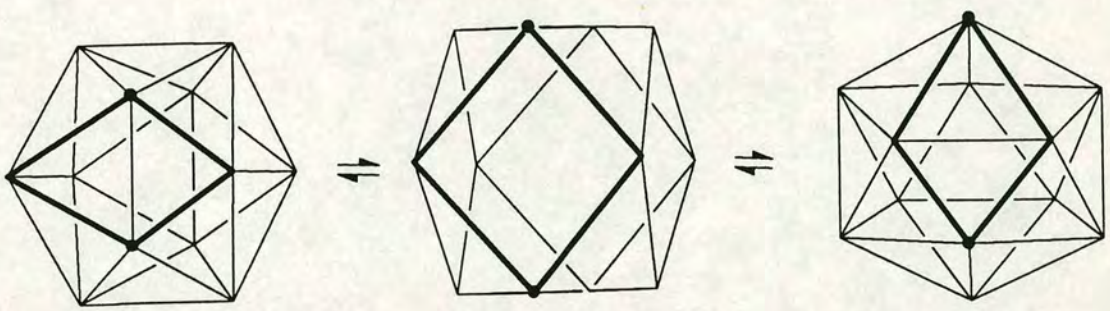

Figure 1.24 *Diamond-Square-Diamond* mechanism for $C_2B_{10}H_{12}$ isomerisation

This mechanism does not explain the *meta-* to *para-* isomerisation: it must be modified so that rotations of triangular faces in the cubeoctahedral intermediate are allowed. Indeed, a number of alternative mechanisms have been proposed. The first of these, put forward by Grafstein and Dvorak **[93]**, involves mutual rotation of the two pentagonal pyramids into which the icosahedron may be split, and can satisfactorily account for both the observed isomerised products obtained from *ortho*-carbaborane thermolysis.

Another rotational mechanism has also been proposed. In this Muetterties and Knoth **[101]** suggested that, by itself, rotation of a triangular face (or faces) would afford the above observed products without the need for rather more severe gross structural deformation. An elaboration of this by Wu and Jones **[102]** gave rise to the *extended triangle rotation* mechanism, which likewise explains experimental evidence.

A final mechanism, which is fundamentally different from the others, was first postulated by Wong and Lipscomb **[103]**, and was more recently examined in some detail by Edvenson and Gaines **[104]**. This mechanism, which involves the closed cage opening to form a *nido intermediate*, then reclosing by a different route to yield an isomeric product, is successful in accounting for previously-observed isomerisations; indeed, it was shown that some of the above, alternative mechanistic schemes are extensions of this "nido intermediate" mechanism.

In the case of the *C*-phenyl carbaplatinaborane system described earlier a diamond-square-diamond mechanism is demonstrably inappropriate, since after one set of DSD operations - the situation in the vicinity of the PtC_2 face is illustrated in figure 1.25 below - the *C*-phenyl analogues of the species whose formation is illustrated in figure 1.15 are formed.

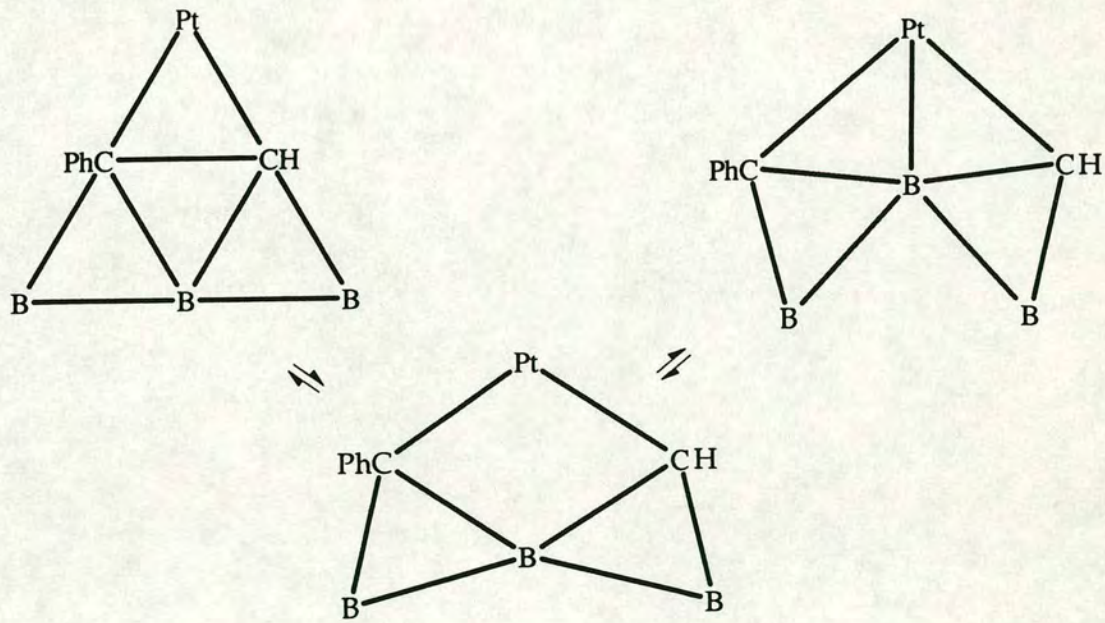

Figure 1.25 Effect of DSD operations in the vicinity of the PtC_2 face in 1-Ph-3,3-$(R_3P)_2$-3,1,2-$PtC_2B_9H_{10}$

Compounds of this type are known and should be stable; the preferred ground state, shown in figure 1.26 below, is spatially accessible and ought not to suffer any steric congestion. No further isomerisation would be expected to occur and the observed products would, therefore, not be obtained.

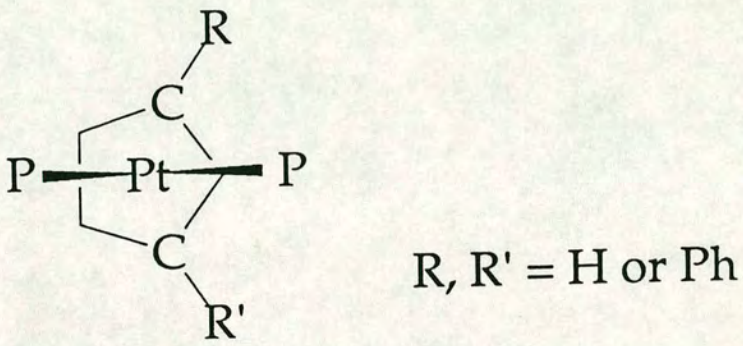

Figure 1.26 Orientation of {P_2Pt} fragment over $CBCB_2$ carbaborane face

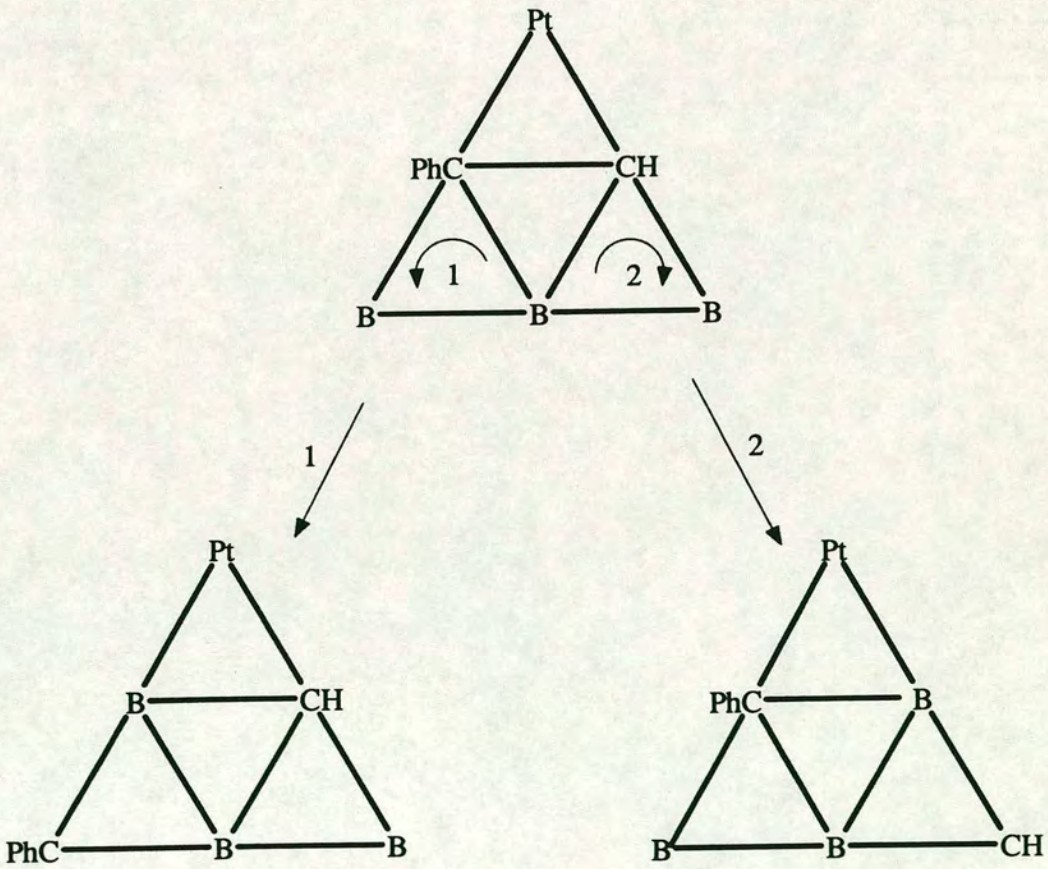

Figure 1.27 Triangular face rotation for 1-Ph-3,3-$(R_3P)_2$-3,1,2-$PtC_2B_9H_{10}$

A more satisfactory explanation involving the mechanism of triangular face rotation successfully accounts for the observed behaviour in the present case. (This bypasses the need for an "unusually unstable" intermediate of the kind represented in figure 1.26.) The situation where only one C_{cage} atom bears a phenyl moiety is shown in figure 1.27 above; that where both C_{cage} atoms bear a phenyl group is shown in figure 1.28 below.

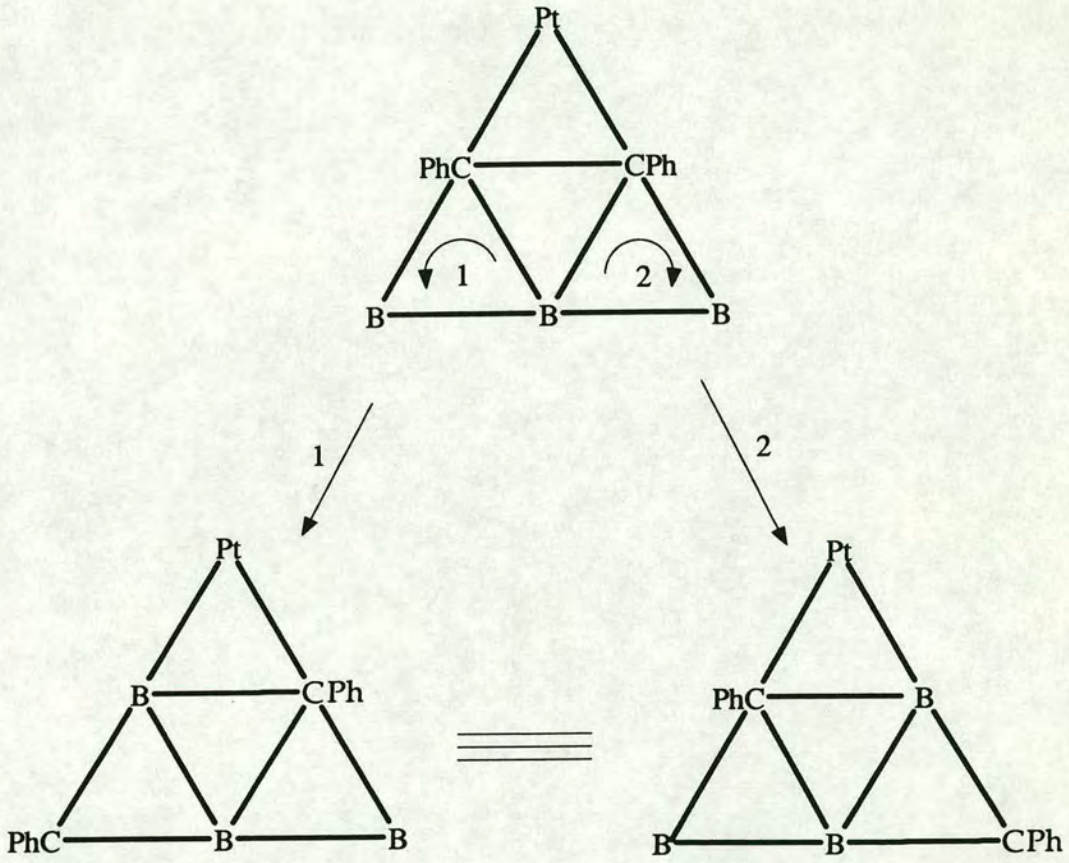

Figure 1.28 Triangular face rotation for 1,2-Ph_2-3,3-$(R_3P)_2$-3,1,2-$PtC_2B_9H_9$

Some considerations of molecular deformations [such as C_{cage}—C_{cage} elongation] in relation to movement along possible rearrangement pathways are presented in Chapter 2. In any event, it seems likely that the mechanisms of rearrangement of polyhedral boranes and their derivatives will continue to be the subject of intense debate for some time to come.

"Anomalous" Structures

Despite the generally broad and successful application of established electron counting rules there nevertheless exist a number of examples of boron cluster species whose geometries are considered "anomalous". Often these can be probed by means such as molecular orbital methods, which may reveal electronic features that cause a "non-conventional" structure to be adopted.

There are several 8-vertex species which display anomalous structural behaviour. The compound B_8H_{12} has for a long time been recognised as one of the few binary boranes which do not conform to Wadian electron counting rules: 10 skeletal electron pairs are present in this 8-vertex species which should, therefore, adopt a *nido* geometry rather than the observed **[105]** *arachno* one. Recent molecular orbital calculations **[106]** suggest that the observed structure is more stable for a neutral species than for the corresponding dianion; the additional electron pair would be required to occupy a strongly destabilising molecular orbital.

The 8-vertex metallaboranes $(\eta\text{-}C_5H_5)_4M_4B_4H_4$ (M = Co **[107]**, Ni **[108]**) both display *closo* structures, despite the fact that neither has the correct electron count for such a geometry: the cobalt compound has n, and the nickel compound $n+2$, skeletal electron pairs rather than the $n+1$ required by Wade's rules. This system has been the subject of much theoretical interest **[109]**, and it seems clear that the origin of the problem here lies in the fact that several of the possible geometries for 8-vertex species have very similar energies.

In the above and other examples, it must be realised that simple electron counting rules fail to take into account such features as steric factors which may limit the extent to which ideal geometries may be achieved, kinetic factors which might apparently stabilise formally unstable geometries, and substituents whose electronic properties may alter cluster electron density in an unexpected manner.

Structural variation may commonly be monitored by comparison of a single parameter such as the bond length of interest in a series of related species. It is, nevertheless, very often more appropriate to consider the whole structure; boron cluster compounds display highly delocalised bonding using truly *molecular* orbitals so that as one parameter varies the whole structure is affected *via* this delocalised bonding. For example, compounds of the type [{M}{$B_{10}H_{12}$}] may be described as either

$$\{M\}^{2+} + \textit{nido}\text{-}\{B_{10}H_{12}\}^{2-} \quad \underline{OR} \quad \{M\}^{4+} + \textit{arachno}\text{-}\{B_{10}H_{12}\}^{4-}.$$

Both borane fragments, represented in figure 1.29 below, have the same connectivity pattern but differ in electron count.

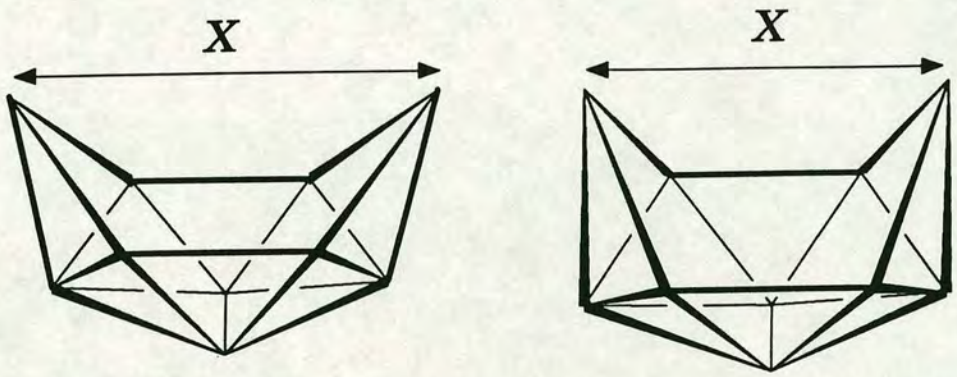

Figure 1.29 *nido*-{$B_{10}H_{12}$}$^{2-}$ and *arachno*-{$B_{10}H_{12}$}$^{4-}$

In these compounds the distance *X* is often taken as a crude measure of whether the fragment is of the *nido* or *arachno* type; a more sensitive measure of the change in overall cage geometry is to consider the whole structure, and comparison with suitable model fragments has allowed the electronic nature of the ligating boranes to be assigned and correlated with other physical data **[110]**. (Detailed structural comparisons of this kind constitute part of Chapter 4 of this work.)

As has been suggested earlier, structural analyses accompanied by methods such as both spectroscopic and molecular orbital studies, provide powerful tools by which structural changes may be monitored, rationalised, or "tracked" along some pathway such as the beginnings of a rearrangement process.

Scope of Present Work

In the previous section were discussed a number of directions in which structural *misbehaviour* in the polyhedral boranes and their derivatives may take place. The three following discussion chapters address some of these aspects in relation to several systems of heteroboranes which show potentially unusual behaviour.

Previous findings of the author's coworkers prompted a systematic study of several substituted *C*-phenyl dicarbadodecaboranes in which the influence of increasing steric congestion between exopolyhedral substituents was monitored *via* single crystal *X*-ray diffraction studies and detailed structural analyses.

Allied to this, several platinum complexes of a potentially sterically demanding carbaborane ligand, in which the platinum-bound phosphine ligands varied in steric requirement, were prepared and studied by both spectroscopic and structural means.

Finally, two separate systems of 11-vertex heterometallaboranes which display anomalous structural behaviour were analysed in detail in an attempt to rationalise these phenomena. In the first case, relatively simple structural examination readily resolved the problem whereas, in the second system, the situation appeared rather less straightforward. For this latter group of compounds a hitherto unrecognised structural possibility was proposed and (with this in mind) attempts to prepare "non-anomalous" analogues yielded a number of unexpected and rather novel species.

Chapter 2

Synthesis and Characterisation of *C*-Substituted Phenyl Carbaboranes

Introduction

This chapter describes the synthesis and characterisation of several 2-substituted 1-phenyl-1,2-*closo*-dicarbadodecaboranes, and focusses upon the influence of the varying steric demands of the C_{cage}-bound substituent upon structure.

In particular, four of these carbaboranes have been the subject of single crystal *X*-ray diffraction studies which reveal these compounds to exhibit essentially the same gross *pseudo*-icosahedral structure which is well known for species of this type **[29]**. There is, however, indication of a significant steric effect in the geometries of these species. Thus, both 1-Ph-2-Me-1,2-*closo*-$C_2B_{10}H_{10}$, **1**, and 1-Ph-2-Br-1,2-*closo*-$C_2B_{10}H_{10}$, **2**, demonstrate relatively little spatial overcrowding and the latter may be taken to be a "reference" member of this series; in contrast, the two silyl carbaboranes 1-Ph-2-Me_3Si-1,2-*closo*-$C_2B_{10}H_{10}$, **3**, and 1-Ph-2-^{t}BuMe$_2$Si-1,2-*closo*-$C_2B_{10}H_{10}$, **4**, show evidence for some intramolecular steric interaction between the cage-bound phenyl and trialkylsilyl substituents. The solid state structures of these four carbaboranes are considered with particular reference to sterically-induced distortions and whether there is, associated with this, any evidence of movement along a particular rearrangement pathway.

Three further carbaboranes are also discussed. 1-Ph-2-^{i}Pr$_3$Si-1,2-*closo*-$C_2B_{10}H_{10}$, **5**, constitutes a further member of the above series for which diffraction quality crystals could not be obtained; whilst 1-^{t}Bu-1,2-*closo*-$C_2B_{10}H_{11}$, **6**, and 1-^{t}Bu-2-Br-1,2-*closo*-$C_2B_{10}H_{10}$, **7**, were prepared as possible precursors to a further crowded species, namely 1-Ph-2-^{t}Bu-1,2-*closo*-$C_2B_{10}H_{10}$.

Synthesis, Characterisation and N.M.R. study of 1-Ph-2-Me-1,2-*closo*-$C_2B_{10}H_{10}$, 1

1 is prepared in good yield by the interaction of 1-phenyl-1-propyne (PhC≡CMe) and decaborane ($B_{10}H_{14}$) in refluxing benzene or toluene in the presence of *N,N*-dimethylaniline as a Lewis base. (The yield and ease of work-up are dramatically reduced, and the reaction time considerably increased, if acetonitrile is used as Lewis base.) Evaporation of the reaction mixture and addition of small amounts of ice-cold methanol, followed by decantation of the yellow supernatant liquid (until the methanolic washings are colourless), yields on drying an analytically pure product. (Several further crops of product may be obtained by evaporation of the washings and further treatment of the residue with methanol.) As far as the author is aware, this is the first reported synthesis of this carbaborane by this route and represents a considerable overall improvement upon the previous synthesis **[111]** which utilised the reaction of the lithium salt 1-Ph-2-Li-1,2-*closo*-$C_2B_{10}H_{10}$ with methyl iodide.

The identity of the product was confirmed by microanalysis, and infrared and n.m.r. spectroscopies. Consideration of the *Cs* molecular symmetry of **1** predicts six peaks in the $^{11}B\{^1H\}$ n.m.r. spectrum in the ratio 1:1:2:2:2:2. These could not be adequately dispersed, even at 192.5MHz; instead a peak ratio of 1:1:4:4 was obtained. In an attempt to achieve at least partial assignment of the n.m.r. resonances, a number of more sophisticated spectra were recorded.

A "two-dimensional" $^{11}B\{^1H\}-^{11}B\{^1H\}$ correlation (*COSY*) spectrum, figure 2.1, shows "cross-peaks" corresponding to correlations between all four of the resonances in the conventional one-dimensional spectrum, so that no additional information could be obtained from this experiment.

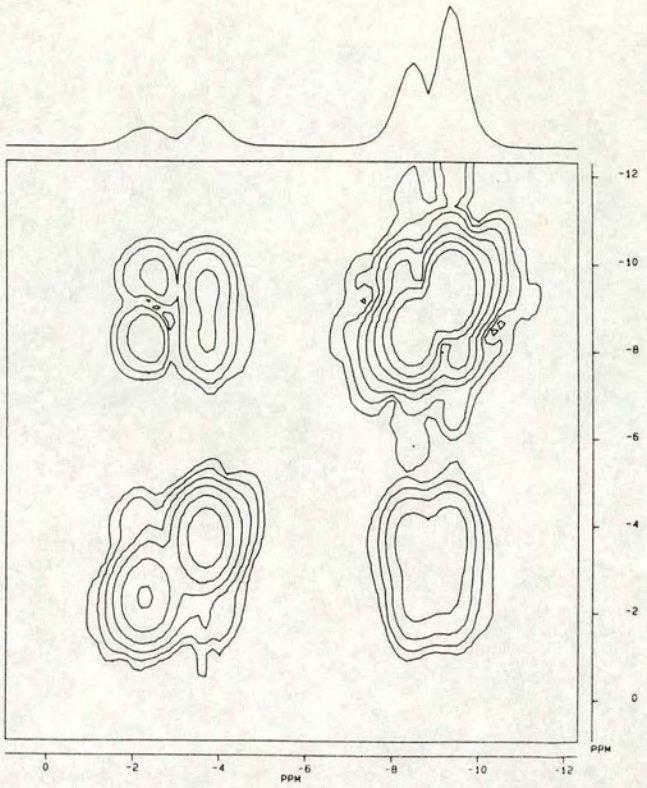

Figure 2.1 $^{11}B\{^1H\}$—$^{11}B\{^1H\}$ ***COSY*** spectrum of **1**

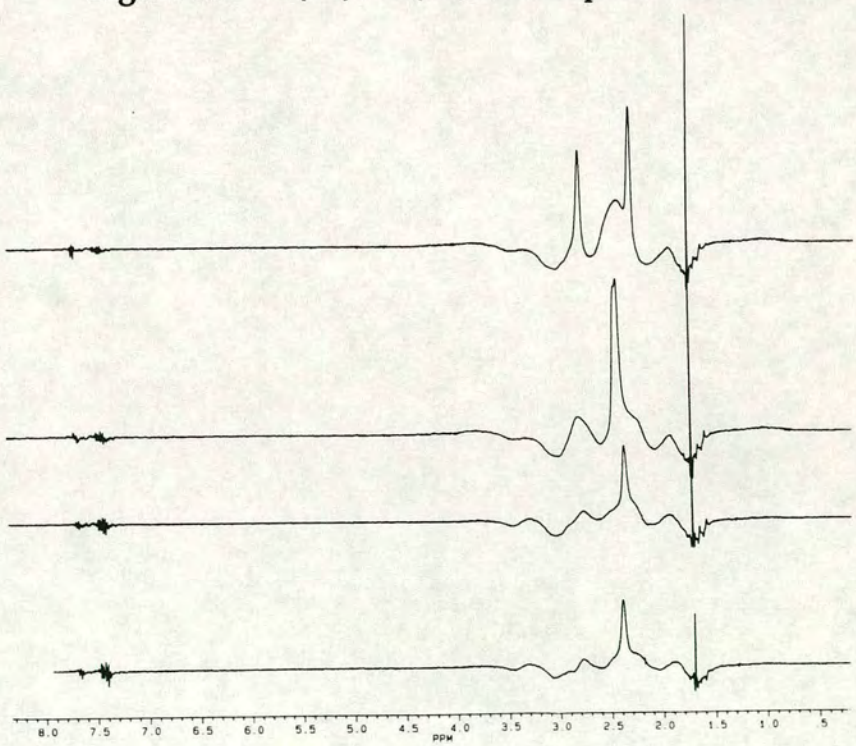

Figure 2.2 $H\{^{11}B_{selective}\}$ difference spectra for **1** (From top to bottom, the spectra correspond to irradiation at $\delta(^{11}B)$ = -9.37, -8.53, -3.76 and -2.36 p.p.m. respectively)

Selective boron decoupling of the ^1H spectrum - difference spectra are shown in figure 2.2 - revealed somewhat better separation of the cage proton resonances; only two of these coincide (at δ_H = 2.38 p.p.m.). Accordingly, a proton-proton [$^1H\{^{11}B\}$—$^1H\{^{11}B\}$] *COSY* experiment was performed. The resulting spectrum is shown in figure 2.3 (the resonance at *ca.* 2.15 p.p.m. is an impurity). This spectrum shows extensive correlation between the diagonal peaks, but again a full (or even partial) unambiguous assignment from this is impossible.

Figure 2.3 $^1H\{^{11}B\}$—$^1H\{^{11}B\}$ *COSY* spectrum for **1**

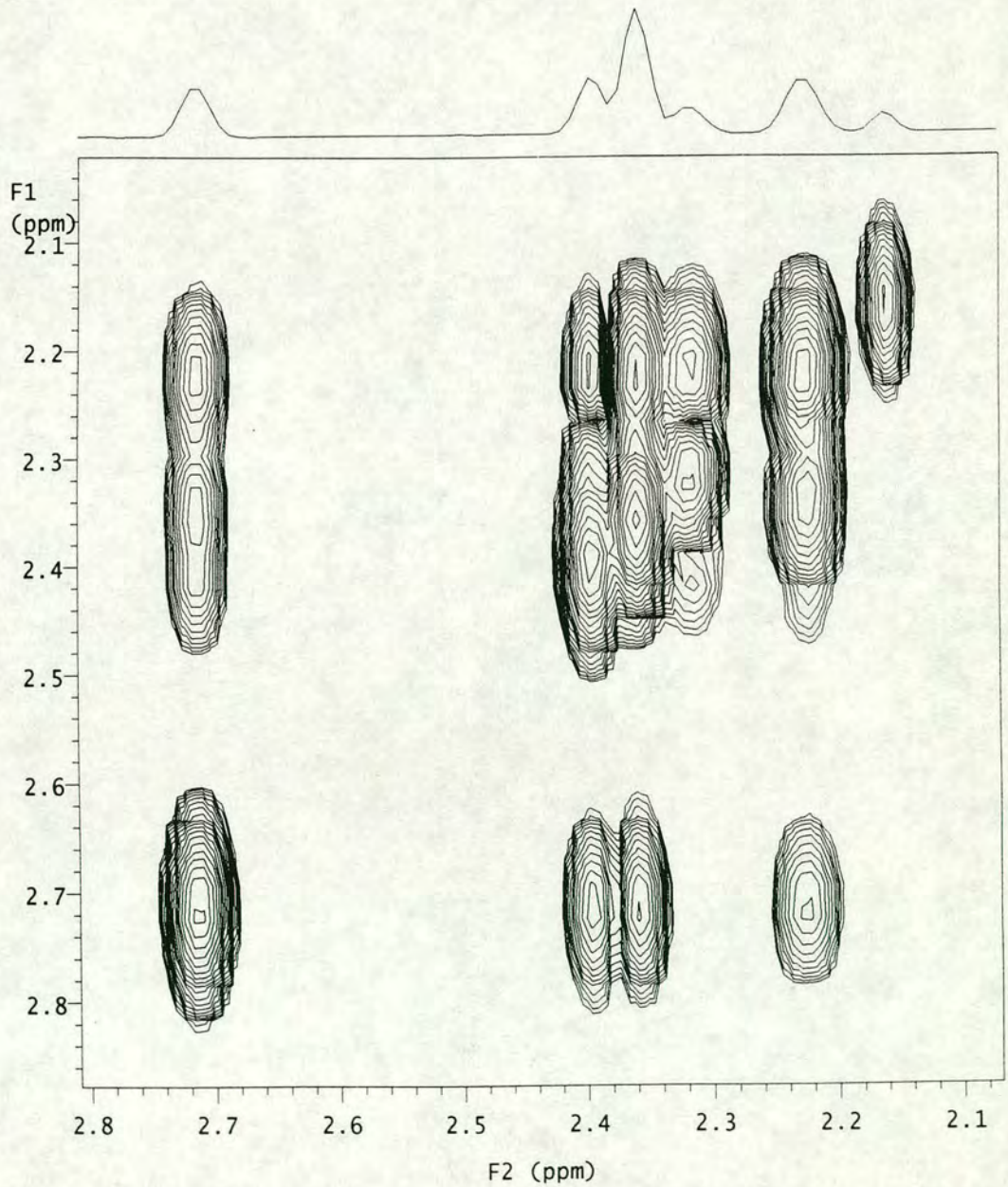

Crystallographic Study of 1

It has been demonstrated [89, 99] that unusual polyhedral structures and unusually facile polyhedral isomerisations can result as a consequence of intramolecular crowding in carbametallaboranes. These findings prompted a study of the stereochemical consequences of systematically varying the amount of crowding within a homologous series of heteroboranes. The molecular structures of a series of *closo* carbaboranes 1-Ph-2-R-1,2-$C_2B_{10}H_{10}$ in which the steric demand of the changing group R is gradually increased have been studied and are considered herein. In the present case, the R = Me species is examined as a relatively "uncrowded" member of this series.

Colourless *plates* of diffraction quality were obtained by slow diffusion of water into a methanolic solution of **1** at 4ºC.

Data were collected at ambient temperature and the structure was solved by direct methods [112] for C and B atoms, and by difference Fourier synthesis [113] for phenyl H atoms; H atoms bound to the cage, and those in the methyl group, were set in idealised positions. All non-H atoms were allowed anisotropic thermal refinement. Both C and H atoms of the phenyl substituent were allowed positional refinement in an attempt to detect any distortion in this moiety which might arise from close intramolecular approaches. In the event, no such effect was noted.

Four molecules of **1** crystallise in the monoclinic space group $P2_1/n$ with no crystallographically imposed symmetry and with no close intermolecular contacts in the crystal lattice.

A perspective view of a single molecule of **1**, and the numbering scheme employed, are shown in figure 2.4. (For consistency in this structure and the following ones, the C_{cage} atom bearing the phenyl group has been labelled **C(1)**; the phenyl ring is numbered cyclically.) Selected interatomic distances and interbond angles are detailed in table 2.1.

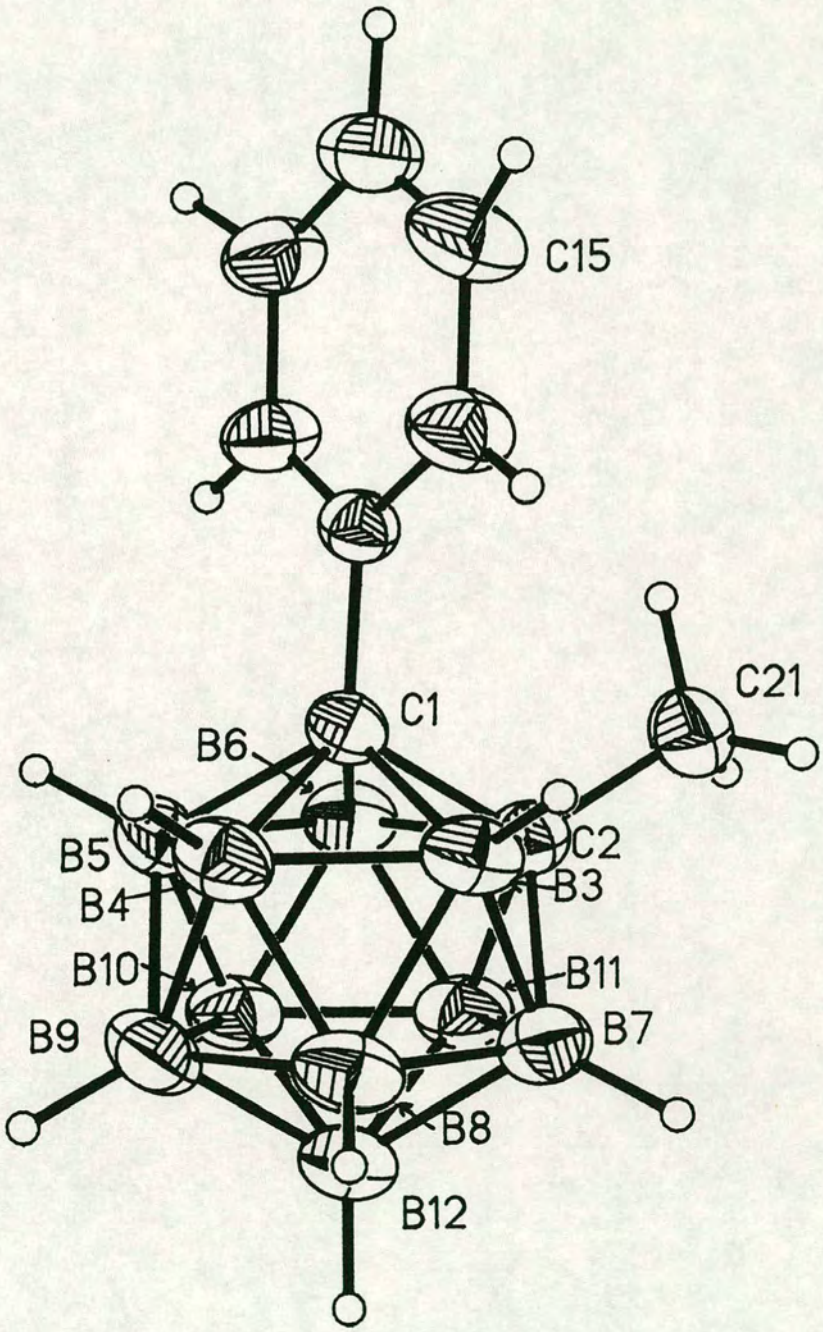

Figure 2.4 Perspective view of **1**
(50% thermal ellipsoids; H atoms have radii of 0.1Å for clarity)

Table 2.1 Selected interatomic distances (Å) and interbond angles (°) in **1**

C(1) - C(2)	1.696(5)	B(5) -B(10)	1.752(7)
C(1) - B(3)	1.715(6)	B(6) -B(10)	1.747(6)
C(1) - B(4)	1.700(6)	B(6) -B(11)	1.762(7)
C(1) - B(5)	1.720(6)	B(7) -B(8)	1.787(7)
C(1) - B(6)	1.732(6)	B(7) -B(11)	1.771(7)
C(1) -C(11)	1.514(5)	B(7) -B(12)	1.788(7)
C(2) - B(3)	1.713(6)	B(8) - B(9)	1.764(7)
C(2) - B(6)	1.710(6)	B(8) -B(12)	1.784(7)
C(2) - B(7)	1.703(6)	B(9) -B(10)	1.789(7)
C(2) -B(11)	1.704(6)	B(9) -B(12)	1.759(7)
C(2) -C(21)	1.518(6)	B(10) -B(11)	1.766(7)
B(3) - B(4)	1.769(6)	B(10) -B(12)	1.785(7)
B(3) - B(7)	1.771(7)	B(11) -B(12)	1.779(7)
B(3) - B(8)	1.776(7)	C(11) -C(12)	1.377(5)
B(4) - B(5)	1.775(7)	C(11) -C(16)	1.388(6)
B(4) - B(8)	1.773(7)	C(12) -C(13)	1.381(6)
B(4) - B(9)	1.762(7)	C(13) -C(14)	1.388(7)
B(5) - B(6)	1.770(6)	C(14) -C(15)	1.373(7)
B(5) - B(9)	1.775(7)	C(15) -C(16)	1.389(7)

C(2) - C(1) - B(3)	60.29(22)	B(10)-B(6) -B(11)	60.5(3)
C(2) - C(1) - B(6)	59.86(22)	C(2) - B(7) - B(3)	59.06(25)
C(2) - C(1) -C(11)	119.0(3)	C(2) - B(7) -B(11)	58.7(3)
B(3) - C(1) - B(4)	62.38(25)	B(3) - B(7) - B(8)	59.9(3)
B(3) - C(1) -C(11)	119.3(3)	B(8) - B(7) -B(12)	59.9(3)
B(4) - C(1) - B(5)	62.55(25)	B(11)-B(7) -B(12)	60.0(3)
B(4) - C(1) -C(11)	122.7(3)	B(3) - B(8) - B(4)	59.8(3)
B(5) - C(1) - B(6)	61.71(24)	B(3) - B(8) - B(7)	59.6(3)
B(5) - C(1) -C(11)	120.9(3)	B(4) - B(8) - B(9)	59.8(3)
B(6) - C(1) -C(11)	116.8(3)	B(7) - B(8) -B(12)	60.1(3)
C(1) - C(2) - B(3)	60.40(22)	B(9) - B(8) -B(12)	59.4(3)
C(1) - C(2) - B(6)	61.10(23)	B(4) - B(9) - B(5)	60.3(3)
C(1) - C(2) -C(21)	118.3(3)	B(4) - B(9) - B(8)	60.4(3)
B(3) - C(2) - B(7)	62.4(3)	B(5) - B(9) -B(10)	58.9(3)
B(3) - C(2) -C(21)	118.5(3)	B(8) - B(9) -B(12)	60.9(3)
B(6) - C(2) -B(11)	62.1(3)	B(10)-B(9) -B(12)	60.4(3)
B(6) - C(2) -C(21)	116.7(3)	B(5) - B(10) - B(6)	60.8(3)
B(7) - C(2) -B(11)	62.6(3)	B(5) - B(10) - B(9)	60.1(3)
B(7) - C(2) -C(21)	121.7(3)	B(6) - B(10) -B(11)	60.2(3)
C(11)- C(2) -C(21)	120.8(3)	B(9) - B(10) -B(12)	59.0(3)
C(1) - B(3) - C(2)	59.31(22)	B(11)-B(10) -B(12)	60.1(3)
C(1) - B(3) - B(4)	58.40(23)	C(2) - B(11) - B(6)	59.12(25)
C(2) - B(3) - B(7)	58.50(25)	C(2) - B(11) - B(7)	58.6(3)

B(4) - B(3) - B(8)	60.0(3)	B(6) - B(11) -B(10)	59.3(3)
B(7) - B(3) - B(8)	60.5(3)	B(7) - B(11) -B(12)	60.5(3)
C(1) - B(4) - B(3)	59.22(24)	B(10)-B(11) -B(12)	60.5(3)
C(1) - B(4) - B(5)	59.26(24)	B(7) - B(12) - B(8)	60.0(3)
B(3) - B(4) - B(8)	60.2(3)	B(7) - B(12) -B(11)	59.5(3)
B(5) - B(4) - B(9)	60.2(3)	B(8) - B(12) - B(9)	59.7(3)
B(8) - B(4) - B(9)	59.8(3)	B(9) - B(12) -B(10)	60.6(3)
C(1) - B(5) - B(4)	58.19(24)	B(10)-B(12) -B(11)	59.4(3)
C(1) - B(5) - B(6)	59.48(24)	C(1) - C(11) -C(12)	119.8(3)
B(4) - B(5) - B(9)	59.5(3)	C(1) - C(11) -C(16)	121.2(3)
B(6) - B(5) -B(10)	59.4(3)	C(12)-C(11) -C(16)	119.0(4)
B(9) - B(5) -B(10)	61.0(3)	C(11)-C(12) -C(13)	120.9(4)
C(1) - B(6) - C(2)	59.04(22)	C(12)-C(13) -C(14)	120.1(4)
C(1) - B(6) - B(5)	58.81(23)	C(13)-C(14) -C(15)	119.1(4)
C(2) - B(6) -B(11)	58.77(25)	C(14)-C(15) -C(16)	120.8(5)
B(5) - B(6) -B(10)	59.8(3)	C(11)-C(16) -C(15)	120.0(4)

The orientation of a carbaborane-bound phenyl group has been discussed **[54]** in terms of the angle θ describing the conformation of the ring relative to the $C_{cage}\cdots C_{cage}$ connectivity. (θ is defined simply **[55]** as the modulus of the average of the two [C_{cage}-C_{cage}-C-C] torsion angles about the C_{cage}—C_{phenyl} bond.) E.H.M.O. studies indicate that the electronically-preferred orientation is that where the ring eclipses this C—C connectivity, that is where θ = 90°. This is supported by the results of *ab initio* calculations **[53]**, which similarly predict a preference for large θ values, giving a position of minimum energy at around θ = 65°. (Intramolecular interactions between the β-H atoms of the phenyl ring and those H atoms bound to the adjacent B_{cage} and C_{cage} atoms are thought to limit the freedom of the phenyl group to further twist towards a higher θ value.) Clearly the presence, as here, of a *C*-substituent bound adjacent to the phenyl moiety prohibits attainment of this *ideal* orientation. Although a twist of the aryl group away from the θ = 90° situation is energetically relatively inexpensive, smaller values of θ are believed **[54]** to contribute electronically to a lengthening of the $C_{cage}\cdots C_{cage}$ distance.

In the case of **1**, the introduction of a cage-bound methyl group results in θ = 16.7°. As a consequence of this phenyl twist, C(1)-C(2) is 1.696(5)Å, significantly longer than in the unsubstituted 1-Ph-1,2-*closo*-$C_2B_{10}H_{11}$ **[53]**, where θ = 68.8° and C(1)-C(2) = 1.646(8)Å for the crystallographically ordered molecule in the asymmetric fraction of the unit cell. Despite the

manifest influence of the pendant methyl group upon the conformation of the phenyl substituent there is, in the structure adopted, no significant intramolecular contact between the two. Thus, analysis of the C(11)-C(1)-X and the C(21)-C(2)-Y angles reveals no mutual bendback of the exopolyhedral groups; nor is there a measurable twist of phenyl and methyl substituents about the C(1)-C(2) vector. [The C(11)-C(1)-C(2)-C(21) torsion angle is 0.6(5)°.]

Species of the type 1-Ph-2-R-1,2-*closo*-$C_2B_{10}H_{10}$ (where R ≠ H) are likely to demonstrate similar structures with θ close to zero. Therefore, in systematically varying R and monitoring any resulting effect upon cage geometry, it is desirable to chose as a reference structure one in which θ is roughly zero and the group R is relatively undemanding sterically. Given the comparatively large θ value observed in **1**, it was decided that although this compound is almost ideal in many respects, a species with a smaller value of θ should be sought. Compound **2**, 1-Ph-2-Br-1,2-*closo*-$C_2B_{10}H_{10}$ was considered for this purpose.

[Further, detailed analysis of the cage geometry of **1**, and comparison with other phenylcarbaboranes, is discussed later in this chapter.]

Synthesis and Characterisation of 1-Ph-2-Br-1,2-*closo*-$C_2B_{10}H_{10}$, 2. Reaction with MeLi

The synthesis of **2** was by a variation of the published method **[38]**. The interaction of the *C*-lithium salt of 1-Ph-1,2-*closo*-$C_2B_{10}H_{11}$ with Br_2 in benzene proceeds at room temperature, evidenced by the rapid production of insoluble LiBr. Evaporation of the reaction mixture, extraction of the residue with dichloromethane, and recrystallisation of the evaporated extract from methanol, gives **2** in good yield.

Microanalytical data, and both infrared and n.m.r. spectra, confirmed the identity of the product. Compound **2** has C_s molecular symmetry, consistent with which is the 1:1:2:2:2:2 pattern of resonances observed in the $^{11}B\{^1H\}$ n.m.r. spectrum. The high frequency shift of these resonances, compared to those obtained for 1-Ph-1,2-*closo*-$C_2B_{10}H_{11}$ **[114]** and 1-Ph-2-Me-1,2-*closo*-$C_2B_{10}H_{10}$ are appropriate to the replacement of H or Me by the electronegative Br atom.

When a benzene solution of **2** is treated with methyllithium, a white, insoluble material (thought to be LiBr) is deposited. Analysis of the filtered and evaporated reaction mixture by proton n.m.r. revealed the principal component to be **1**; that is, the C_{cage}-bound bromine atom is displaced by the methyl group, with concomitant formation of lithium bromide. This has important implications as a possible synthetic route to *C*-substituted carbaboranes, and will be returned to later.

Crystallographic Study of 2

The crystallographic study of **1** described earlier was intended to establish a reference structure for a series of 1-Ph-2-R-1,2-*closo*-$C_2B_{10}H_{10}$ compounds with gradually more sterically demanding substituents R. As has been noted above, the length of the C_{cage}—C_{cage} connectivity in species of this type is sensitive to θ, the twist angle of the phenyl group. With this in mind, it was hoped to characterise structurally a series of compounds with differing groups R and θ roughly zero: a measure of the influence of changing R alone was thereby sought. However, in **1** (R = Me) θ was found to be 16.7°, somewhat larger than ideally desired. Accordingly, the molecular structure of another, relatively uncrowded member of this series, namely 1-Ph-2-Br-1,2-*closo*-$C_2B_{10}H_{10}$, **2**, was determined. Since the van der Waals radii of Me and Br are both around 2.0Å, and given that C-Br is expected to be longer than C-Me, compound **2** could in principle be taken as somewhat less crowded than **1**.

Poor quality, colourless *plates* of **2** may be grown by slow diffusion of water into a methanolic solution at 4ºC. However, far superior colourless *blocks* suitable for analysis *via* a single crystal *X*-ray diffraction study were obtained by slow evaporation and cooling of a warm, concentrated methanol solution of **2**.

The intensities of diffracted *X*-radiation over one octant were measured at ambient temperatures. Inspection of a Patterson map **[113]** revealed the location of the Br atom; the remaining non-H atoms and cage H atoms were found by difference Fourier syntheses **[113]**. Phenyl H atoms were set in idealised positions and the aryl ring constrained to be a regular hexagon. H atoms bound directly to the cage were allowed positional refinement subject to a common B-H distance; all non-H atoms were refined anisotropically.

Eight molecules of **2** crystallise in the orthorhombic space group *Pbca*, with no close approaches between molecules.

A perspective view of a single molecule of **2** and the numbering scheme employed are shown in figure 2.5. (For consistency, the C_{cage} atom bearing the phenyl moiety has again been labelled **C(1)**; the phenyl ring is numbered

cyclically.) In table 2.2 are tabulated selected interatomic distances and interbond angles.

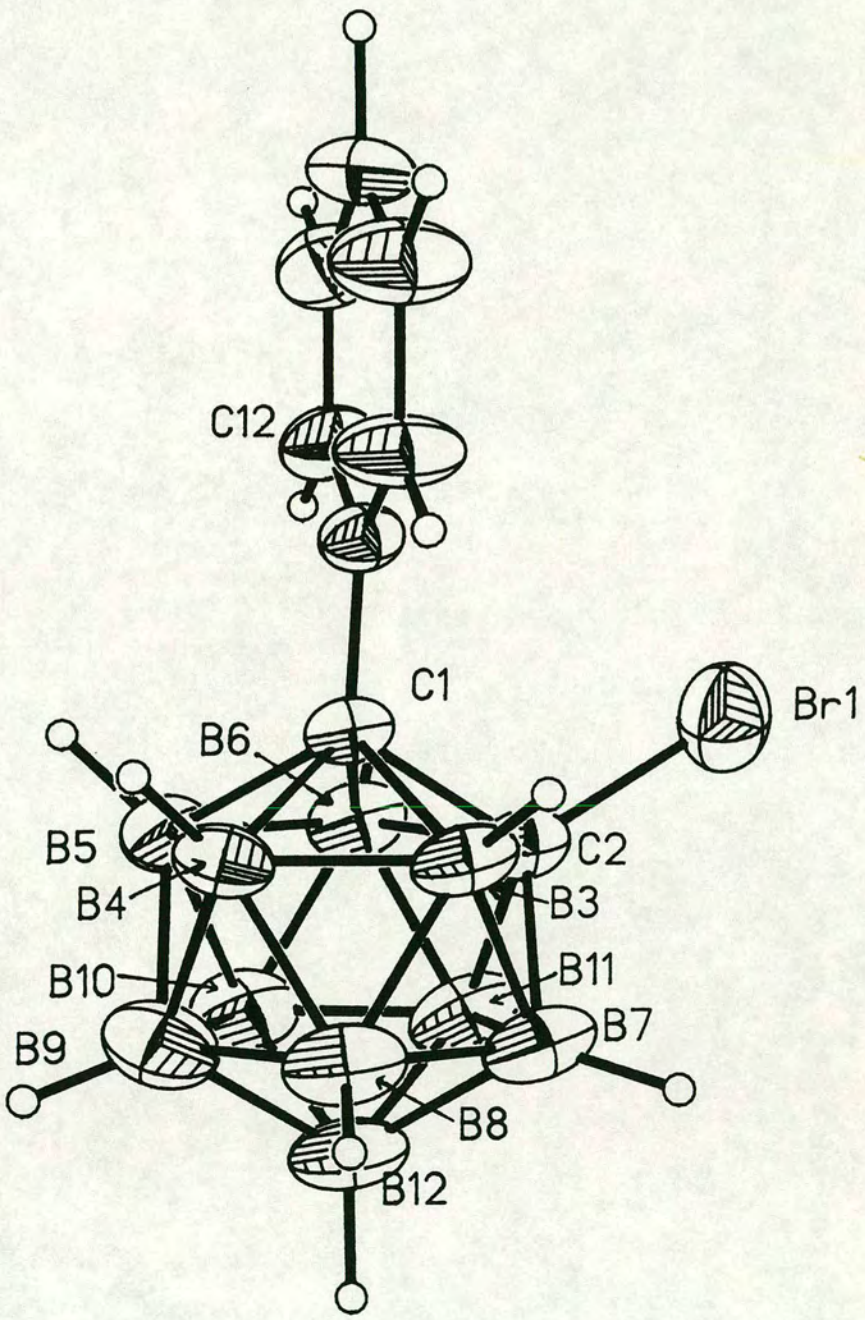

Figure 2.5 Perspective view of **2**
(50% thermal ellipsoids; H atoms have radii of 0.1Å for clarity)

Table 2.2 Selected interatomic distances (Å) and interbond angles (°) in **2**

Br(1) - C(2)	1.888(6)	B(4) - B(9)	1.758(12)
C(1) - C(2)	1.692(8)	B(5) - B(6)	1.764(10)
C(1) - B(3)	1.735(9)	B(5) - B(9)	1.780(12)
C(1) - B(4)	1.728(9)	B(5) -B(10)	1.773(11)
C(1) - B(5)	1.714(9)	B(6) -B(10)	1.755(11)
C(1) - B(6)	1.737(9)	B(6) -B(11)	1.780(11)
C(1) -C(11)	1.494(7)	B(7) - B(8)	1.770(12)
C(2) - B(3)	1.701(9)	B(7) -B(11)	1.804(12)
C(2) - B(6)	1.721(9)	B(7) -B(12)	1.790(12)
C(2) - B(7)	1.693(10)	B(8) - B(9)	1.772(12)
C(2) -B(11)	1.725(10)	B(8) -B(12)	1.800(12)
B(3) - B(4)	1.763(11)	B(9) -B(10)	1.766(12)
B(3) - B(7)	1.769(11)	B(9) -B(12)	1.744(13)
B(3) - B(8)	1.735(11)	B(10) -B(11)	1.741(12)
B(4) - B(5)	1.792(11)	B(10) -B(12)	1.755(12)
B(4) - B(8)	1.755(11)	B(11) -B(12)	1.755(12)

C(2) - C(1) - B(3)	59.5(4)	C(1) - B(6) - B(5)	58.6(4)
C(2) - C(1) - B(6)	60.3(4)	C(2) - B(6) -B(11)	59.0(4)
C(2) - C(1) -C(11)	121.1(4)	B(5) - B(6) -B(10)	60.5(4)
B(3) - C(1) - B(4)	61.2(4)	B(10) - B(6) -B(11)	59.0(5)
B(3) - C(1) -C(11)	118.0(4)	C(2) - B(7) - B(3)	58.8(4)
B(4) - C(1) - B(5)	62.8(4)	C(2) - B(7) -B(11)	59.0(4)
B(4) - C(1) -C(11)	120.9(4)	B(3) - B(7) - B(8)	58.7(4)
B(5) - C(1) - B(6)	61.5(4)	B(8) - B(7) -B(12)	60.7(5)
B(5) - C(1) -C(11)	121.7(4)	B(11) - B(7) -B(12)	58.5(5)
B(6) - C(1) -C(11)	119.5(4)	B(3) - B(8) - B(4)	60.7(4)
Br(1) - C(2) - C(1)	116.7(4)	B(3) - B(8) - B(7)	60.6(5)
Br(1) - C(2) - B(3)	117.7(4)	B(4) - B(8) - B(9)	59.8(5)
Br(1) - C(2) - B(6)	115.9(4)	B(7) - B(8) -B(12)	60.2(5)
Br(1) - C(2) - B(7)	120.8(4)	B(9) - B(8) -B(12)	58.4(5)
Br(1) - C(2) -B(11)	120.5(4)	B(4) - B(9) - B(5)	60.9(5)
C(1) - C(2) - B(3)	61.5(4)	B(4) - B(9) - B(8)	59.6(5)
C(1) - C(2) - B(6)	61.2(4)	B(5) - B(9) -B(10)	60.0(5)
B(3) - C(2) - B(7)	62.8(4)	B(8) - B(9) -B(12)	61.6(5)
B(6) - C(2) -B(11)	62.2(4)	B(10) - B(9) -B(12)	60.0(5)
B(7) - C(2) -B(11)	63.7(4)	B(5) -B(10) - B(6)	60.0(4)
C(1) - B(3) - C(2)	59.0(4)	B(5) -B(10) - B(9)	60.4(5)
C(1) - B(3) - B(4)	59.2(4)	B(6) -B(10) -B(11)	61.2(5)
C(2) - B(3) - B(7)	58.4(4)	B(9) -B(10) -B(12)	59.4(5)
B(4) - B(3) - B(8)	60.2(4)	B(11) -B(10) -B(12)	60.3(5)
B(7) - B(3) - B(8)	60.7(5)	C(2) -B(11) - B(6)	58.8(4)

C(1) - B(4) - B(3)	59.6(4)	C(2) -B(11) - B(7)	57.3(4)
C(1) - B(4) - B(5)	58.2(4)	B(6) -B(11) -B(10)	59.8(5)
B(3) - B(4) - B(8)	59.1(4)	B(7) -B(11) -B(12)	60.4(5)
B(5) - B(4) - B(9)	60.2(4)	B(10) -B(11) -B(12)	60.3(5)
B(8) - B(4) - B(9)	60.6(5)	B(7) -B(12) - B(8)	59.1(5)
C(1) - B(5) - B(4)	59.0(4)	B(7) -B(12) -B(11)	61.2(5)
C(1) - B(5) - B(6)	59.9(4)	B(8) -B(12) - B(9)	60.0(5)
B(4) - B(5) - B(9)	59.0(4)	B(9) -B(12) -B(10)	60.6(5)
B(6) - B(5) -B(10)	59.5(4)	B(10) -B(12) -B(11)	59.5(5)
B(9) - B(5) -B(10)	59.6(5)	C(1) -C(11) -C(12)	119.8(4)
C(1) - B(6) - C(2)	58.6(4)	C(1) -C(11) -C(16)	120.1(4)

In **2**, the C(1)-C(11) distance is 1.494(7)Å, some 0.020(9)Å shorter than in **1**. However, C(1)-C(2) in **2** is 1.692(8)Å, identical to that observed in the 2-Me analogue; the C(2)-Br(1) distance is effectively the same as that between C(2) and C(21) in **1** when the difference in covalent radii between an sp^3-C atom and a Br atom is taken into account **[115]**.

The measured value of θ in **2** is only 2.2°; that is, the plane of the phenyl group lies essentially perpendicular to the non-crystallographic mirror plane which bisects the molecule. As was the case for **1**, there is no significant twist about C(1)-C(2): the torsion angle C(11)-C(1)-C(2)-Br(1) is only 2.2(6)°. Although the five angles C(11)-C(1)-X do not much internally vary - they lie in the range 118.0(4) to 121.7(4)° - there is some evidence for greater asymmetry in the Br(1)-C(2)-Y angles: those to B(3), C(1) and B(6), average 116.8(6)°, being significantly narrower than those to B(7) and B(11), average 120.7(6)°. Such an effect, although small, could perhaps be taken as evidence of a weak intramolecular interaction between the bromine atom and the β-phenyl group. [A similar, small deformation is apparent in both crystallographically-independent molecules of 1,1-dibromo-2-phenyl-2-(2'-propenyl)cyclopropane **[116]**.] It is possible that such an interaction could contribute to the very small value of θ observed in the molecular structure of **2**.

This study, along with that of **1**, affords reference 1-Ph-2-R-1,2-*closo*-$C_2B_{10}H_{10}$ structures against which more crowded analogues may be compared; the low θ value in **2** makes it particularly well suited for this purpose. These more detailed structural analyses (in particular of cage geometry) are the subject of a later part of this chapter.

Synthesis and Characterisation of 1-Ph-2-Me_3Si-1,2-*closo*-$C_2B_{10}H_{10}$, 3

The compound 1-Ph-2-Me_3Si-1,2-*closo*-$C_2B_{10}H_{10}$, **3**, is formed in good yield (≥90%) by an improvement upon the published synthesis **[117]**. Reaction of the *C*-lithio derivative of phenylcarbaborane with Me_3SiCl in benzene proceeds smoothly, and yields on work-up an essentially pure product. An alternative preparation of this compound has been reported **[48]** which relies upon the formation of a *C*-LnI (Ln = lanthanide) derivative of phenyl carbaborane and interaction of this with Me_3SiCl, to give **3** in reported yields similar to the present route. Further consideration of these routes was not made since that *via* the *C*-lithium salt is simpler and as effective.

Compound **3** was identified and characterised by standard techniques of microanalysis, and infrared and multinuclear n.m.r. spectroscopies. The $^{11}B\{^1H\}$ spectrum is not fully dispersed, showing one coincidence, but is nevertheless consistent with the anticipated C_s molecular symmetry of the species. In the ^1H n.m.r. spectrum, both the ^{29}Si and the ^{13}C satellites at the resonance corresponding to the trimethylsilyl group could be distinguished and hence $^1J_{^{13}CH}$ and $^2J_{^{29}SiH}$ could be approximately determined.

Crystallographic Study of 3

Compounds **1** and **2** were examined as potential reference members of a series of compounds 1-Ph-2-R-1,2-*closo*-$C_2B_{10}H_{10}$ with the group R varying in steric demand, in the anticipation that the exopolyhedral Me or Br substituent would afford relatively little Ph···X congestion, whilst establishing a common reference orientation for the phenyl substituent. In the light of these studies, **2** was chosen as the more suitable reference point for this series. The structure of the 2-Me_3Si analogue, **3**, which is liable to intramolecular crowding of greater significance, is now described.

Slow diffusion of water into a methanolic solution of **3** at 4°C yielded colourless *plates* suitable for a single crystal *X*-ray diffraction study.

One hemisphere of diffraction data was collected at ambient temperatures. Compound **3** was found to crystallise ($Z = 2$) in the monoclinic space group $P2_1/m$, with crystallographically-imposed C_s symmetry. Each molecule lies on a mirror plane through atoms C(1), C(2), B(9) and B(12). All non-H atoms were located by automated direct methods **[112]**, and were ultimately refined anisotropically. Methyl and phenyl H atoms, and those cage H atoms lying on the crystallographic mirror plane were set in idealised positions; the remaining cage H atoms were allowed positional refinement subject to a common B-H distance. No close intermolecular approaches within the crystal lattice were detected.

Figure 2.6 shows a perspective view of a single whole molecule of **3**, and the atomic numbering scheme adopted. (As before, the numbering in the asymmetric fraction was chosen so as to be consistent with that in related species discussed herein. Mirror image atoms are suffixed A.) Table 2.3 lists selected internuclear distances and interbond angles, and includes some bonds and angles lying across the mirror plane.

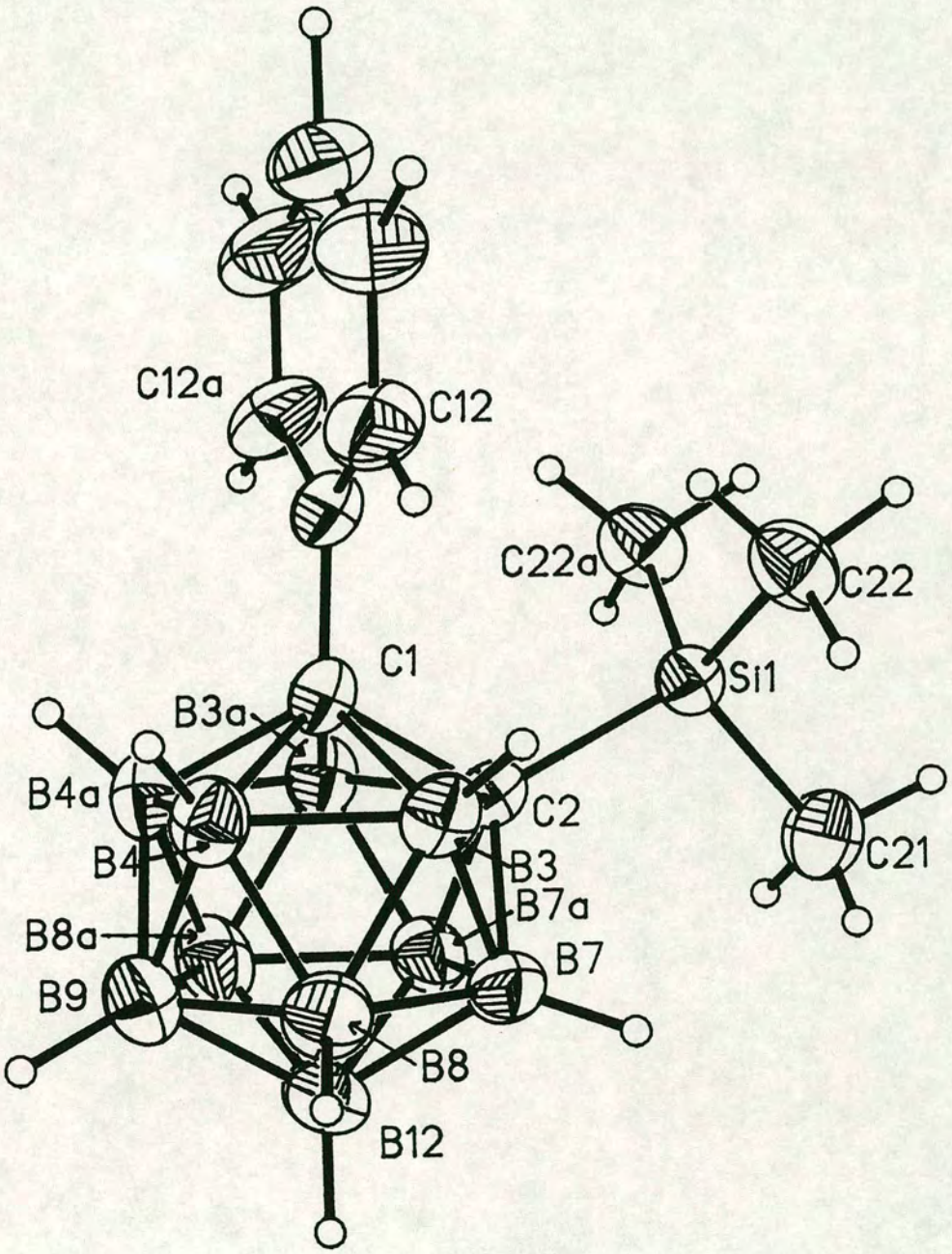

Figure 2.6 Perspective view of **3**
(50% thermal ellipsoids; H atoms have radii of 0.1Å for clarity.
Symmetry equivalent atoms. A: *x*, ½-*y*, *z*)

Table 2.3 Selected interatomic distances (Å) and interbond angles (°) in **3**

C(1) - C(2)	1.708(4)	B(4) -B(4A)	1.772(5)
C(1) - B(3)	1.717(4)	B(7) - B(8)	1.774(5)
C(1) - B(4)	1.711(4)	B(7) -B(12)	1.773(5)
C(1) -C(11)	1.511(4)	B(7) -B(7A)	1.776(5)
C(2) - B(3)	1.728(4)	B(8) - B(9)	1.780(6)
C(2) - B(7)	1.714(4)	B(8) -B(12)	1.784(5)
C(2) -Si(1)	1.931(3)	B(9) -B(12)	1.776(6)
B(3) - B(4)	1.773(5)	C(11) -C(12)	1.389(4)
B(3) - B(7)	1.764(4)	C(12) -C(13)	1.377(5)
B(3) - B(8)	1.766(5)	C(13) -C(14)	1.376(6)
B(4) - B(8)	1.769(5)	Si(1) -C(21)	1.851(4)
B(4) - B(9)	1.781(5)	Si(1) -C(22)	1.855(3)

C(2) - C(1) - B(3)	60.60(17)	B(3) - B(7) - B(8)	59.88(19)
C(2) - C(1) -C(11)	120.05(23)	B(8) - B(7) -B(12)	60.40(21)
B(3) - C(1) - B(4)	62.29(18)	B(12) - B(7) -B(7A)	59.94(20)
B(3) - C(1) -C(11)	118.51(23)	B(3) - B(8) - B(4)	60.22(19)
B(4) - C(1) -C(11)	119.90(24)	B(3) - B(8) - B(7)	59.80(19)
B(4) - C(1) -B(4A)	62.37(19)	B(4) - B(8) - B(9)	60.24(21)
C(1) - C(2) - B(3)	59.97(17)	B(7) - B(8) -B(12)	59.76(20)
C(1) - C(2) -Si(1)	122.89(18)	B(9) - B(8) -B(12)	59.78(22)
B(3) - C(2) - B(7)	61.68(18)	B(4) - B(9) - B(8)	59.56(21)
B(3) - C(2) -Si(1)	119.67(18)	B(4) - B(9) -B(4A)	59.66(20)
B(7) - C(2) -Si(1)	119.20(19)	B(8) - B(9) -B(12)	60.21(22)
B(7) - C(2) -B(7A)	62.41(18)	B(7) -B(12) - B(8)	59.83(20)
C(1) - B(3) - C(2)	59.43(17)	B(7) -B(12) -B(7A)	60.12(20)
C(1) - B(3) - B(4)	58.68(18)	B(8) -B(12) - B(9)	60.00(22)
C(2) - B(3) - B(7)	58.75(17)	C(1) -C(11) -C(12)	120.6(3)
B(4) - B(3) - B(8)	59.97(19)	C(12) -C(11) -C(12A)	118.6(3)
B(7) - B(3) - B(8)	60.32(19)	C(11) -C(12) -C(13)	120.3(3)
C(1) - B(4) - B(3)	59.03(18)	C(12) -C(13) -C(14)	120.8(4)
C(1) - B(4) -B(4A)	58.82(18)	C(13) -C(14) -C(13A)	119.2(4)
B(3) - B(4) - B(8)	59.81(19)	C(2) -Si(1) -C(21)	105.51(14)
B(8) - B(4) - B(9)	60.19(21)	C(2) -Si(1) -C(22)	110.02(13)
B(9) - B(4) -B(4A)	60.17(20)	C(21) -Si(1) -C(22)	110.50(15)
C(2) - B(7) - B(3)	59.57(17)	C(22) -Si(1) -C(22A)	110.19(14)
C(2) - B(7) -B(7A)	58.79(17)		

Symmetry equivalent atoms A: x, ½-y, z

As a direct consequence of the constraint imposed by crystallographic mirror symmetry, any molecular distortion in **3** which relieves steric congestion must clearly maintain this symmetry. Thus both the angle θ and the torsion angle C(11)-C(1)-C(2)-Si(1), must be exactly zero, and hence no relief from crowding may here be achieved by a mutual twisting away of substituents *via* a combination of these modes.

In **3** the C(1)-C(11) distance is 1.511(4)Å, essentially the same as in the 2-Me analogue (**1**) [1.514(4)Å], but 0.017(8)Å longer than in the corresponding 2-Br species (**2**) [1.494(8)Å]. However, the C(1)-C(2) connectivity in **3**, at 1.708(4)Å, is only slightly longer than the corresponding distance in these less crowded relatives [1.696(5) and 1.692(8)Å respectively]. Although this latter minor elongation may perhaps be attributed in part to the predicted weakening of the C_{cage}—C_{cage} bond which is associated with this "lowest-possible" θ value, it is nevertheless surprising that replacement of Me or Br by $SiMe_3$ apparently causes such a small change in C(1)-C(2). Closer examination of the structure of **3** affords a rationalisation of this anomaly: both cluster substituents bend measurably away from each other, thus minimising their reciprocal steric congestion.

The phenyl ring is essentially planar (deviation < 0.02Å). However, the angles at C(11) do not sum to 360°, with the aryl ring bending away from Si(1) by some 3.6(3)°. Although small, this bend back angle is greater than that in either **1** [1.0(3)°] or **2** [2.7(5)°]. Moreover, there is a concomitant bending back of the $SiMe_3$ group, which apparently takes two forms. Firstly, bend back at silicon, since C(22)-Si(1)-C(2) is greater than C(21)-Si(1)-C(2) by *ca.* 5°; and secondly, bend back at C(2), since the largest Si(1)-C(2)-X angle is that to C(1).

Such bending-back mechanisms are not without precedent. In the uncrowded 1-Me_3Si-1,2-*closo*-$C_2B_{10}H_{11}$ **[118]** there is no deformation of the $SiMe_3$ group and an actual *bend forward* of this whole group towards the other cage carbon atom; whereas in the more congested relative 1-Me-2-Me_3Si-1,2-*closo*-$C_2B_{10}H_{10}$ **[119]** the trimethylsilyl group behaves in a manner similar to that observed in **3**, albeit to a slightly lesser extent.

This structural study of **3** has revealed further possible modes by which *C*-substituted 1-phenyl-*closo*-1,2-carbaboranes may accommodate steric overcrowding; namely, bending back of exopolyhedral substituents and internal distortions of these substituents. These are in addition to previously-recognised modes, principally lengthening of the $C_{cage}\cdots C_{cage}$ connectivity, and twist of the phenyl group. These phenomena will be further addressed in the structural characterisation of **4** below; and a more detailed analysis and comparison of carbaborane cage geometries is presented later in this Chapter.

Synthesis and Characterisation of 1-Ph-2-^{t}BuMe$_2$Si-1,2-*closo*-$C_2B_{10}H_{10}$, 4

The new carbaborane, 1-Ph-2-^{t}BuMe$_2$Si-1,2-*closo*-$C_2B_{10}H_{10}$, **4**, was prepared - albeit in poorer yield - by a procedure similar to that which affords the 2-Me$_3$Si analogue, **3**; namely the reaction between the *C*-Li intermediate derived from phenylcarbaborane, and the appropriate trialkylsilyl chloride. It would appear that the considerably more sterically congested nature of the target carbaborane **4** renders necessary the treatment of the starting carbaborane with excess reagents and thermal encouragement of the reaction. In addition, a considerable amount of phenylcarbaborane starting material (identified by microanalysis and comparison of *Rf* value with an authentic sample) may be recovered from the product mixture. Nevertheless, **4** may be isolated in an acceptable yield of somewhat over 30% by chromatographic means: it may be that optimisation may further improve this figure.

The product was characterised initially by crystallographic means (discussed below), following the fortuitous growth of good quality crystals by attempted fractional crystallisation (!). More conventional characterisation was, meanwhile, also obtained: microanalysis, and infrared and ^{1}H and ^{11}B{^{1}H} n.m.r. spectroscopies, confirmed the anticipated product formulation. In particular, the ^{11}B n.m.r. spectrum of **4** shows a pattern of resonances very similar to that obtained for **3**. It is of interest to note, however, that the weighted average boron chemical shift in **4** is -6.53 p.p.m. (*c.f.* -6.97 p.p.m. in **3**) despite the introduction of what is, in principle, formally a better electron-donating silyl substituent in the case of **4**. This latter feature may be a consequence of molecular deformation which arises from the congested nature of this species, and will be returned to later.

Crystallographic Study of 4

Having established reference members (compounds **1** and **2**) of the present series of 2-substituted phenylcarbaboranes, and considered the molecular structure of the modestly congested 2-Me_3Si species, **3**, it was appropriate now to consider the solid-state structure of **4** where intramolecular crowding to a much greater degree is anticipated.

Colourless, single-crystalline *blocks* of diffraction quality were grown by fractional crystallisation of crude **4** *via* slow diffusion of water into a methanolic carbaborane solution.

Diffraction data were collected over one hemisphere at ambient temperatures. Two molecules of **4** crystallise in the triclinic space group *P*bar1, with no crystallographically-imposed symmetry and no close intermolecular contacts. Non-H atoms were located by automated direct methods **[112]**, and cage H atoms were found by inspection of a difference Fourier map **[113]**. Other H atoms were set in idealised positions and the phenyl ring was constrained to be a hexagon. All non-H atoms were allowed anisotropic refinement.

In figure 2.7 is shown a perspective view of a single molecule of **4**, and the atomic numbering scheme adopted. (The numbering scheme has again been chosen so as to be consistent with that in the related carbaboranes discussed herein.) Table 2.4 lists selected internuclear distances and interbond angles.

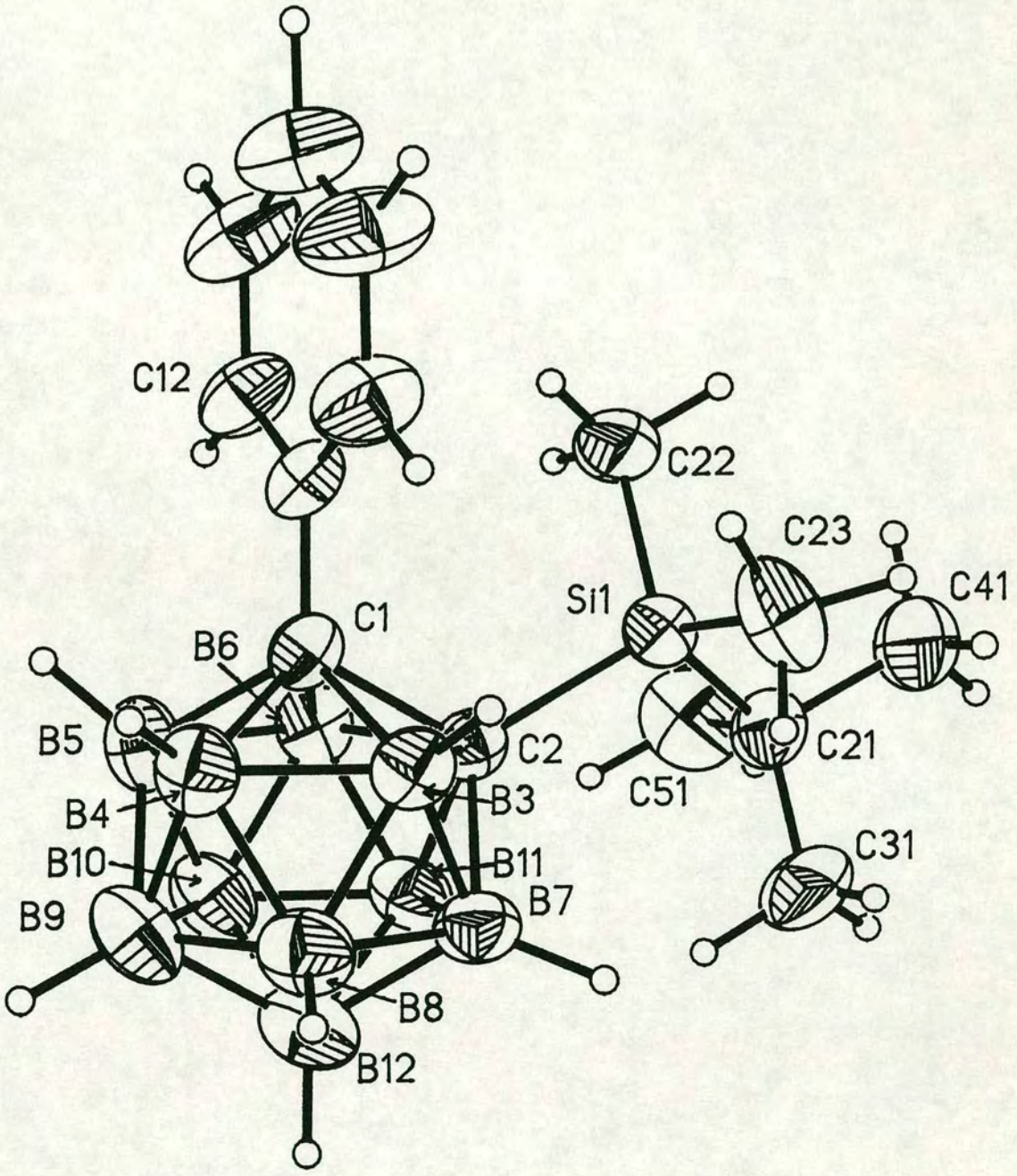

Figure 2.7 Perspective view of **4**
(50% thermal ellipsoids; H atoms have radii of 0.1Å for clarity)

Table 2.4 Selected interatomic distances (Å) and interbond angles (°) in **4**

Si(1) - C(2)	1.948(4)	B(4) - B(9)	1.781(8)
Si(1) -C(21)	1.894(5)	B(5) - B(6)	1.784(7)
Si(1) -C(22)	1.844(5)	B(5) - B(9)	1.771(8)
Si(1) -C(23)	1.864(5)	B(5) -B(10)	1.757(8)
C(1) - C(2)	1.742(5)	B(6) -B(10)	1.764(8)
C(1) - B(3)	1.730(6)	B(6) -B(11)	1.747(7)
C(1) - B(4)	1.709(7)	B(7) - B(8)	1.763(8)
C(1) - B(5)	1.707(7)	B(7) -B(11)	1.755(7)
C(1) - B(6)	1.713(6)	B(7) -B(12)	1.770(8)
C(1) -C(11)	1.494(5)	B(8) - B(9)	1.781(8)
C(2) - B(3)	1.748(6)	B(8) -B(12)	1.773(9)
C(2) - B(6)	1.710(6)	B(9) -B(10)	1.763(8)
C(2) - B(7)	1.716(7)	B(9) -B(12)	1.771(9)
C(2) -B(11)	1.695(7)	B(10) -B(11)	1.745(8)
B(3) - B(4)	1.772(7)	B(10) -B(12)	1.758(9)
B(3) - B(7)	1.756(7)	B(11) -B(12)	1.768(8)
B(3) - B(8)	1.741(8)	C(21) -C(31)	1.525(7)
B(4) - B(5)	1.776(8)	C(21) -C(41)	1.543(7)
B(4) - B(8)	1.763(8)	C(21) -C(51)	1.537(7)

C(2) -Si(1) -C(21)	111.85(19)	C(1) - B(6) - B(5)	58.4(3)
C(2) -Si(1) -C(22)	110.53(20)	C(2) - B(6) -B(11)	58.7(3)
C(2) -Si(1) -C(23)	106.24(20)	B(5) - B(6) -B(10)	59.4(3)
C(21) -Si(1) -C(22)	108.36(22)	B(10) - B(6) -B(11)	59.6(3)
C(21) -Si(1) -C(23)	109.52(22)	C(2) - B(7) - B(3)	60.4(3)
C(22) -Si(1) -C(23)	110.33(23)	C(2) - B(7) -B(11)	58.5(3)
C(2) - C(1) - B(3)	60.46(24)	B(3) - B(7) - B(8)	59.3(3)
C(2) - C(1) - B(6)	59.32(24)	B(8) - B(7) -B(12)	60.2(3)
C(2) - C(1) -C(11)	121.6(3)	B(11) - B(7) -B(12)	60.2(3)
B(3) - C(1) - B(4)	62.0(3)	B(3) - B(8) - B(4)	60.8(3)
B(3) - C(1) -C(11)	119.6(3)	B(3) - B(8) - B(7)	60.1(3)
B(4) - C(1) - B(5)	62.6(3)	B(4) - B(8) - B(9)	60.3(3)
B(4) - C(1) -C(11)	118.7(3)	B(7) - B(8) -B(12)	60.1(3)
B(5) - C(1) - B(6)	62.9(3)	B(9) - B(8) -B(12)	59.8(3)
B(5) - C(1) -C(11)	118.9(3)	B(4) - B(9) - B(5)	60.0(3)
B(6) - C(1) -C(11)	119.3(3)	B(4) - B(9) - B(8)	59.4(3)
Si(1) - C(2) - C(1)	121.01(24)	B(5) - B(9) -B(10)	59.6(3)
Si(1) - C(2) - B(3)	117.5(3)	B(8) - B(9) -B(12)	59.9(3)
Si(1) - C(2) - B(6)	121.4(3)	B(10) - B(9) -B(12)	59.7(3)
Si(1) - C(2) - B(7)	120.2(3)	B(5) -B(10) - B(6)	60.9(3)
Si(1) - C(2) -B(11)	123.5(3)	B(5) -B(10) - B(9)	60.4(3)
C(1) - C(2) - B(3)	59.43(24)	B(6) -B(10) -B(11)	59.7(3)
C(1) - C(2) - B(6)	59.50(24)	B(9) -B(10) -B(12)	60.4(3)

B(3) - C(2) - B(7)	60.9(3)	B(11) -B(10) -B(12)	60.6(3)
B(6) - C(2) -B(11)	61.7(3)	C(2) -B(11) - B(6)	59.5(3)
B(7) - C(2) -B(11)	61.9(3)	C(2) -B(11) - B(7)	59.6(3)
C(1) - B(3) - C(2)	60.11(24)	B(6) -B(11) -B(10)	60.7(3)
C(1) - B(3) - B(4)	58.4(3)	B(7) -B(11) -B(12)	60.3(3)
C(2) - B(3) - B(7)	58.7(3)	B(10) -B(11) -B(12)	60.1(3)
B(4) - B(3) - B(8)	60.3(3)	B(7) -B(12) - B(8)	59.7(3)
B(7) - B(3) - B(8)	60.6(3)	B(7) -B(12) -B(11)	59.5(3)
C(1) - B(4) - B(3)	59.6(3)	B(8) -B(12) - B(9)	60.3(3)
C(1) - B(4) - B(5)	58.6(3)	B(9) -B(12) -B(10)	59.9(3)
B(3) - B(4) - B(8)	59.0(3)	B(10) -B(12) -B(11)	59.3(3)
B(5) - B(4) - B(9)	59.7(3)	C(1) -C(11) -C(12)	119.2(3)
B(8) - B(4) - B(9)	60.3(3)	C(1) -C(11) -C(16)	120.8(3)
C(1) - B(5) - B(4)	58.7(3)	Si(1) -C(21) -C(31)	115.0(3)
C(1) - B(5) - B(6)	58.7(3)	Si(1) -C(21) -C(41)	106.6(3)
B(4) - B(5) - B(9)	60.3(3)	Si(1) -C(21) -C(51)	111.4(3)
B(6) - B(5) -B(10)	59.7(3)	C(31) -C(21) -C(41)	107.6(4)
B(9) - B(5) -B(10)	60.0(3)	C(31) -C(21) -C(51)	109.1(4)
C(1) - B(6) - C(2)	61.17(25)	C(41) -C(21) -C(51)	106.7(4)

The C(1)-C(11) distance in **4** is 1.494(5)Å, the same as in the 2-Br species **2** [1.494(7)Å], but slightly shorter than in the 2-Me [1.514(5)Å] and 2-Me_3Si [1.511(4)Å] relatives (**1** and **3** respectively). There is some asymmetry in the C(11)-C(1)-X angles: the angle C(11)-C(1)-C(2) is 121.6(3)°; whereas the other four angles at C(1) all lie in the range 118.7(3) to 119.6(3)°, demonstrating a bending back of the phenyl group *away* from the silyl moiety. However, in contrast to the situation in **3**, there is no evidence for bend back of the phenyl ring at C(11) in the present compound, evidenced by angles at C(11) which sum to 360° and the fact that C(1) lies within 0.002Å of the plane of the ring (the equivalent displacement in the 2-Me_3Si analogue is 0.044Å). Equally, the trialkylsilyl group in **4** appears not to bend back significantly, and so does not give rise to a wide C(1)-C(2)-Si(1) angle. Instead, the phenyl group is twisted about C(1)-C(11) resulting in $\theta = 7.6°$ [C(16) moving towards the silyl group] and the ^{t}BuMe$_2$Si group appears to bend slightly towards B(3). The torsion angle C(11)-C(1)-C(2)-Si(1) is 2.9(4)°; that is, there is a small but significant mutual twisting away of the two exopolyhedral substituents, about the C(1)—C(2) vector.

In **4** the single most important deformation by which the molecule avoids overcrowding is the *anti* disposition of the ^{t}Bu group of the trialkylsilyl

moiety relative to the cage-bound phenyl substituent. This, however, brings the ^{t}Bu group closer to the carbaborane surface, arguably an equally unfavourable intramolecular approach. A reduction in the extent of this latter movement is afforded by lengthening of the C(1)—C(2) connectivity to 1.742(5)Å, the second longest reported C_{cage}—C_{cage} distance in an aryl 1,2-*closo*-dicarbadodecaborane species with (simple) σ-bound C_{cage} substituents. [In 1,2-[4'-(4''-{$MeCO_2$}-C_6H_4)-C_6H_4-]$_2$-1,2-*closo*-$C_2B_{10}H_{10}$ the C(1)—C(2) separation is 1.747(4)Å **[120]**.] Recent, unpublished work by the author's co-workers **[41]** has revealed numerically even longer C(1)—C(2) distances: in one of the two crystallographically-independent molecules in the asymmetric fraction of the unit cell of 1-Ph-2-[4'-Br-C_6F_4]-1,2-*closo*-$C_2B_{10}H_{10}$, the C(1)—C(2) separation is 1.751(9)Å; whilst in the related 1-^{t}Bu-2-[4'-Br-C_6F_4]- compound C(1)—C(2) is 1.765(8)Å.

Other trialkylsilyl-substituted *closo*-dicarbadodecaboranes **[45, 118, 119]**, and related species in which the carbaborane moiety is part of a disila-, six-membered heterocycle of the type {(cage)—SiX_2—(cage)—SiX_2—} (X = Cl **[121]**, Me **[122]**), have C(1)—C(2) distances in the range 1.660(3) to 1.707(7)Å. The chemically most closely related analogue of **4** is the 2-Me_3Si species, **3**, in which C(1)-C(2) is only 1.708(4)Å. As C(1)-C(2) in **4** is stretched the B(3)···B(6) distance shortens, being 2.830(7)Å compared to 2.847(6), 2.865(10) and 2.848(5)Å in the 2-Me, 2-Br and 2-Me_3Si analogues respectively. This situation resembles that in *pseudocloso*-MC_2B_9 complexes **[87, 89]** and species whose geometries appear to be intermediate between *closo* and *pseudocloso* **[88]**. This observation is worthy of particular note since, as is the case for **4**, both these groups of metallacarbaboranes show an increase in weighted average ^{11}B n.m.r. shifts thought to be associated with the onset of cluster structural deformation. More detailed analysis of the deformation of the cage in the present case is not straightforward, and will constitute part of a later section in this Chapter, where further consideration of this and related structures is presented.

Synthesis and Characterisation of 1-Ph-2-^{i}Pr$_3$Si-1,2-*closo*-$C_2B_{10}H_{10}$, 5

Compound **5** was prepared in a manner analogous to that which afforded **3** and **4**, namely the interaction of the *C*-lithium derivative of phenylcarbaborane with tri-isopropylsilyl chloride. The reaction did not proceed in good yield, and isolation of the product proved difficult. Nevertheless, preliminary microanalytical data and (^{1}H and ^{11}B) n.m.r. evidence do suggest some conversion of the phenylcarbaborane precursor to the desired C(2)-substituted product. Furthermore, the weighted average ^{11}B n.m.r. chemical shift for **5** (-6.32 p.p.m.) is slightly greater than that found for **4** (-6.53 p.p.m.); this fact is consistent with the increase in molecular congestion which is expected for compound **5** relative to compound **4**.

Clearly, this compound represents a further, potentially very crowded, member of the series of 1-Ph-2-R-1,2-*closo*-$C_2B_{10}H_{10}$ species discussed here. However, crystals of a quality suitable for an *X*-ray diffraction structural study could not be obtained: rather inferior *plates* could be obtained by cooling methanolic solutions of **5**, but their extreme fragility on removal from the mother liquor prohibited any information being obtained by this means.

Synthesis and Characterisation of 1-^{t}Bu-1,2-*closo*-$C_2B_{10}H_{11}$, 6, and 1-^{t}Bu-2-Br-1,2-*closo*-$C_2B_{10}H_{10}$, 7. Comments on the Attempted Preparation of 1-Ph-2-^{t}Bu-1,2-*closo*-$C_2B_{10}H_{10}$

Direct insertion of ^{t}BuC≡CH into $B_{10}H_{14}$ in the presence of *N,N'*-dimethylaniline gives **6** in good yield. The product was identified by microanalysis; and by ^{1}H and ^{11}B n.m.r. spectroscopy, which confirmed the presence of the cage-bound ^{t}Bu group and the characteristic C_{cage}-***H*** resonance, and showed ^{11}B resonances typical of a dicarbaborane of this type.

Treatment of **6** with alkyllithium followed by Br_2 yielded, on work-up and crystallisation, microcrystalline **7** which was identified from microanalytical and spectroscopic data. The high frequency shifts in both the ^{1}H and ^{11}B n.m.r. spectra are consistent with the replacement of C_{cage}-H in **6** by C_{cage}-Br.

A number of unsuccessful attempts were made to prepare 1-Ph-2-^{t}Bu-1,2-*closo*-$C_2B_{10}H_{10}$ from these two precursors. Conversion of **6** to the *C*-lithium or *C*-copper(I) derivatives, followed by treatment with iodobenzene (or the more reactive analogue 4-iodotoluene) afforded **6** as the only isolated carbaborane product. Likewise, treatment of **7** with phenyllithium yielded only **6** on work-up (*c.f.* reaction of **2** with MeLi to yield **1**); and reaction of **2** with ^{t}BuLi similarly yielded only 1-Ph-1,2-*closo*-$C_2B_{10}H_{11}$. It seems likely that a more successful route to the target carbaborane may lie through direct insertion of the acetylene ^{t}BuC≡CPh into $B_{10}H_{14}$ in a similar manner to the preparations of **1** and **6** discussed above. (However, no commercial source of this acetylene, nor any reliable synthesis, could be found. An as yet untested synthetic route may be the reaction of ^{t}BuLi with PhC≡CX, X = Br, I.) It is encouraging to note that the related *p-bromotetrafluoro*phenyl species has recently been prepared by reaction of *C*-lithio-*t*-butylcarbaborane with C_6F_5Br **[41]**: clearly there is no steric impediment to the formation of the 1-Ph-2-^{t}Bu- compound. It may be the case that the unsubstituted arene precursor requires some activation to bring about successful reaction: interaction of the complex [(η-ClC_6H_5)$Cr(CO)_3$] with the *C*-lithium derivative of **6** may prove fruitful in this respect. (This would be analogous to a procedure published recently **[123]**, by which halophenyl analogues of **1** were formed by reaction of *C*-lithio-methylcarbaborane with appropriate chromium reagents of the above type.)

Detailed Structural Analysis of Carbaboranes 1 to 4

A major consideration in the present structural analysis of these species is whether sterically-induced deformations occur in a manner which indicates the beginnings of movement along a particular rearrangement pathway. Given that separation of the C_{cage} atoms generally characterises the products of an isomerisation process, some means which brings about an increase in C_{cage}—C_{cage} distance almost certainly pushes the structure towards a state where rearrangement is inevitable. Hence, molecular destabilisation, brought about by conditions such as engineered steric congestion, may simplistically be viewed as the onset of an "uphill" movement towards the transition state of some molecular reorganisation process which (in the example here) will relieve this crowding. It is not unreasonable, therefore, to expect that increasing sterically-induced distortion will follow this same path which would ultimately lead to the same isomerisation process.

The first, and arguably still the most popular mechanism to explain the *ortho-* to *meta-* isomerisation of species of the type 1-R-2-R'-1,2-*closo*-$C_2B_{10}H_{10}$ is the *diamond—square—diamond* (DSD) mechanism **[100]** introduced in Chapter 1 (p. 43). This is characterised by synchronous elongation of three orthogonal pairs of connectivities; namely C(1)—(2) and B(9)—B(12), B(4)—B(5) and B(7)—B(11), and B(3)—B(8) and B(6)—B(10). Table 2.5 below details the distances of these connectivities in the carbaboranes **1** to **4** discussed herein, and those derived from structural studies of related phenylcarbaboranes and other dicarbaboranes which display unusually long C_{cage}—C_{cage} separations. (These carbaboranes, or related species, have been introduced earlier.)

A is the crystallographically ordered molecule of phenylcarbaborane **[53]**; **B** and **C** are the two crystallographically independent molecules ("*B*" and "*A*" respectively) of diphenylcarbaborane **[54]**; **D** and **E** are the two crystallographically independent molecules ("*B*" and "*A*" respectively) of 1-Ph-2-[4'-Br-C_6F_4]-1,2-*closo*-$C_2B_{10}H_{10}$, and **F** is 1-^{t}Bu-2-[4'-Br-C_6F_4]-1,2-*closo*-$C_2B_{10}H_{10}$ **[41]**. **G**, **H** and **J** are dicarbadodecaboranes in which the two C_{cage} atoms are externally linked *via* a macrocyclic group: in **G** this linkage is {-S-CH_2CH_2-O-CH_2CH_2-S-} **[85]**; whilst **H** and **J** are the two crystallographically independent molecules ("*50*" and "*0*" respectively) of the species in which the linking unit is {-S-(-CH_2CH_2-O-)$_2$-CH_2CH_2-S-} **[86]**.

Distance:	C1—C2	B9—B12	B4—B5	B7—B11	B3—B8	B6—B10
Compound						
A	1.646(8)	1.750(11)	1.778(10)	1.771(12)	1.729(10)	1.754(10)
1	1.696(5)	1.759(7)	1.775(7)	1.771(7)	1.776(7)	1.747(6)
2	1.692(8)	1.744(13)	1.792(11)	1.804(12)	1.735(11)	1.755(11)
3	1.708(4)	1.776(6)	1.772(5)	1.776(5)	1.766(5)	1.766(5)
B	1.720(4)	1.757(6)	1.773(6)	1.777(6)	1.746(6)	1.757(6)
C	1.733(4)	1.760(7)	1.771(8)	1.759(7)	1.742(6)	1.750(6)
D	1.739(10)	1.739(18)	1.794(16)	1.776(15)	1.785(15)	1.756(15)
4	1.742(5)	1.771(9)	1.776(8)	1.755(7)	1.741(8)	1.764(8)
E	1.751(9)	1.764(14)	1.793(13)	1.749(13)	1.730(14)	1.742(14)
F	1.765(8)	1.763(13)	1.785(12)	1.727(11)	1.760(12)	1.761(12)
G	1.816(7)	1.772(9)	1.779(9)	1.781(9)	1.779(8)	1.763(8)
H	1.825(5)	1.762(6)	1.784(6)	1.773(5)	1.776(6)	1.766(5)
J	1.858(5)	1.745(5)	1.787(5)	1.774(5)	1.779(5)	1.779(5)

Table 2.5 Interatomic distances (Å) relevant to the DSD-type mechanism in selected carbaboranes (*See text for key to Compounds*)

The above table demonstrates no particular pattern in the connectivities considered, and certainly no general elongation as movement along the diamond→square→diamond pathway would require. On the basis of this (albeit rather rudimentary) analysis, therefore, it may be observed that in the species considered *no evidence to support the DSD mechanism* was found.

However, a more general trend is revealed upon consideration of the localised "diamond" formed by the two adjacent faces defined by C(1), B(3), C(2) and B(6). It is in these faces that sterically-induced distortion occurs in the species [(arene)M{$C_2B_9H_9Ph_2$}], discussed previously in this chapter and in Chapter 1. Specifically, as intramolecular repulsions force the two C_{cage} atoms C(1) and C(2) to separate, the two adjacent atoms M(3) and B(6) are pulled closer together. A similar situation is evidenced here, with B(3)···B(6) shortening as C(1)—C(2) lengthens: this is best seen by consideration of table 2.6.

Distance:	C1—C2	B3 ··· B6	θ / °
Compound			
A	1.646(8)	2.910(10)	68.8
1	1.696(5)	2.847(6)	16.7
2	1.692(8)	2.865(10)	2.2
3	1.708(4)	2.848(5)	0
B	1.720(4)	2.841(5)	9.2, 8.0
C	1.733(4)	2.831(6)	2.4, 2.3
D	1.739(10)	2.873(13)	7.4, 9.6†
4	1.742(5)	2.830(7)	7.6
E	1.751(9)	2.845(13)	2.0, 2.2†
F	1.765(8)	2.852(11)	0.1†
G	1.816(7)	2.816(8)	—
H	1.825(5)	2.811(5)	—
J	1.858(5)	2.797(5)	—

Table 2.6 Interatomic distances (Å) associated with movement towards a *pseudocloso*-type structure, and values of θ (where appropriate), in selected carbaboranes. (*See text for key to Compounds*) † 4'-Br-C_6F_4 ring

The three species **D**, **E** and **F**, might be expected to behave anomalously given that each bears a cage-bound 4'-Br-C_6F_4 group. One might, for example, postulate a gross electronic effect arising from the polyhaloaryl moiety, which causes the C(1)—C(2) connectivity to lengthen by some process such as depopulation of the appropriate bonding molecular orbital. Detailed examination of such properties in these 3 compounds is, however, not appropriate here but will undoubtedly be considered elsewhere [for example, **41**]. This potentially (relatively) unpredictable structural behaviour of **D**, **E** and **F** renders them somewhat unreliable in terms of these detailed considerations of carbaborane geometry; the following discussion will, therefore, largely ignore these three species.

Nevertheless, excepting the compounds **D**, **E** and **F**, it is clear that as the C_{cage}—C_{cage} connectivity lengthens there is a concomitant shortening of the B(3)···B(6) vector. This resembles the beginnings of a localised, single diamond-square-diamond operation which, as has been noted earlier, may

formally convert a *closo* ("diamond") species through a *pseudocloso* ("square") intermediate to a *hypercloso* ("diamond") product; it does not, however, explain rearrangements of the *ortho*- to *meta*-carbaborane type.

It appears in addition that the increase in the C_{cage}—C_{cage} distance is accompanied by a small movement of the C_{cage} atoms away from the polyhedral centroid. Although such a movement (if sufficiently large) could, by itself, result in the observed elongation of C_{cage}—C_{cage}, it cannot explain the observed simultaneous *decrease* in B(3)···B(6) (the distance of these atoms from the centroid does not appear to vary as the C—C connectivity is lengthened); nor can this alone account for other aspects of the cluster distortion discussed below.

A number of further points arising from the above table(s) are worthy of note at this juncture. The influence of the angle θ (describing C_{cage}—aryl orientation) upon the C_{cage}—C_{cage} distance has been discussed in an earlier section. Examination of the θ values tabulated in table 2.6 above reveals that whilst there is a perceptible effect due to variations in θ, other factors such as intramolecular repulsions (especially between exopolyhedral groups), and even crystal packing effects, must be considered. Thus, comparison of the C_{cage}—C_{cage} distances in **B** and **C** (diphenylcarbaborane) shows that in the absence of other factors the larger θ values in **B** cause a shortening of the C—C connectivity relative to that in **C**. In contrast, **3** has a lower θ value than either **B** or **C**, and the combination of exopolyhedral substituents (Me_3Si + Ph) in **3** is arguably more sterically demanding than in **B** and **C** (Ph_2); yet **3** has a shorter C—C connectivity. (This may perhaps be attributed to the different packing environments in the crystalline state of these two species.)

Ultimately, the detailed observed geometry is likely, therefore, to arise from an interplay of several factors such as steric effects, crystal packing forces, the influence of aryl substituents' orientation (θ), and so on. However, regardless of how and to what extent these factors interact to effect a cluster's structure, it seems clear that in the <u>*actual structure adopted*</u> the geometry genuinely reflects an approximate position along some (rearrangement?) pathway. That is, as some parameter such as the C(1)—C(2) separation varies in a (*quasi*-)homologous series of carbaboranes, the rest of the cage structure responds in a manner which is repeated throughout the series.

In an effort further to analyse the structural changes associated with lengthening of the C_{cage}—C_{cage} connectivity - and particularly in the region defined by C(1), C(2), B(3) and B(6) - a further series of structural parameters may be examined.

It has been noted that the extension of the C(1)—C(2) connectivity in several icosahedral dicarbadodecaboranes is accompanied by a simultaneous shortening of the B(3)···B(6) distance: the precise nature of the underlying structural processes by which this is accomplished have not yet been established.

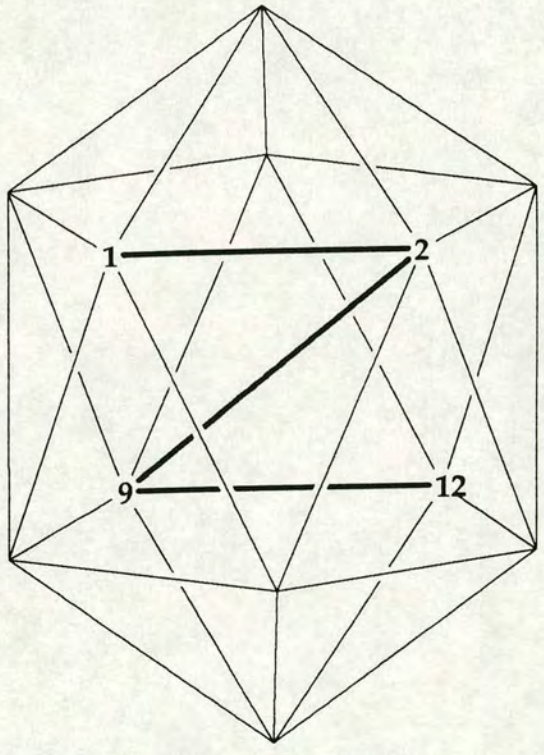

Figure 2.8 Representation of one of the 15 unique "opposite-edge" torsions in an icosahedron

In an icosahedron torsion angles involving opposite edges and the polyhedral centre (for example, 1-2-9-12, 4-8-6-11, and so on: figure 2.8) are ideally 180°. All fifteen such unique angles have been calculated for the

carbaboranes **1** to **4** and **A** to **J** being considered here, and are listed in table 2.7 below. Examination of this table reveals very definite asymmetry among each set of torsions. Thus, whereas the compounds **A, 1, 2** and **3** with shorter C_{cage}—C_{cage} distances show torsion values not differing greatly from 180°; structure **J**, having the longest C_{cage}—C_{cage} here, shows a range of torsions and several which deviate by some 6° from the ideal situation. (The absence of torsion asymmetry in the relatively undistorted species serves to confirm the significance of this effect, and that it arises not merely from replacement of {BH} vertices by {CH}.)

On following page:

Table 2.7 Values of the "opposite-edge" torsions in selected carbaboranes [*See text for key to compounds; notation thus*: 1,2,9,12 *is the torsion* C(1)-C(2)-B(9)-B(12)]

compound \ *torsion:*	1,2,9,12	1,3,10,12	1,4,11,12	1,5,7,12	1,6,8,12	2,3,10,9	3,4,11,10	4,5,7,11	5,6,8,7	6,2,9,8	2,7,5,9	3,7,5,10	3,8,6,10	4,8,6,11	4,9,2,11
A	179.5(5)	-180.0(5)	-179.0(6)	-179.7(6)	179.6(5)	180.0(6)	179.8(6)	179.5(6)	-178.8(6)	179.7(5)	179.4(6)	-179.4(5)	-179.7(6)	179.3(6)	179.9(6)
1	179.7(3)	-178.2(3)	-179.5(4)	178.7(3)	178.7(3)	178.3(3)	-179.0(4)	-179.9(4)	179.5(4)	-179.3(3)	-179.7(4)	179.2(4)	-179.8(3)	-179.8(4)	-179.1(3)
2	178.8(6)	-179.0(6)	-179.6(6)	179.7(6)	178.4(6)	178.8(6)	-179.0(6)	178.3(6)	179.3(6)	-178.5(6)	179.8(6)	-179.8(6)	179.7(6)	-177.9(6)	-179.1(6)
3	180.0	-179.3(3)	-179.9(3)	179.9(3)	179.3(3)	178.5(3)	-179.6(2)	-180.0	179.6(2)	-178.5(3)	179.2(3)	179.5(2)	180.0(3)	-179.5(2)	-179.2(2)
B	179.2(3)	-178.7(3)	-178.7(3)	-179.9(3)	178.2(3)	178.2(3)	-179.6(3)	-179.8(3)	179.9(3)	-178.7(3)	179.0(3)	179.2(3)	-179.8(3)	-179.7(3)	-178.9(3)
C	-180.0(3)	-178.2(3)	-179.1(3)	179.0(3)	178.2(3)	178.5(3)	-179.1(3)	-179.6(3)	179.0(3)	-178.8(3)	179.8(3)	179.1(3)	-179.8(3)	-179.4(3)	-179.5(3)
D	179.0(8)	-178.0(8)	-178.0(8)	178.9(8)	176.7(8)	-179.6(8)	179.4(8)	-179.8(8)	178.7(8)	-179.5(8)	-179.4(8)	-179.5(8)	179.9(8)	-178.9(8)	-179.7(8)
4	-179.4(4)	-178.4(4)	-179.2(4)	179.1(4)	177.5(4)	179.2(4)	179.8(4)	-179.7(4)	178.6(4)	-178.0(4)	178.9(4)	179.8(4)	-180.0(4)	-178.6(4)	-179.6(4)
E	179.1(7)	-177.6(7)	-178.4(7)	179.0(7)	178.7(7)	178.9(7)	-178.8(7)	179.1(7)	-179.4(7)	-179.3(7)	179.8(7)	179.6(7)	179.3(7)	179.7(7)	-179.6(7)
F	179.2(6)	178.6(6)	178.7(6)	-178.2(6)	-178.8(6)	-178.8(6)	179.4(6)	179.9(6)	-178.8(6)	178.0(6)	-179.7(6)	179.7(6)	-179.6(6)	-180.0(6)	-179.7(6)
G	-179.4(4)	-175.5(4)	-179.1(5)	177.9(5)	175.6(4)	175.7(4)	-176.8(4)	179.4(5)	177.3(4)	-175.9(4)	178.4(5)	177.3(4)	-179.7(4)	-176.6(4)	-178.6(4)
H	179.9(3)	-175.7(3)	-177.7(3)	179.3(3)	175.7(3)	174.8(3)	-176.0(3)	179.8(3)	177.8(3)	-175.7(3)	177.4(3)	176.3(3)	-179.6(3)	-177.6(3)	-179.2(3)
J	-180.0(3)	174.3(3)	177.4(3)	-178.6(3)	-175.2(3)	-174.3(3)	176.5(3)	179.2(3)	-176.6(3)	174.0(3)	-177.4(3)	-175.7(3)	-179.2(3)	177.6(3)	178.2(3)

Crucially, those torsions which differ most from 180° *all* involve one of the C_{cage}—B(3 *or* 6) edges. Closer analysis of the data reveals a "pivoting" motion whereby C_{cage}—B(3 *or* 6) bonds appear to rotate about the C_{cage} position in a manner such that the two vicinal boron atoms [B(3) and B(6)] are brought closer together; obviously this is, in reality, accompanied by the C_{cage}—C_{cage} separation process. This combination equates, effectively, to *rotations* of the C_{cage}—B(3 *or* 6) edges such that C(1)-C(2) is extended and B(3)···B(6) is reduced.

[It may be of interest to note that in **4** those torsions involving only the two C_{cage}—B(6) bonds deviate most. As a consequence of these apparent rotations there is a marked asymmetry in certain chemically equivalent connectivities in the structure of **4**; for example, C(1)—B(6) [1.713(6)Å] is less than C(1)—B(3) [1.730(6)Å] and C(2)—B(6) [1.710(6)Å] is quite significantly shorter than C(2)—B(3) [1.748(6)Å]. The origin of this slight anomaly is unclear: it may arise simply as a consequence of the precise steric interactions between the particular exopolyhedral groups present in this species, or from some more subtle cluster electronic feature.]

The above observation of very definite evidence for C—B rotations which occur as the C_{cage}—C_{cage} distance lengthens may be of some relevance to the controversy surrounding the mechanism of isomerisation in carbaboranes, their metal derivatives and related species. The principle of edge rotation represents a further possible mechanism whereby these rearrangements may be effected. In Chapter 1 (pp. 41-46) the related carbaplatinaborane system [1-Ph-3,3-$(R_3P)_2$-3,1,2-$PtC_2B_9H_{10}$] was discussed, and the mechanism of triangular face rotation was suggested to be appropriate in describing the facile isomerisation process observed there. Likewise, the *closo*→*pseudocloso*→*hypercloso* transformations referred to earlier may similarly be viewed in terms of rotations of triangular faces. Rotation of two adjacent faces by some 30° achieves a *closo*→*pseudocloso* conversion (figure 2.9); whilst a further 30° rotation of the same two faces arrives at a *hypercloso*-type structure.

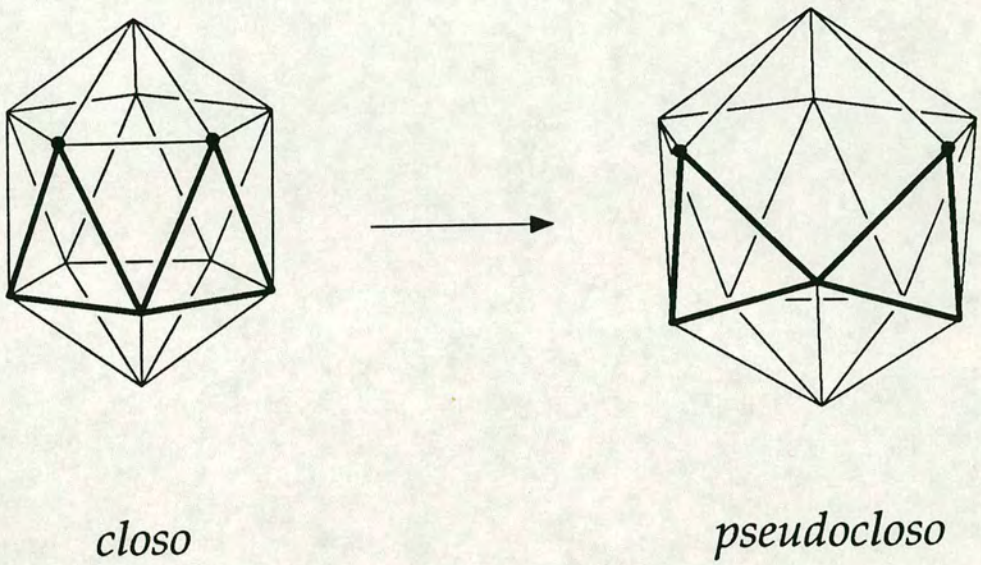

Figure 2.9 The *closo*→*pseudocloso* transformation viewed as triangular face rotation

It may be of interest to note that edge rotation provides a similar, alternative description of these processes. Recognition of this mechanistic possibility here has prompted a determination, for comparison, of the relative twists of triangular faces in the icosahedral carbaboranes under discussion here.

In an ideal icosahedron, there are 10 pairs of faces which are related by a centre of inversion located at the polyhedral centre. A projection of one such pair of faces is shown in figure 2.10.

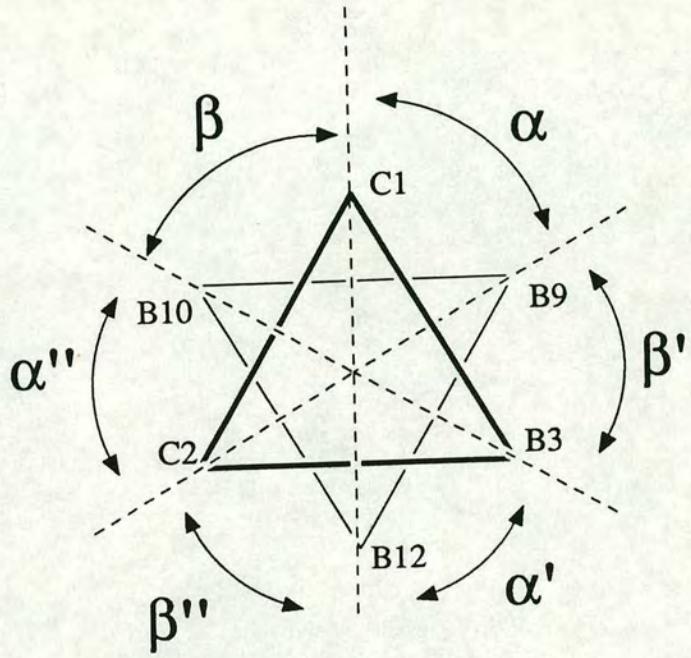

$$\delta = |\alpha - \beta|$$

$$\delta' = |\alpha' - \beta'|$$

$$\delta'' = |\alpha'' - \beta''|$$

$$\partial = [\delta + \delta' + \delta'']/3$$

Figure 2.10 Projection of the C(1)C(2)B(3) and B(9)B(10)B(12) faces in an icosahedron, and definitions of the twist angles α, β, δ and ∂

The twist angle α and β are obtained as torsions involving the centroids [say X(1) and X(2)] of the two faces. Thus the triangle vertex C(1) has an associated twist α to the right - "towards" B(9) - which is the modulus of the torsion C(1)-X(1)-X(2)-B(9), and a twist β to the left - "towards" B(10) - which is the modulus of the C(1)-X(1)-X(2)-C(2) torsion. The twist δ for the C(1) vertex is then the modulus of the difference between α and β; the overall twist angle ∂ for the pair of faces is the average of the three individual δ values. (In an ideal icosahedron all the pairs of faces are perfectly staggered, so that all α and β angles are 60° and hence all values of δ and ∂ are *zero*.) Values of ∂ for the carbaboranes being considered here are tabulated in table 2.8.

twist:	1,2,3 / 9,10,12	1,3,4 / 10,11,12	1,4,5 / 7,11,12	1,5,6 / 7,8,12	1,2,6 / 8,9,12	2,3,7 / 5,9,10	3,4,8 / 6,10,11	4,5,9 / 2,7,11	5,6,10 / 3,7,8	2,6,11 / 4,8,9
Compound										
A	3.04	1.45	2.27	0.94	2.47	2.44	0.77	1.78	1.70	1.79
1	0.70	1.98	1.54	1.97	1.51	1.79	0.83	1.61	1.05	2.18
2	1.11	1.44	2.57	1.60	2.09	2.23	1.71	1.99	0.80	2.81
3	0.70	1.90	1.64	1.90	0.69	1.74	1.71	0.57	0.57	1.75
B	0.76	2.06	1.70	1.56	0.76	2.14	0.77	1.05	0.91	2.30
C	0.29	2.31	1.62	2.46	0.39	1.91	0.97	0.71	1.45	1.93
4	0.80	1.81	1.64	2.85	0.80	1.27	0.80	0.70	1.09	2.25
G	2.38	5.09	3.35	5.56	2.46	5.20	4.17	1.55	3.17	5.44
H	2.67	6.39	2.77	4.32	1.27	6.86	4.14	1.39	3.28	4.60
J	3.40	7.10	2.89	5.80	3.13	7.61	3.11	1.74	5.18	6.27

Table 2.8 Values of the "overall twist angle" ∂ for the 10 pairs of triangular faces in selected carbaboranes [*See text for key to compounds; notation thus*: 1,2,3/9,10,12 *is overall twist of face* C(1)C(2)B(3) *relative to face* B(9)B(10)B(12) *and* vice-versa]

twist:	1/9,10	2/10,12	3/9,12	1/10,11	3/11,12	4/10,12	1/7,11	4/7,12	5/11,12	1/7,8	5/8,12	6/7,12	1/8,9	2/8,12	6/9,12
compound															
A	4.97	3.12	1.02	2.18	0.69	1.49	1.16	2.90	2.76	0.36	2.45	0.01	2.63	3.83	0.94
1	1.43	0.65	0.01	1.83	3.78	0.33	1.08	2.30	2.22	2.36	0.21	3.34	1.24	1.20	2.02
2	2.69	0.20	0.45	1.74	2.26	0.31	1.10	2.37	4.25	2.65	0.04	2.11	1.94	2.29	2.05
3	0.90	0.29	0.90	1.21	2.74	1.76	0.00	2.46	2.46	1.21	1.76	2.73	0.90	0.28	0.90
B	1.59	0.70	0.00	2.75	3.03	0.39	0.55	3.42	1.12	1.13	0.77	2.79	0.39	1.17	0.73
C	0.71	0.04	0.11	2.80	3.87	0.26	0.17	2.71	1.99	2.63	0.31	4.43	0.77	0.32	0.08
4	1.55	0.84	0.02	1.98	2.70	0.76	0.19	2.53	2.19	3.13	0.02	5.39	1.10	1.14	0.17
G	3.47	2.88	0.80	8.01	7.24	0.01	2.28	3.46	4.32	6.62	1.96	8.10	3.33	3.63	0.43
H	3.17	4.44	0.41	6.81	9.82	2.54	1.96	3.51	2.85	6.06	1.06	5.83	3.46	3.09	0.38
J	4.20	5.06	0.93	8.29	9.45	3.57	1.77	4.34	2.56	7.45	1.91	8.05	3.55	5.04	0.80

twist:	2/5,10	3/5,9	7/9,10	3/6,11	4/6,10	8/10,11	4/2,7	5/2,11	9/7,11	5/3,8	6/3,7	10/7,8	2/4,8	6/4,9	11/8,9
compound															
A	1.90	1.78	3.63	1.46	0.27	0.58	3.22	1.56	0.56	2.50	1.98	0.62	0.94	0.64	3.79
1	1.82	2.52	1.04	0.45	0.70	1.34	1.12	2.18	1.54	1.70	0.55	0.91	1.12	3.43	2.00
2	0.83	3.57	2.30	0.93	1.28	2.91	3.49	2.06	0.42	0.14	0.53	1.73	2.96	4.95	0.53
3	2.28	2.91	0.04	0.14	0.91	0.66	0.85	0.85	0.01	0.91	0.14	0.66	2.28	2.92	0.06
B	2.57	3.73	0.11	0.33	0.20	1.77	1.23	1.54	0.38	0.77	0.73	1.22	2.57	3.27	1.07
C	2.25	2.96	0.51	0.02	0.50	2.39	0.41	1.62	0.11	1.90	0.58	1.88	1.94	3.01	0.85
4	2.32	1.47	0.01	0.11	1.02	1.26	1.20	0.68	0.22	2.09	0.22	0.97	2.81	3.36	0.59
G	6.72	7.88	1.00	3.26	4.80	4.45	1.56	1.62	1.48	3.57	2.22	3.71	5.97	7.59	2.75
H	7.79	9.12	3.68	2.55	5.64	4.23	3.56	0.78	0.53	3.34	3.17	3.34	7.16	6.53	0.10
J	8.92	9.65	4.25	2.54	3.72	3.06	2.50	2.67	0.06	6.41	4.82	4.31	8.91	8.79	1.10

On preceding page:

Table 2.9 Values of the "individual twist angles" δ for the 10 pairs of triangular faces in selected carbaboranes [*See text for key to compounds; notation thus*: 1/9,10 *is twist of vertex* 1 *towards* 9 *or* 10 - i.e., "δ" *in figure 2.10*]

The values of the overall twist angle ∂ entered in table 2.8 suggest very little movement of this kind, even in the most distorted carbaboranes considered. However, where this does to some extent occur, the observed twists are generally of triangular faces which involve a C_{cage} atom and are in a direction which produces an increase in the C_{cage}—C_{cage} distance; this is entirely consistent with a face rotation mechanism. Furthermore, it appears that the process of averaging the three values δ, δ' and δ" (tabulated individually in table 2.9) to give the "overall" parameter ∂ somewhat masks the fact that the "moving" faces do, in fact, pivot about a point close to one of their vertices (that is, the axis of rotation lies near to a face corner, rather than through the centre of a face). The distinction, between this view of the cluster deformation process and its description in terms of *edge* rotations, is a fine one and these analyses cannot dismiss one of these two (almost equivalent) descriptions in favour of the other.

Further Work

The current paucity of structural data on crowded (or otherwise distorted) icosahedral carbaboranes severely limits the scope of detailed analyses of the type discussed in this chapter. A priority in extending the present work must be the synthesis and structural characterisation of crowded phenylcarbaboranes, such as the 2-^{t}Bu- and 2-^{i}Pr$_3$Si- derivatives referred to earlier. Other trialkyl- (or mixed alkyl/aryl-) silyl species ought to show similar (or more) congestion; the compounds [(1-Ph-1,2-*closo*-$C_2B_{10}H_{10}$-2-)$_2$-SiR_2] (R = alkyl, aryl) may possess unique steric properties. Additional steric demands may be imposed by *B*-substitution adjacent to the C_{cage}—C_{cage} connectivity; the geometries of species such as 1,2-Ph_2-3-R-1,2-*closo*-$C_2B_{10}H_9$ would be of interest in this respect.

Finally, it would be informative to determine (by, for example, molecular orbital calculations) what electronic and energetic changes are associated with the molecular deformation and reorganisation phenomena described above. It is likely that calculations of this type will help shed light on the feasibility of the proposed mechanism(s).

Conclusions

The synthesis and characterisation of 4 *C*-substituted derivatives of phenylcarbaborane, and of three related carbaborane species, have been presented. The 2-Me, 2-Br, 2-Me_3Si and 2-^{t}BuMe$_2$Si relatives of 1-Ph-1,2-*closo*-$C_2B_{10}H_{11}$ were the subject of single crystal *X*-ray diffraction structural determinations. These four species constitute part of a series of such carbaboranes in which the exopolyhedral substituents have gradually increasing steric requirement; detailed examination of these structures revealed new ways in which increasing intramolecular congestion in such compounds may be accommodated. In the structures of the 2-trialkylsilyl species, there is evidence of *bending back* of the C_{cage}-bound substituents so as to reduce intramolecular repulsions; this may occur not only at the C_{cage} vertex itself, but also at the substituent atom which is the point of attachment to the cage. Substituent flexibility may also allow internal distortions of the pendant group which relieve crowding.

Considerably more detailed analyses of the geometry of the carbaborane nucleus in these four species, and in a number of related clusters which suffer significant C_{cage}—C_{cage} elongation, were performed. These studies provided no evidence in support of the *diamond—square—diamond* mechanism of polyhedral rearrangement. Instead, the results appear to favour a reorganisation mechanism which is localised near the C_{cage} atoms. In particular, evidence was presented which is consistent with an "*edge rotation*" mechanism, ***or*** a closely related mechanism of *triangular face "pivoting"*; these discussions generally lend support to mechanisms of the rotational type.

Chapter 3

Synthesis and Characterisation of *bis*-(Phosphine)Platinum Complexes of Methylphenylcarbaborane, and Some Related Reactions

Introduction

In the present Chapter are presented the syntheses and characterisation of several *bis*(phosphine) platinum derivatives of a sterically demanding {η^5-carbaborane} ligand. These studies are viewed in the context of their relation to the corresponding derivatives of 1-phenyl-1,2-*closo*-dicarbadodecaborane whose facile isomerisations have been discussed in Chapter 1.

The deboronation of the *closo*-carbaborane precursor 1-Ph-2-Me-1,2-$C_2B_{10}H_{10}$ to form [7-Ph-8-Me-7,8-*nido*-$C_2B_9H_9$]$^{2-}$, **8**, and the characterisation of both this latter species and its protonated relative $8H^+$ are reported. Related "decapitation" reactions of both the parent *C*-phenyl-carbaborane (to yield [7-Ph-7,8-*nido*-$C_2B_9H_{11}$]$^-$, $9H^+$), and of more crowded, trialkylsilyl derivatives, are also discussed.

Interaction of the carbaborane ligand **8** with appropriate dichloro- salts of the {$(R_3P)_2Pt$} fragment afforded the platinum complexes 3,3-$(R_3P)_2$-1-Ph-2-Me-3,1,2-$PtC_2B_9H_9$ (R_3 = Me_2Ph, **10**; R = Et, **11**; Ph, **12**; *p*-tol, **13**); the synthesis and characterisation of these compounds, and the results of single-crystal *X*-ray diffraction experiments on **11** and **12** (for which two separate crystalline modifications were studied), are presented. Molecules of **11**, and the two crystalline modifications of **12**, **12A** and **12B**, contain a "carbons adjacent" C_2B_9 carbaborane moiety, and there is evidence of a significant steric influence upon the structures adopted; this is attributed to intramolecular interaction between the C_{cage}-bound groups and those attached to the platinum-bound phosphorus ligands. Some discussion of these species in relation to the facile thermal rearrangement of the analogous derivatives of **9** then follows.

Formation of Ligands of the Type [7-Ph-8-R-7,8-*nido*-$C_2B_9H_9$]$^{2-}$ *

Deboronation of 1-Ph-2-Me-1,2-*closo*-$C_2B_{10}H_{10}$, 1. Formation of [7-Ph-8-Me-7,8-*nido*-$C_2B_9H_9$]$^{2-}$, 8, and [7-Ph-8-Me-7,8-*nido*-$C_2B_9H_{10}$]$^-$, 8H$^+$

The *closo*-carbaborane 1-Ph-2-Me-1,2-$C_2B_{10}H_{10}$, **1**, discussed in some detail in the preceding Chapter, constitutes the precursor to a moderately sterically-demanding *nido*-carbaborane ligand from which may be prepared a homologous series of *bis*(phosphine) platinum complexes.

Treatment of **1** with excess KOH in refluxing ethanol affords the carbaborane dianion [7-Ph-8-Me-7,8-*nido*-$C_2B_9H_9$]$^{2-}$, 8, in reasonable yield. This species is conveniently isolated as the *dithallium* salt, a useful reagent in the formation of metal complexes. An entirely analogous procedure has previously been employed in the preparation of Tl[(Tl){7-R-8-R'-7,8-*nido*-$C_2B_9H_9$}] salts (R = R' = H **[77]**; R = Ph, R' = H **[88]**; R = R' = Ph **[89]**); in the present case the poorer yields and longer required reaction time are fully consistent with the greater steric crowding in **1** than in the unsubstituted 1,2-*closo*-$C_2B_{10}H_{12}$ parent. Future optimisation of this route (in particular, perhaps, by further increased reaction time) may improve the final yield.

The identity of the Tl[(Tl)8] product was confirmed by infrared spectroscopy, and by microanalysis.

An alternative method of decapitation of **1** uses an excess of the cyclic amine piperidine (pip), in refluxing benzene. This affords the *monoanionic nido*-carbaborane [7-Ph-8-Me-7,8-*nido*-$C_2B_9H_{10}$]$^-$, 8H$^+$, as the piperidinium salt in good yield. Similar facile degradations of *closo*-carbaboranes have been reported **[124]**; again, the present substrate (**1**) appears to undergo reaction less readily than the corresponding, comparatively unhindered, analogues.

---

* As in the previous chapter, the C_{cage} atom bearing the phenyl group has - for consistency - been made the lowest-numbered carbon vertex in both these *nido*-carbaborane anions and the platinum complexes discussed below.

The piperidinium salt [pipH][8H] was identified and characterised by C, H, N microanalysis, and both infrared and n.m.r. (^{1}H, ^{11}B) spectroscopies. The $^{11}B\{^{1}H\}$ n.m.r. spectrum shows nine resonances (two are coincident) corresponding to the presence of nine inequivalent boron atoms, fully consistent with the absence of molecular symmetry in **8**. Upon retention of proton coupling, the ^{11}B spectrum contains eight doublets arising from coupling to terminal H_{cage} atoms ($^{1}J_{BH}$ 135 - 152 Hz), and one doublet of doublets corresponding to the boron atom [B(10) by analogy to the situation in the unsubstituted $\{C_2B_9H_{12}\}^-$ parent **[125]**] bearing both an *exo*- and an *endo*-H atom; the proton couplings to this unique boron atom are typical, being $^{1}J_{BH(exo)}$ 137 and $^{1}J_{BH(endo)}$ 55 Hz.

Formation of $[PhCH_2NMe_3]^+[7\text{-Ph-}7,8\text{-}nido\text{-}C_2B_9H_{11}]^-$, BTMA[9H], and $[C_5H_{10}NH_2]^+[7\text{-Ph-}7,8\text{-}nido\text{-}C_2B_9H_{11}]^-$, [pipH][9H]. Comments on the Attempted Deboronation of 1-Ph-2-Me_3Si-1,2-*closo*-$C_2B_{10}H_{10}$, 3, and of 1-Ph-2-^{t}BuMe$_2$Si-1,2-*closo*-$C_2B_{10}H_{10}$, 4.

The monoanionic *nido*-eleven vertex carbaborane $[7\text{-Ph-}7,8\text{-}nido\text{-}C_2B_9H_{11}]^-$, $9H^+$, was readily prepared in good yield by mild base degradation of the parent carbaborane 1-Ph-1,2-*closo*-$C_2B_{10}H_{11}$ in ethanol, and isolated as the benzyltrimethylammonium salt BTMA 9H. Microanalytical and spectroscopic data confirmed the identity of the product.

In common with that of $8H^+$, the ^{11}B n.m.r. spectrum of BTMA[9H] shows nine separate resonances, consistent with the absence of molecular symmetry. Likewise, all nine of these resonances show typical couplings to *exo*- (terminal) H_{cage} atoms ($^1J_{BH}$ 120 - 162 Hz), with one of these showing additional coupling ($^1J_{BH(endo)}$ 54 Hz) to an *endo*-H atom.

An unusual result was obtained in the parallel deboronation reaction of the same parent carbaborane using piperidine. Microanalysis of the product is consistent with its formulation as [pipH][9H]. However, in solution it appears that a counterion effect occurs: the ^{11}B n.m.r. spectrum of this species is somewhat different to that obtained for the above BTMA salt. Again there are 9 separate resonances (with slightly different chemical shifts) showing coupling to terminal H_{cage} atoms ($^1J_{BH}$ 125 - 156 Hz); however, there is no evidence of any additional coupling to an *endo*-H atom. It may be that some loose ion-pair formation occurs, which causes the previously *endo*-H atom to switch to a bridging position (for which an additional coupling is generally not seen).

Deboronation of 1-Ph-2-Me_3Si-1,2-*closo*-$C_2B_{10}H_{10}$, 3, using piperidine was partly successful in that a decapitated product was obtained. However, comparison of the ^{11}B n.m.r. spectrum of the product with that of [pipH][9H] discussed above demonstrated that the trimethylsilyl moiety had been lost during the reaction: the product was, in fact, simply an impure form of [pipH][9H]. Thus, since it would be expected that a considerably longer reaction period would be required for the deboronation of 3 than the less

crowded carbaboranes discussed above, it seems likely that the competing reactions of trimethylsilyl substitution followed by phenylcarbaborane deboronation prevail. The sensitivity of the C_{cage}—$SiMe_3$ bond to nucleophiles has been demonstrated elsewhere **[44, 45]** and it seems that, despite the sterically hindered nature of **3**, the loss of the cage-bound trimethylsilyl group is a direct consequence of the conditions required for deboronation.

In an attempt to overcome this problem, the deboronation of the even more crowded carbaborane **4** was attempted; it has been shown **[44, 45]** that the C_{cage}—Si bond in species of this type is considerably more robust. However, even after several days of treatment of compound **4** with 3 equivalents of piperidine or KOH in refluxing benzene or ethanol respectively, ^{1}H and ^{11}B n.m.r. spectroscopy of the product showed that it was essentially unchanged by such treatment. It may be the case that even more prolonged reaction will effect decapitation, but it is equally likely that the competing reactions discussed above may continue adversely to affect this system .

Platinum Complexes of [7-Ph-8-Me-7,8-*nido*-$C_2B_9H_9$]$^{2-}$

The intention in preparing this series of platinum complexes of the carbaborane ligand **8** was to synthesise several compounds in which the "cone angle" (see below) of the phosphine ligands gradually increases. In so doing it was anticipated that the exopolyhedral (C_{cage}- and platinum-bound) groups would suffer increasing steric interaction; the molecule would undergo gradually more cluster distortion, and ultimately would relieve this crowding by isomerisation. It was hoped that structural characterisations (by means of single-crystal *X*-ray diffraction analysis) would allow a tracking of the sites of cluster distortion along the path towards the expected isomerisation. Valuable mechanistic information would thereby be obtained.

The π frontier orbitals of a *nido*-icosahedral {η^5-carbaborane} ligand have the form shown in figure 3.1, which also shows the interactions of these with the appropriate orbitals of an angular ML_2 fragment - such as {$Pt(PR_3)_2$}. [A molecular orbital calculation **[126]** has shown that the C_{cage} substitution in **8** has minimal *qualitative* effect upon the form and energies of the cage π orbitals.] The metal-based LUMO ($1a_1$) is of symmetry suitable for overlap with the lowest OMO (a') of the carbaborane (this interaction has no conformational preference); whilst the interaction of the metal fragment OMOs with the carbaborane frontier orbitals will determine the preferred conformation of the angular {$Pt(PR_3)_2$} fragment with respect to the ligating C_2B_3 face [*c.f.* figure 1.23(a)]. Two pairs of these latter interactions are possible [namely $1b_1$···a"/$1b_2$···a' (shown) *or* $1b_2$···a"/$1b_1$···a'] and these two situations define orthogonal metal fragment orientations; the electronically preferred orientation will be the one which affords greater stabilisation. (The first member of each of the above pairs is two-electron, stabilising and the second four-electron, destabilising.) The former of the two above pairs of interactions is found to be the preferred one: the $1b_1$···a" overlap is highly stabilising (the two orbitals are well matched in energy), whilst the poor energy match of the $1b_2$ and a' orbitals gives relatively lower destabilisation. Hence the preferred conformation of the metal fragment is that where the P_2Pt plane is oriented perpendicular to the notional mirror plane of the carbaborane.

Figure 3.1 Qualitative representation of the frontier orbitals of $\{\eta^5\text{-}C_2B_9H_{11}\}$ and $\{Pt(PR_3)_2\}$

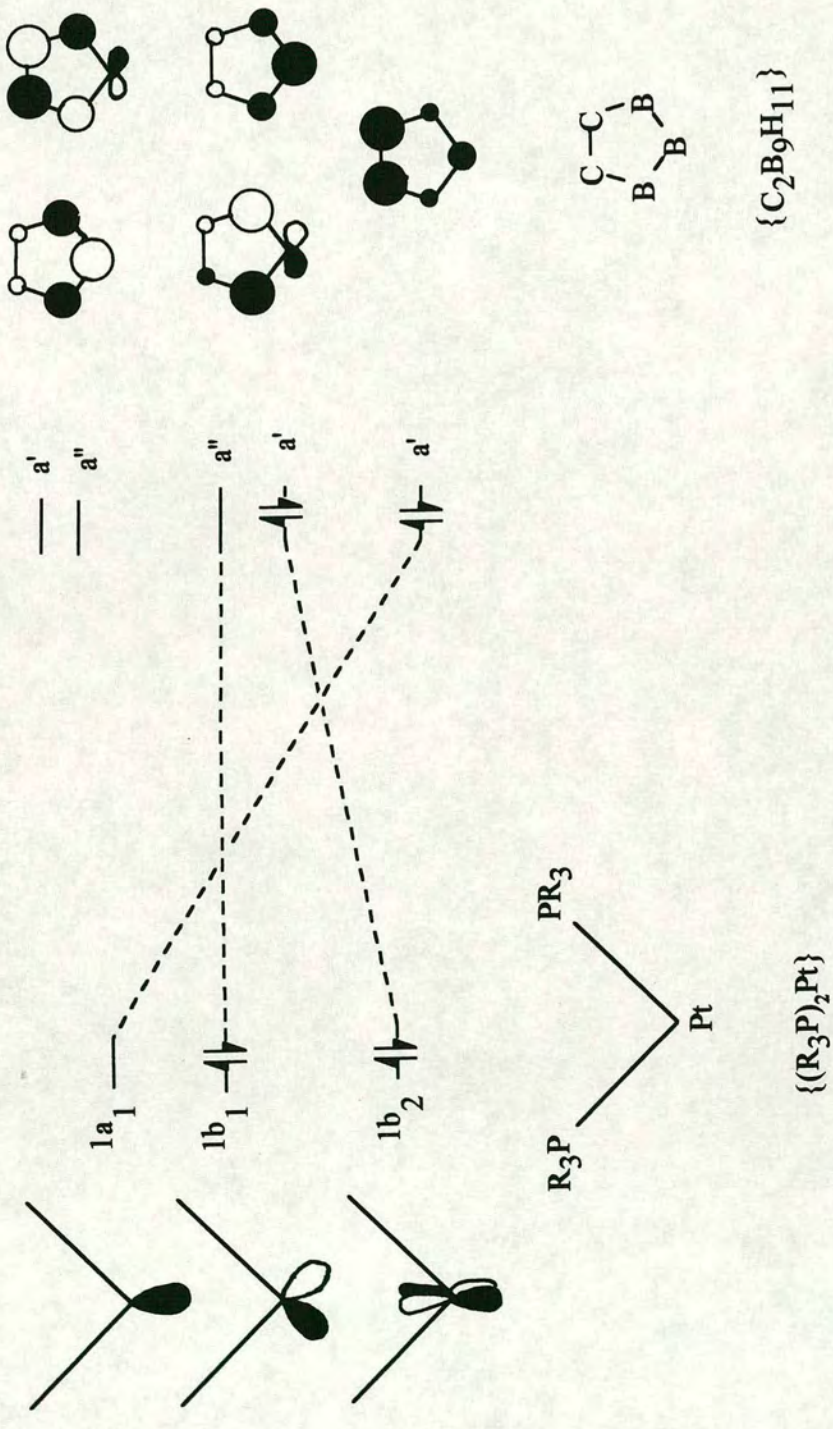

The above stabilising interaction is further enhanced by a positive *slip* **[77]** [*c.f.* figure 1.17; i.e., $\Delta > 0$] of the platinum fragment towards the unique boron atom of the open face; whereas this reduces the extent of the destabilising orbital overlap. [This contrasts with the situation in which $\{Pt(PR_3)_2\}$ is replaced by conical {Ru(arene)} - or, indeed, by {BH} - where the ligated fragment is preferentially located over the centre of the C_2B_3 face, with correspondingly low Δ.] As the metal fragment slips thus, an additional interaction, between the metal LUMO ($1a_1$) and the carbaborane HOMO (a'), is also established. The corresponding *folding* **[77]** of the ligating C_2B_3 face serves to further reduce the destabilising $1b_2 \cdots a'$ interaction and the two carbon atoms, in effect, move *away* from the metal atom towards the lower pentagonal belt of the cage.

Phosphine ligands may be conveniently discussed in terms of their "cone angle" Θ (figure 3.2 below), a concept introduced by Tolman **[129]** to quantify the varying steric influence of these ligands which potentially has a marked effect upon the properties of the corresponding metal complexes.

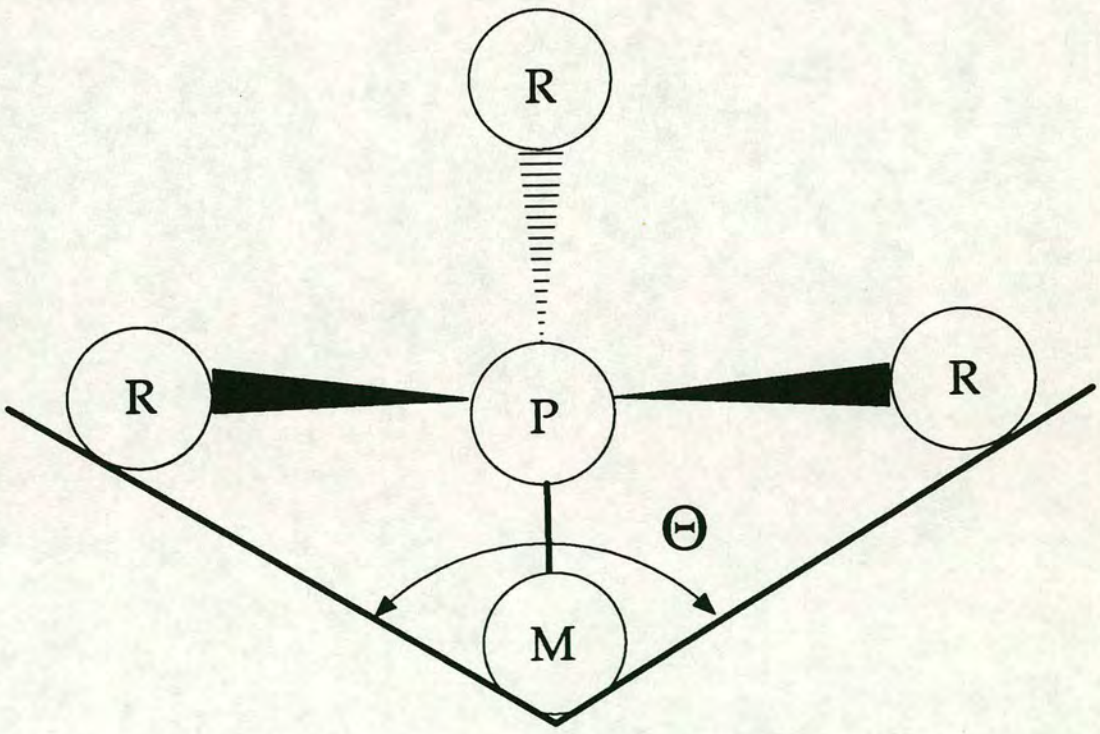

Figure 3.2 The Tolman cone angle Θ for a phosphine ligand R_3P bound to a metal centre M

Θ is essentially the apex angle of a cylindrical cone, centred 2.28Å from the middle of the phosphorus atom, which just touches the spheres defined by the van der Waals radii of the outermost atoms. Although this representation considerably simplifies reality and suffers several limitations, it does nevertheless provide a fairly reliable means of comparing the influence upon sterics of variation in the nature of metal-bound phosphines. For example, the M—P distance is set at 2.28Å, but even large deviations from this value do not substantially affect the value of Θ; in this chapter, all the metal complexes have platinum-bound phosphines and hence may reasonably be compared in terms of this parameter.

Values of Θ for the phosphines present in the platinum complexes described below are listed in table 3.1.

Phosphine	*Cone Angle, Θ / °*
Me_2PhP	122
Et_3P	132
Ph_3P	145
$(p\text{-tol})_3P$	145

Table 3.1 Cone angles for selected phosphine ligands

Several *bis*(phosphine)-platinum complexes of *nido*-icosahedral carbaborane ligands have been structurally characterised previously. These species, of general type 1-R-3,3-{P}$_2$-3,1,2-$PtC_2B_9H_{10}$ show similar cluster geometries, with folding of the ligating C_2B_3 face and modest slippage of the metal fragment *away* from the C_{cage} atoms. The C_{cage}—C_{cage} distance, along with values of the slipping (Δ) and folding (θ, ϕ) parameters and metal atom elevation (above the mean C_2B_3 face) are tabulated in table 3.2 below. [The parameters Δ, θ and ϕ have been defined in Chapter 1 (figure 1.17).] Compound **A** has {P} = Et_3P, R = H **[77]**; **B** has {P}$_2$ = $Ph_2PCH_2CH_2PPh_2$, R = H **[130]**; **C** is {P} = Me_2PhP, R = Ph **[99]**; and **D** and **E** are two crystallographically-independent molecules for the compound with {P} = Me_2PhP, R = —CH_2OCH_3 **[131]**. Note that the fold axis lies through C(2) and B(4) in **C** and C(1) and B(8) in **D** and **E**, rather than through B(4) and B(7), in

part as a consequence of rotation of the metal fragment about the Pt···cage vector.

Table 3.2 C—C distance, values of Δ, θ and ϕ, and metal atom elevation for species 1-R-3,3-{P}$_2$-3,1,2-PtC$_2$B$_9$H$_{10}$. (*See text for key to compounds*)

Compound:	C—C /Å	Δ/Å	θ/°	ϕ/°	Pt elevation/Å
A	1.529(10)	0.42	4.7	4.4	1.86
B	1.53 (3)	0.35	5.4	6.2	1.81
C	1.594(14)	0.39	2.8	7.2	1.81
D	1.550(12)	0.41	2.3	8.3	1.81
E	1.527(12)	0.44	3.0	8.3	1.82

As has been discussed above, the electronically-preferred conformation of the {P$_2$Pt} fragment over the C$_2$B$_3$ face is that lying parallel to the C$_{cage}$—C$_{cage}$ connectivity. In reality this situation is not realised as the metal fragment rotates to reduce interactions between the metal ligand set and the *exo*polyhedral substituents and H atoms bound to the carbaborane facial atoms. Thus, in **A** and **B** the P$_2$Pt plane is rotated by 13.9° and 6.9° respectively from the preferred conformation; whilst in **C** a sterically-induced rotation of some 37.2° is observed, as a consequence of the presence of the C$_{cage}$-bound phenyl substituent. There is evidence **[132]** that in **D** and **E** the C$_{cage}$-bound ether group modifies the cage π frontier orbitals, so that in these two species the preferred orientation of the platinum fragment is somewhat rotated from that for unsubstituted (and simply substituted) cages; as a result the metal fragments in the two molecules **D** and **E** have rotated by 33.1° and 28.0° respectively from a disposition parallel to the C$_{cage}$—C$_{cage}$ bond.

With the exception of **C**, the length of the C—C connectivity in the above-mentioned complexes is fairly constant at around 1.53 to 1.55Å. Electronic factors may account for the elongation of this distance in **C**: as the metal fragment rotates (under steric influence) from its preferred conformation, the carbaborane second UMO (a" - see figure 3.1) becomes partially populated by interaction with the metal OMOs. This carbaborane orbital is strongly *antibonding* between the two C$_{cage}$ atoms and hence the C—C connectivity lengthens.

Very few metal complexes of *nido*-eleven-vertex carbaborane ligands containing both C_{cage}—Me and C_{cage}—Ph groups have been reported and structurally characterised **[13(f), 88, 133]**. Of these, only the {(arene)Ru} complex 3-(*p*-cym)-1-Ph-2-Me-3,1,2-$RuC_2B_9H_9$ **[88]** contains a 3,1,2-MC_2B_9 polyhedron in which the C_{cage} atoms both lie in the metal-ligating face and are mutually adjacent. In this compound, a sterically-induced cluster deformation is reported for one of the two crystallographically-independent molecules in the asymmetric portion of the unit cell.

The *bis*(phosphine) platinum complexes **10** — **13** described below represent the first reported {ML_2} derivatives of **8**; crystallographic studies of **11** and two crystalline forms of **12** reveal significant influence of steric factors upon structure.

Synthesis and Characterisation of 1-Ph-2-Me-3,3-$(Me_2PhP)_2$-3,1,2-$PtC_2B_9H_9$, 10

Reaction of $[(Me_2PhP)_2PtCl_2]$ with the dithallium salt of **8** in CH_2Cl_2 readily forms **10**; the progress of the reaction is evidenced by the appearance of an orange colouration in the CH_2Cl_2 solution. The filtered and concentrated reaction mixture was purified by preparative thin layer chromatography (prep. t.l.c.) (CH_2Cl_2/*n*-hexane, 4:1); isolation of the only mobile band (*Rf* 0.8) afforded **10** in good yield as a yellow-orange powder. The identity of the product was confirmed by satisfactory C, H, N microanalytical data, and by infrared and multinuclear (^1H, ^{31}P, ^{11}B) n.m.r. spectroscopy.

The ^{31}P n.m.r. spectrum (figure 3.3) consists of a single resonance with ^{195}Pt satellites; the magnitude of the coupling $^1J_{PPt}$ (*ca.* 3040 Hz) is typical of a *cis*-$[(R_3P)_2Pt]^{2+}$ fragment; whilst the appearance of only one resonance is fully consistent with unhindered rotation (at room temperature) of the $\{(Me_2PhP)_2Pt\}$ moiety about the Pt···cage vector.

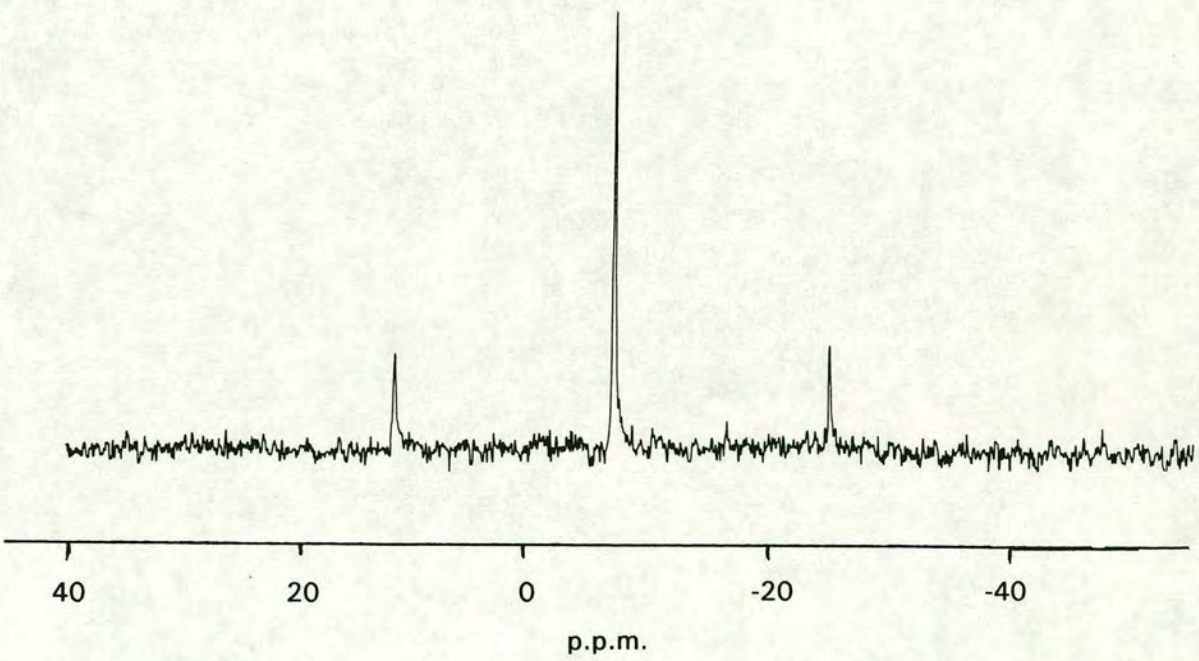

Figure 3.3 81.02 MHz ^{31}P n.m.r. spectrum of **10**

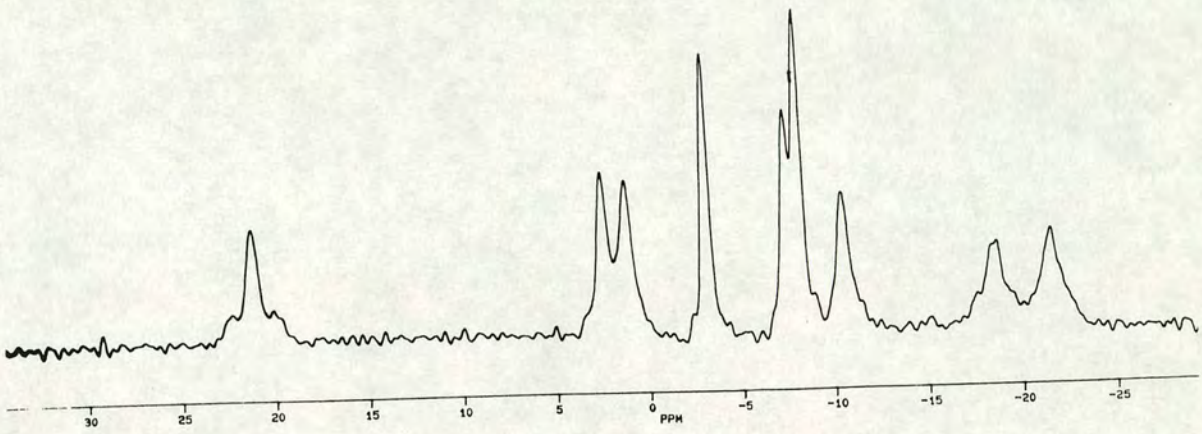

Figure 3.4 115.55 MHz $^{11}B\{^1H\}$ n.m.r. spectrum of **10**

The ^{11}B n.m.r. spectrum (figure 3.4 above) contains nine separate resonances, in accord with the anticipated absence of molecular (mirror) symmetry. Crucially, the highest-frequency resonance (at 21.10 p.p.m.) in this spectrum is substantially separated (to high chemical shift) from the other eight peaks (range 2.37 to -21.68 p.p.m.), and shows clear ^{195}Pt satellites ($^1J_{BPt}$ is *ca.* 300Hz). The appearance of such a resonance has been proposed **[80]** to be diagnostic of a non-isomerised 3,1,2-PtC_2B_9 cluster architecture, and the peak may be assigned as the unique boron atom [B(8)] on the C_2B_3 ligating carbaborane face. Consistent with this is the presence of two further, ^{195}Pt-coupled boron resonances (at -18.89 and - 21.68 p.p.m.) which have smaller coupling constants ($^1J_{BPt}$ here is *ca.* 200Hz), and which are jointly assigned to the other two boron atoms [B(4), B(7)] on the C_2B_3 face. [The observation of a larger ^{195}Pt-^{11}B coupling constant for B(8) than for B(4) and B(7) is not inconsistent with the anticipated stronger bonding between platinum and the former atom, on the basis of the molecular orbital description presented earlier.]

Synthesis and Characterisation of 1-Ph-2-Me-3,3-$(Et_3P)_2$-3,1,2-$PtC_2B_9H_9$, 11

Compound **11** was prepared and characterised in a manner analogous to that for **10** above. The reaction of $[(Et_3P)_2PtCl_2]$ with Tl[(Tl)8] in CH_2Cl_2, followed by filtration and chromatographic work-up (prep. t.l.c.; CH_2Cl_2/*n*-hexane, 3:1; product *Rf* 0.8) gives **11** in good yield.

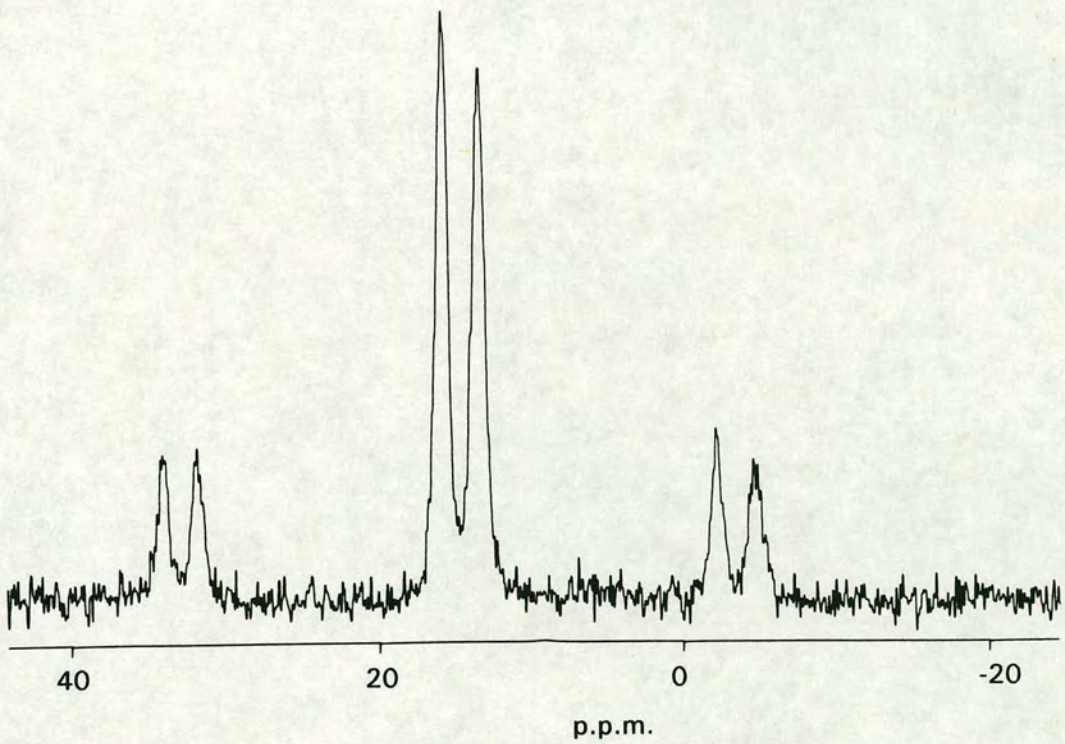

Figure 3.5 81.02 MHz ^{31}P n.m.r. spectrum of **11**

The phosphorus (^{31}P) n.m.r. spectrum of **11** (figure 3.5) is significantly different from that of **10**. Hindered rotation of the $\{(Et_3P)_2Pt\}$ is inferred from the presence of two separate, platinum-coupled phosphorus resonances (at

16.09 and 13.72 p.p.m.). (In the ^{1}H n.m.r. spectrum, the region corresponding to those protons of the ethyl groups is complex but appears, nevertheless, likewise to correlate with inequivalence of the two phosphine ligands.) Again, the two values of $^{1}J_{PPt}$ (*ca.* 2930 and 2950 Hz respectively) are typical of a *cis* arrangement of the two phosphine ligands. All six signals are broadened by two-bond phosphorus-phosphorus coupling ($^{2}J_{PP}$ between the two inequivalent ligands); this second coupling is not resolved, but appears to be of the order of 10Hz.

In contrast, the ^{11}B n.m.r. spectrum of **11** is very similar to that of **10**. There are again nine resonances (with one coincidence), of which eight lie in the range 2.52 to -21.93 p.p.m. The ninth boron peak is shifted considerably to high frequency (22.17 p.p.m.) and shows apparent platinum-195 satellites ($^{1}J_{BPt}$ is approximately 270Hz). This spectrum again indicates the presence of a 3,1,2-PtC_2B_9 cluster geometry.

Crystallographic Study Of 11

Diffraction quality orange *blocks* of **11** were obtained by the slow evaporation of a moderately concentrated solution of **11** at ambient temperatures. (Good quality crystals could also be obtained by slow diffusion of *i*-hexane into a dichloromethane solution of **11** at -30°C, but those obtained by the former method were deemed to be of a far superior quality.)

One quadrant of diffracted *X*-radiation was measured at ambient temperature, and the structure was solved **[113]** by Patterson (Pt) and difference Fourier (P, C, B) syntheses. The structure was refined by iterative least squares on *F* with alkyl, aryl and cage H atoms in idealised positions, and with the phenyl ring constrained as a planar regular hexagon. The data benefited from an empirical absorption correction and, following this, all non-H atoms were allowed to refine with anisotropic thermal parameters.

Four molecules of **11** crystallise in the monoclinic space group $P2_1/n$ with no significant intermolecular approaches.

In figure 3.6 are shown a perspective view of a single molecule of **11** and the atomic numbering scheme employed; the phenyl ring is numbered cyclically. Selected internuclear distances and interbond angles are listed in table 3.3.

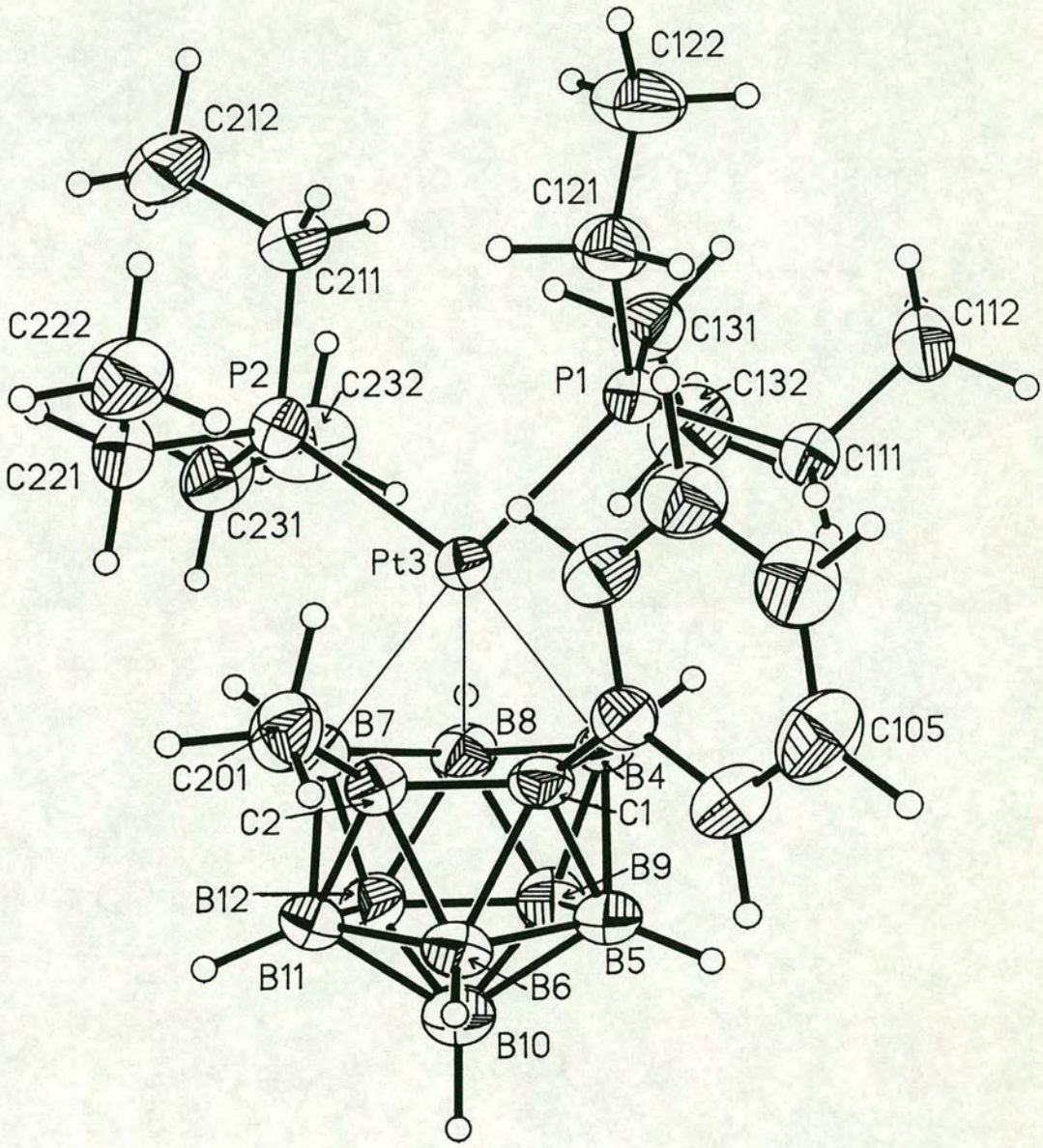

Figure 3.6 Perspective view of a single molecule of **11** (50% thermal ellipsoids; H atoms given radii of 0.1Å for clarity)

Table 3.3 Selected Interatomic Distances (Å) and Interbond Angles (°) for **11**

Pt(3) - P(1)	2.2952(13)	B(4) - B(8)	1.806(8)
Pt(3) - P(2)	2.2972(14)	B(4) - B(9)	1.832(9)
Pt(3) - C(1)	2.834(5)	B(5) - B(6)	1.749(9)
Pt(3) - C(2)	2.835(5)	B(5) - B(9)	1.770(9)
Pt(3) - B(4)	2.276(6)	B(5) -B(10)	1.796(9)
Pt(3) - B(7)	2.272(6)	B(6) -B(10)	1.757(10)
Pt(3) - B(8)	2.182(6)	B(6) -B(11)	1.766(9)
P(1) -C(111)	1.834(6)	B(7) - B(8)	1.792(9)
P(1) -C(121)	1.855(6)	B(7) -B(11)	1.811(9)
P(1) -C(131)	1.824(6)	B(7) -B(12)	1.826(9)
P(2) -C(211)	1.836(6)	B(8) - B(9)	1.757(9)
P(2) -C(221)	1.819(6)	B(8) -B(12)	1.761(9)
P(2) -C(231)	1.822(7)	B(9) -B(10)	1.753(10)
C(1) - C(2)	1.532(7)	B(9) -B(12)	1.753(10)
C(1) - B(4)	1.786(7)	B(10) -B(11)	1.764(10)
C(1) - B(5)	1.673(8)	B(10) -B(12)	1.755(10)
C(1) - B(6)	1.727(8)	B(11) -B(12)	1.736(10)
C(1) -C(101)	1.507(6)	C(111)-C(112)	1.531(8)
C(2) - B(6)	1.724(8)	C(121)-C(122)	1.492(9)
C(2) - B(7)	1.783(8)	C(131)-C(132)	1.538(10)
C(2) -B(11)	1.666(9)	C(211)-C(212)	1.540(9)
C(2) -C(201)	1.515(8)	C(221)-C(222)	1.527(10)
B(4) - B(5)	1.838(9)	C(231)-C(232)	1.520(10)

P(1) -Pt(3) - P(2)	97.81(5)	Pt(3) - B(4) - B(8)	63.4(3)
P(1) -Pt(3) - C(1)	108.65(10)	Pt(3) - B(4) - B(9)	119.9(3)
P(1) -Pt(3) - C(2)	134.91(11)	C(1) - B(4) - B(5)	55.0(3)
P(1) -Pt(3) - B(4)	97.54(15)	C(1) - B(4) - B(8)	109.7(4)
P(1) -Pt(3) - B(7)	171.03(16)	B(5) - B(4) - B(9)	57.7(3)
P(1) -Pt(3) - B(8)	128.12(17)	B(8) - B(4) - B(9)	57.8(3)
P(2) -Pt(3) - C(1)	137.66(10)	C(1) - B(5) - B(4)	60.9(3)
P(2) -Pt(3) - C(2)	108.39(11)	C(1) - B(5) - B(6)	60.5(3)
P(2) -Pt(3) - B(4)	163.86(15)	B(4) - B(5) - B(9)	61.0(3)
P(2) -Pt(3) - B(7)	91.00(16)	B(6) - B(5) -B(10)	59.4(4)
P(2) -Pt(3) - B(8)	117.42(17)	B(9) - B(5) -B(10)	58.9(4)
C(1) -Pt(3) - C(2)	31.35(14)	C(1) - B(6) - C(2)	52.7(3)
C(1) -Pt(3) - B(4)	39.02(17)	C(1) - B(6) - B(5)	57.5(3)
C(1) -Pt(3) - B(7)	63.11(18)	C(2) - B(6) -B(11)	57.0(3)
C(1) -Pt(3) - B(8)	70.32(19)	B(5) - B(6) -B(10)	61.6(4)
C(2) -Pt(3) - B(4)	63.04(18)	B(10) - B(6) -B(11)	60.1(4)
C(2) -Pt(3) - B(7)	38.93(18)	Pt(3) - B(7) - C(2)	87.9(3)

C(2) -Pt(3) - B(8)	70.07(19)	Pt(3) - B(7) - B(8)	63.7(3)
B(4) -Pt(3) - B(7)	73.85(21)	Pt(3) - B(7) -B(11)	137.2(4)
B(4) -Pt(3) - B(8)	47.76(22)	Pt(3) - B(7) -B(12)	120.7(4)
B(7) -Pt(3) - B(8)	47.39(22)	C(2) - B(7) - B(8)	110.1(4)
Pt(3) - P(1) -C(111)	115.07(18)	C(2) - B(7) -B(11)	55.2(3)
Pt(3) - P(1) -C(121)	115.88(19)	B(8) - B(7) -B(12)	58.3(4)
Pt(3) - P(1) -C(131)	112.10(20)	B(11) - B(7) -B(12)	57.0(4)
C(111)- P(1) -C(121)	102.2(3)	Pt(3) - B(8) - B(4)	68.8(3)
C(111)- P(1) -C(131)	102.0(3)	Pt(3) - B(8) - B(7)	69.0(3)
C(121)- P(1) -C(131)	108.2(3)	Pt(3) - B(8) - B(9)	129.1(4)
Pt(3) - P(2) -C(211)	122.41(19)	Pt(3) - B(8) -B(12)	129.3(4)
Pt(3) - P(2) -C(221)	116.45(20)	B(4) - B(8) - B(7)	98.8(4)
Pt(3) - P(2) -C(231)	107.29(21)	B(4) - B(8) - B(9)	61.8(4)
C(211)- P(2) -C(221)	102.6(3)	B(7) - B(8) -B(12)	61.8(4)
C(211)- P(2) -C(231)	104.0(3)	B(9) - B(8) -B(12)	59.8(4)
C(221)- P(2) -C(231)	101.6(3)	B(4) - B(9) - B(5)	61.3(3)
Pt(3) - C(1) - C(2)	74.3(3)	B(4) - B(9) - B(8)	60.4(3)
Pt(3) - C(1) - B(4)	53.34(22)	B(5) - B(9) -B(10)	61.3(4)
Pt(3) - C(1) - B(5)	113.9(3)	B(8) - B(9) -B(12)	60.2(4)
Pt(3) - C(1) - B(6)	128.6(3)	B(10) - B(9) -B(12)	60.1(4)
Pt(3) - C(1) -C(101)	107.2(3)	B(5) -B(10) - B(6)	59.0(4)
C(2) - C(1) - B(4)	109.5(4)	B(5) -B(10) - B(9)	59.8(4)
C(2) - C(1) - B(6)	63.6(3)	B(6) -B(10) -B(11)	60.2(4)
C(2) - C(1) -C(101)	120.0(4)	B(9) -B(10) -B(12)	60.0(4)
B(4) - C(1) - B(5)	64.1(3)	B(11) -B(10) -B(12)	59.1(4)
B(4) - C(1) -C(101)	118.4(4)	C(2) -B(11) - B(6)	60.3(4)
B(5) - C(1) - B(6)	61.9(3)	C(2) -B(11) - B(7)	61.5(3)
B(5) - C(1) -C(101)	120.1(4)	B(6) -B(11) -B(10)	59.7(4)
B(6) - C(1) -C(101)	118.5(4)	B(7) -B(11) -B(12)	61.9(4)
Pt(3) - C(2) - C(1)	74.3(3)	B(10) -B(11) -B(12)	60.2(4)
Pt(3) - C(2) - B(6)	128.7(3)	B(7) -B(12) - B(8)	59.9(4)
Pt(3) - C(2) - B(7)	53.21(23)	B(7) -B(12) -B(11)	61.1(4)
Pt(3) - C(2) -B(11)	112.9(3)	B(8) -B(12) - B(9)	60.0(4)
Pt(3) - C(2) -C(201)	110.3(3)	B(9) -B(12) -B(10)	60.0(4)
C(1) - C(2) - B(6)	63.7(3)	B(10) -B(12) -B(11)	60.7(4)
C(1) - C(2) - B(7)	109.8(4)	C(1) -C(101)-C(102)	119.9(3)
C(1) - C(2) -C(201)	120.1(4)	C(1) -C(101)-C(106)	120.0(3)
B(6) - C(2) -B(11)	62.8(4)	P(1) -C(111)-C(112)	115.4(4)
B(6) - C(2) -C(201)	115.6(4)	P(1) -C(121)-C(122)	120.2(4)
B(7) - C(2) -B(11)	63.3(4)	P(1) -C(131)-C(132)	112.1(5)
B(7) - C(2) -C(201)	119.9(4)	P(2) -C(211)-C(212)	116.0(4)
B(11) - C(2) -C(201)	118.5(5)	P(2) -C(221)-C(222)	114.9(5)
Pt(3) - B(4) - C(1)	87.6(3)	P(2) -C(231)-C(232)	114.6(5)
Pt(3) - B(4) - B(5)	137.0(4)		

Molecules of **11** adopt a solid-state structure that is fully consistent with the (solution) n.m.r. spectra discussed earlier; the vertices of the dicarbaplatinaborane moiety describe a rather distorted icosahedron of 3,1,2-PtC_2B_9 formulation similar to that observed in the analogous compounds **A** to **E** discussed above. The angular metal fragment has a *pseudo* square planar geometry, with P(1)-Pt(3)-P(2) 97.81(5)°; the plane defined by the atoms P(1), P(2) and Pt(3) lies at an angle of some 6.0° to the predicted [77] electronically-preferred conformation, with P(2) moving away from the C_{cage}-bound substituents. The platinum atom is elevated 1.89Å above the least squares plane through the ligating C_2B_3 face, somewhat greater than that found in **A** to **E** above. In both phosphine ligands there is some distortion from tetrahedral geometry at the phosphorus atom, with some enlargement and compression of the Pt—P—C and C—P—C angles arising from close intramolecular approaches between pendant groups; this behaviour is similar to that observed previously (for example, in **A**). In addition, the largest Pt—P—C angles are those for the ethyl groups closest to the C_{cage}-bound substituents, consistent with the crowded nature of this molecule.

The cage-bound phenyl group is oriented relative to the C_2B_3 face of the carbaborane ligand to afford a value of θ_{Ph} (see Chapter 2) of 33.2°*, much larger than in the parent *closo* carbaborane **1** (where θ_{Ph} = 16.7°), despite the unfavourable {C_{cage}—Me}···{C_{cage}—Ph} approach this produces. This conformation appears to allow the cage-bound phenyl substituent to "*insert*" between the two triethylphosphine ligands (see figure 3.7). A further consequence of - or perhaps the reason for - this orientation of the phenyl group, is a close Pt···H approach: Pt(3)···H(102) is only 2.762Å. (There is no evidence for such an interaction in the room-temperature solution ^{1}H n.m.r. spectrum.) The phenyl and methyl groups bound to the carbaborane moiety at C(1) and C(2) have values of χ [elevation relative to the B(5, 6, 11, 12, 9) plane] of 28.2° and 24.8° respectively (*c.f.* χ = 26° for an ideal icosahedron); this occurs despite the fact that this (unfavourably) brings the C_{cage}-bound phenyl substituent closer to the area of space occupied by the two phosphines.

---

* Note that in this chapter the twist angle of the C_{cage}-bound phenyl substituent is denoted θ_{Ph}, to distinguish this from the cage "folding" parameter θ.

Figure 3.7 Space filling representation of **11** showing cage-bound phenyl group lying between Et_3P ligands, and proximity of H(102) to Pt(3)

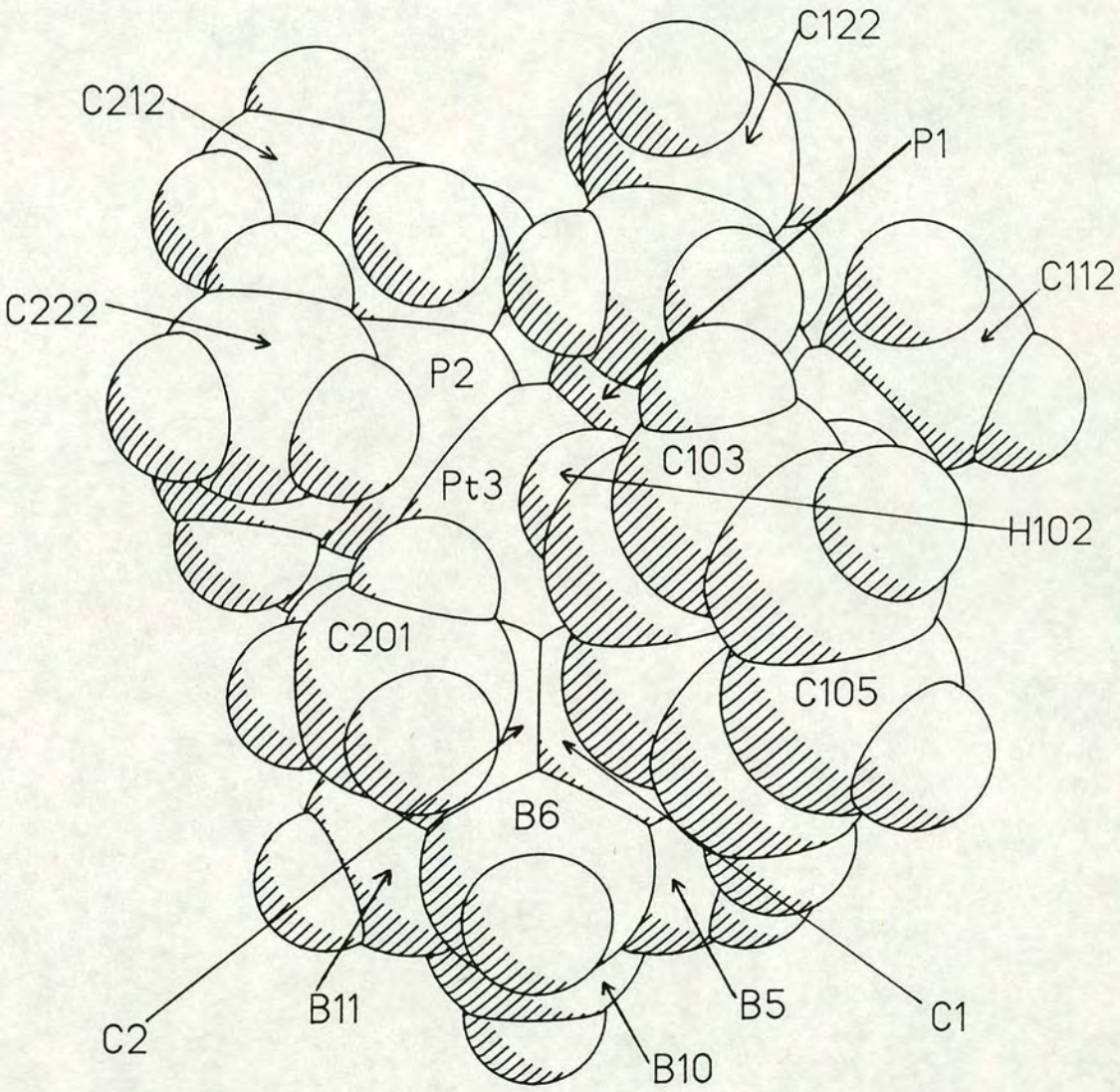

The C(1)—C(2) distance in **11** is 1.532(7)Å, which is essentially the same as in the analogues **A**, **B**, **D** and **E**. Likewise, the ligating carbaborane face in **11** is folded about the B(4)···B(7) vector, resulting in $\theta = 5.53°$ and $\phi = 8.11°$; these are comparable to, but slightly larger than, those found in **A**, **B** and **C**. However, in contrast to the previous analogues **A** to **E**, the value of the slip parameter Δ is substantially greater, being 0.74Å. This is reflected in distances to the C_{cage} atoms [Pt(3)···C(1) is 2.834(5), and Pt(3)···C(2) is 2.835(5)Å] in **11** which are much longer than previously (average 2.51Å) - and indeed are almost non-bonding - and a correspondingly much shorter Pt(3)—B(8) distance of 2.182(6)Å (*c.f.* previous average 2.25Å); the Pt(3)—B(4) and Pt(3)—B(7) distances are 2.276(6) and 2.272(6)Å, similar to those observed formerly (average 2.27Å) - perhaps as a consequence of the slightly increased folding of the ligating C_2B_3 face in **11**. The upper C_2B_3 face is also slightly slipped with respect to the lower B_5 belt, by some 0.08Å [towards the midpoint of the B(9)—B(12) vector]: this slightly enhances Δ, but it is, even so, still very much greater than in the aforementioned analogous platinum complexes which suffer similar interplane slippages. The close proximity of H(102) to the platinum atom is likely to contribute to the above slippage: a filled d_{z^2} orbital points towards this H atom, a probable consequence of which is a repulsive Pt···H interaction.

Synthesis and Characterisation of 1-Ph-2-Me-3,3-$(Ph_3P)_2$-3,1,2-$PtC_2B_9H_9$, 12

Reaction of equimolar quantities of $[(Ph_3P)_2PtCl_2]$ with Tl[(Tl)8] in CH_2Cl_2 over *ca.* 15 hours, followed by filtration, affords an orange solution of **12**. This filtrate was concentrated and applied to a chromatographic column (Florisil®, prewashed with eluant; CH_2Cl_2/*n*-hexane, 9:1) which, upon elution, gave a single mobile orange band which was collected and identified as **12**.

In common with that of **11**, the ^{31}P n.m.r. spectrum of **12** shows two (mutually *cis*) platinum-bound phosphine ligands which are inequivalent on the n.m.r. timescale, rotation about the Pt···cage vector being hindered by intramolecular crowding [values of $^1J_{PPt}$ are 3075 (δ_P = 29.13 p.p.m.) and 3295 (δ_P = 22.16 p.p.m.); $^2J_{PP}$ not resolved]. Likewise, the ^{11}B n.m.r. spectrum of **12**, although poorly resolved as a consequence of the compound's low solubility, shows a comparable pattern of resonances to those for **10** and **11**; there is again a separated, high frequency resonance (25.83 p.p.m.; *c.f.* 4.95 to -24.65 p.p.m. for the eight other resonances), although in this instance platinum satellites cannot definitely be detected.

This similarity in the boron n.m.r. spectrum of **12** to that of the two previous analogues confirms that, despite the somewhat larger cone angle of the present phosphine, the overall PtC_2B_9 polyhedron retains a 3,1,2-arrangement of vertices; *i.e.*, that even a molecule which suffers intramolecular crowding to the degree anticipated in **12** does not spontaneously isomerise at ambient temperatures. However, the structural studies of **12** described below will demonstrate a significant influence of steric crowding upon the molecular structure of the complex.

Synthesis and Characterisation of 1-Ph-2-Me-3,3-(p-tol$_3$P)$_2$-3,1,2-PtC$_2$B$_9$H$_9$, 13

Similarly, the interaction of [(p-tol$_3$P)$_2$PtCl$_2$] with Tl[(Tl)8] in CH_2Cl_2 over *ca.* 18 hours, followed by filtration, column chromatographic purification (Florisil®, prewashed with eluant; CH_2Cl_2/n-hexane, 9:1), and evaporation of the mobile orange band collected, affords **13** as an orange solid. The identity of the product was confirmed by conventional microanalytical and spectroscopic means.

Structurally, **12** and **13** would be expected to have very similar properties (the two phosphines have identical cone angles); indeed, their n.m.r. spectra show similar patterns of resonances with **13** confirmed to have hindered metal fragment rotation, and a 3,1,2-PtC$_2$B$_9$ cluster structure. Again, poor solubility limits the resolution of the ^{11}B n.m.r. spectrum and it cannot be said definitely whether the high frequency resonance found for **13** couples to a platinum atom.

Poor quality orange *plates* of **13** (probably as the dichloromethane solvate) were obtained by slow diffusion of n-hexane into a CH_2Cl_2 solution of **13** at -30°C. These were, however, somewhat unstable with respect to solvent loss, and were consequently deemed unsuitable for *X*-ray diffraction analysis. (In any case, it was anticipated that the molecular structure of **13** would be very similar to that of **12**.)

Crystallographic Study of 12 .0.5CH_2Cl_2

Diffraction quality yellow-orange *blocks* of **12** as the 0.5-dichloromethane solvate were obtained by the slow diffusion of *n*-hexane into a concentrated CH_2Cl_2 solution at -30°C.

One hemisphere of *X*-ray diffraction data was collected at ambient temperatures. The structure was solved without difficulty; the Pt atom was located by inspection of the Patterson function **[113]**, whilst the remaining non-H atoms were found from difference Fourier maps. All H atoms were set in calculated positions, and the phenyl rings were constrained to be rigid, planar hexagons. An empirical absorption correction was applied, and all non-H atoms (except those of the solvate) were allowed to refine with anisotropic temperature factors.

In the present crystalline modification, two molecules of **12** cocrystallise with one of dichloromethane in the triclinic space group *P*bar1. There are no close intermolecular contacts. However, the solvate molecule is located close to an inversion centre (½, ½, ½) and is therefore found, on average, in 50% of asymmetric fractions; the one molecule per unit cell is effectively shared statistically between the two symmetry-related sites.

A perspective view of a single molecule of **12** (termed **12A** in this crystalline form), and the atomic numbering scheme employed, are shown in figure 3.8; phenyl rings are labelled cyclically. In table 3.4 are listed selected internuclear distances and interbond angles for both **12A** and the solvate molecule.

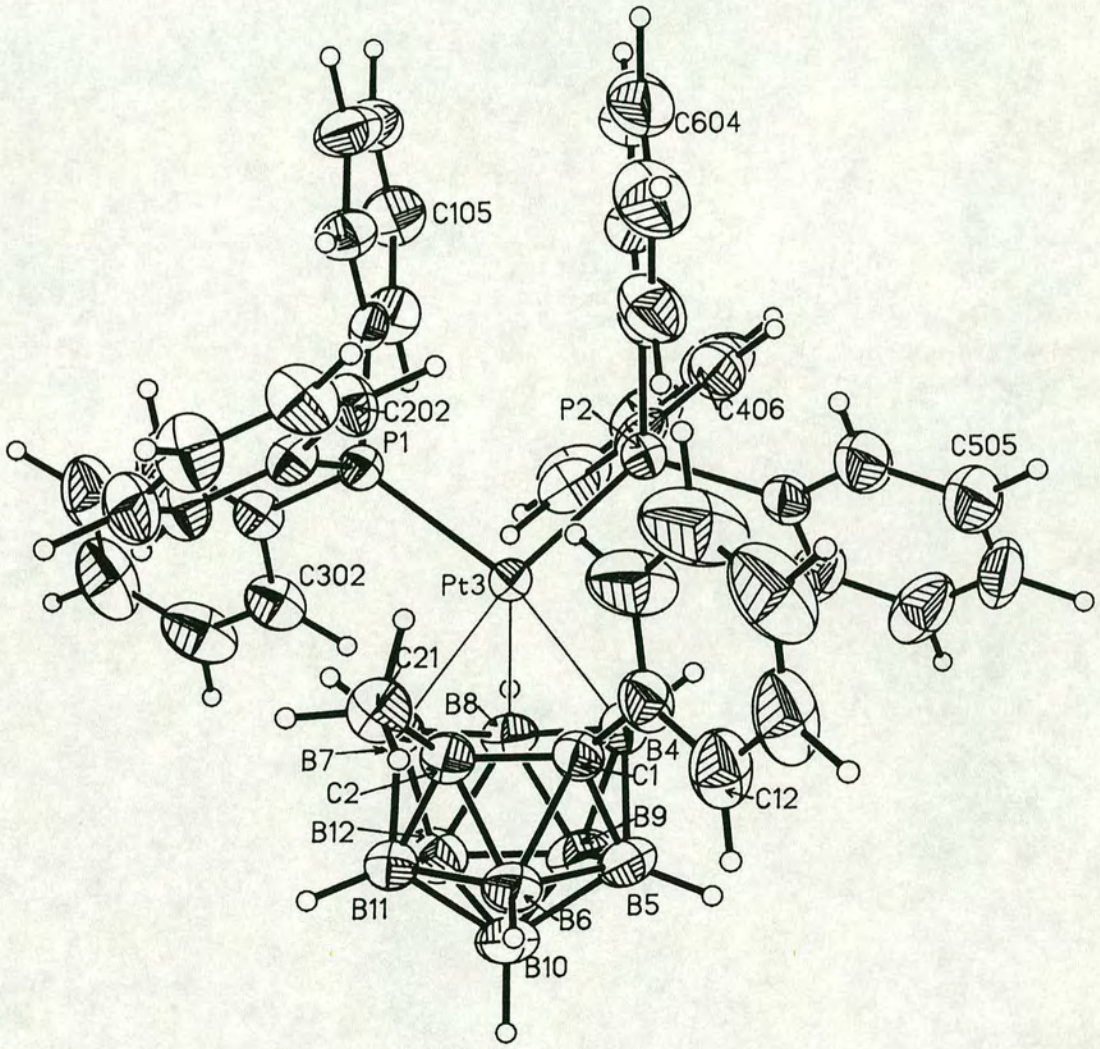

Figure 3.8 Perspective view of a single molecule of **12A** in **12 .0.5CH_2Cl_2** (50% thermal ellipsoids; H atoms given radii of 0.1Å for clarity)

Table 3.4 Selected Interatomic Distances (Å) and Interbond Angles (°) for **12A** and the solvate molecule in **12 .0.5CH_2Cl_2**

C(1) - C(2)	1.525(9)	B(5) -B(10)	1.772(12)
C(1) -Pt(3)	3.003(6)	B(6) -B(10)	1.748(12)
C(1) - B(4)	1.765(10)	B(6) -B(11)	1.767(11)
C(1) - B(5)	1.658(10)	B(7) - B(8)	1.850(10)
C(1) - B(6)	1.713(10)	B(7) -B(11)	1.801(10)
C(1) -C(11)	1.502(8)	B(7) -B(12)	1.861(11)
C(2) -Pt(3)	2.980(6)	B(8) - B(9)	1.742(11)
C(2) - B(6)	1.730(10)	B(8) -B(12)	1.762(11)
C(2) - B(7)	1.728(9)	B(9) -B(10)	1.762(12)
C(2) -B(11)	1.643(9)	B(9) -B(12)	1.759(12)
C(2) -C(21)	1.513(9)	B(10) -B(11)	1.778(11)
Pt(3) - B(4)	2.324(8)	B(10) -B(12)	1.734(12)
Pt(3) - B(7)	2.291(7)	B(11) -B(12)	1.756(11)
Pt(3) - B(8)	2.143(7)	P(1) -C(101)	1.843(4)
Pt(3) - P(1)	2.3140(15)	P(1) -C(201)	1.818(4)
Pt(3) - P(2)	2.2940(16)	P(1) -C(301)	1.830(4)
B(4) - B(5)	1.797(11)	P(2) -C(401)	1.830(5)
B(4) - B(8)	1.826(11)	P(2) -C(501)	1.837(5)
B(4) - B(9)	1.849(11)	P(2) -C(601)	1.831(5)
B(5) - B(6)	1.751(12)	C(1S) -Cl(1S)	1.31(4)
B(5) - B(9)	1.766(12)	C(1S) -Cl(2S)	1.47(3)

C(2) - C(1) -Pt(3)	74.4(3)	C(2) - B(7) -Pt(3)	94.7(4)
C(2) - C(1) - B(4)	109.0(5)	C(2) - B(7) - B(8)	111.3(5)
C(2) - C(1) - B(6)	64.3(4)	C(2) - B(7) -B(11)	55.4(4)
C(2) - C(1) -C(11)	118.9(5)	Pt(3) - B(7) - B(8)	61.2(3)
Pt(3) - C(1) - B(4)	50.6(3)	B(8) - B(7) -B(12)	56.7(4)
Pt(3) - C(1) -C(11)	108.4(3)	B(11) - B(7) -B(12)	57.3(4)
B(4) - C(1) - B(5)	63.2(4)	Pt(3) - B(8) - B(4)	71.2(3)
B(4) - C(1) -C(11)	118.6(5)	Pt(3) - B(8) - B(7)	69.6(3)
B(5) - C(1) - B(6)	62.6(4)	B(4) - B(8) - B(7)	94.9(5)
B(5) - C(1) -C(11)	122.3(5)	B(4) - B(8) - B(9)	62.3(4)
B(6) - C(1) -C(11)	118.8(5)	B(7) - B(8) -B(12)	62.0(4)
C(1) - C(2) -Pt(3)	76.1(3)	B(9) - B(8) -B(12)	60.3(5)
C(1) - C(2) - B(6)	63.1(4)	B(4) - B(9) - B(5)	59.6(4)
C(1) - C(2) - B(7)	110.6(5)	B(4) - B(9) - B(8)	61.1(4)
C(1) - C(2) -C(21)	120.3(5)	B(5) - B(9) -B(10)	60.3(5)
Pt(3) - C(2) - B(7)	50.0(3)	B(8) - B(9) -B(12)	60.4(5)
Pt(3) - C(2) -C(21)	110.3(4)	B(10) - B(9) -B(12)	59.0(5)
B(6) - C(2) -B(11)	63.1(4)	B(5) -B(10) - B(6)	59.7(5)

B(6) - C(2) -C(21)	117.2(5)	B(5) -B(10) - B(9)	60.0(5)
B(7) - C(2) -B(11)	64.5(4)	B(6) -B(10) -B(11)	60.1(4)
B(7) - C(2) -C(21)	117.6(5)	B(9) -B(10) -B(12)	60.4(5)
B(11) - C(2) -C(21)	118.2(5)	B(11) -B(10) -B(12)	60.0(5)
C(1) -Pt(3) - C(2)	29.53(16)	C(2) -B(11) - B(6)	60.8(4)
C(1) -Pt(3) - B(4)	35.93(22)	C(2) -B(11) - B(7)	60.0(4)
C(1) -Pt(3) - B(7)	58.93(21)	B(6) -B(11) -B(10)	59.1(4)
C(1) -Pt(3) - B(8)	68.07(23)	B(7) -B(11) -B(12)	63.1(4)
C(1) -Pt(3) - P(1)	131.41(12)	B(10) -B(11) -B(12)	58.8(5)
C(1) -Pt(3) - P(2)	115.52(12)	B(7) -B(12) - B(8)	61.4(4)
C(2) -Pt(3) - B(4)	59.25(22)	B(7) -B(12) -B(11)	59.6(4)
C(2) -Pt(3) - B(7)	35.31(21)	B(8) -B(12) - B(9)	59.3(5)
C(2) -Pt(3) - B(8)	68.20(23)	B(9) -B(12) -B(10)	60.6(5)
C(2) -Pt(3) - P(1)	105.15(12)	B(10) -B(12) -B(11)	61.2(5)
C(2) -Pt(3) - P(2)	142.83(12)	C(1) -C(11) -C(12)	120.1(4)
B(4) -Pt(3) - B(7)	71.9(3)	C(1) -C(11) -C(16)	119.9(4)
B(4) -Pt(3) - B(8)	48.1(3)	Pt(3) - P(1) -C(101)	123.97(14)
B(4) -Pt(3) - P(1)	163.35(19)	Pt(3) - P(1) -C(201)	108.02(14)
B(4) -Pt(3) - P(2)	97.91(19)	Pt(3) - P(1) -C(301)	113.67(14)
B(7) -Pt(3) - B(8)	49.2(3)	C(101)- P(1) -C(201)	104.70(19)
B(7) -Pt(3) - P(1)	91.96(18)	C(101)- P(1) -C(301)	98.31(19)
B(7) -Pt(3) - P(2)	168.69(18)	C(201)- P(1) -C(301)	106.71(19)
B(8) -Pt(3) - P(1)	123.50(20)	Pt(3) - P(2) -C(401)	112.03(15)
B(8) -Pt(3) - P(2)	120.32(20)	Pt(3) - P(2) -C(501)	116.03(16)
P(1) -Pt(3) - P(2)	98.50(5)	Pt(3) - P(2) -C(601)	117.91(17)
C(1) - B(4) -Pt(3)	93.5(4)	C(401)- P(2) -C(501)	97.54(21)
C(1) - B(4) - B(5)	55.5(4)	C(401)- P(2) -C(601)	105.74(21)
C(1) - B(4) - B(8)	111.4(5)	C(501)- P(2) -C(601)	105.23(22)
Pt(3) - B(4) - B(8)	60.8(3)	P(1) -C(101)-C(102)	123.3(3)
B(5) - B(4) - B(9)	57.9(4)	P(1) -C(101)-C(106)	116.7(3)
B(8) - B(4) - B(9)	56.6(4)	P(1) -C(201)-C(202)	117.7(3)
C(1) - B(5) - B(4)	61.3(4)	P(1) -C(201)-C(206)	122.3(3)
C(1) - B(5) - B(6)	60.2(4)	P(1) -C(301)-C(302)	121.7(3)
B(4) - B(5) - B(9)	62.5(5)	P(1) -C(301)-C(306)	118.3(3)
B(6) - B(5) -B(10)	59.5(5)	P(2) -C(401)-C(402)	119.9(3)
B(9) - B(5) -B(10)	59.7(5)	P(2) -C(401)-C(406)	119.9(3)
C(1) - B(6) - C(2)	52.6(4)	P(2) -C(501)-C(502)	117.0(3)
C(1) - B(6) - B(5)	57.2(4)	P(2) -C(501)-C(506)	123.0(3)
C(2) - B(6) -B(11)	56.0(4)	P(2) -C(601)-C(602)	122.1(4)
B(5) - B(6) -B(10)	60.8(5)	P(2) -C(601)-C(606)	117.9(4)
B(10) - B(6) -B(11)	60.8(4)	Cl(1S)-C(1S) -Cl(2S)	134.7(24)

Structurally **12A** appears very similar to **11**, with the PtC_2B_9 polyhedron being a distorted icosahedron in which the three heteroatoms (Pt, 2C) occupy mutually adjacent vertices of a triangular face. The metal fragment is again of a *pseudo*-square planar geometry [P(1)-Pt(3)-P(2) is 98.50(5)°]; and the geometry at the two phosphorus atoms is essentially tetrahedral, with the Pt—P—C angles showing some distortions effected by intramolecular interactions, resembling the situation in **11** (in the present case, however, the exact origin of these appears to be a subtle combination of inter-substituent repulsions and perhaps "graphitic" interactions between the various phenyl groups). Similar steric influences cause slight bending of the phosphino phenyl groups at their respective points of attachment to phosphorus; significant deviations from the (ideal) 120° angle are noted for several angles P-C(*n*01)-C(*n*02) and P-C(*n*01)-C(*n*06) (for $n = 1, 2, 5, 6$).

The platinum atom in **12A** is located at an elevation of 1.90Å above the least-squares plane through the ligating C(1)C(2)B(4)B(8)B(7) face of the carbaborane ligand (slightly more than in **11**), and the plane defined by the platinum and two phosphorus ligands is again rotated by 6.0° from its electronically-preferred position - although this appears to occur in the opposite direction to that found in **11**, perhaps in response to steric influences.

In **12A**, as in **11**, the C_{cage}-bound phenyl group has a conformation which is not far from orthogonal to the C(1)—C(2) connectivity, with $\theta_{Ph} = 28.2°$ slightly smaller than in **11**. Likewise, this again appears to afford this phenyl substituent a *niche* between the two triphenylphosphine ligands; and there is a β-H atom [H(16)] which is close to Pt(3) [Pt(3)···H(16) is only 2.835Å]. The pendant phenyl and methyl groups bound to C(1) and C(2) respectively have angles of elevation (χ) of 29.0° and 26.2° respectively relative to the plane defined by B(5, 6, 11, 12, 9) (compared to $\chi = 26°$ in a regular icosahedron), mirroring the situation in **11**.

The C(1)—C(2) distance in **12A** is 1.525(9)Å, essentially the same as that in **11**, and in the analogues **A**, **B**, **D** and **E**. In common with these prior examples of such species, the upper C_2B_3 face of the carbaborane ligand in **12A** is folded - about B(4)···B(7) - giving rise to folding angles θ and ϕ of 6.4° and 8.9° respectively which are slightly larger than in the above-mentioned

relatives. However, **12A** differs significantly from these latter compounds in that the metal fragment is now *very substantially slipped*: the slip parameter Δ is 0.94Å. Thus, although Δ is again slightly increased by an additional lateral "interplane slippage" [0.06Å, towards the midpoint of B(9)—B(12)] of the C_2B_3 face relative to the lower B_5 girdle, the platinum fragment is perhaps more appropriately described as *pseudo*-σ-bonded to B(8). [In the "truly" σ-bound complex 10-*endo*-{PPh_3Hg}-7,8-$C_2B_9H_{11}$ **[79]**, Δ is 0.92Å and the interplane slip is *ca.* 0.15Å.] The large value of Δ is reflected in the Pt(3)···{cage} distances The Pt(3)···C_{cage} distances are now essentially non-bonding [Pt(3)···C(1) is 3.003(6)Å and Pt(3)···C(2) is 2.980(6)Å, much larger than previously]; the Pt(3)···B(4, 7) distances are also somewhat increased [Pt(3)—B(4) is 2.324(8)Å and Pt(3)—B(7) is 2.291(7)Å]; whilst the Pt(3)—B(8) bond [2.143(7)Å] is very short. It is additionally striking to recall that the substantial Pt fragment slippage has occurred *in addition* to the somewhat enhanced elevation of the metal atom above the ligating face.

The effect of the basicity of the metal-bound ligands upon slippage in systems of this type has been discussed **[134]**, and it has been demonstrated that - in the absence of other influences such as steric factors - ligands of higher basicity (which increase the electron density at the metal centre) cause an increased slippage. Thus, in the case of compounds **11** and **12**, intramolecular crowding has presumably overcome the electronic tendency for **11** to display a larger Δ value than **12**. The remarkable, sterically-induced slip distortion in **12A** might again be enhanced by the proposed Pt···$(\beta\text{-}H)_{Ph(cage)}$ interaction discussed above.

Crystallographic Study of 12 .(unknown solvent)

Slow diffusion of *n*-hexane into an n.m.r. sample [d^6-acetone/CH_2Cl_2 solvents] of **12** at -30°C afforded a modest number of well-formed yellow/orange *blocks*.

The intensities of one quadrant of diffracted *X*-radiation from one of these were measured at ambient temperature. The starting coordinates of the Pt atom were obtained by Patterson methods **[113]**, and the structure developed by difference Fourier syntheses (P, C, B atoms); methyl, phenyl and cage H atoms were set in calculated positions, and the phenyl rings constrained to be rigid hexagons. Inspection of ΔF maps also revealed an area in the asymmetric fraction of the unit cell apparently containing several peaks of electron density well separated from molecules of **12**. However, the chemical identity of this (solvate) species could not definitely be established, and was ultimately modelled as five carbon atoms of fixed arbitrary isotropic thermal parameter whose positions and occupancies were allowed some refinement before being set at fixed values. It is thought that this solvate portion consists of various, random molecules of acetone, dichloromethane and hexane in poorly-defined proportions.

Four molecules of **12** cocrystallise with unknown solvent molecules in the monoclinic space group $P2_1/n$, with no significant intermolecular approaches between the heteroborane and the solvate molecules.

A perspective view of a single molecule of **12** (identified as **12B** in this crystalline form) is shown in figure 3.9, wherein the atomic numbering scheme employed is also indicated (phenyl rings are labelled cyclically). In table 3.5 are listed selected internuclear distances and interbond angles for molecules of **12B**.

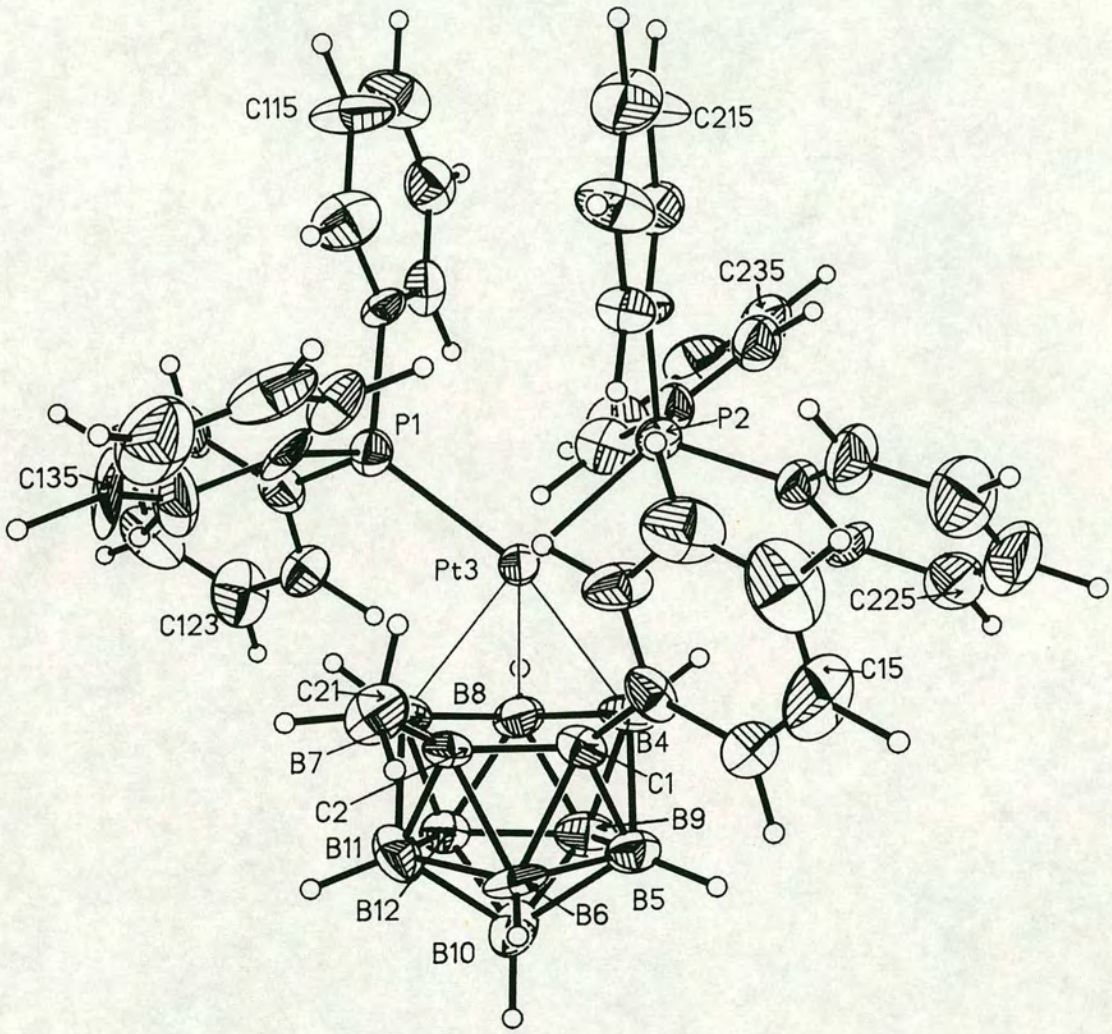

Figure 3.9 Perspective view of a single molecule of **12B** in **12.(unknown solvent)** (50% thermal ellipsoids; H atoms given radii of 0.1Å for clarity)

Table 3.5 Selected Internuclear Distances (Å) And Interbond Angles (°) for **12B** in **12.(unknown solvent)**

C(1) - C(2)	1.554(19)	B(5) - B(9)	1.78(3)
C(1) -Pt(3)	2.933(14)	B(5) -B(10)	1.79(3)
C(1) - B(4)	1.809(22)	B(6) -B(10)	1.75(3)
C(1) - B(5)	1.691(22)	B(6) -B(11)	1.76(3)
C(1) - B(6)	1.747(23)	B(7) - B(8)	1.844(25)
C(1) -C(11)	1.504(17)	B(7) -B(11)	1.82(3)
C(2) -Pt(3)	2.952(14)	B(7) -B(12)	1.832(25)
C(2) - B(6)	1.767(23)	B(8) - B(9)	1.72(3)
C(2) - B(7)	1.756(22)	B(8) -B(12)	1.700(24)
C(2) -B(11)	1.638(23)	B(9) -B(10)	1.78(3)
C(2) -C(21)	1.514(21)	B(9) -B(12)	1.73(3)
Pt(3) - B(4)	2.294(18)	B(10) -B(11)	1.78(3)
Pt(3) - B(7)	2.320(18)	B(10) -B(12)	1.81(3)
Pt(3) - B(8)	2.171(17)	B(11) -B(12)	1.80(3)
Pt(3) - P(1)	2.301(4)	P(1) -C(111)	1.854(10)
Pt(3) - P(2)	2.309(4)	P(1) -C(121)	1.822(11)
B(4) - B(5)	1.844(25)	P(1) -C(131)	1.824(11)
B(4) - B(8)	1.754(25)	P(2) -C(211)	1.815(10)
B(4) - B(9)	1.83(3)	P(2) -C(221)	1.842(12)
B(5) - B(6)	1.76(3)	P(2) -C(231)	1.811(10)

C(2) - C(1) -Pt(3)	75.4(7)	B(10) - B(6) -B(11)	61.0(10)
C(2) - C(1) - B(4)	109.1(11)	C(2) - B(7) -Pt(3)	91.8(9)
C(2) - C(1) - B(6)	64.4(9)	C(2) - B(7) - B(8)	109.3(12)
C(2) - C(1) -C(11)	121.2(11)	C(2) - B(7) -B(11)	54.5(9)
Pt(3) - C(1) - B(4)	51.5(7)	Pt(3) - B(7) - B(8)	61.6(7)
Pt(3) - C(1) -C(11)	105.6(7)	B(8) - B(7) -B(12)	55.1(9)
B(4) - C(1) - B(5)	63.5(9)	B(11) - B(7) -B(12)	58.9(10)
B(4) - C(1) -C(11)	116.2(11)	Pt(3) - B(8) - B(4)	70.6(8)
B(5) - C(1) - B(6)	61.5(10)	Pt(3) - B(8) - B(7)	70.0(8)
B(5) - C(1) -C(11)	120.8(11)	B(4) - B(8) - B(7)	99.1(12)
B(6) - C(1) -C(11)	121.1(11)	B(4) - B(8) - B(9)	63.8(10)
C(1) - C(2) -Pt(3)	74.0(7)	B(7) - B(8) -B(12)	62.1(10)
C(1) - C(2) - B(6)	63.1(9)	B(9) - B(8) -B(12)	60.8(10)
C(1) - C(2) - B(7)	109.7(11)	B(4) - B(9) - B(5)	61.4(10)
C(1) - C(2) -C(21)	121.0(12)	B(4) - B(9) - B(8)	59.1(10)
Pt(3) - C(2) - B(7)	51.8(7)	B(5) - B(9) -B(10)	60.6(10)
Pt(3) - C(2) -C(21)	113.1(9)	B(8) - B(9) -B(12)	59.1(10)
B(6) - C(2) -B(11)	62.3(10)	B(10) - B(9) -B(12)	62.1(10)
B(6) - C(2) -C(21)	114.9(12)	B(5) -B(10) - B(6)	59.5(10)
B(7) - C(2) -B(11)	64.7(10)	B(5) -B(10) - B(9)	59.6(10)

B(7) - C(2) -C(21)	119.6(12)	B(6) -B(10) -B(11)	59.9(10)
B(11) - C(2) -C(21)	117.1(12)	B(9) -B(10) -B(12)	57.5(10)
C(1) -Pt(3) - C(2)	30.6(4)	B(11) -B(10) -B(12)	59.9(10)
C(1) -Pt(3) - B(4)	38.1(5)	C(2) -B(11) - B(6)	62.5(10)
C(1) -Pt(3) - B(7)	60.8(5)	C(2) -B(11) - B(7)	60.8(10)
C(1) -Pt(3) - B(8)	67.9(5)	B(6) -B(11) -B(10)	59.1(10)
C(1) -Pt(3) - P(1)	132.9(3)	B(7) -B(11) -B(12)	60.9(10)
C(1) -Pt(3) - P(2)	111.9(3)	B(10) -B(11) -B(12)	60.8(10)
C(2) -Pt(3) - B(4)	61.6(5)	B(7) -B(12) - B(8)	62.8(10)
C(2) -Pt(3) - B(7)	36.5(5)	B(7) -B(12) -B(11)	60.2(10)
C(2) -Pt(3) - B(8)	68.0(5)	B(8) -B(12) - B(9)	60.1(10)
C(2) -Pt(3) - P(1)	105.4(3)	B(9) -B(12) -B(10)	60.4(10)
C(2) -Pt(3) - P(2)	139.5(3)	B(10) -B(12) -B(11)	59.2(10)
B(4) -Pt(3) - B(7)	72.8(6)	C(1) -C(11) -C(12)	118.8(9)
B(4) -Pt(3) - B(8)	46.2(6)	C(1) -C(11) -C(16)	121.2(10)
B(4) -Pt(3) - P(1)	164.1(5)	Pt(3) - P(1) -C(111)	123.2(3)
B(4) -Pt(3) - P(2)	96.5(5)	Pt(3) - P(1) -C(121)	113.4(4)
B(7) -Pt(3) - B(8)	48.4(6)	Pt(3) - P(1) -C(131)	110.7(4)
B(7) -Pt(3) - P(1)	91.2(4)	C(111)- P(1) -C(121)	97.0(5)
B(7) -Pt(3) - P(2)	169.2(4)	C(111)- P(1) -C(131)	104.0(5)
B(8) -Pt(3) - P(1)	122.4(5)	C(121)- P(1) -C(131)	106.8(5)
B(8) -Pt(3) - P(2)	122.7(5)	Pt(3) - P(2) -C(211)	117.3(4)
P(1) -Pt(3) - P(2)	99.42(14)	Pt(3) - P(2) -C(221)	114.7(4)
C(1) - B(4) -Pt(3)	90.5(8)	Pt(3) - P(2) -C(231)	112.3(3)
C(1) - B(4) - B(5)	55.1(9)	C(211)- P(2) -C(221)	103.1(5)
C(1) - B(4) - B(8)	110.1(12)	C(211)- P(2) -C(231)	105.6(5)
Pt(3) - B(4) - B(8)	63.2(8)	C(221)- P(2) -C(231)	102.1(5)
B(5) - B(4) - B(9)	57.8(10)	P(1) -C(111)-C(112)	116.2(7)
B(8) - B(4) - B(9)	57.1(10)	P(1) -C(111)-C(116)	123.7(7)
C(1) - B(5) - B(4)	61.4(9)	P(1) -C(121)-C(122)	120.9(7)
C(1) - B(5) - B(6)	60.8(10)	P(1) -C(121)-C(126)	119.1(7)
B(4) - B(5) - B(9)	60.8(10)	P(1) -C(131)-C(132)	115.5(8)
B(6) - B(5) -B(10)	59.0(10)	P(1) -C(131)-C(136)	124.5(8)
B(9) - B(5) -B(10)	59.9(10)	P(2) -C(211)-C(212)	115.7(7)
C(1) - B(6) - C(2)	52.5(8)	P(2) -C(211)-C(216)	124.3(7)
C(1) - B(6) - B(5)	57.7(9)	P(2) -C(221)-C(222)	122.8(9)
C(1) - B(6) -B(11)	97.6(12)	P(2) -C(221)-C(226)	117.2(8)
C(2) - B(6) - B(5)	99.5(12)	P(2) -C(231)-C(232)	120.1(7)
C(2) - B(6) -B(11)	55.3(9)	P(2) -C(231)-C(236)	119.9(7)
B(5) - B(6) -B(10)	61.5(10)		

Not unexpectedly, the molecules of **12** in the crystalline modification **12B** are rather similar to those found in **12A**, discussed above; gross differences

between the two forms arise from differing dispositions of the pendant phenyl groups.

The *pseudo* square planar {($Ph_3P)_2Pt$} fragment [P(1)—Pt(3)—P(2) is 99.42(14)°] is elevated 1.92Å above the C_2B_3 face, and is rotated by only 1.8° from its "electronically-preferred" orientation above this face; the geometry at phosphorus is again close to tetrahedral, and there is again evidence of significant "bending" of the phosphino phenyl groups at their points of attachment to the corresponding phosphorus atoms.

The phenyl substituent in **12B** is somewhat more twisted (about the C_{cage}—C_{Ph} bond) than in either **11** or **12A**, and has a θ_{Ph} value of 44.6°; this probably arises from the different metal fragment orientation (in **12A** and **12B**) which is ultimately a function of crystal packing forces. This metal fragment orientation does, nevertheless, again provide a close β-H approach, with Pt(3)···H(102) only 2.94Å. The elevations (χ) of the cage-bound methyl and phenyl groups relative to the B(5, 6, 11, 12, 9) plane show a similar pattern to that found in the related species **11**and **12A**, with somewhat larger deviations from χ = 26° (ideal icosahedron) in the present case: values of χ for the cage-bound phenyl and methyl groups are, respectively, 31.5° and 23.5°.

In **12B** the C(1)—C(2) distance is 1.554(19)Å, numerically slightly longer than in the species considered above. The upper C_2B_3 face of the carbaborane ligand is again folded about B(4)···B(7) with resulting fold angles θ and ϕ of 4.9° and 10.5° respectively; the latter angle is significantly larger than in the related complexes already discussed. In common with the situation encountered in **12A**, the value of the slip parameter Δ in **12B** suffers a substantial, sterically-induced enhancement: Δ is 0.91Å, with (as before) an accompanying interplane slippage of 0.10Å. This slippage is comparable to that in **12A** and gives rise to similar distances between the platinum atom and the atoms of the ligating carbaborane face: Pt(3)···C(1) and Pt(3)···C(2) are slightly shorter, at 2.933(14) and 2.952(14)Å respectively; Pt(3)—B(4) is 2.294(18)Å and Pt(3)—B(7) is 2.320(18)Å, essentially the same as in **12A**; whilst the Pt(3)—B(8) distance [2.171(17)Å] is perhaps slightly longer.

Isomerisation of Platinum Complexes of Aryl Carbaboranes

The facile polyhedral rearrangements observed in *bis*(phosphine)-platinum complexes of **9** (such as compound **C** discussed above) **[99]** have been discussed in some detail in Chapter 1. To recap, the sterically-induced rotation of the {$(R_3P)_2Pt$} fragment from its electronically-preferred orientation over the ligating carbaborane face is proposed to result in "*ground state destabilisation*" (*g.s.d.*) which facilitates isomerisation at relatively low temperatures. Thus, although the original aim of structurally characterising a series of increasingly crowded complexes of the ligand **8** - which undergo increasing cluster distortion and ultimately isomerise - was unsuccessful it is, nevertheless, of interest to examine compounds such as **10** - **13** under similar mild thermolysis conditions. However, a $CHCl_3$ solution of **12**, heated to reflux for several hours, did not appear to undergo any change. Thus, although **12** is considerably more crowded than **C**, the former species does not undergo rearrangement under conditions which isomerise the latter.

This observation supports the proposed influence of *g.s.d.* in **C** (this is absent in **12**); it appears that in complexes such as **12**, the enhanced lateral slippage Δ of the metal fragment can adequately accommodate the increased intramolecular crowding without facilitating any isomerisation at moderate temperature. It may also be of significance that the C_{cage}—C_{cage} connectivity in **C** [1.594(14)Å] is rather longer (and therefore weaker) than in, for example, **12A** [1.525(9)Å], and it is possible that this feature hinders rearrangement. Indeed, it may be the case that the lengthening of the C_{cage}—C_{cage} connectivity in **C** represents the beginning of the isomerisation process.

Conclusions

The synthesis and characterisation of the sterically-demanding ligand [7-Ph-8-Me-7,8-*nido*-$C_2B_9H_9$]$^{2-}$ as the dithallium salt, and of the piperidinium salt of its protonated counterpart, have been presented. Deboronation reactions of several other phenylcarbaboranes have also been considered. For the parent 1-Ph-1,2-*closo*-$C_2B_{10}H_{11}$ carbaborane, a counterion-dependence has been proposed to affect the exact nature of the *nido*-icosahedral anion produced by decapitation; whilst the 2-Me_3Si and 2-^{t}BuMe$_2$Si derivatives of the parent carbaborane failed satisfactorily to deboronate.

Several *bis*(phosphine)platinum complexes of the first ligand have been prepared; these have been shown - by a combination of spectroscopic evidence and *X*-ray diffraction structural analysis - to suffer increasing intramolecular crowding as the steric demands of the metal-bound phosphine become greater. In particular, single crystal *X*-ray diffraction studies of the triethylphosphine derivative and two different crystalline forms of the triphenylphosphine compound have demonstrated that this substantial intramolecular crowding is accommodated by a very significantly enhanced (*c.f.* less crowded analogues) lateral slippage of the platinum fragment across the ligating C_2B_3 face of the carbaborane ligand, away from the C_{cage} atoms. The magnitude of this slip enhancement appears to be sterically-controlled, and overrides the opposing electronic tendency.

Despite their more congested nature, the present complexes appear not to isomerise under conditions which effect rearrangement of the less crowded analogues 1-Ph-3,3-$(R_3P)_2$-3,1,2-$PtC_2B_9H_{10}$. It is suggested that this observation supports the previously-proposed influence of *ground state destabilisation* in these latter compounds.

Further Work

The somewhat anomalous ^{11}B n.m.r. spectra obtained for $9H^+$ have not yet been fully explained. It seems probable that further n.m.r. experiments - and in particular the $^1H\{^{11}B_{selective}\}$ n.m.r. spectra - will resolve this situation.

Additional, detailed n.m.r. studies of the compounds **10** - **13** may prove instructive with regard to the extent of lateral slip of the metal fragment. On the basis of the molecular orbital discussions presented earlier the magnitude of the coupling $^1J_{PtB}$ [between Pt(3) and B(8)] should correlate directly with the extent of slippage, and it is of interest to ascertain whether the very large slip found in the solid-state structures of **12** is retained in solution. The proposed interaction between the platinum atom and a β-H atom of the cage-bound phenyl ring should be probed further to determine whether this is genuine or simply a recurrent artefact of molecular packing; variable temperature n.m.r. experiments, and/or a high-quality, low-temperature *X*-ray diffraction study (with the appropriate H atom allowed positional refinement) would prove informative in this respect.

The parallel synthesis and structural characterisation of analogous $\{(R_3P)_2Pt\}$ complexes of even more sterically demanding ligands [7-Ph-8-R-7,8-*nido*-$C_2B_9H_9]^{2-}$ (such as R = ^{t}Bu or Me_3Si), with a view to comparing the properties of these compounds with the present species **10** to **13**, may ultimately allow realisation of the original aim of this work; namely, the detailed study of a series of "sterically-engineered" carbaplatinaboranes which suffer increasing polyhedral distortion (and ultimately isomerisation), with a view to examining the mechanism of rearrangement in complexes of this type. The structural behaviour of such compounds would be of interest in its own right, as they would constitute examples of severely crowded heteroboranes.

Chapter 4

Structural Studies on Selected Heterometallaboranes

Introduction

In this chapter, members of two separate systems of 11-vertex heterometallaboranes are considered with particular reference to certain of these species whose structures are "anomalous" in terms of conventional electron counting rules such as those discussed in Chapter 1.

Structural studies were performed using the technique of *root mean square* (*r. m. s.*) *misfit* calculations which has proved effective in the analysis of the geometries of other metallaboranes **[110]**. However, prior to performing the structural calculations, it was necessary first to establish certain criteria which govern the detailed nature of the models which may be chosen for comparison by this method. This is of particular importance where subtle structural differences are involved, as in the present two series of compounds.

The first of these two systems consists of two dicarbaplatinaboranes **[135, 136]** which are based ostensibly on a 9,7,8-PtC_2B_8 nucleus, namely 9-H-9,9-$(Et_3P)_2$-$\mu_{10,11}$-H-9,7,8-$PtC_2B_8H_{10}$, **14**, and 9-H-9,10-$(Et_3P)_2$-9,7,8-$PtC_2B_8H_9$, **15**; the observed anomalous behaviour here is readily resolved upon consideration of the results of *r. m. s. misfit* calculations.

The second group of heterometallaboranes studied are species containing a 8,7-$RhSB_9$ cluster, and are exemplified by 8,8-$(Ph_3P)_2$-$\mu_{9,10}$-H-8,7-$RhSB_9H_9$ **[137]**, **16**, and 8,8,8-$(Me_2PhP)_3$-$\mu_{9,10}$-H-8,7-$RhSB_9H_9$ **[138]**, **17**; structural studies in this case served to *confirm* the apparently anomalous behaviour. An

unusual, common structural motif was found and a related, hitherto unnoticed, aspect of the metal coordination sphere is proposed to account for the observed geometry in **16**. However, attempts to prepare compounds which are direct analogues of **16**, and which meanwhile have the structure predicted on the basis of cluster electron count (with a more "normal" metal coordination sphere), were unsuccessful. Nevertheless, these synthetic studies did yield a number of new metallathiaboranes which were fully characterised by means of both spectroscopic and single crystal *X*-ray diffraction experiments. The compound 8-(dppe)-$\mu_{9,10}$-H-8,7-$RhSB_9H_9$ (dppe = $Ph_2P—CH_2CH_2—PPh_2$), **18**, exhibits "anomalous" structural behaviour similar to that noted in species such as **16**. A related reaction unexpectedly yielded as the major isolated products a number of novel, twelve vertex, *dirhodium* clusters including *cis*-2,3-$(CO)_2$-$\mu_{2,3}$-CO-7-Cl-2,3-$(PPh_3)_2$-2,3,1-*closo*-$Rh_2SB_9H_8$, **19**.

The *R. M. S. Misfit* Method

Structural comparisons which consider only one or two bond lengths or angles (and which, therefore, use the coordinates of only a few atoms) may be useful where the remainder of the structure is genuinely invariant (or is so to a good approximation). However, the selectivity implicit in such comparisons somewhat limits their value since further useful information may be contained in the positions of all the atoms in the molecular or polyhedral array. Indeed, as has been discussed earlier (Chapter 1), the delocalised bonding in polyboron clusters implies that structural changes are communicated to the *whole molecule* and, as a direct consequence of this, the *whole molecule* should be considered. A useful technique, and the one employed extensively in the present work, involves the calculation of *r. m. s. misfit* values; the procedure is outlined in principle below.

The two structures are placed at a common centre of gravity, then one is rotated relative to the other so as to minimise the quantity

$$\Sigma_i \delta_i^2$$

(where δ_i is the distance between the ith pair of corresponding atoms in the two structures). This is achieved *via* an iterative least-squares process, with convergence for two similar structures generally occurring within three or four cycles, to give an *r. m. s. misfit* defined as

$$[\{\Sigma_i \delta_i^2\}/n]^{1/2}$$

for n atoms. The relative values of the individual atom misfits δ_i at convergence may provide information useful in tracking the site(s) of structural perturbations.

In general, as n becomes greater, two coordinate sets are liable to poorer fit; as the number of individual δ_i values to be accommodated increases, so does the overall misfit. More importantly, it is crucial to recognise and eliminate possible sources of systematic error (which may arise where, for example, structural changes are due simply to variation in pendant groups) and thereby to ensure that any significantly poorer fits obtained are genuine. In such instances, the *rational* removal of specific atoms from the coordinate sets compared lends the analysis greater integrity and reliability than where atoms are merely ignored in order to simplify calculations and comparisons.

Generally, the technique is limited to comparison of the positions of heavy (non-H) atoms, since hydrogen atom locations are often poorly defined in structural determinations by *X*-ray diffraction methods, and are commonly set in calculated positions. In addition, the present studies are limited to cluster vertices' coordinates; the locations of exopolyhedral groups are often determined by external forces such as crystal packing effects or - as has been demonstrated in Chapter 2 - by intramolecular steric factors.

A number of criteria have to be satisfied in the choice of fragments to be compared. In general, enantiomers are non-superimposable and it is, therefore, often necessary to adjust atomic coordinates derived from crystallographic studies so that molecular (mirror) symmetry is present. In addition, it clearly is necessary only to compare "like with like" where more than one atom type is present; the differing radii of (for example) carbon and boron atoms implies slightly different bond lengths to these atoms and their positions are perturbed as a result. Likewise, the presence or absence of bridging hydrides - which generally lengthen the bridged connectivity - cannot be ignored since this, again, can affect atom locations.

A further feature which cannot be ignored is the presence of an exopolyhedral substituent, such as where a {B—H} vertex is replaced by {B—PR_3} or - perhaps to a somewhat lesser extent - where {C—H} is replaced by {C—Ph}. In the former case, an important electronic change has taken place at the vertex in question: the two-electron donor {B—H} unit is replaced by the three-electron-donating {B—PR_3} group. The effect of such a difference is likely to be not insignificant in terms of atomic positions.

In order to test the above suggestion, the two following species, illustrated schematically in figure 4.1 below, have been compared: *nido*-$[B_{11}H_{14}]^-$ **[139]**, **A**, and *nido*-8-Ph_3P-7-$CB_{10}H_{12}$ **[140]**, **B** (the coordinate set of the former cluster has crystallographically-imposed mirror symmetry, and so does not require "idealisation"). With the exception of the cage atom 10, the two structures otherwise conform to the criteria set out thus far.

[Note that, here and elsewhere, the models have non-standard cage numbering schemes for consistency and ease of comparison.]

The results of the *r. m. s. misfit* calculation comparing the appropriate B_{10} fragments are tabulated in table 4.1.

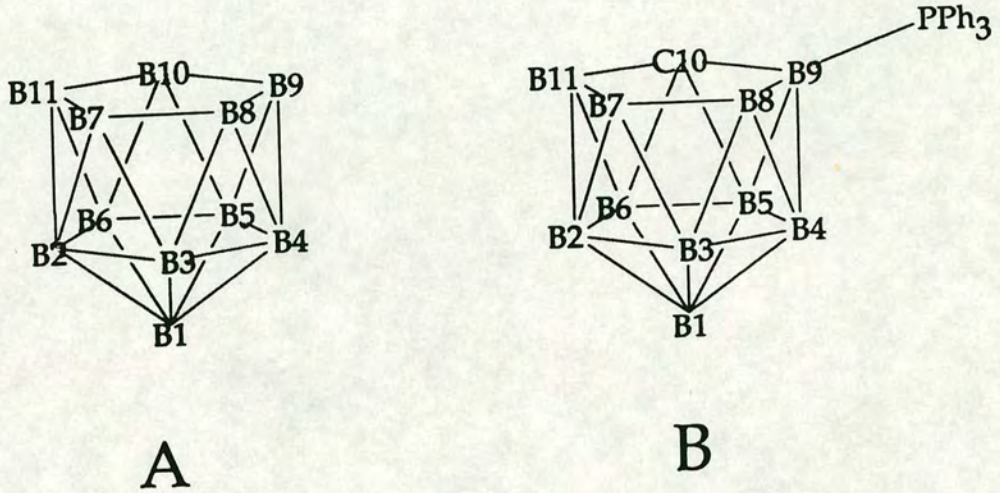

Figure 4.1 Representation of the structures **A** and **B** with numbering scheme (*See text for key to compounds*; B(7)-B(11) and B(8)-B(9) are H-bridged)

Table 4.1 Results of *r. m. s. misfit* calculation ($x10^3$Å) for B_{10} fragments of **A** and **B**

Vertex:	B(1)	B(2)	B(3)	B(4)	B(5)	B(6)	B(7)	B(8)	B(9)	B(11)	*Overall misfit*
models											
A/B	14	18	29	37	75	38	36	22	**191**	173	88

The above results clearly demonstrate a significant misfit for the boron atom [B(9)] which bears the pendant phosphine ligand in **B**. [A rather poor fit for B(11), formally the symmetry equivalent of B(9), might be attributable to problems of crystallographic disorder in the structural determination of **B** **[140]**] On the basis of this, it is proposed that this additional constraint be placed upon the choice of model fragments for use in *r. m. s. misfit* calculations.

The PtC_2B_8 System

The compounds 9-H-9,9-$(Et_3P)_2$-$\mu_{10,11}$-H-9,7,8-$PtC_2B_8H_{10}$, **14** (figure 4.2), and 9-H-9,10-$(Et_3P)_2$-9,7,8-$PtC_2B_8H_9$, **15** (figure 4.3), were first reported in 1980 **[135]**. **14** is formed by the direct oxidative insertion of the platinum(0) nucleophile $\{Pt(PEt_3)_2\}$ - derived from $[Pt_2(\mu\text{-cod})(PEt_3)_4]$ - into 5,6-*nido*-$C_2B_8H_{12}$; an X-ray diffraction study showed **14** to have a *nido* cluster architecture (figure 4.4). Thermolysis of a toluene solution of **14** at 100°C affords **15** in good yield; a further single crystal X-ray diffraction experiment established the cluster geometry of **15** to be that shown in figure 4.5. **15** is seen apparently to adopt a similar cage structure to that found in **14**, with some distortion towards a more closed geometry **[136]**. In particular, the Pt atom in **14** lies 0.52Å elevated above the least-squares plane through C(7), C(8), B(10) and B(11); whereas in **15** this elevation is 0.71Å. [In the rhodium analogue of **14**, 9-H-9,9-$(Ph_3P)_2$-$\mu_{10,11}$-H-*nido*-9,7,8-$RhC_2B_8H_{10}$ **[141]**, the corresponding value is 0.56Å.]

The cluster electron counts of these two 11-vertex (that is, $n = 11$) species are as shown below:

14

2 x {CH}	= 2 x (4 + 1 - 2)	= 6
8 x {BH}	= 8 x (3 + 1 - 2)	=16
{μ-H}		= 1
$\{(Et_3P)_2(H)Pt\}$	= 10 + [(2 x 2)+1] - 12	= 1
		26 electrons = $(n + 2)$ pairs
		predict *nido*

15

2x{CH}	= 2 x (4 + 1 - 2)	= 6
7x{BH}	= 7 x (3 + 1 - 2)	=14
{B-(PEt_3)}	= 3 + 2 - 2	= 3
$\{(Et_3P)(H)Pt\}$	= 10 + (2+1) - 12	= 1
		24 electrons = $(n + 1)$ pairs
		predict *closo*

Thus, in terms of cluster electron count, the observed *nido*-icosahedral structure of **14** conforms to that expected; whereas, the polyhedron in **15** has one less skeletal electron pair and would, therefore, be expected to adopt a *closo*- geometry. Herein lies the "anomalous" behaviour of **15**: electron counting predicts a *closo*-octadecahedral architecture, yet an essentially *nido*-structure is observed.

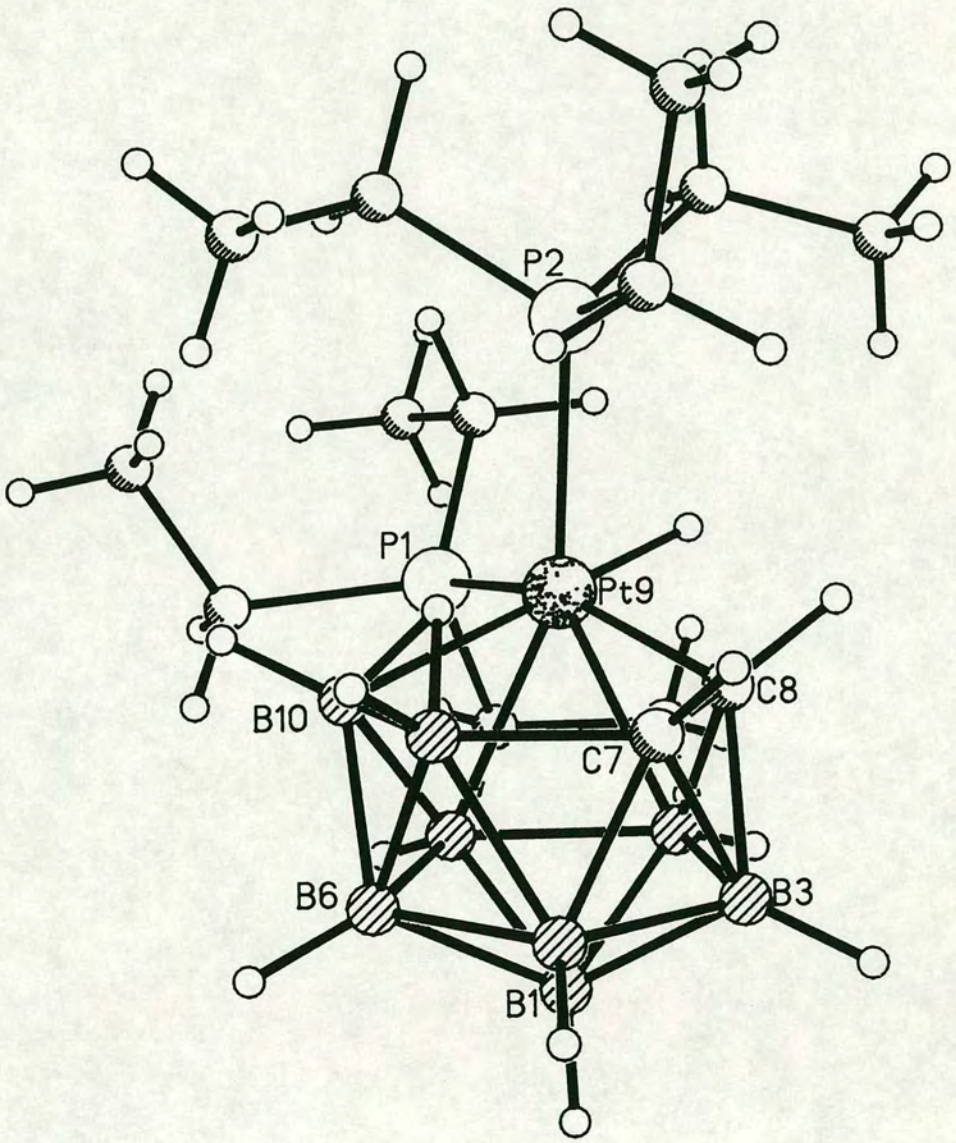

Figure 4.2 Structure of **14** from an X-ray diffraction study
(Cage, some ethyl, and the Pt-bound H atoms were not located; these were included in calculated positions, their existence inferred from spectroscopic data.)

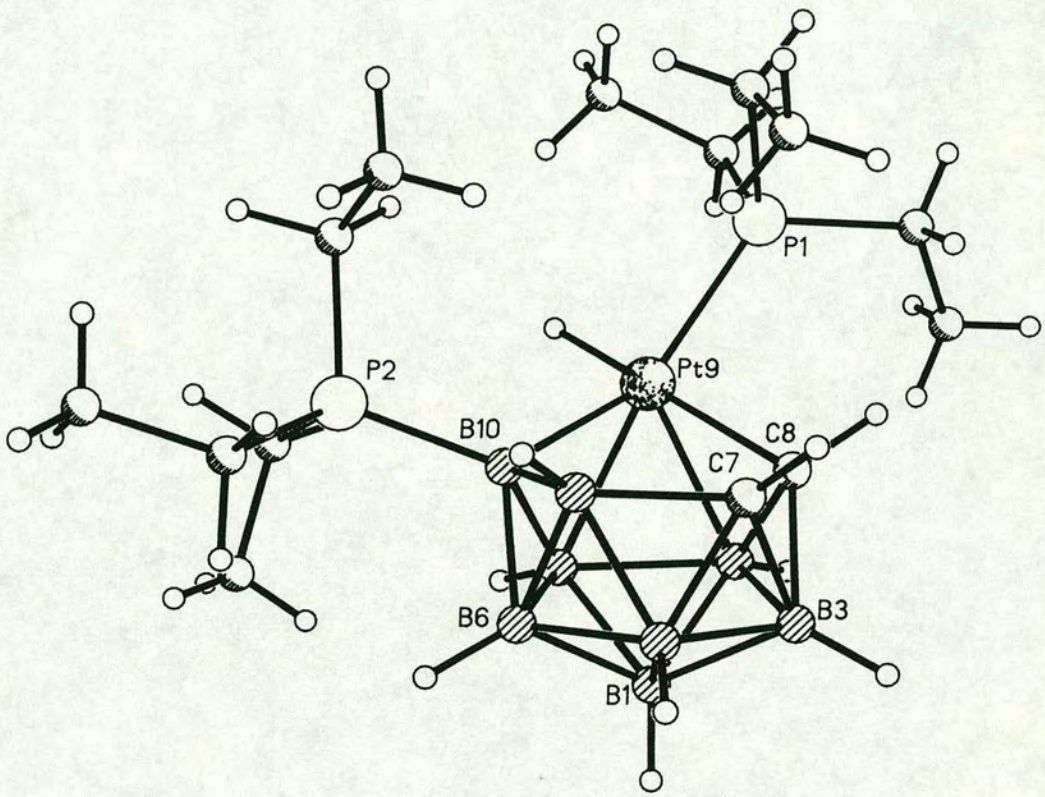

Figure 4.3 Structure of **15** from an X-ray diffraction study

(Some ethyl and the Pt-bound H atoms were located; these were included in calculated positions, their existence inferred from spectroscopic data. Cage H atoms were located and positionally refined)

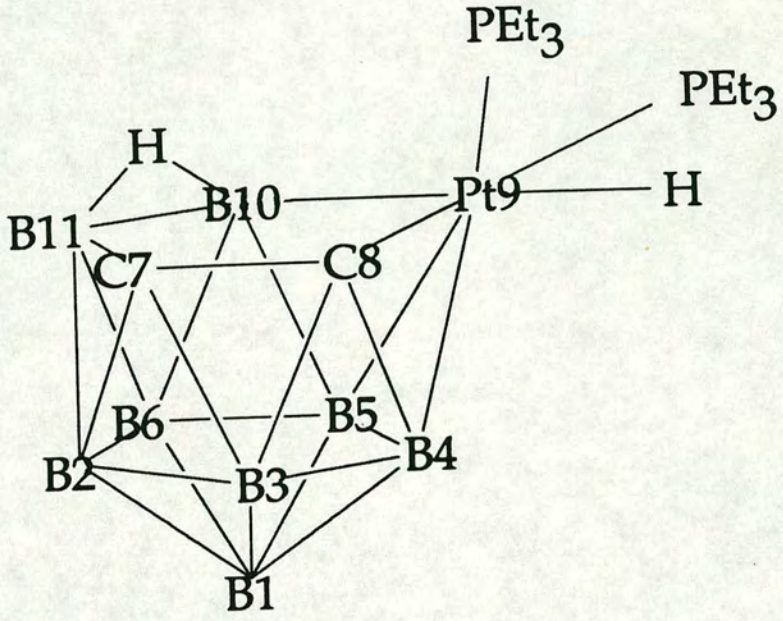

Figure 4.4 Cluster geometry in **14**

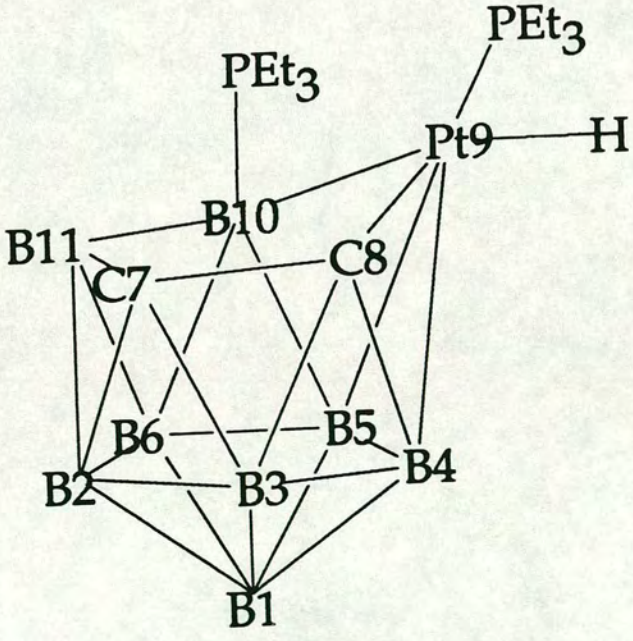

Figure 4.5 Cluster geometry in **15**

In both the present PtC_2B_8 system and that involving $RhSB_9$ species below, the clusters considered are all of an eleven vertex construction and may be either *nido* fragments of a closed 12-vertex polyhedron, or are themselves *closo*, eleven vertex clusters. This means that genuine *nido* and *closo* eleven vertex polyhedral (hetero)boranes are required as models against which the present heterometallaboranes may be compared. For this purpose, *nido*-$[B_{11}H_{14}]^-$, **A**, and *nido*-$[7,8\text{-}C_2B_9H_{12}]^-$ **[125]**, **C**, were chosen to represent the former class of structures; and *nido*-$B_{10}H_{14}$ **[142]**, **D** (a *nido* fragment of a *closo* eleven vertex parent), and *closo*-$[2\text{-}(Me_3Si)_2CH\text{-}2\text{-}CB_{10}H_{10}]^-$ **[37]**, E, belong to the latter category of model. (The choice of models was limited to those structures which have been determined crystallographically, whilst avoiding as far as possible models which do not comply with the criteria set out earlier; the structure of one further, potentially useful, species - namely *closo*-$2,3\text{-}Me_2\text{-}2,3\text{-}C_2B_9H_9$ **[143]** - has been determined but the coordinates were not deposited. In the case of **D**, only one of the two crystallographically-independent molecules was used; the two polyhedra have been shown **[144]** to be virtually superimposable.) The structures C and E were adjusted to molecular C_s symmetry; **D** was modified to full C_{2v} symmetry. C, D and E are represented in figure 4.6 below.

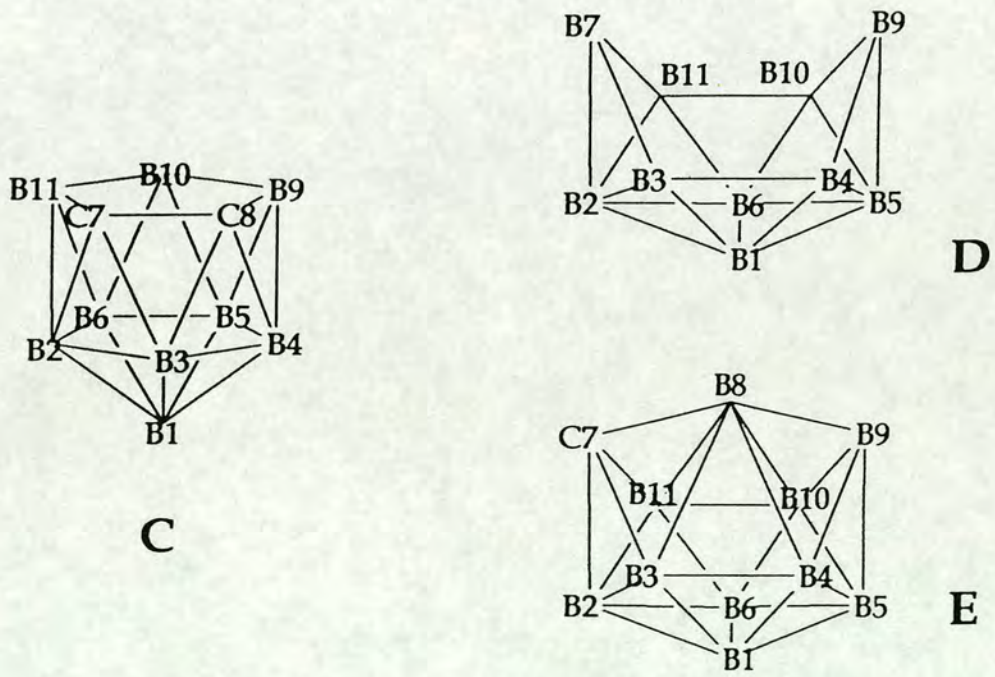

Figure 4.6 Representation of structures C, D and E with numbering scheme
(See text for key to compounds)

The nature of the two carbaplatinaboranes **14** and **15** dictates that several of their cluster vertices must be omitted in order that the *r. m. s. misfit* calculations are acceptable in terms of the criteria put forward earlier. The models themselves possess limited functionality, but do differ from each other and from **14** and **15** in several respects. For example, **C** has two carbon cluster vertices, but lacks the two bridging H atoms which lie on the open face of **A** (which has all boron vertices). Likewise, the "open" faces of **14** and **15** contain boron, carbon and platinum atoms, and a bridging hydrogen atom and a boron-bound phosphine group (in **14** and **15** respectively). To satisfy all necessary conditions, the situation reduces to a comparison of the appropriate "pentagonal pyramids" derived from both the model species and from **14** and **15**, as illustrated in figure 4.7 below.

[It is interesting to note that the two pentagonal pyramids do differ distinctly. Thus, whereas that derived from a *nido* eleven vertex parent contains an essentially planar B_5 belt, the corresponding fragment derived from a *closo* parent has a somewhat folded B_5 plane. This is apparent in the individual atom misfits δ_i tabulated for the atoms in the B(2)B(3)B(4)B(5)B(6) "planes".]

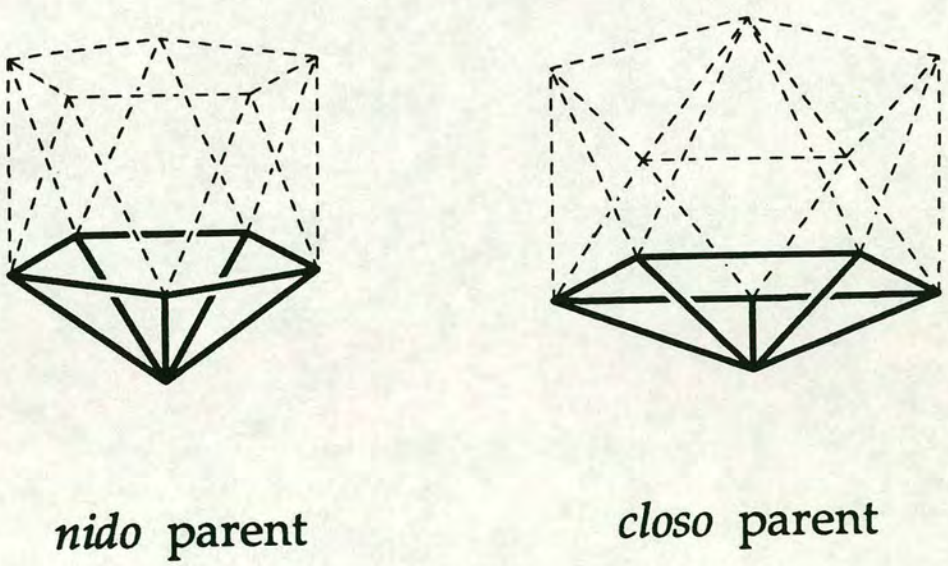

Figure 4.7 Derivation of pentagonal pyramidal B_6 fragments from *closo* and *nido* eleven vertex parent polyhedra

In order to establish the typical value of the overall *r. m. s. misfit* calculated here, the models themselves were first compared by the same technique. The results of this evaluation are tabulated in table 4.2.

Table 4.2 Results of comparison by the *r. m. s. misfit* method (x10^3 Å) of B_6 fragments derived from *closo* and *nido* eleven vertex polyhedra

Vertex:	B(1)	B(2)	B(3)	B(4)	B(5)	B(6)	*Overall misfit*
model / model							
(a) *closo / closo*							
D / E	64	28	38	89	77	59	63
(b) *nido / nido*							
A / C	14	13	10	13	23	23	16
(c) *closo / nido*							
A / D	89	103	125	109	116	115	110
A / E	27	130	111	51	44	91	84
C / D	100	103	133	111	125	108	114
C / E	39	130	120	52	54	92	89

This establishes the typical magnitude of the *r. m. s. misfit* which might be expected in comparisons of polyhedral fragments which may be thought of as "similar" or "non-similar" in terms of cluster electron count.

The results of *r. m. s. misfit* calculations comparing the appropriate B_6 fragments of **14** and **15** with the corresponding model fragments are listed in table 4.3 below.

Table 4.3 Individual atom and overall *r. m. s. misfit* results ($x10^3$ /Å) for comparison of B_6 fragments of **14** and **15** with model fragments

Vertex:	B(1)	B(2)	B(3)	B(4)	B(5)	B(6)	*Overall misfit*
Complex / model							
14/A	33	46	37	31	32	37	**36**
14/C	44	41	45	32	38	27	**38**
14/D	58	65	99	80	87	86	80
14/E	18	93	81	35	28	66	61
15/A	39	105	106	85	95	61	85
15/C	38	110	115	92	96	57	89
15/D	87	41	51	66	41	76	**63**
15/E	38	48	25	54	64	42	**47**
[**14/15**	45	83	72	65	63	30	62]

From this it is apparent that (as would be expected) **14** shows significantly better fits to *nido* eleven-vertex models than to *closo* ones. **15**, whilst generally fitting both sets of models rather more poorly, does appear to be more congruent to the *closo* models. Therefore, on the basis of the above analysis, it would appear that Wade's Rules are not broken, with **15** adopting a very distorted, *closo* structure.

The origin of this severe distortion of the polyhedral geometry of **15** remains uncertain, but it has been suggested **[136]** that the {Pt(H)(PEt_3)} fragment in **15** is unable adequately to bond to the six-atom ligating face of the carbaborane. (A similar situation has been encountered in the "slippage" of {Pt(PR_3)$_2$} fragments bound to *nido*-icosahedral carbaborane ligands, discussed in the previous Chapter.) This phenomenon may ultimately be understood *via* the results of (fragment) molecular orbital and/or *ab initio* studies.

The $RhSB_9$ System

Reaction of Wilkinson's catalyst [$RhCl(PPh_3)_3$] with the thiaborane precursor Cs[6-*arachno*-SB_9H_{12}] affords 8,8-$(Ph_3P)_2$-$\mu_{9,10}$-H-8,7-$RhSB_9H_9$, **16** (figure 4.8), in yields of around 80% **[137]**. **16** may be converted by ethanolysis to 9-OEt-8,8-$(Ph_3P)_2$-$\mu_{9,10}$-H-8,7-$RhSB_9H_8$, **16A** **[145]**. Both **16** and **16A** have been studied by X-ray diffraction methods and are found to have the same gross *nido*-icosahedral geometry shown in figure 4.10. Treatment of **16** with an excess of Me_2PhP gives 8,8,8-$(Me_2PhP)_3$-$\mu_{9,10}$-H-8,7-$RhSB_9H_9$, **17** (figure 4.9) **[138]**, whilst prolonged thermal reaction with CS_2 converts **16** to 8,8-$(Ph_3P)_2$-$\mu_{8,9}$-S_2CH-$\mu_{9,10}$-H-8,7-$RhSB_9H_8$, **17A** **[137]**. Single crystal X-ray diffraction studies of **17** and **17A** reveal both to have similar cluster structures (figure 4.11) to **16** and **16A** with the crucial difference that the former pair of compounds possess a *tris*(ligand) metal vertex, whereas **16** and **16A** appear to bear only two pendant, metal-bound ligands.

Explicit cluster electron counting for these four 11-vertex (n = 11) species is as follows:

16

9 x {BH}	= 9 x (3 + 1 - 2)	=18
S	= 6 + 0 - 2	= 4
{μ-H}		= 1
$\{(Ph_3P)_2Rh\}$	= 9 + [(2 x 2)] - 12	= 1
		24 electrons = (n + 1) pairs
		predict *closo*

16A

8 x {BH}	= 9 x (3 + 1 - 2)	=16
{B—OEt}	= 3 + 1 - 2	= 2
S	= 6 + 0 - 2	= 4
{μ-H}		= 1
$\{(Ph_3P)_2Rh\}$	= 9 + [(2 x 2)] - 12	= 1
		24 electrons = (n + 1) pairs
		predict *closo*

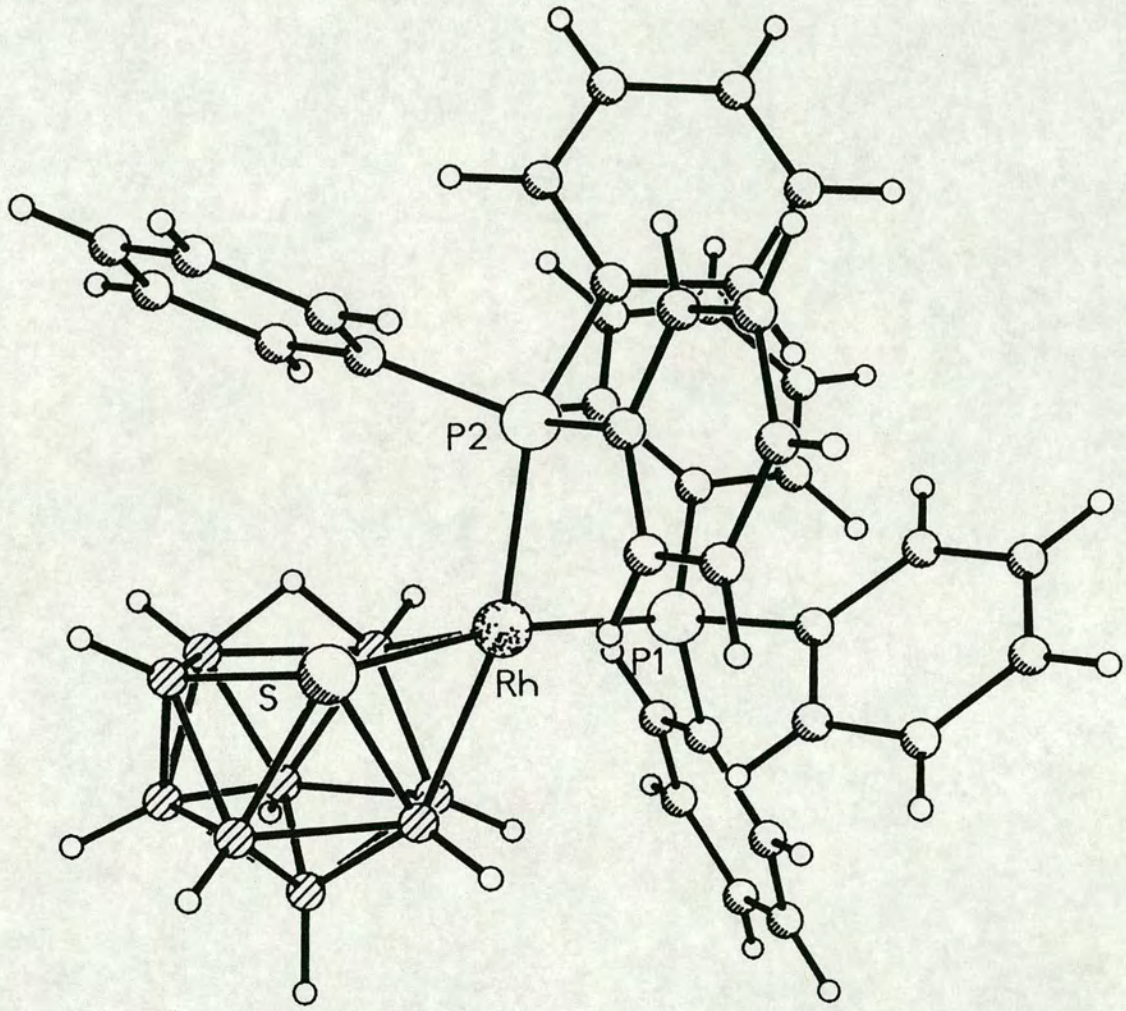

Figure 4.8 Structure of **16** from an X-ray diffraction study

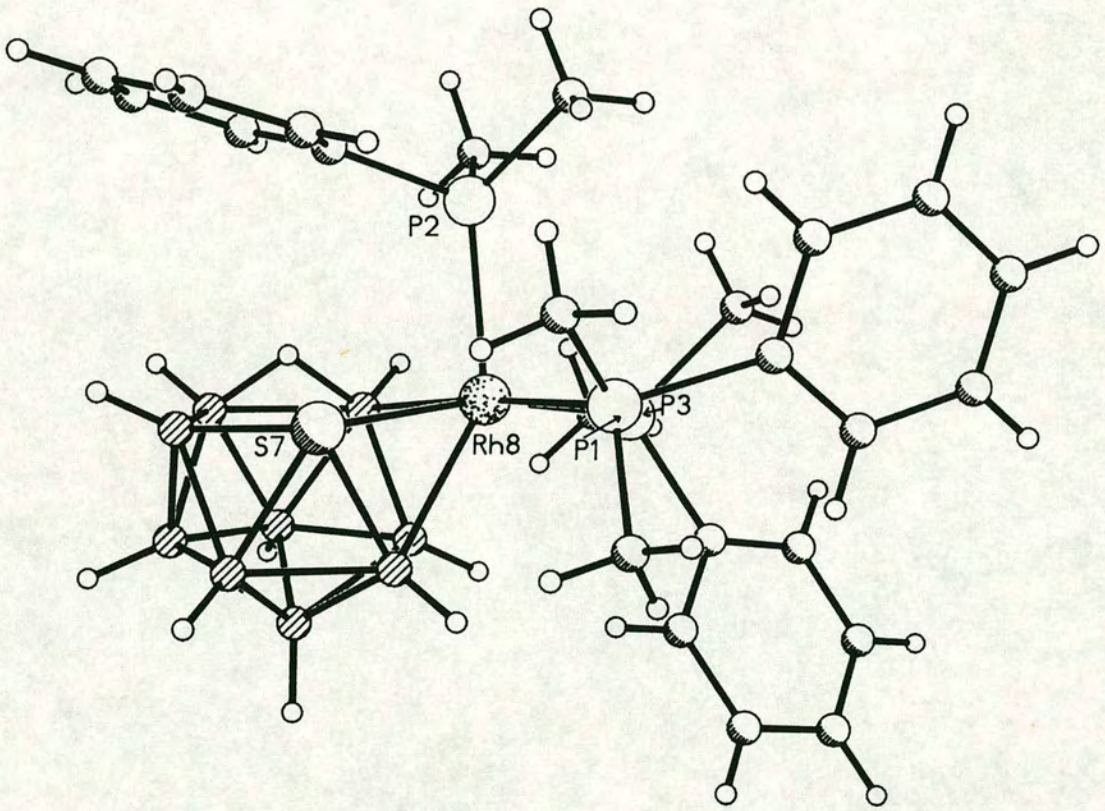

Figure 4.9 Structure of **17** from an X-ray diffraction study

17

9 x {BH}	= 9 x (3 + 1 - 2)	=18
S	= 6 + 0 - 2	= 4
{μ-H}		= 1
{($Me_2PhP)_3Rh$}	= 9 + [(3 x 2)] - 12	= 3
		26 electrons = (n + 2) pairs
		predict *nido*

17A*

8 x {BH}	= 8 x (3 + 1 - 2)	=16
{B—SC(H)=S}	= 3 + 1 - 2	= 2
S	= 6 + 0 - 2	= 4
{μ-H}		= 1
{($Ph_3P)_2$[SC(H)=S:]Rh}	= 9 + [(3 x 2)] - 12	= 3
		26 electrons = (n + 2) pairs
		predict *nido*

Electron counting has thus revealed another instance of anomalous structural behaviour. All of **16, 16A, 17** and **17A** appear to adopt a *nido*-icosahedral cluster architecture and yet **16** and **16A** are predicted to have *closo* geometries.

The cluster structures of all four compounds have been analysed by the *r. m. s. misfit* technique discussed above. As before, this was performed *via* comparison of models' B_6 fragments with the appropriate fragments derived from the present four complexes. The results of these calculations are presented in table 4.4 below.

* The dithioformato moiety may be considered as either of two equivalent forms: (a) B—S σ-bond with C=S acting as Lewis base (2 electron donor) towards Rh (*c. f.* phosphine); or (b) Rh—S σ-bond with C=S acting as 2 electron donor to B vertex. In either view, the μ-HCS_2 group contributes a total of 3 electrons to Rh and B(9).

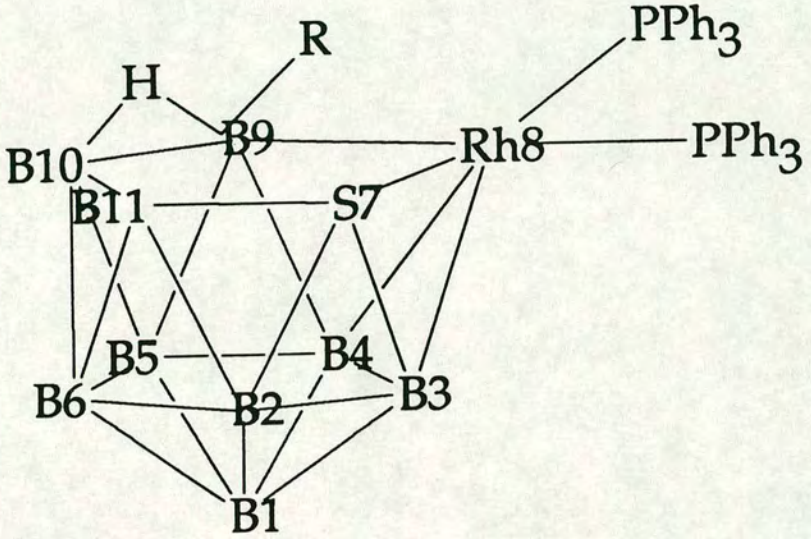

Figure 4.10 Cluster geometry in **16** (R = H) and **16A** (R = OEt)

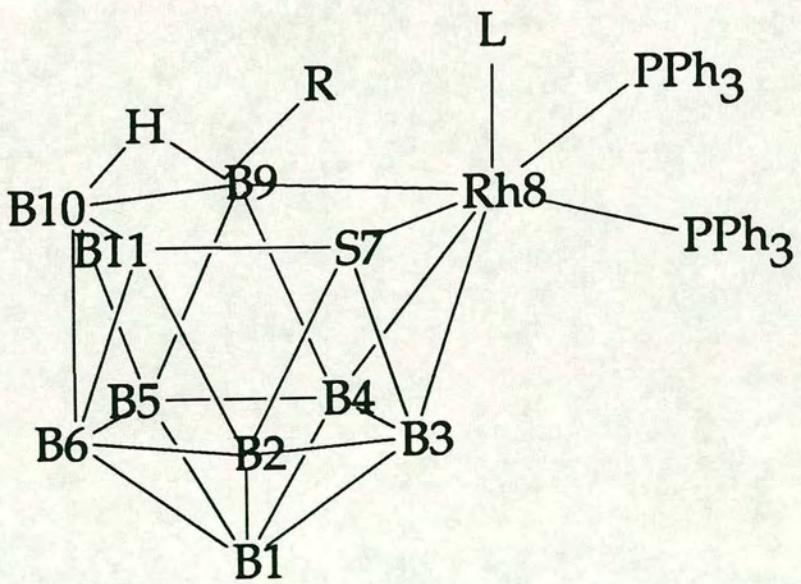

Figure 4.11 Cluster geometry in **17** (L = Me_2PhP, R = H) and **17A** (L⌒R = μ-HCS_2)

Table 4.4 Individual atom and overall *r. m. s. misfit* results (x10^3 / Å) for the comparison of B_6 fragments of **16, 16A, 17** and **17A** with model fragments

Vertex:	B(1)	B(2)	B(3)	B(4)	B(5)	B(6)	*Overall misfit*
Complex / model							
16 / A	41	82	54	20	21	32	**47**
16 / C	50	87	52	29	35	33	**51**
16 / D	83	174	135	112	120	141	130
16 / E	46	198	130	69	56	124	116
16A / A	56	88	55	27	15	33	**52**
16A / C	63	94	53	29	22	32	**55**
16A / D	87	182	141	119	117	136	134
16A / E	61	206	134	78	52	123	121
17 / A	47	68	63	24	23	20	**45**
17 / C	53	75	68	35	35	27	**52**
17 / D	90	151	95	120	105	126	116
17 / E	55	173	93	63	45	110	100
17A / A	50	60	65	13	16	21	**43**
17A / C	57	67	68	25	34	30	**50**
17A / D	88	145	103	116	108	117	114
17A / E	56	168	100	61	42	103	98

The above *r. m. s. misfit* calculations' results appear to confirm the irregular behaviour of **16** and **16A**; there is no evidence from these analyses to suggest that these two compounds possess anything other than a truly *nido* cluster geometry.

This conclusion prompts a search for an alternative interpretation of these two clusters' solid state structures, which might shed some light upon this problem. In particular, the question of whether the (in principle) *closo* complexes have acquired an additional electron pair must be addressed.

In this connection, it is appropriate to note the observation **[137]** that the ^{11}B n.m.r. spectrum of **16** displays a pattern of resonances consistent with the presence of an *arachno*-B_9 fragment; that is, that the $RhSB_9$ polyhedron may be of the *closo* type in solution. This tends to suggest that the observed *nido*-$RhSB_9$ skeleton arises from some solid-state effect which, although small, may be of adequate significance to effect the *closo* → *nido* structural change. [Such a phenomenon would not be without precedent. A facile *closo*/*nido* interchange has been observed in a related system **[146]**; namely the solution exchange between the two 11-vertex dicarbarhodaboranes $[\{(PEt_3)_2(H)Rh\}C_2B_8H_{10}]$ and $[\{(PEt_3)_2Rh\}C_2B_8H_{11}]$ respectively.]

The compounds **16** and **16A** both co-crystallise with dichloromethane solvate molecules in the two structural determinations reported. Conceivably, a Rh···Cl(solvent) interaction might in both instances provide the metal centre (and hence the cluster) with an additional electron pair. This, however, may be ruled out upon consideration of distances of Rh···Cl closest approach, which are 6.617(2)Å in **16** and 6.713(35)Å in **16A**.

An alternative explanation requires the sulphur (*exo*-) lone pair to have become involved in cluster bonding; that is, the sulphur vertex switches from four-electron to six-electron donation. Under such circumstances, it might be expected that bond lengths to this atom would show some perturbation; this appears not to be the case. The S—B distances in **16** and **16A** lie within the same approximate range (1.90 - 2.10Å), and show corresponding patterns of variation within this range, to that found in metallathiaboranes (**17**, **17A**) which lack any structural anomaly. (In any event such a scenario seems unlikely, since such an effect might be expected to persist in solution and not to be confined merely to the solid state.) Indeed, such an effect would be entirely at variance with the "$v + x - 2$" rule which is observed by the many "naked main group" heteroboranes such as those mentioned in Chapter 1 (p. 27).

A third possibility exists which is, at present, substantially the most favourable. Close examination of the structures of **16** and **16A** reveals that, in both cases, each of the rhodium-bound PPh_3 ligands have one phenyl ring oriented such that a β-H atom on this ring points almost directly towards the

metal centre. This situation is illustrated in figure 4.12 and schematically in figure 4.13 below.

Figure 4.12 Close Rh···H approaches in **16** showing location of **X**

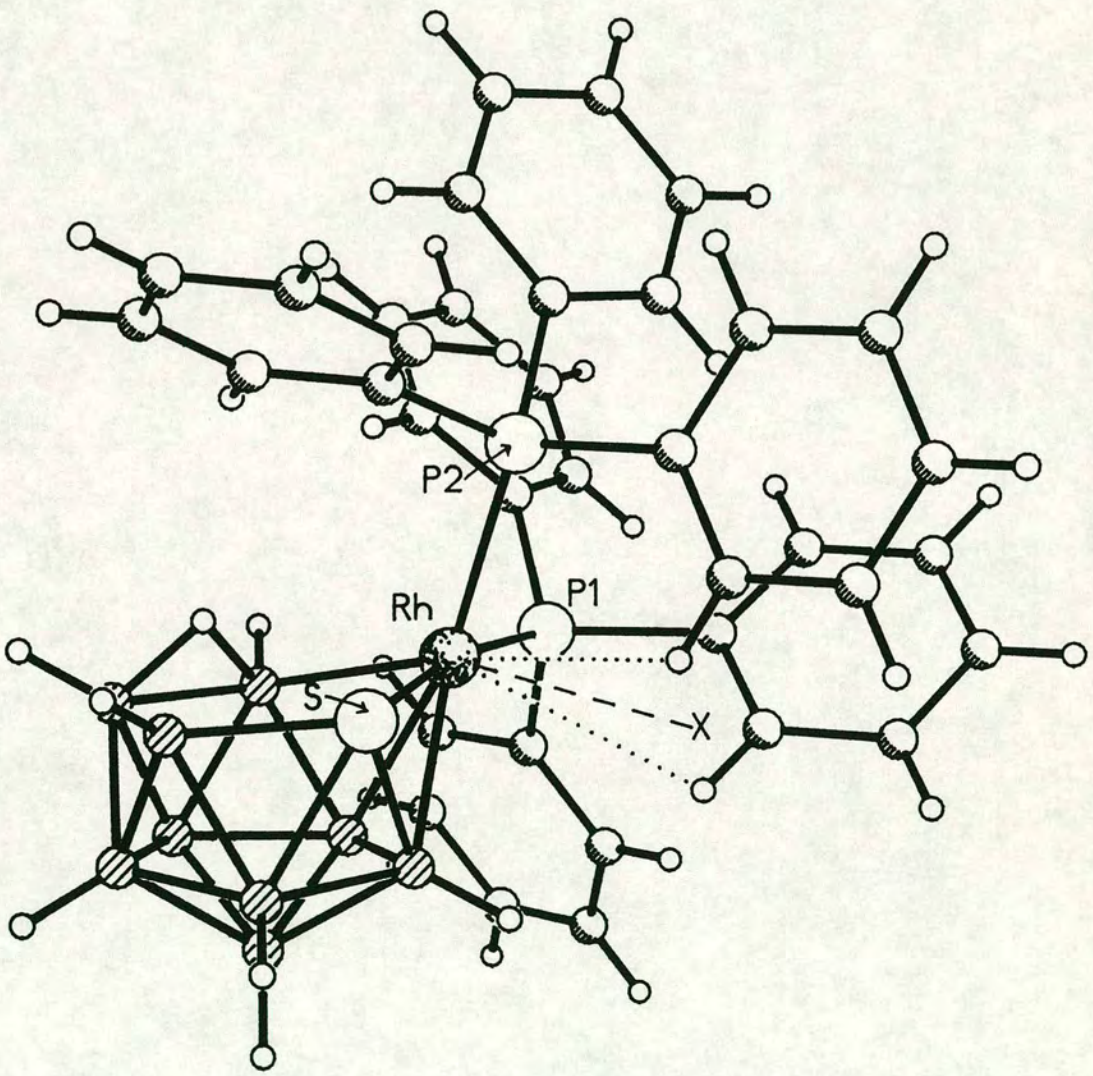

Figure 4.13 Schematic representation of Rh···β-H interactions in **16**

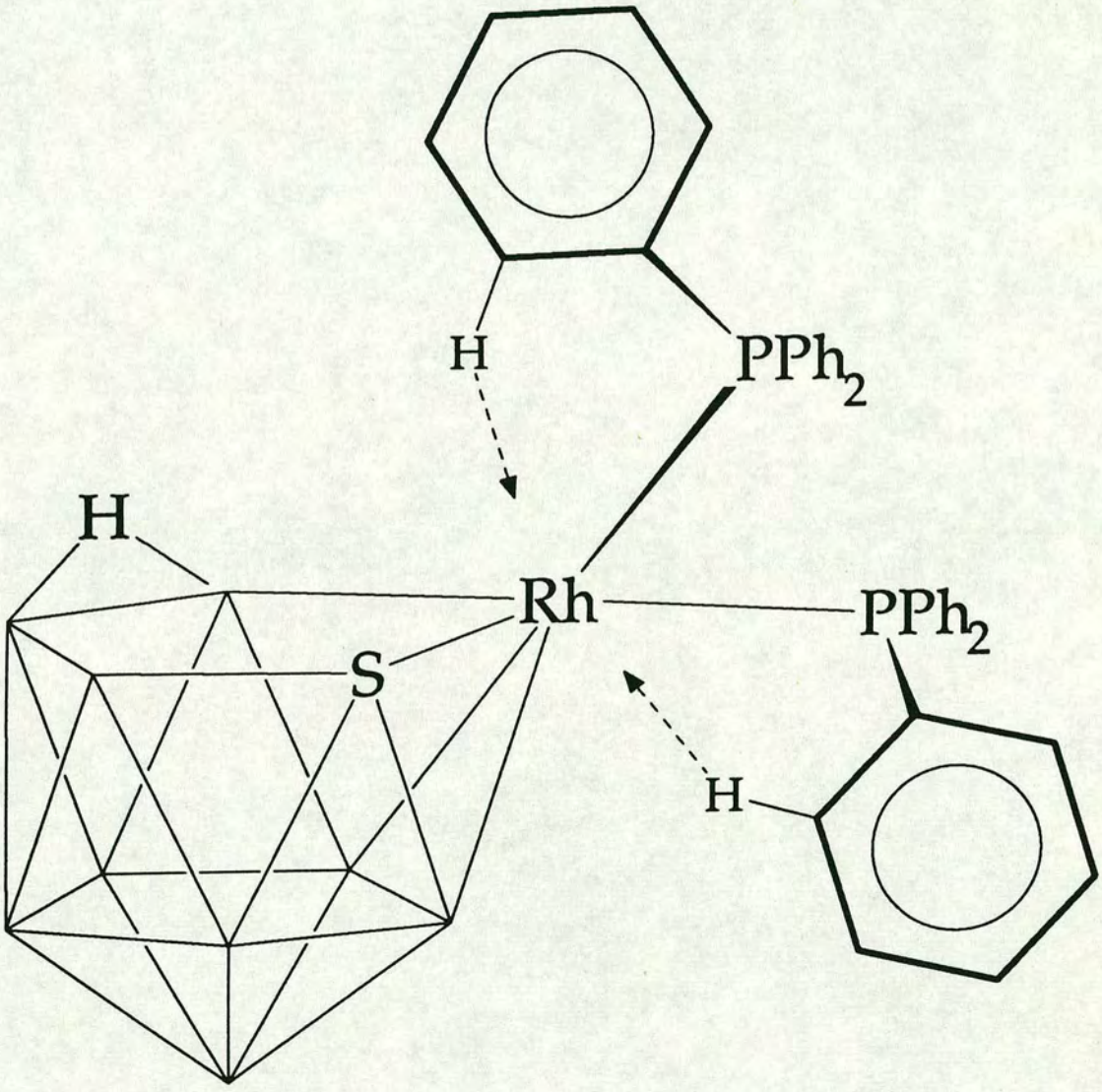

Furthermore, the position **X** (figure 4.12), defined by the average of the two β-H atoms' locations*, lies almost exactly in the direction of the vacant octahedral site on the rhodium vertex, so that {Rh(**X**)(PPh_3)$_2$} effectively constitutes a distorted conical fragment. The Rh···(β-H) and Rh···**X** distances, and relevant angles at Rh involving **X** and/or PPh_3, are tabulated below (table 4.5), along with the appropriate P-Rh-P angles in **17** for comparison.

Table 4.5 Parameters (Å, °) for proposed conical Rh geometry in **16** and **16A**, with corresponding angles (°) at Rh in **17**

	$(Rh\cdots H)_1$	$(Rh\cdots H)_2$	Rh···X	$P_{(1)}$-Rh-$P_{(2)}$	$P_{(1)}$-Rh···X	$P_{(2)}$-Rh···X
Compound						
16	2.955	3.007	2.621	98.50(2)	84.83	82.84
16A	3.150	2.872	2.528	101.35(5)	76.07	95.90
				$P_{(1)}$-Rh-$P_{(2)}$	$P_{(1)}$-Rh-$P_{(3)}$	$P_{(2)}$-Rh-$P_{(3)}$
17				95.88(2)	94.06(2)	99.44(2)

On the basis of this, it is proposed that two weak agostic-type **[147]** Rh∠—H—C interactions exist in the solid state structures of **16** and **16A** which between them provide, in effect, an additional skeletal electron pair which satisfies cluster bonding requirements.

Such an interaction might be expected to be lost in solution, consistent with the ^{11}B n.m.r. data discussed earlier and the accompanying published ^1H n.m.r. data **[137]**. Furthermore, it would indeed be curious that *both* **16** and **16A** happen to display the similar phosphine phenyl ring orientations noted above. It may be the case that low temperature (or perhaps solid-state) ^1H or ^{13}C n.m.r. experiments would show the presence of this agostic-type bonding.

* In the crystallographic determinations of **16** and **16A**, the phenyl H atoms were set riding in calculated positions; thus the actual location of the β-H atoms may in fact be in even greater agreement with this proposal.

Attempts to Prepare "Non-Anomalous" Rhodathiaboranes

The rhodium coordination arrangement proposed above prompted attempts to prepare, independently, direct analogues **LL'**$RhSB_9H_{10}$ of **16** which display a *closo* architecture in the crystalline state.

In particular, it was thought that species which lack (or have restricted) the ability to form the two five-membered {Rh-P-C-C-H} "rings" described above would be suitable target species. Thus, species of this type with **L** = **L'** = PMe_3, CO, $CH_2{=}CH_2$; or **L⌒L'** = $Me_2PCH_2CH_2PMe_2$, 1,5-cyclo-C_8H_{12}, for example, and perhaps their Ir analogues, were considered. However, the attempted syntheses were largely unsuccessful; all of the required ligands appear not to bind adequately strongly to Rh. Almost all of the product mixtures either proved intractable, or any product which could be isolated did not contain a thiaborane moiety (by infrared spectroscopy) or was found to be a *tris*(ligand) rhodathiaborane complex.

A second strategy may be to prepare a complex with a chelating phosphine **L⌒L'** whose geometric restrictions might not permit phenyl rings to fully realise the orientation whereby the above agostic-type interactions may occur. Somewhat greater success was had in this area: reaction of $[(dppe)RhCl]_2$ with a thiaborane precursor afforded 8-(dppe)-8,7-$RhSB_9H_{10}$, **18** (dppe = Ph_2P—CH_2-CH_2—PPh_2), whose synthesis, characterisation and crystallographic study are discussed below.

Synthesis and Characterisation of 18

The compound **18** is synthesised in good yield by the interaction of $[Rh(dppe)_2Cl]_2$, formed *in situ* (*c.f.* **[148]**), and the thiaborane precursor $Cs[SB_9H_{12}]$ under oxygen-free conditions. The progress of the reaction is evidenced by a marked darkening of the reaction mixture over several hours. Following filtration and evaporation of the crude orange product, **18** is isolated in a pure form by preparative thin layer chromatography. [One other borane-containing (infrared spectrum) species, which also contained the diphosphine ligand (^1H n.m.r. evidence), appeared to be formed in very poor yield. However, no further data could be obtained upon this product.]

Microanalysis, and both infrared and (^1H, ^{31}P and ^{11}B) n.m.r. spectral evidence, confirmed the identity of **18**. The ^1H (figure 4.14) and ^{31}P (figure 4.15) n.m.r. spectra suggest the two phosphorus atoms to be *quasi*-inequivalent at room temperature on the n.m.r. timescale.

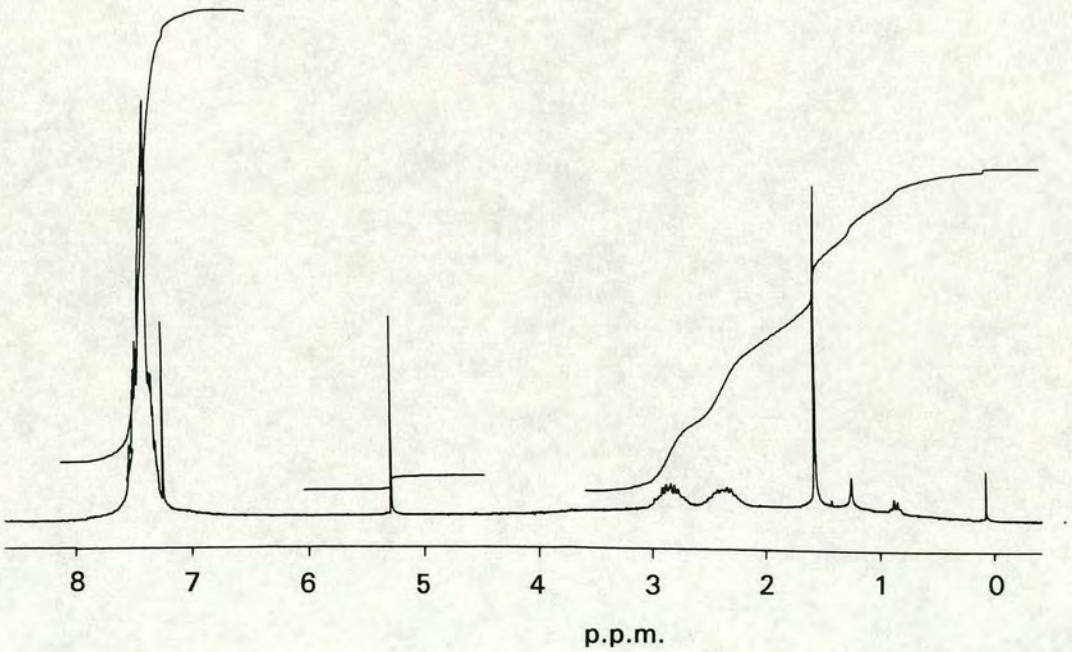

Figure 4.14 ^1H n.m.r. spectrum of **18**

The two separate multiplets centred at $\delta(^1H)$ = *ca.* 2.4 and 2.8 p.p.m., corresponding to the two sets of methylene protons in the dppe ligand, are consistent with inequivalent phosphorus environments. The broadness of the two components of the rhodium coupled doublet in the ^{31}P n.m.r. spectrum, and the apparent absence therein of the two-bond coupling ($^2J_{PP}$), is perhaps somewhat at odds with the ^1H spectrum. This is thought to be due in part to the poor resolution of the spectrum, a consequence of this species' poor solubility; it is suggested that the two anticipated ^{31}P resonances almost coincide, and have similar values of the coupling $^1J^{103}_{RhP}$, so that the spectrum illustrated in figure 4.15 is obtained.

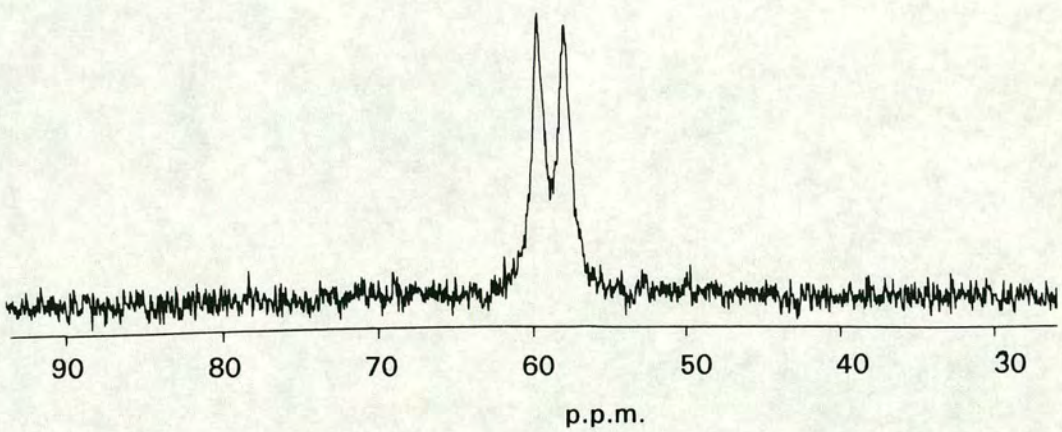

Figure 4.15 ^{31}P n.m.r. spectrum of **18**

Crystallographic Study of 18 .2CH_2Cl_2

Diffraction quality crystals of **18** as the *bis*(dichloromethane) solvate were obtained by diffusion of *n*-hexane into a dichloromethane solution at -30°C.

The crystal lattice was found to be very unstable with respect to solvent loss. This was so severe that crystal growth (by solvent diffusion) had to be arrested after *ca.* 12 hours to avoid diffusion of dichloromethane out of the lattice. To further minimise problems arising from potential solvent loss from the crystal, all crystal transfer and handling operations were performed at 195K (dry ice bath); and diffraction data were collected at 210K. Despite this latter precaution, some crystal decay - presumably arising from partial loss of solvate CH_2Cl_2 - was detected towards the end of data collection and occasioned a minor truncation of the data set.

The position of the rhodium atom was solved by inspection of the Patterson function **[113]**; the remaining heavy atoms, and the μ-H atom were located by difference Fourier syntheses. (The cage bridging H atom was not permitted positional refinement following its location.) The remaining cage H atoms, and the H atoms of the hydrocarbon functions, were set in calculated positions; the phenyl rings were constrained to be planar, regular hexagons. No correction for absorption was applied and all non-H atoms were allowed final anisotropic thermal refinement.

Two molecules of **18** cocrystallise with four of dichloromethane in the triclinic space group *P*bar1, with no close intermolecular contacts.

Figure 4.16 below shows a perspective view of a single molecule of **18** and the atomic numbering scheme adopted (phenyl rings are labelled cyclically); in table 4.5 are tabulated selected internuclear distances and interbond angles.

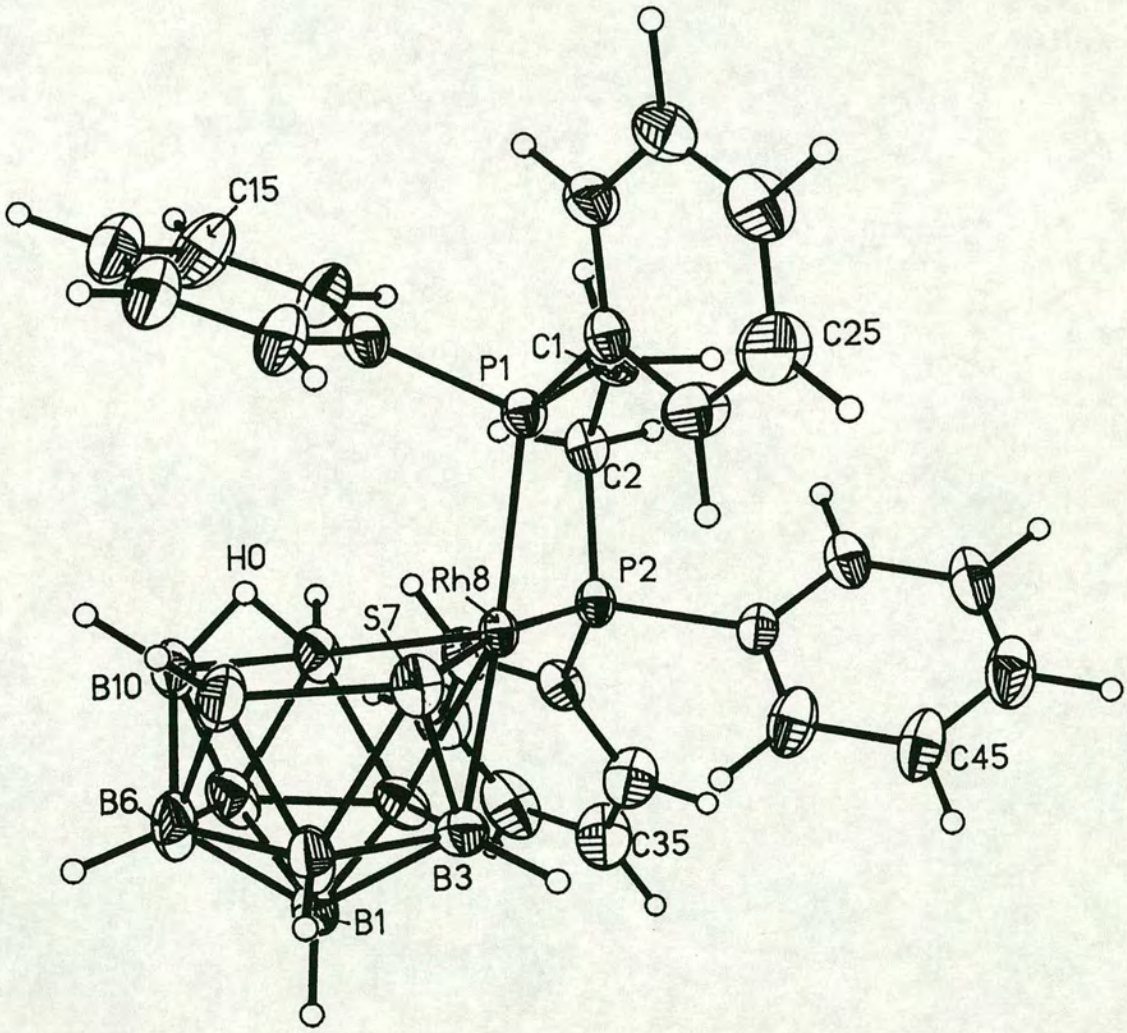

Figure 4.16 Perspective view of **18**
(50% thermal ellipsoids; H atoms have radii of 0.1Å for clarity)

Table 4.5 Selected Interatomic Distances (Å) and Interbond Angles (°) for **18**.2CH_2Cl_2

Rh(8) - S(7)	2.3659(17)	B(4) - B(9)	1.843(10)
Rh(8) - B(3)	2.239(7)	B(5) - B(6)	1.790(11)
Rh(8) - B(4)	2.228(7)	B(5) - B(9)	1.773(11)
Rh(8) - B(9)	2.139(7)	B(5) -B(10)	1.797(11)
Rh(8) - P(1)	2.3214(16)	B(6) -B(10)	1.752(11)
Rh(8) - P(2)	2.2365(16)	B(6) -B(11)	1.730(12)
S(7) - B(2)	1.996(8)	B(9) -B(10)	1.866(10)
S(7) - B(3)	2.062(8)	B(10) -B(11)	1.859(11)
S(7) -B(11)	1.918(9)	P(1) - C(1)	1.834(6)
B(1) - B(2)	1.757(11)	P(1) -C(11)	1.829(4)
B(1) - B(3)	1.759(10)	P(1) -C(21)	1.814(4)
B(1) - B(4)	1.783(10)	P(2) - C(2)	1.838(6)
B(1) - B(5)	1.791(11)	P(2) -C(31)	1.823(4)
B(1) - B(6)	1.770(11)	P(2) -C(41)	1.815(4)
B(2) - B(3)	1.879(11)	C(1) - C(2)	1.542(9)
B(2) - B(6)	1.768(11)	C(1S) -Cl(1S)	1.763(8)
B(2) -B(11)	1.840(12)	C(1S) -Cl(2S)	1.766(8)
B(3) - B(4)	1.787(10)	C(2S) -Cl(3S)	1.748(10)
B(4) - B(5)	1.771(11)	C(2S) -Cl(4S)	1.750(10)

S(7) -Rh(8) - B(3)	53.13(19)	B(6) - B(5) -B(10)	58.5(4)
S(7) -Rh(8) - B(4)	90.05(20)	B(9) - B(5) -B(10)	63.0(4)
S(7) -Rh(8) - B(9)	94.39(20)	B(1) - B(6) - B(2)	59.6(4)
S(7) -Rh(8) - P(1)	99.22(6)	B(1) - B(6) - B(5)	60.4(4)
S(7) -Rh(8) - P(2)	170.62(6)	B(2) - B(6) -B(11)	63.5(5)
B(3) -Rh(8) - B(4)	47.2(3)	B(5) - B(6) -B(10)	61.0(4)
B(3) -Rh(8) - B(9)	85.9(3)	B(10) - B(6) -B(11)	64.5(5)
B(3) -Rh(8) - P(1)	151.89(19)	Rh(8) - B(9) - B(4)	67.6(3)
B(3) -Rh(8) - P(2)	122.28(19)	Rh(8) - B(9) -B(10)	113.8(4)
B(4) -Rh(8) - B(9)	49.9(3)	B(4) - B(9) - B(5)	58.6(4)
B(4) -Rh(8) - P(1)	152.35(20)	B(5) - B(9) -B(10)	59.1(4)
B(4) -Rh(8) - P(2)	90.81(20)	B(5) -B(10) - B(6)	60.5(4)
B(9) -Rh(8) - P(1)	103.15(20)	B(5) -B(10) - B(9)	57.9(4)
B(9) -Rh(8) - P(2)	93.30(20)	B(6) -B(10) -B(11)	57.2(4)
P(1) -Rh(8) - P(2)	84.22(6)	B(9) -B(10) -B(11)	111.0(5)
Rh(8) - S(7) - B(2)	107.10(23)	S(7) -B(11) - B(2)	64.1(4)
Rh(8) - S(7) - B(3)	60.28(21)	S(7) -B(11) -B(10)	113.9(5)
Rh(8) - S(7) -B(11)	105.6(3)	B(2) -B(11) - B(6)	59.3(4)
B(2) - S(7) - B(3)	55.1(3)	B(6) -B(11) -B(10)	58.3(4)
B(2) - S(7) -B(11)	56.1(3)	Rh(8) - P(1) - C(1)	109.25(21)

B(3) - S(7) -B(11)	96.7(3)	Rh(8) - P(1) -C(11)	110.02(14)
B(2) - B(1) - B(3)	64.6(4)	Rh(8) - P(1) -C(21)	120.07(14)
B(2) - B(1) - B(6)	60.2(4)	C(1) - P(1) -C(11)	106.29(24)
B(3) - B(1) - B(4)	60.6(4)	C(1) - P(1) -C(21)	105.12(24)
B(4) - B(1) - B(5)	59.4(4)	C(11) - P(1) -C(21)	105.20(18)
B(5) - B(1) - B(6)	60.3(4)	Rh(8) - P(2) - C(2)	110.11(20)
S(7) - B(2) - B(3)	64.2(3)	Rh(8) - P(2) -C(31)	124.68(14)
S(7) - B(2) -B(11)	59.8(4)	Rh(8) - P(2) -C(41)	104.37(14)
B(1) - B(2) - B(3)	57.7(4)	C(2) - P(2) -C(31)	104.54(23)
B(1) - B(2) - B(6)	60.3(4)	C(2) - P(2) -C(41)	105.97(24)
B(6) - B(2) -B(11)	57.3(4)	C(31) - P(2) -C(41)	105.84(19)
Rh(8) - B(3) - S(7)	66.59(22)	P(1) - C(1) - C(2)	110.3(4)
Rh(8) - B(3) - B(4)	66.1(3)	P(2) - C(2) - C(1)	108.5(4)
S(7) - B(3) - B(2)	60.6(3)	P(1) -C(11) -C(12)	117.4(3)
B(1) - B(3) - B(2)	57.6(4)	P(1) -C(11) -C(16)	122.4(3)
B(1) - B(3) - B(4)	60.4(4)	P(1) -C(21) -C(22)	121.3(3)
Rh(8) - B(4) - B(3)	66.7(3)	P(1) -C(21) -C(26)	118.7(3)
Rh(8) - B(4) - B(9)	62.5(3)	P(2) -C(31) -C(32)	120.3(3)
B(1) - B(4) - B(3)	59.0(4)	P(2) -C(31) -C(36)	119.7(3)
B(1) - B(4) - B(5)	60.5(4)	P(2) -C(41) -C(42)	121.8(3)
B(5) - B(4) - B(9)	58.7(4)	P(2) -C(41) -C(46)	118.2(3)
B(1) - B(5) - B(4)	60.1(4)	Cl(1S)-C(1S) -Cl(2S)	110.7(4)
B(1) - B(5) - B(6)	59.3(4)	Cl(3S)-C(2S) -Cl(4S)	110.5(6)
B(4) - B(5) - B(9)	62.7(4)		

The $RhSB_9$ polyhedron in **18** has a gross *nido*-icosahedral geometry, similar to that found in the closely analogous 8,8-$(PPh_3)_2$- and 8,8-$(PPh_3)_2$-9-(OEt)-species **16** and **16A** respectively. The Rh(8)-S(7) distance in **18** is 2.3659(17)Å, shorter than in **16** and **16A**, where the corresponding separations are 2.3769(6) and 2.375(2)Å respectively. In all three compounds the equivalent Rh—B and S—B distances are essentially similar. Likewise, the Rh(8)-P(2) distance (*trans* to sulphur) is 2.2365(16)Å, somewhat less than Rh(8)-P(1) (*cis* to sulphur) which is 2.3214(16)Å [*c.f.* 2.2906(5) and 2.4197(5)Å in **16**; and 2.278(2) and 2.417(1)Å in **16A**]. Cage B—B separations lie in the range 1.730(12) to 1.879(11)Å, typical of metalla(hetero)boranes of this kind.

The diphosphine ligand is somewhat distorted from ideal tetrahedral geometry at both P(1) and P(2), presumably as a consequence of accommodating coordination to the rhodium centre; a similar situation around the ligating phosphorus atoms is found in **16** and **16A**. The bridging CH_2—CH_2 unit appears rather more regular in geometry (both P-C-C angles

are close to being tetrahedral), save that metal coordination requires a low P(1)—C(1)—C(2)—P(2) angle, only -44.6(5)° .

Relative to the least squares plane throught the other four atoms [S(7), B(9), B(10), B(11)] of the open face, the rhodium atom is elevated by some 0.25Å; in compounds **16** and **16A** the corresponding rhodium elevations are 0.30 and 0.25Å respectively. Thus, **18** shows little or no "upward" movement of the rhodium vertex towards η^6-coordination by the cage (*i.e.*, towards a *closo* geometry). In the "non-anomalous", *nido*-structured species **17** and **17A**, this parameter has values of 0.20 and 0.22Å respectively; whilst in the related compounds [(η^6-C_6H_5Me)$FeSB_9H_{11}$] **[73]** and [(η^5-C_5Me_5)$IrSB_9H_{10}Cl$] **[67]** it has values of 0.06, and 0.25 and 0.20 (two crystallographically independent molecules), respectively.

Since **18** is isoelectronic with **16**, the cluster structural features discussed above confirm the former compound to be another example of an eleven vertex rhodathiaborane with a *nido* cluster geometry, but a cluster electron count more appropriate to a *closo* polyhedron. This is further verified by the results of *r. m. s. misfit* calculations, table 4.6, which demonstrate a far closer fit of **18** to *nido* than to *closo* models. (It is interesting to note in passing the very close similarity between these results and those for **16** in table 4.4; the overall misfit between the B_6 fragments of **16** and **18** is only 0.016Å.)

Table 4.6 Individual atom and overall *r. m. s. misfit* results (x10^3 /Å) for comparison of B_6 fragments of **18** with model fragments

Vertex:	B(1)	B(2)	B(3)	B(4)	B(5)	B(6)	*Overall misfit*
Complex / model							
18 / A	43	83	45	30	28	27	**47**
18 / C	51	89	43	39	24	32	**51**
18 / D	91	179	128	120	115	138	131
18 / E	52	203	123	76	55	120	117

In common with the metal coordination geometry observed in **16** and **16A**, the environment of the rhodium atom in **18** resembles a distorted octahedron with a vacant coordination site *trans* to B(9). Once again, the presence of two close Rh···H approaches in the vicinity of this vacant position has been noted; and again the coordinates of the mid-point (**X**) of the corresponding H—H vector lie in the direction of this unoccupied site. The exopolyhedral geometry around Rh(8) in **18** is described in table 4.7 below.

Table 4.7 Parameters (Å, °) for Rh geometry in **18**, with corresponding values for **16** and **16A**

Compound	$(Rh\cdots H)_1$	$(Rh\cdots H)_2$	Rh···**X**	$P_{(1)}$-Rh-$P_{(2)}$	$P_{(1)}$-Rh···**X**	$P_{(2)}$-Rh···**X**
18	**3.174**	**2.809**	**2.395**	**84.22(6)**	**87.69**	**86.63**
16	2.955	3.007	2.621	98.50(2)	84.83	82.84
16A	3.150	2.872	2.528	101.35(5)	76.07	95.90

Thus it appears that, despite the more constrained nature of the bridged diphosphine ligand, there remains adequate internal freedom within this ligand which allows two phenyl rings again to adopt a position where the postulated Rh···H interactions are possible. [Likewise, there is again an apparent requirement of the presence of <u>two</u> diphenylphosphino units; it seems unlikely that two phenyl groups bound to the *same* phosphorus atom could successfully achieve the correct mutual orientation relative to the metal centre.]

In light of this observation, it seems that the alternative strategy - namely that of altogether removing the possibility of formation of agostic-type Rh···H interactions by judicious choice of metal-bound ligands - is rather more attractive. In particular, the thiaborane complex of the {Rh(CO)(PPh_3)} fragment would, on the basis of the above arguments, be highly likely to adopt a *closo* structure. Indeed, a closely related, B_{cage}-PPh_3-substituted analogue of the target species - [(CO)(PPh_3)$RhSB_9H_9$(*B*-PPh_3)] - has been prepared by Spalding and co-workers **[149]**, and displays the expected *closo*-

1,2-$RhSB_9$ cage geometry. This confirms that there is no intrinsic instability in *closo*-structured LL'$RhSB_9$ clusters; in addition the close relation between the latter compound and the present target species adds considerable weight to the chosen strategy and, therefore, to the postulate of agostic-type Rh···H interactions. The above-referenced work, however, fails to address the *nido* structure adopted by **16** and **16A**; the intriguing converse question is also raised of whether the *B*-PPh_3 analogues of **16** and **16A** would adopt *closo* or *nido* geometries. This also calls into question the possible importance of having to accommodate a μ-H atom in a formally *closo* structure (such as that originally anticipated for **16**). Such a situation, however, is not without precedent; the *closo* carbaborane CB_5H_7 **[150]** carries an "additional" μ_3-H atom over a B_3 face.

The interaction of $Cs[SB_9H_{12}]$ with $[(CO)Rh(PPh_3)_2Cl]$ fails to yield the desired product, but instead the known **[149]** *tris*(ligand)Rh complex $[(CO)(PPh_3)_2RhSB_9H_{10}]$ (identified by infrared and ^{31}P n.m.r. spectroscopies) is formed.

With the metal precursor $[(CO)Rh(PPh_3)Cl]_2$, however, several other, unexpected rhodathiaboranes are isolated. The icosahedral *dirhodium* thiaborane *cis*-2,3-$(CO)_2$-$\mu_{2,3}$-CO-7-Cl-2,3-$(PPh_3)_2$-2,3,1-*closo*-$Rh_2SB_9H_8$, **19**, described below, has been fully characterised by both spectroscopic means and a single crystal X-ray diffraction study. Two other twelve-vertex dirhodathiaboranes, *cis*-2,3-$(CO)_2$-$\mu_{2,3}$-CO-2,3-$(PPh_3)_2$-2,3,1-*closo*-$Rh_2SB_9H_9$, **19A**, and **19B** - thought to be either the *trans*-$(CO)_2$ isomer of **19A**, or a different 7-substituted analogue - were also isolated from this system and have been partially characterised **[151]**.

Synthesis and Characterisation of 19, 19A and 19B

Interaction of $[(CO)_2RhCl]_2$ and PPh_3 (one equivalent per Rh atom) readily forms the dimer $[(CO)Rh(PPh_3)Cl]_2$; subsequent reaction of this, *in situ*, with $Cs[SB_9H_{12}]$ affords a number of borane-containing (by infrared spectroscopy) products which may be (partially) separated by preparative thin layer chromatography.

The major isolated product is *cis*-2,3-$(CO)_2$-$\mu_{2,3}$-CO-7-Cl-2,3-$(PPh_3)_2$-2,3,1-*closo*-$Rh_2SB_9H_8$, **19**, which was characterised by conventional means. Infrared spectroscopy confirmed the presence of a borane moiety, and of both bridging and terminal CO groups. *Cs* molecular symmetry was inferred from the $^{11}B\{^1H\}$ n.m.r. spectrum; on retention of proton coupling the n.m.r. spectrum for this nucleus showed one boron vertex to have suffered replacement of the terminal H atom. Full, unambiguous characterisation, and identification of the B_{cage} substituent, was not possible until the results of the X-ray diffraction study (described below) were known.

The compounds **19A** and **19B** could not be separated by chromatographic means, being two overlapping bands under a variety of conditions. However, infrared and microanalytical data strongly suggest a mixture (presumably two isomers) of non-Cl-substituted analogues of **19**. Attempted separation by fractional crystallisation (CH_2Cl_2/*i*-hexane solvent diffusion at -30°C) afforded apparently only one crystalline modification which formed as dark orange *rods*, extremely susceptible to solvent loss. Further recrystallisation (solvent diffusion, as above) yielded in addition two distinct crystalline species as both red and (mainly) yellow *blocks*. One of these red *blocks* has been structurally characterised **[151]** by an *X*-ray diffraction study and shown to be composed largely of **19A**, the 7-H analogue of **19**. [One quarter of these molecules, however, were tentatively identified as bearing a terminal hydroxyl substituent bound to B(7).] A diffraction quality crystal of yellow **19B** has not yet been obtained.

Crystallographic Study of 19

Slow diffusion of *i*-hexane into a dichloromethane solution of **19** at -30°C yielded dark red *blocks* suitable for analysis *via* an X-ray diffraction study.

Data were collected at ambient temperature, and the positions of the two rhodium atoms determined by inspection of the Patterson synthesis **[113]**; those of the B, C, O, P, S, Cl and cage H atoms were obtained by difference Fourier synthesis. The phenyl rings were constrained to be planar, regular hexagons with H atoms set in idealised positions. An empirical absorption correction was applied, and all heavy atoms were permitted anisotropic refinement.

Two molecules of **19** crystallise in the triclinic space group *P*bar1, with no close approaches between molecules.

A perspective view of a single molecule of **19** and the numbering scheme employed are shown in figure 4.17. In table 4.8 are tabulated selected interatomic distances and interbond angles.

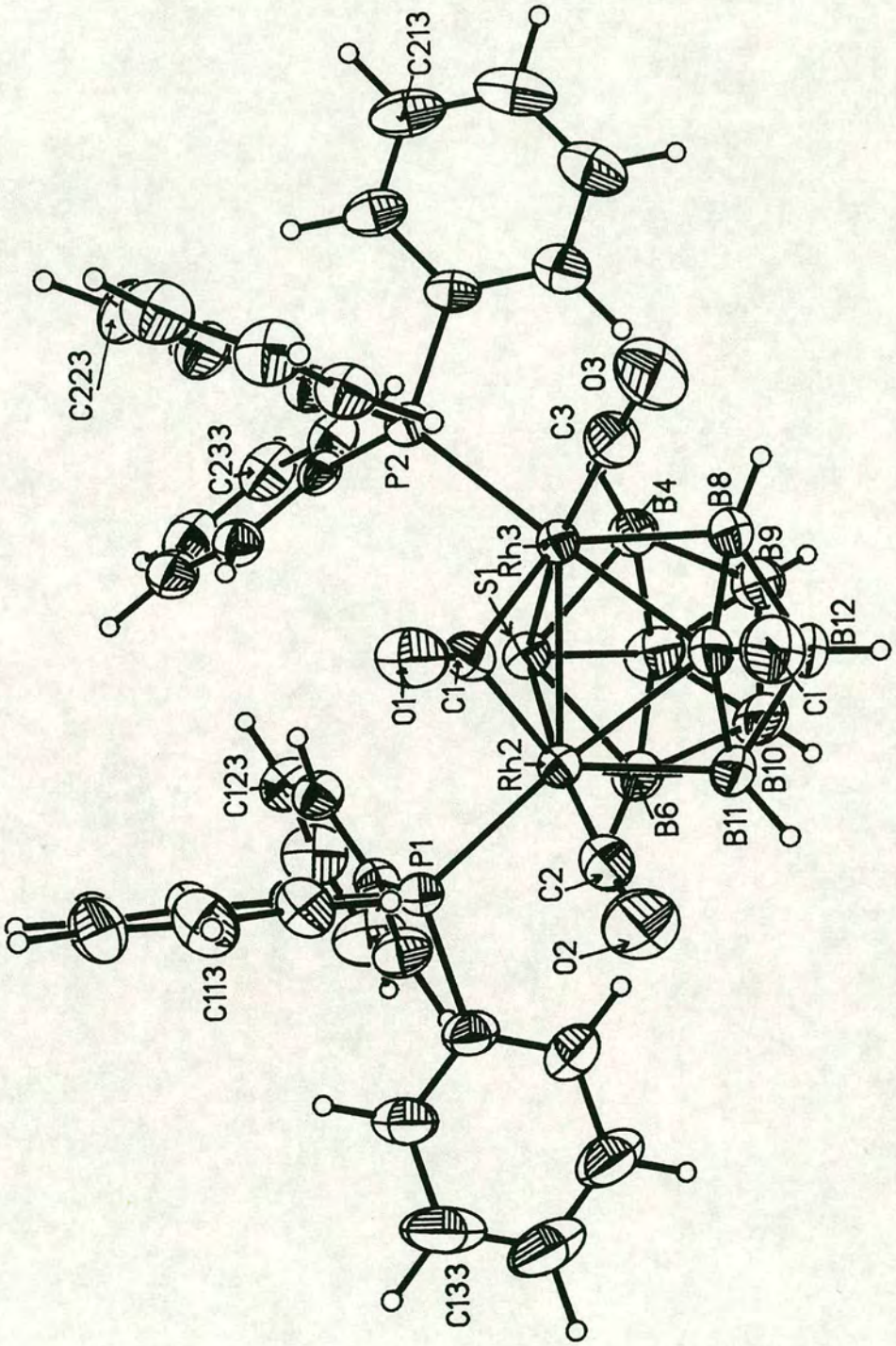

Figure 4.17 Perspective view of **19**
(50% thermal ellipsoids; H atoms have radii of 0.1Å for clarity)

Table 4.8 Selected Interatomic Distances (Å) and Interbond Angles (°) for **19**

S(1) -Rh(2)	2.4189(8)	B(5) -B(10)	1.768(7)
S(1) -Rh(3)	2.4522(8)	B(6) -B(10)	1.751(7)
S(1) - B(4)	2.072(4)	B(6) -B(11)	1.779(6)
S(1) - B(5)	1.996(5)	B(7) - B(8)	1.858(6)
S(1) - B(6)	2.108(4)	B(7) -B(11)	1.852(6)
Rh(2) -Rh(3)	2.7491(3)	B(7) -B(12)	1.770(6)
Rh(2) - B(6)	2.312(4)	B(7) - Cl	1.835(4)
Rh(2) - B(7)	2.307(4)	B(8) - B(9)	1.768(7)
Rh(2) -B(11)	2.259(4)	B(8) -B(12)	1.773(7)
Rh(2) - P(1)	2.3764(8)	B(9) -B(10)	1.762(7)
Rh(2) - C(1)	2.114(3)	B(9) -B(12)	1.759(7)
Rh(2) - C(2)	1.857(4)	B(10) -B(11)	1.774(7)
Rh(3) - B(4)	2.336(4)	B(10) -B(12)	1.751(7)
Rh(3) - B(7)	2.311(4)	B(11) -B(12)	1.776(7)
Rh(3) - B(8)	2.269(5)	P(1) -C(111)	1.8196(23)
Rh(3) - P(2)	2.3751(8)	P(1) -C(121)	1.8253(21)
Rh(3) - C(1)	2.116(3)	P(1) -C(131)	1.827(3)
Rh(3) - C(3)	1.849(4)	P(2) -C(211)	1.8404(23)
B(4) - B(5)	1.870(7)	P(2) -C(221)	1.8349(23)
B(4) - B(8)	1.800(6)	P(2) -C(231)	1.8208(22)
B(4) - B(9)	1.748(6)	C(1) - O(1)	1.143(4)
B(5) - B(6)	1.887(7)	C(2) - O(2)	1.137(5)
B(5) - B(9)	1.763(7)	C(3) - O(3)	1.133(5)

Rh(2) - S(1) -Rh(3)	68.713(23)	B(9) - B(5) -B(10)	59.9(3)
Rh(2) - S(1) - B(6)	60.97(12)	S(1) - B(6) -Rh(2)	66.17(13)
Rh(3) - S(1) - B(4)	61.51(12)	S(1) - B(6) - B(5)	59.65(20)
B(4) - S(1) - B(5)	54.70(18)	Rh(2) - B(6) -B(11)	65.51(20)
B(5) - S(1) - B(6)	54.67(19)	B(5) - B(6) -B(10)	58.0(3)
S(1) -Rh(2) -Rh(3)	56.218(20)	B(10) - B(6) -B(11)	60.3(3)
S(1) -Rh(2) - B(6)	52.86(11)	Rh(2) - B(7) -Rh(3)	73.07(13)
S(1) -Rh(2) - B(7)	85.16(11)	Rh(2) - B(7) -B(11)	64.72(19)
S(1) -Rh(2) -B(11)	85.93(12)	Rh(2) - B(7) - Cl	114.57(20)
S(1) -Rh(2) - P(1)	95.64(3)	Rh(3) - B(7) - B(8)	64.86(19)
S(1) -Rh(2) - C(1)	91.49(9)	Rh(3) - B(7) - Cl	113.27(20)
S(1) -Rh(2) - C(2)	171.13(13)	B(8) - B(7) -B(12)	58.43(25)
Rh(3) -Rh(2) - B(6)	95.81(11)	B(8) - B(7) - Cl	118.4(3)
Rh(3) -Rh(2) - B(7)	53.54(10)	B(11) - B(7) -B(12)	58.69(25)
Rh(3) -Rh(2) -B(11)	93.22(11)	B(11) - B(7) - Cl	119.0(3)
Rh(3) -Rh(2) - P(1)	131.829(22)	B(12) - B(7) - Cl	114.4(3)
Rh(3) -Rh(2) - C(1)	49.51(9)	Rh(3) - B(8) - B(4)	68.99(20)

Rh(3) -Rh(2) - C(2)	126.39(12)	Rh(3) - B(8) - B(7)	67.27(19)
B(6) -Rh(2) - B(7)	81.20(15)	B(4) - B(8) - B(9)	58.7(3)
B(6) -Rh(2) -B(11)	45.80(16)	B(7) - B(8) -B(12)	58.31(25)
B(6) -Rh(2) - P(1)	94.19(11)	B(9) - B(8) -B(12)	59.6(3)
B(6) -Rh(2) - C(1)	142.73(14)	B(4) - B(9) - B(5)	64.4(3)
B(6) -Rh(2) - C(2)	118.82(16)	B(4) - B(9) - B(8)	61.6(3)
B(7) -Rh(2) -B(11)	47.84(16)	B(5) - B(9) -B(10)	60.2(3)
B(7) -Rh(2) - P(1)	173.59(11)	B(8) - B(9) -B(12)	60.3(3)
B(7) -Rh(2) - C(1)	85.75(14)	B(10) - B(9) -B(12)	59.6(3)
B(7) -Rh(2) - C(2)	90.56(16)	B(5) -B(10) - B(6)	64.9(3)
B(11) -Rh(2) - P(1)	125.81(12)	B(5) -B(10) - B(9)	59.9(3)
B(11) -Rh(2) - C(1)	133.58(15)	B(6) -B(10) -B(11)	60.6(3)
B(11) -Rh(2) - C(2)	85.45(17)	B(9) -B(10) -B(12)	60.1(3)
P(1) -Rh(2) - C(1)	100.58(9)	B(11) -B(10) -B(12)	60.5(3)
P(1) -Rh(2) - C(2)	87.77(13)	Rh(2) -B(11) - B(6)	68.69(20)
C(1) -Rh(2) - C(2)	95.94(15)	Rh(2) -B(11) - B(7)	67.44(19)
S(1) -Rh(3) -Rh(2)	55.069(20)	B(6) -B(11) -B(10)	59.0(3)
S(1) -Rh(3) - B(4)	51.21(10)	B(7) -B(11) -B(12)	58.37(25)
S(1) -Rh(3) - B(7)	84.30(11)	B(10) -B(11) -B(12)	59.1(3)
S(1) -Rh(3) - B(8)	84.87(12)	B(7) -B(12) - B(8)	63.3(3)
S(1) -Rh(3) - P(2)	96.66(3)	B(7) -B(12) -B(11)	62.9(3)
S(1) -Rh(3) - C(1)	90.52(9)	B(8) -B(12) - B(9)	60.1(3)
S(1) -Rh(3) - C(3)	167.24(12)	B(9) -B(12) -B(10)	60.3(3)
Rh(2) -Rh(3) - B(4)	93.62(10)	B(10) -B(12) -B(11)	60.4(3)
Rh(2) -Rh(3) - B(7)	53.39(10)	Rh(2) - P(1) -C(111)	117.68(8)
Rh(2) -Rh(3) - B(8)	92.52(12)	Rh(2) - P(1) -C(121)	114.09(7)
Rh(2) -Rh(3) - P(2)	128.876(22)	Rh(2) - P(1) -C(131)	111.24(9)
Rh(2) -Rh(3) - C(1)	49.44(9)	C(111)- P(1) -C(121)	106.13(10)
Rh(2) -Rh(3) - C(3)	128.91(12)	C(111)- P(1) -C(131)	103.01(12)
B(4) -Rh(3) - B(7)	80.76(15)	C(121)- P(1) -C(131)	103.19(11)
B(4) -Rh(3) - B(8)	45.99(16)	Rh(3) - P(2) -C(211)	112.61(8)
B(4) -Rh(3) - P(2)	98.15(10)	Rh(3) - P(2) -C(221)	117.90(8)
B(4) -Rh(3) - C(1)	140.23(14)	Rh(3) - P(2) -C(231)	114.84(8)
B(4) -Rh(3) - C(3)	116.61(16)	C(211)- P(2) -C(221)	102.75(10)
B(7) -Rh(3) - B(8)	47.86(16)	C(211)- P(2) -C(231)	104.21(10)
B(7) -Rh(3) - P(2)	177.64(11)	C(221)- P(2) -C(231)	102.88(10)
B(7) -Rh(3) - C(1)	85.58(14)	Rh(2) - C(1) -Rh(3)	81.06(12)
B(7) -Rh(3) - C(3)	90.03(16)	Rh(2) - C(1) - O(1)	139.2(3)
B(8) -Rh(3) - P(2)	130.01(12)	Rh(3) - C(1) - O(1)	138.9(3)
B(8) -Rh(3) - C(1)	133.44(15)	Rh(2) - C(2) - O(2)	178.5(4)
B(8) -Rh(3) - C(3)	82.85(16)	Rh(3) - C(3) - O(3)	177.0(3)
P(2) -Rh(3) - C(1)	96.55(9)	P(1) -C(111)-C(112)	116.71(17)
P(2) -Rh(3) - C(3)	88.60(12)	P(1) -C(111)-C(116)	123.05(17)
C(1) -Rh(3) - C(3)	100.46(15)	P(1) -C(121)-C(122)	117.65(15)
S(1) - B(4) -Rh(3)	67.29(12)	P(1) -C(121)-C(126)	122.35(15)
S(1) - B(4) - B(5)	60.59(20)	P(1) -C(131)-C(132)	120.97(20)

Rh(3) - B(4) - B(8)	65.02(20)	P(1) -C(131)-C(136)	118.83(20)
B(5) - B(4) - B(9)	58.2(3)	P(2) -C(211)-C(212)	119.31(16)
B(8) - B(4) - B(9)	59.8(3)	P(2) -C(211)-C(216)	120.68(16)
S(1) - B(5) - B(4)	64.71(20)	P(2) -C(221)-C(222)	120.80(16)
S(1) - B(5) - B(6)	65.68(21)	P(2) -C(221)-C(226)	118.97(16)
B(4) - B(5) - B(9)	57.4(3)	P(2) -C(231)-C(232)	121.29(16)
B(6) - B(5) -B(10)	57.1(3)	P(2) -C(231)-C(236)	118.68(16)

This accurate structure determination shows **19** to be a twelve-vertex dirhodathiaborane in which the Rh_2SB_9 polyhedron defines a distorted icosahedron, with (ignoring pendant phenyl groups) approximate *Cs* symmetry fully consistent with the solution ^{11}B n.m.r. spectrum. A sulphur and two rhodium atoms occupy the three vertices of a single triangular face, whilst the unique boron atom [B(7)] mutually adjacent to the two rhodia is *exo*-substituted by a chlorine atom. (The proximity of this boron atom to both metal atoms presumably activates this site towards substitution.) The remaining thiaborane fragment of the polyhedron is substantially regular and Rh—B, B—S and B—B distances are typical of such a species. Minor deviations from ideal mirror symmetry are evidenced by, for example, the environment of the sulphur atom which is somewhat asymmetrically disposed with respect to the notional molecular mirror plane; S(1) is 2.4189(8)Å from Rh(2), but 2.4522(8)Å from the chemically equivalent Rh(3).

Icosahedral complexes of formulation M_2SB_9 are not without precedent: the dirhodium species [7-Cl-2,3-(η^5-C_5Me_5)$_2$-2,3,1-*closo*-$Rh_2SB_9H_8$] **[152]** and [3-Cl-$\mu_{2,3}$-Cl-2,3-$(PPh_3)_2$-2-($Ph_2PC_6H_4$-)-2,3,1-*closo*-$Rh_2SB_9H_8$-7-]* **[137]**, and the 2,3-dicobalt and 7-iodo-2,3-dicobalt analogues of the former compound **[153]**, have been reported. A common feature in compounds of this type is the presence of some substituent in the B(7) position. The present compound **19** - and the relatives **19A** and **19B** - constitute the first examples of M_2SB_9 clusters in which both metal atoms are formally in a univalent oxidation state.

* In this compound the {$Ph_2PC_6H_4$—} moiety is *ortho*-cycloboronated to B(7) of the cage.

Each rhodium vertex has a coordination environment which resembles a distorted octahedron in which a conical {(CO)(μ-CO)(PPh_3)Rh} fragment is η^5-coordinated to the cage *via* the "ligating" $RhSB_3$ face of a *nido*-$RhSB_9$ polyhedron. The two terminal carbonyl groups, and likewise the two triphenylphosphine ligands, are mutually *cisoid*; the rhodium—rhodium connectivity is (essentially) symmetrically bridged by one further carbonyl ligand.

Both terminal CO groups appear to be bound to the rhodium vertices in a typical fashion: distances to rhodium Rh(2)—C(2) and Rh(3)—C(3) are 1.857(4) and 1.849(4)Å; the internal C—O distances C(2)—O(2) and C(3)—O(3) are 1.137(5) and 1.133(5)Å respectively; and the angles at carbon are essentially linear, being 178.5(4) and 177.0(3)° for Rh(2)—C(2)—O(2) and Rh(3)—C(3)—O(3) respectively. Likewise, the phosphorus to rhodium coordination is unremarkable. The Rh(2)—Rh(3) internuclear distance at 2.7491(3)Å is rather long, but not exceptionally so; it is larger than in the above μ-Cl-Rh_2 compound [2.6307(9)Å], but shorter than in the unbridged (and perhaps, therefore, less restricted) (η^5-C_5Me_5)$_2$ analogue [2.778(1)Å]. (A steric factor arising from the presence of bulky PPh_3 groups might also be invoked here.)

One consequence, however, of this rather large metal atom separation in **19** is relatively long distances to the bridging carbonyl moiety; Rh(2)—C(1) is 2.114(3)Å and Rh(3)—C(1) is 2.116(3). This, in turn, affords relatively poor overlap between rhodium *d*-hybrid and carbonyl σ and π orbitals resulting in a C(1)—O(1) distance of 1.143(4)Å, relatively short for a μ-CO function. [This is reflected in the relatively high value of $\nu_{\mu\text{-CO}}$ (1880cm^{-1}) for **19**. The low rhodium oxidation state will also contribute to these features.] The Rh(2)—Rh(3) and C(1)—O(1) vectors do, nevertheless, lie close to coplanar; O(1) is distant only 0.12Å from the plane defined by Rh(2), Rh(3) and C(1), the O atom bending slightly away from S(1) in response (perhaps) to the steric influence of the P-bound phenyl groups.

[In the related compounds [1,1,2,2,-(CO)$_4$-$\mu_{1,2}$-CO-L_2-1,2-*closo*-$Co_2B_{10}H_8$] (**L**$_2$ = 4,7-(Et_2S)$_2$, 4,11-(Et_2S)$_2$) **[154]**, the μ-CO ligands appear to bond rather better to the dicobalt unit with correspondingly longer C—O distance and, hence, lower CO stretching frequency.]

Conclusions

The application of the technique of *r. m. s. misfit* calculations to polyhedral boranes has been further explored and evaluated with particular reference to two series of eleven-vertex heterometallaboranes displaying "anomalous" cluster geometries. In the course of these studies, the presence of an *exo*polyhedrally-bound group such as phosphine was established as significant in terms of vertex atom positions; this was shown to be particularly so where subtle differences in structure are involved.

A pair of dicarbaplatinaundecaboranes were examined using the *r. m. s. misfit* method, by comparison of the appropriate pentagonal pyramidal B_6 fragments with the corresponding fragments derived from model polyboranes with well-established structures. This analysis readily resolved the structural anomaly in this system; the formally *closo*-, but in the solid state apparently *nido*-structured, member of the pair of platinum complexes was confirmed to have a highly distorted, *closo* architecture.

A series of eleven-vertex rhodathiaboranes were similarly studied and, on the basis of the results obtained, the structural irregularity initially appeared to be genuine. However, closer examination of the rhodium environment in the two complexes displaying anomalous structural behaviour revealed two close intramolecular Rh···H approaches. This prompted the suggestion of two long-range, agostic-type Rh$\swarrow$—H—C interactions which supply the metal centre with an additional two electrons and thereby render a cluster electron count consistent with the observed geometry.

Attempts were made rationally to prepare analogues of the "anomalous" rhodathiaboranes which adopted regular geometries in terms of electron counting formalisms. Although ultimately unsuccessful, these synthetic studies yielded several new rhodathiaboranes which have been characterised by a combination of spectroscopic means and single crystal X-ray diffraction studies. The first of these new species was 8-(dppe)-8,7-$RhSB_9H_{10}$, **18**, which constitutes a further example of the above anomalous behaviour, and in which the metal coordination geometry provides further support for the proposal of agostic-type Rh···H interactions. A second, novel

*dirhoda*thiaborane *cis*-2,3-$(CO)_2$-7-Cl-2,3-$(PPh_3)_2$-2,3,1-*closo*-$Rh_2SB_9H_8$, **19**, was also prepared; whilst two other products isolated from this reaction, **19A** and **19B**, have been identified elsewhere as the 7-H-*cis*- isomeric relative of **19** and (tentatively) the corresponding 7-H-*trans*- compound respectively.

Further Work

Clearly much work remains to be done in the rhodathiaborane area; in particular it would be of considerable interest to successfully synthesise and characterise the species $[(CO)(PPh_3)RhSB_9H_{10}]$, and to confirm this compound to have a *closo* cluster geometry in the solid state. Derivatives of similar formulation $[L(PPh_3)RhSB_9H_{10}]$ - such as the mixed phosphine species $[(PMe_3)(PPh_3)RhSB_9H_{10}]$ formally accessible from the reaction of $Cs[SB_9H_{12}]$, [(1,5-*cyclo*-C_8H_{12})$(PPh_3)RhCl$] and PMe_3 - would also merit study.

The value of low-temperature (or solid-state) n.m.r. experiments in detecting (and confirming) the presence of the proposed agostic-type interactions has also been discussed above. A single-crystal *X*-ray diffraction data set of adequate quality, collected at low temperature, may ultimately be sufficiently well-defined that the "agostic" H atoms may be shown to have unusually long C_{phenyl}—H distances. Molecular orbital treatment of this system might shed some light on whether the *closo* isomeric relative of **16** possesses some inherent instability (although this seems highly unlikely), and could definitively discount the involvement in cluster bonding of the lone pair located on the sulphur vertex. Indeed, it may be found by such studies that the highly (η^6-) coordinated 1- position in *closo*- eleven vertex 1-metalla(hetero)boranes is an undesirable environment for certain metal fragments.

It would likewise be informative to prepare the iridium analogue of **16** and establish the polyhedral geometry of this compound; the isoelectronic cobalt, platinum and palladium relatives $[(PPh_3)_2MSB_9H_{10}]$ of **16** may show similar

novel structural behaviour. The platinum/palladium species would, of course be cationic; however, the corresponding *neutral* $[(PPh_3)_2MSB_9H_9]$ compounds do not have to accommodate the "extra" μ-H atom, and so may be more likely to display *closo* cage geometries. More significantly, the equivalent rhodathiaborane $[(PPh_3)_2RhSB_9H_9]^-$, formally obtained simply by deprotonation of **16**, represents a crucial target species; the anionic nature of this compound may further disfavour formation of the proposed Rh⟋—H—C interactions.

Some work remains to be done in fully characterising the products **19A** and **19B**, and to determine by what mechanism the dirhodium species are formed and whether they can be selectively synthesised. It has yet to be seen whether judicious adjustment of the conditions and reagent stoichiometry in this reaction system could afford the original target compound $[(CO)(PPh_3)RhSB_9H_{10}]$ and whether, for example, diiridium analogues may be similarly prepared. The susceptibility of the B(7) position to nucleophilic attack remains not satisfactorily explained; this feature might ultimately be explained *via* the results of a molecular orbital calculation.

Chapter 5

Experimental

Introduction

This chapter details the synthetic, spectroscopic and crystallographic techniques employed in the preparation and characterisation of the compounds described in Chapters 2, 3 and 4, and a brief mention of the methods employed in the structural calculations discussed in Chapter 4.

First, the various synthetic routes to the compounds discussed herein are presented, along with their characterisation by analytical and spectroscopic data.

The following section gives the parameters derived from the crystallographic studies of compounds **1**, **2**, **3**, **4**, **11**, **12** (two crystalline forms), **18** and **19**; this includes the fractional coordinates, and isotropic and anisotropic thermal parameters, for each structural analysis.

Finally, in the context of the structural analysis and the *R.M.S. Misfit* method employed principally in Chapter 4, the coordinates of models and compounds which were compared by this technique are listed.

Synthesis and Characterisation of Compounds 1 to 19

General Techniques

All syntheses were carried out under an atmosphere of dry, oxygen-free nitrogen using standard Schlenk line techniques; some subsequent manipulations were performed in air. Solvents were stored over appropriate drying agents [Na wire (toluene, benzene, *n*-hexane, *i*-hexane, *n*-pentane, diethyl ether, 1,2-dimethoxyethane, tetrahydrofuran), KOH (pyridine), CaH_2 (dichloromethane) Mg/I_2 (methanol, ethanol), P_2O_5 (acetonitrile)]. Hexanes, 1,2-dimethoxyethane, tetrahydrofuran, dichloromethane, methanol, ethanol and acetonitrile were freshly distilled, and all solvents were degassed, prior to use. Infrared spectra were recorded as solutions (or as KBr discs - where indicated) on a Perkin-Elmer 598 spectrophotometer. Except where otherwise indicated, n.m.r. spectra were recorded as solutions at ambient temperatures on Varian VXR-600, Bruker WH360, WP200SY or JEOL FX-90Q instruments. ^{31}P n.m.r. spectra were always recorded with broad-band ^{1}H decoupling. Chemical shifts are reported relative to external standards: Me_4Si (^{1}H), 85% H_3PO_4 (^{31}P) and $BF_3.OEt_2$ (^{11}B). Microanalyses were performed by the departmental service.

Starting Materials

1-Ph-1,2-*closo*-$C_2B_{10}H_{11}$ **[53]**, $[(Me_2PhP)_2PtCl_2]$ **[155]**, $[(Et_3P)_2PtCl_2]$ **[156]**, $[(Ph_3P)_2PtCl_2]$ **[157, 158]**, [(*p*-$tol_3P)_2PtCl_2$] **[159]**, $Cs[SB_9H_{12}]$ **[64]**, $[(CO)_2RhCl]_2$ **[160]**, $[(CH_2{=}CH_2)RhCl]_2$ **[161]**, [(1,5-*cyclo*-C_8H_{12})$RhCl]_2$ **[162]**, [(1,5-*cyclo*-C_8H_{12})$IrCl]_2$ **[163]**, $[(CO)(PPh_3)_2RhCl]$ **[164]**, $[(CO)(PPh_3)_2IrCl]$ **[165]**, $[(CO)(PMe_3)_2IrCl]$ **[166]**, $[(Me_3P)_3RhCl]$ **[167]**, [(dmpe)$RhCl]_2$ **[168]**, [(dppm)$RhCl]_2$ **[168]**, [(dppe)$RhCl]_2$ **[148]** and $[(CO)(PPh_3)RhCl]_2$ **[169]** were synthesised by previously published routes, and their purity checked by microanalysis and/or appropriate spectroscopic means. [However, the last four compounds were prepared *in situ* and used directly.] $B_{10}H_{14}$ was purified prior to use by dissolution in diethyl ether, filtration and evaporation to dryness. All other starting materials were used as supplied.

Preparation of 1-Ph-2-Me-1,2-*closo*-$C_2B_{10}H_{10}$, 1

Typically, $B_{10}H_{14}$ (0.500g, 4.09mmol), *N,N*-dimethylaniline (0.496g, 4.09mmol) and MeC≡CPh (0.475g, 4.09mmol) were dissolved in toluene (50ml) and the resulting solution refluxed for 3 hours. Evaporation of the mixture *in vacuo* yielded a yellow oily solid. Addition of small amounts (1-2ml in total) of ice-cold MeOH to this residue, and decantation of the resulting yellow supernatant liquid (until these washings were colourless), afforded **1** as a white microcrystalline solid. (The combined methanolic washings were evaporated *in vacuo* and treated with MeOH as before to yield further crops of product.) Total yield: 0.647g (2.76mmol, 67.5%) Found: 46.14 %C; 7.80 %H. Calculated for $C_9H_{18}B_{10}$: 46.13 %C; 7.74 %H. IR (CH_2Cl_2): ν_{BH} = 2590 cm^{-1}. N.M.R. (298K, $CDCl_3$): $\delta(^1H)$ 7.66-7.33 (5H, $C_6\underline{H}_5$), 1.68 (br, 3H, $C\underline{H}_3$) p.p.m.; $\delta(^{11}B)$ -2.36 (1B), -3.76 (1B), -8.53 (4B), -9.37 (4B) p.p.m. $\delta(^1H\{^{11}B_{selective}\})$ [integral, δ_B of irradiation/p.p.m.] 2.74 [2H, -9.37], 2.41 [2H, -8.53], 2.38 [2H, -8.53 + 1H, -2.36], 2.34 [1H, -3.76], 2.25 [2H, -9.37] p.p.m.

Diffraction quality colourless *plates* of **1** were grown by slow diffusion of H_2O into a methanolic solution at 4°C.

Preparation of 1-Ph-2-Br-1,2-*closo*-$C_2B_{10}H_{10}$, 2

Compound **2** was prepared by a variation of the method of Zakharkin and Podvisotskaya **[38]**. 1-Ph-1,2-*closo*-$C_2B_{10}H_{11}$ (0.50g, 2.27mmol) was dissolved in benzene (25ml) and cooled to 0°C. MeLi (2.50mmol, 1.8ml of 1.4M solution in Et_2O) was added dropwise, and the mixture allowed to warm to room temperature. A solution of Br_2 (0.37g, 2.32mmol) in benzene (5ml) was slowly added and the mixture stirred at room temperature for 5 hours, during which time a white precipitate was observed. The reaction mixture was filtered, the filtrate evaporated *in vacuo*, and the residue recrystallised from methanol to yield **2** as a white, microcrystalline solid. Yield 0.51g, 1.70mmol, 75%. Found: 32.16 %C; 5.36 %H. Calculated for $C_8H_{15}B_{10}Br$: 32.11 %C; 5.05 %H. IR (CH_2Cl_2): ν_{BH} = 2605, 2630 cm^{-1}. N.M.R. (298K, $CDCl_3$): $\delta(^1H)$ 7.86-7.50 p.p.m. ($C_6\underline{H}_5$); $\delta(^{11}B)$ -2.07 (1B), -3.07 (1B), -6.61 (2B), -7.30 (2B), -7.93 (2B), -8.60 (2B) p.p.m.

Poor quality *plates* of **2** may be grown by slow diffusion of H_2O into a methanolic solution at 4°C. However, slow evaporation and cooling of a warm, concentrated MeOH solution afforded considerably superior, colourless *blocks* of **2** suitable for an *X*-ray diffraction study.

Reaction of 2 with MeLi

A solution of **2** (0.10g, 0.33mmol) in benzene (10ml) was cooled (ice bath) to 0°C, and to this was added, dropwise, a solution of MeLi (0.42mmol, 0.3ml of 1.4M solution in Et_2O). The stirred solution was permitted to warm to room temperature, and the reaction allowed to proceed for *ca.* 4 hours. (The appearance of some precipitate in the vessel evidenced the occurrence of a reaction.) Upon addition of a small amount of H_2O (3ml) the solution clarified; the ethereal layer was collected, dried over $MgSO_4$, and evaporated *in vacuo* to yield an intractable, very pale yellow oil. This product mixture was found, by ^1H n.m.r. spectroscopy, to consist largely of **1** [$\delta(^1H)$ 7.68-7.29 ($C_6\underline{H}_5$) and 1.69 ($C\underline{H}_3$) p.p.m.], and some 1-Ph-1,2-*closo*-$C_2B_{10}H_{11}$ [$\delta(^1H)$ 7.68-7.29 ($C_6\underline{H}_5$) and 3.97 ($C_{cage}\underline{H}$) p.p.m.].

Reaction of 2 with ^{t}BuLi

By analogy with the above reaction, the present scheme was thought to be a possible route to 1-Ph-2-^{t}Bu-1,2-*closo*-$C_2B_{10}H_{10}$. However, in contrast to the previous reaction, the treatment of **2** with ^{t}BuLi, followed by a similar work-up procedure, afforded 1-Ph-1,2-*closo*-$C_2B_{10}H_{11}$ (by ^1H and ^{11}B n.m.r. spectroscopy) as the only identifiable product.

Preparation of 1-Ph-2-Me_3Si-1,2-*closo*-$C_2B_{10}H_{10}$, 3

Compound **3** was synthesised in very good yield from 1-Ph-1,2-*closo*-$C_2B_{10}H_{11}$ by an improvement upon the method of Zakharkin, *et al* **[117]**. Typically, 1-Ph-1,2-*closo*-$C_2B_{10}H_{11}$ (0.50g, 2.27mmol) was dissolved in benzene (25ml) and cooled to 0°C. MeLi (2.50mmol, 1.8ml of 1.4M solution in Et_2O) was added dropwise, and the mixture allowed to warm to room temperature. A solution of Me_3SiCl (0.27g, 2.49mmol) in benzene (5ml) was added dropwise; the mixture was allowed to stir for 20 hours, and finally warmed to 45°C for 2 hours. Removal of volatiles *in vacuo* yielded a white solid. The product was extracted into CH_2Cl_2 (100ml), and the extract filtered and evaporated to yield **3** as a white powder (0.60g 2.05mmol, 90%). Found: 45.40 %C; 8.51 %H. Calculated for $C_{11}H_{24}B_{10}Si$: 45.17 %C; 8.27 %H. IR (CH_2Cl_2): ν_{CH} = 2980, ν_{BH} = 2570 cm^{-1}. N.M.R. (298K, $CDCl_3$): $\delta(^1H)$ 7.68-7.27 (5H, $C_6\underline{H}_5$), -0.09 (9H, $C\underline{H}_3Si$; $^1J_{^{13}C-H} \approx$ 120Hz, $^2J_{^{29}Si-H} \approx$ 7Hz) p.p.m.; $\delta(^{11}B)$ 1.99 (1B), -1.94 (1B), -7.26 (4B), -9.37 (2B), -10.97 (2B) p.p.m.

Slow diffusion of H_2O into a MeOH solution of **3** at 4°C yielded colourless *plates* of diffraction quality.

Preparation of 1-Ph-2-^{t}BuMe$_2$Si-1,2-*closo*-$C_2B_{10}H_{10}$, 4

Typically, 1-Ph-1,2-*closo*-$C_2B_{10}H_{11}$ (0.500g, 2.27mmol) was dissolved in benzene (25ml) and cooled to 0°C. Excess MeLi (4.20mmol, 3.0ml of 1.4M solution in Et_2O) was added dropwise, and the mixture allowed to warm to room temperature. A solution of an excess of ^{t}BuMe$_2$SiCl (0.800g, 5.31mmol) in benzene (5ml) was added dropwise, and the mixture was heated to reflux for 44 hours. Removal of volatiles *in vacuo* yielded an off-white waxy solid. The product was extracted into CH_2Cl_2 (5x50ml) and the extract filtered and evaporated to yield very crude **4** as a white powder. The pure product was separated from unreacted $PhC_2B_{10}H_{11}$ by fractional crystallisation (colourless *blocks* were obtained by slow diffusion of H_2O into a MeOH solution at 4°C); or, more reliably, by preparative thin layer chromatography [Silica gel; eluent CH_2Cl_2/*n*-hexane (1:19); product R_f = 0.7, $PhC_2B_{10}H_{11}$ R_f = 0.5. (Somewhat less reliable separation could be achieved using neat *n*-hexane as eluent.)]. Yield 0.231g, 0.69mmol, 31% (not optimised). Found: 49.25 %C; 8.24 %H. Calculated for $C_{14}H_{30}B_{10}Si$: 50.26 %C; 9.04 %H. IR (CH_2Cl_2): ν_{CH} = 2980, ν_{BH} = 2565 cm^{-1}. N.M.R. (298K, $CDCl_3$): δ(^{1}H) 7.65-7.26 (5H, $C_6\underline{H}_5$), 0.90 [9H, $Me_2SiC(C\underline{H}_3)_3$], -0.25 [6H, $(C\underline{H}_3)_2Si^{t}Bu$], p.p.m.; δ(^{11}B) 2.91 (1B), -2.13 (1B), -6.68 (4B), -8.54 (2B), -11.16 (2B) p.p.m.

Crystals suitable for a single crystal *X*-ray diffraction study were grown by fractional crystallisation as noted above.

Preparation of 1-Ph-2-^{i}Pr$_3$Si-*closo*-$C_2B_{10}H_{10}$, 5

1-Ph-1,2-*closo*-$C_2B_{10}H_{11}$ (0.500g, 2.27mmol) was dissolved in benzene (25ml) and cooled to 0°C. To this, excess MeLi (4.20mmol, 3.0ml of 1.4M solution in Et_2O) was added dropwise, and the mixture allowed to warm to room temperature. An excess of ^{i}Pr$_3$SiCl (0.950g, 4.93mmol) in benzene (5ml) was added dropwise, and the mixture was heated to reflux for 44 hours. The volatile components of the reaction mixture were removed *in vacuo* to yield an oily, off-white solid. The product was extracted into CH_2Cl_2 (5x50ml) and the extract filtered and evaporated to yield very crude **5** as an off-white powder. The pure product was separated from unreacted $PhC_2B_{10}H_{11}$ by preparative thin layer chromatography [Silica gel; eluent *n*-hexane; product R_f = 0.6, $PhC_2B_{10}H_{11}$ R_f = 0.45.]. Yield: *ca.* 0.128g, 0.36mmol, 16% (not optimised). Found: 53.05 %C; 10.42 %H. Calculated for $C_{15}H_{36}B_{10}Si$: 51.09%C; 10.29 %H. IR (*n*-hexane): ν_{BH} = 2575 cm^{-1}. N.M.R. (298K, $CDCl_3$): $\delta(^1H)$ 7.69-7.26 (5H, $C_6\underline{H}_5$), 1.02 [doublet (slightly obscured), 18H, $\{C\underline{H}_3)_2CH\}_3Si$], 0.85 [septet ($^3J_{HH} \approx$ 5Hz), 3H, $(Me_2C\underline{H})_3Si$], p.p.m.; $\delta(^{11}B)$ 3.47 (1B), -2.57 (1B), -6.19 (4B), -8.35 (2B), -11.32 (2B) p.p.m.

Preparation of 1-^{t}Bu-1,2-*closo*-$C_2B_{10}H_{11}$, 6

Typically, $B_{10}H_{14}$ (0.500g, 4.09mmol), *N,N*-dimethylaniline (0.496g, 4.09mmol) and ^{t}BuC≡CH (0.336g, 4.09mmol) were dissolved in benzene (50ml) and the resulting solution gently refluxed for 12 hours. Evaporation of the mixture *in vacuo* afforded a yellow oil. This residue was extracted with *n*-pentane (5 x 50ml), the extract filtered and evaporated *in vacuo* to crude **6** as an off-white, waxy solid. The product was recrystallised by slow diffusion of H_2O into a methanolic solution of crude **6** at 4°C, affording the essentially pure product as colourless *plates*. Total yield: 0.448g (2.24mmol, 54.7%) Found: 36.36 %C; 10.31 %H. Calculated for $C_6H_{20}B_{10}$: 35.74 %C; 10.06 %H. IR (CH_2Cl_2): ν_{BH} = 2550 cm^{-1}. N.M.R. (298K, $CDCl_3$): $\delta(^1H)$ 3.77 (1H, $C_{cage}\underline{H}$), 1.22 (br, 9H, $C\underline{H}_3$) p.p.m.; $\delta(^{11}B)$ -3.22 (2B), -8.23 (2B), -10.52 (2B), -13.02 (4B) p.p.m.

Preparation of 1-^{t}Bu-2-Br-1,2-*closo*-$C_2B_{10}H_{10}$, 7

In a manner analogous to that by which **2** above was formed by the reaction of *C*-lithio-1-Ph-1,2-*closo*-$C_2B_{10}H_{10}$ with Br_2, **6** (0.25g, 1.25mmol) was treated with MeLi (1.40mmol, 1.0ml of 1.4M Et_2O solution) at 0°C then Br_2 (0.22g, 1.38mmol), and allowed to stir at room temperature for 12 hours. The filtered (Celite®) and evaporated reaction mixture was extracted with *n*-pentane (4 x 40ml); this extract was filtered and evaporated *in vacuo* to afford crude **7** as a rather off-white solid. This product was recrystallised by slow diffusion of H_2O into a methanolic solution of crude **7** at 4°C, affording a small quantity of relatively pure product as colourless *plates*. Total yield: 0.11g (0.39mmol, 31%) Found: 27.43 %C; 7.90 %H. Calculated for $C_6H_{19}B_{10}Br$: 25.81 %C; 6.86 %H. IR (CH_2Cl_2): ν_{BH} = 2625 cm^{-1}. N.M.R. (298K, $CDCl_3$): $\delta(^1H)$ 1.45 (br, 9H, C*H*$_3$) p.p.m.; $\delta(^{11}B)$ -2.76 (1B), -3.75 (1B), -6.15 (2B), -8.25 (2B), -10.36 (4B; shoulder at *ca.* 9.5 p.p.m. - i.e., almost 2B:2B) p.p.m.

Reaction of 7 with PhLi

Compound **7** was treated with PhLi in an analogous manner to those reactions of **2** with MeLi and with ^{t}BuLi reported above. This scheme was viewed as a feasible route to 1-Ph-2-^{t}Bu-1,2-*closo*-$C_2B_{10}H_{10}$. However, upon work-up, the only identifiable product of the reaction was **6** (identified by ^1H and ^{11}B n.m.r. spectroscopy).

Attempted Preparation of Other 1-Ph-2-R-1,2-*closo*-$C_2B_{10}H_{10}$ Species

A number of unsuccessful attempts were made to prepare other carbaboranes of the type 1-Ph-2-R-*closo*-$C_2B_{10}H_{10}$ (where R is a bulky alkyl group, for example) which constitute more crowded analogues of **1**. Thus, treatment of the *C*-lithio or *C*-copper(I) derivatives of 1-Ph-1,2-*closo*-$C_2B_{10}H_{11}$ with an appropriate alkyl halide (such as ^{t}BuCl or ^{i}PrCl) failed to yield the anticipated products, but 1-Ph-1,2-*closo*-$C_2B_{10}H_{11}$ (by microanalysis and/or ^1H and ^{11}B n.m.r. spectroscopy) was instead recovered unchanged. Likewise, the attempted preparation of the above species for R = ^{t}Bu by reaction of the *C*-lithio or *C*-copper(I) derivatives of 1-^{t}Bu-1,2-*closo*-$C_2B_{10}H_{11}$ with an aryl halide (such as PhI or *p*-tolI) failed to convert the starting carbaborane (recovered, and identified as above).

Deboronation of 1 by Ethanolic KOH. Formation of Tl[(Tl)7-Ph-8-Me-7,8-*nido*-$C_2B_9H_9$], Tl[(Tl) 8]

Typically, compound **1** (0.500g, 2.13 mmol) was dissolved in EtOH (50ml), and to this was added powdered KOH (0.72g, 12.8 mmol). The mixture was heated to reflux and stirred for *ca.* 26 hours, allowed to cool, and evaporated to dryness *in vacuo*. To the resulting waxy solid was added H_2O (50ml), and the aqueous solution of K_2[7-Ph-8-Me-*nido*-7,8-$C_2B_9H_9$], **K2**8, filtered (Celite®, 1 atm) to remove unreacted **1**. CH_3CO_2Tl (1.68g, 6.38 mmol) was dissolved in H_2O (5ml), and this solution added to the above filtrate, instantaneously precipitating yellow, solid Tl[(Tl)**8**]. The precipitate was collected by filtration, washed with H_2O (2 x 5ml), and dried *in vacuo* in a foil-covered Schlenk tube. Yield 0.370g, 0.586 mmol, 27.4%. Found: 19.32 %C; 3.43 %H. Calculated for $C_9H_{17}B_9Tl_2$: 17.12 %C; 2.72 %H (poor combustion?). IR (KBr disc): ν_{BH} = 2515 cm^{-1}

Deboronation of 1 by Piperidine. Formation of Piperidinium 7-Ph-8-Me-7,8-*nido*-$C_2B_9H_{10}$, [pipH][8H]

Typically, **1** (0.500g, 2.13mmol) was dissolved in benzene (25ml) and piperidine (0.80g, 9.40mmol) was added. The solution was heated to reflux temperature for 20 hours, cooled, evaporated *in vacuo*, and recrystallised from benzene. The product was dried *in vacuo* for several days, affording essentially pure [pipH][8H] in good yield. Yield 0.532g, 1.72mmol, 80.6%. Found: 53.41%C; 10.12 %H; 6.96%N. Calculated for $C_{14}H_{30}B_9N$: 54.30 %C; 9.74 %H; 4.52 %N. I.R. (Nujol Mull): ν_{BH} = 2520 cm^{-1}. N.M.R. (298K, d^6-acetone): $\delta(^1H)$ 7.29 - 7.01 (m, 5H, $C_6\underline{H}_5$), 3.04 (br, m, 4H, -N-C$\underline{H}_2$-), *ca.* 2.1 (C$\underline{H}_3$, obscured by solvent), 1.77 (br, m, 6H, -N-CH_2-C$\underline{H}_2$- and -N-$(CH_2)_2$-C$\underline{H}_2$-) p.p.m. $\delta(^{11}B)$ [integral, $^1J_{BH}$ /Hz] -6.48 [1B, 138], -7.24 [1B, 138], -9.98 [1B, 152], -15.09 [1B, *ca.* 134], -16.12 [2B, 141], -17.39 [1B, 150], -30.05 [1B, $^1J_{BH(endo)}$ 55, $^1J_{BH(exo)}$ 137], -34.47 [1B, 135] p.p.m.

Formation of $[PhCH_2NMe_3]^+[7\text{-Ph-}7,8\text{-}nido\text{-}C_2B_9H_{11}]^-$, BTMA [9H]

1-Ph-1,2-*closo*-$C_2B_{10}H_{11}$ (0.400g, 1.82 mmol) was dissolved in EtOH (50ml) and powdered KOH (0.30g, 5.35 mmol) added. The solution was heated to reflux temperature for 6 hours, cooled to room temperature and bubbled with CO_2; the resulting faintly cloudy mixture was filtered and evaporated to dryness *in vacuo*. The off-white residue was dissolved in H_2O (25ml) and filtered to remove traces of unreacted parent carbaborane. To the filtrate was added a solution of BTMACl (0.65g, 3.50 mmol) in H_2O (5ml), producing an immediate copious slightly off-white precipitate This was collected, washed with H_2O (2 x 10ml), and dried *in vacuo*. Yield 0.56g, 1.56mmol, 85.7%. Found: 59.17 %C; 8.98 %H; 3.89 %N. Calculated for $C_{18}H_{32}B_9N$: 60.10 %C; 8.97 %H; 3.64 %N. I.R. (CH_2Cl_2): ν_{BH} = 2525 cm^{-1}. N.M.R. (298K, d^6-acetone): $\delta(^1H)$ 7.70 - 7.55 (m, 5H, N-$C_6\underline{H}_5$), 7.25 - 6.97 (m, 5H, C_{cage}-$C_6\underline{H}_5$), 4.76 (2H, N-$C\underline{H}_2$-), 3.85 (br, 1H, C_{cage}—H), 3.34 (9H, N-$C\underline{H}_3$) p.p.m. $\delta(^{11}B)$ [$^1J_{BH}$ /Hz] -2.80 [140], -4.27 [135], -7.65 [162], -10.44 [139], -12.10 [*ca.* 120], -13.56 [149], -16.84 [150], -26.70 [$^1J_{BH(endo)}$ 54, $^1J_{BH(exo)}$ 133], -28.90 [136] p.p.m. (all integrals 1B).

Reaction of 1-Ph-1,2-*closo*-$C_2B_{10}H_{11}$ with Piperidine

In an analogous manner to the above reaction of **1** with piperidine, 1-Ph-1,2-*closo*-$C_2B_{10}H_{11}$ (0.500g, 2.27 mmol) was treated with piperidine (0.95g, 11.2mmol) in benzene (50ml) at reflux temperature for 4 hours, and the product recrystallised from benzene as before. Yield: 0.579g, 1.96mmol, 86.3%. Found: 52.66 %C; 9.54 %H; 6.87 %N. Calculated for $C_{13}H_{28}B_9N$: 52.81 %C; 9.55 %H; 4.74 %N. I.R. (Nujol Mull): ν_{BH} = 2525 cm^{-1}. N.M.R. (298K, d^6-acetone): $\delta(^1H)$ 7.24 - 7.05 (m, 5H, C_{cage}-$C_6\underline{H}_5$), *ca.* 4.1 (br, 1H, C_{cage}-$\underline{H}$) 3.11 (br, m, 4H, -N-$C\underline{H}_2$-), 1.75 (br, m, 6H, -N-CH_2-$C\underline{H}_2$- and -N-$(CH_2)_2$-$C\underline{H}_2$-) p.p.m. $\delta(^{11}B)$ [$^1J_{BH}$ /Hz] -7.25 [138], -8.67 [136], -11.90 [149], -14.49 [156], -16.33 [*ca.* 125], -17.55 [152], -20.94 [151], -30.72 [$^1J_{BH(endo)}$ absent, $^1J_{BH(exo)}$ 131], -34.00 [139] p.p.m. (all integrals 1B).

Reaction of 3 with Piperidine

The reaction of **3** with piperidine was performed similarly, save that a longer reaction time (26 hours) was employed. After this time, the pale yellow oily residue obtained was analysed by n.m.r. spectroscopy (^{1}H and ^{11}B), and found to be essentially identical to that obtained from 1-Ph-1,2-*closo*-$C_2B_{10}H_{11}$ above.

Attempted Deboronation of 4

The deboronation of **4** was attempted using both of the deboronating agents (KOH and piperidine) employed above in the "decapitation" of 1-Ph-1,2-*closo*-$C_2B_{10}H_{11}$. However, n.m.r. spectroscopic analysis (^{1}H and ^{11}B spectra) of the product suggested that, even after reaction times of 2-3 days, **4** was recovered unchanged.

Preparation of 1-Ph-2-Me-3,3-($Me_2PhP)_2$-3,1,2-$PtC_2B_9H_9$, 10

To a frozen (77K) solution of [$(Me_2PhP)_2PtCl_2$] (0.200g, 0.369mmol) in CH_2Cl_2 (20ml) was added solid Tl[(Tl)8] (0.233g, 0.369mmol); the mixture was allowed slowly to warm to room temperature and stirred for *ca.* 20 hours. During this period, the progress of the reaction was evidenced by the formation of a yellow-orange solution. The reaction mixture was filtered (Celite®, 1 atm) and concentrated by evaporation *in vacuo* to *ca.* 5ml. Preparative t.l.c. (silica gel, CH_2Cl_2/*n*-hexane 4:1) of this reduced filtrate yielded only one mobile coloured band (*Rf* 0.8) which was collected and identified as **10**. Yield 0.131g, 0.188mmol, 51.2%. Found: 43.44 %C; 5.35%H. Calculated for $C_{25}H_{39}B_9P_2Pt$: 43.27 %C; 5.67 %H. IR (CH_2Cl_2): ν_{BH} = 2520 cm^{-1}. N.M.R. (298K, d^6-acetone): $\delta(^1H)$ 8.33-8.28 (br, m, 2H, C_{cage}-$C_6\underline{H}_5$), 7.74-7.36 (m, 13H, C_{cage}-$C_6\underline{H}_5$ and P-$C_6\underline{H}_5$), *ca.* 2.1 (C_{cage}-$C\underline{H}_3$, obscured by acetone solvent), 1.80 (br, 12H, P-$C\underline{H}_3$) p.p.m.; $\delta(^{31}P)$ -7.74 ($^1J_{PtP}$ 3037Hz) p.p.m. $\delta(^{11}B)$ 21.10 [1B, B(8); $^1J_{PtB}$ ~ 280Hz], 2.37 (1B), 1.08 (1B), -3.19 (1B), -7.57 (1B), -8.24 (1B), -10.58 (1B), -18.89 [1B, B(4 or 7); $^1J_{PtB}$ ~ 190Hz], -21.68 [1B, B(4 or 7); apparent $^1J_{PtB}$ unresolved] p.p.m.

Preparation of 1-Ph-2-Me-3,3-($Et_3P)_2$-3,1,2-$PtC_2B_9H_9$, 11

Similarly, a solution of [$(Et_3P)_2PtCl_2$] (0.250g, 0.498mmol) in CH_2Cl_2 (20ml) was frozen to 77K, and to this was added solid Tl[(Tl)8] (0.315g, 0.500mmol). The mixture was allowed gradually to warm to ambient temperature and stirred for *ca.* 16 hours. Filtration of the reaction mixture (Celite®, 1 atm) afforded an orange solution which was reduced by evaporation *in vacuo* to *ca.* 5ml, and subjected to preparative t.l.c. (silica gel, CH_2Cl_2/*n*-hexane 3:1). A single mobile orange band (*Rf* 0.8) was obtained; this was collected and identified as **11**. Yield 0.241g, 0.369mmol, 74.1%. Found: 38.41 %C; 7.76 %H. Calculated for $C_{21}H_{47}B_9P_2Pt$: 38.51 %C; 7.24 %H. IR (CH_2Cl_2): ν_{BH} = 2548 (sh), 2536 cm^{-1}. N.M.R. (298K, $CDCl_3$): $\delta(^1H)$ 8.24-8.20 (m, 2H, $C_6\underline{H}_5$), 7.26-7.21 (m, 3H, $C_6\underline{H}_5$), 2.06-1.62 (m, 12H, $C\underline{H}_2$), 1.95 (br, s, 3H, C_{cage}-$C\underline{H}_3$), 1.27-1.01 (m, 18H, P-CH_2-$C\underline{H}_3$) p.p.m.; $\delta(^{31}P)$ 16.09 ($^1J_{PtP}$ ~ 2933Hz), 13.72 ($^1J_{PtP}$ ~ 2947Hz) p.p.m.; $^2J_{PP}$ not resolved. $\delta(^{11}B)$ 22.17 [1B, B(8); $^1J_{PtB}$ ~ 270Hz], 3.42 (1B), 1.49 (1B), -4.31 (1B), -7.98 (2B), -10.34 (1B), -20.64 [1B, B(4 or 7); apparent $^1J_{PtB}$ not resolved], -23.38 [1B, B(4 or 7); apparent $^1J_{PtB}$ unresolved] p.p.m.

Slow diffusion of *i*-hexane into a concentrated CH_2Cl_2 solution of **11** at -30°C afforded well-formed *blocks*. However, very slow evaporation of a CH_2Cl_2 solution of **11** under ambient conditions yielded superior quality *blocks*, one of which was the subject of an *X*-ray diffraction analysis.

Preparation of 1-Ph-2-Me-3,3-$(Ph_3P)_2$-3,1,2-$PtC_2B_9H_9$, 12

$[(Ph_3P)_2PtCl_2]$ (0.250g, 0.316mmol) was dissolved in CH_2Cl_2 (20ml) and the solution frozen to 77K. To this was added solid Tl[(Tl)8] (0.202g, 0.320mmol), the mixture was warmed to room temperature and stirred for *ca.* 24 hours. The filtered (Celite®, 1 atm) reaction mixture was concentrated by evaporation *in vacuo*, and the resulting dark orange solution applied to a chromatographic column (20 x 2cm, Florisil® prewashed with eluent; CH_2Cl_2/*n*-hexane, 9:1). Upon elution, a single mobile orange band was obtained; this was collected and evaporated *in vacuo* to yield **12** as an orange solid. Yield 0.103g, 0.109mmol, 35.7%. Found: 56.31 %C; 5.91 %H. Calculated for $C_{45}H_{47}B_9P_2Pt$: 57.36 %C; 5.03 %H. IR (CH_2Cl_2): ν_{BH} = 2524 cm^{-1}. N.M.R. [298K, $CDCl_3$ (^1H), d^6-acetone (^{31}P, ^{11}B)]: $\delta(^1H)$ 7.94-7.00 (m, 35H, $C_6\underline{H}_5$), *ca.* 2.17 (3H, C_{cage}-$C\underline{H}_3$) p.p.m.; $\delta(^{31}P)$ 29.13 ($^1J_{PtP}$ ~ 3075Hz), 22.16 ($^1J_{PtP}$ ~ 3295Hz) p.p.m.; $^2J_{PP}$ not resolved. $\delta(^{11}B)$ 25.83 [1B, B(8); $^1J_{PtB}$ not resolved], 4.95 (br, 1B), 3.61 (2B), -6.62 (2B), -8.88 (1B), -20.80 [1B, B(4 or 7); apparent $^1J_{PtB}$ not resolved], -24.65 [1B, B(4 or 7); apparent $^1J_{PtB}$ unresolved] p.p.m.

Diffraction quality crystals of **12** were obtained by slow diffusion of *n*-hexane into a CH_2Cl_2 solution of **12** at -30°C. A second crystalline modification of **12** was obtained by diffusion of *n*-hexane into an n.m.r. sample (CH_2Cl_2/d^6-acetone solvents) of **12**. Both of these crystalline forms of **12** were studied by *X*-ray diffraction techniques.

Attempted Thermolysis of 12

A sample of **12** (*ca.* 50 mg) was dissolved in $CHCl_3$ (10ml), and warmed to reflux temperature (61°C) for several hours. Spectroscopic analysis (^{31}P, ^{11}B n.m.r.) of the recovered material suggested that **12** had not been affected by the thermolysis.

Preparation of 1-Ph-2-Me-3,3-(*p*-tol$_3$P)$_2$-3,1,2-PtC$_2$B$_9$H$_9$, 13

In a manner analogous to that which afforded the closely-related compound **12** above, a frozen (77K) CH_2Cl_2 (20ml) solution of [(*p*-tol$_3$P)$_2$PtCl$_2$] (0.250g, 0.286mmol) was allowed to react with solid Tl[(Tl)8] (0.181g, 0.287mmol) while warming to room temperature. After being stirred for *ca.* 25 hours, the reaction mixture was filtered (Celite®, 1 atm) and the filtrate concentrated by evaporation *in vacuo*. The resulting orange solution was applied to a chromatographic column (20 x 2cm, Florisil® prewashed with eluent; CH_2Cl_2/*n*-hexane, 9:1), and the mixture eluted to afford a single mobile orange band. This was collected, evaporated *in vacuo* and identified as **13** by conventional means. Yield 0.094g, 0.092mmol, 32.1%. Found: 57.11 %C; 5.62 %H. Calculated for $C_{51}H_{59}B_9P_2Pt$: 59.68 %C; 5.79 %H. IR (CH_2Cl_2): ν_{BH} = 2525 cm^{-1}. N.M.R. [298K, $CDCl_3$ (^1H), d^6-acetone (^{31}P, ^{11}B)]: $\delta(^1H)$ 7.92 (m, 2H, C_{cage}-$C_6\underline{H}_5$), 7.33 (t, 12H, P-$C_6\underline{H}_4$; $^3J_{HH}$ ~ 8.5Hz), 7.17-7.02 (m, 3H, C_{cage}-$C_6\underline{H}_5$), 6.89 (t, 12H, P-$C_6\underline{H}_4$; $^3J_{HH}$ ~ 8.5Hz), 2.29 (s, 9H, P-C_6H_4-$C\underline{H}_3$), 2.27 (s, 9H, P-C_6H_4-$C\underline{H}_3$), 2.16 (s, 3H, C_{cage}-$C\underline{H}_3$) p.p.m.; $\delta(^{31}P)$ 27.67 ($^1J_{PtP}$ ~ 2986Hz), 26.72 ($^1J_{PtP}$ ~ 3175Hz) p.p.m.; $^2J_{PP} \approx$ 20Hz. $\delta(^{11}B)$ 25.30 [1B, B(8); $^1J_{PtB}$ not resolved], 3.84 (br, 2B), -3.26 (2B), -6.97 (2B), -21.59 [br, 1B, B(4 or 7)], -24.44 [br, 1B, B(4 or 7)] p.p.m.

Poor quality orange *plates* of (solvated) **13** - which were somewhat unstable with respect to solvent loss - could be obtained by slow diffusion of *n*-hexane into a CH_2Cl_2 solution of **13** at -30°C.

Attempted Preparations of LL'RhSB$_9$H$_{10}$ Species

A number of unsuccessful attempts were made to prepare thiaborane complexes of the above type (in addition to the two "productive" reactions discussed later), by reaction of Cs[SB$_9$H$_{12}$] with an appropriate metal salt. Thus, interaction of Cs[SB$_9$H$_{12}$] with [(CO)$_2$RhCl]$_2$ or [(CH$_2$=CH$_2$)$_2$RhCl]$_2$ gave an apparent reaction [evidenced by colour change, and monitored by IR spectroscopy (CO stretching region) in the former case]; the product mixtures, however, proved intractable. A similar situation obtained in the reactions with [(1,5-*cyclo*-C$_8$H$_{12}$)MCl]$_2$ (M = Rh, Ir); after a variety of reaction times no soluble, borane-containing (by IR) product was obtained.

With metal substrates of the "Vaska's compound" type [(CO)(PR$_3$)$_2$MCl], it is believed that the *tris*-ligand metallathiaboranes were obtained. With R = Ph, M = Rh, the known **[149]** species 8-CO-8,8-(PPh$_3$)$_2$-8,7-*nido*-RhSB$_9$H$_{10}$ (identified by microanalysis, and IR and ^{31}P n.m.r. spectroscopies) was isolated in excellent yield; for R = Ph, M = Ir and R = Me, M = Ir, it is thought (on the basis of preliminary IR spectroscopic evidence) that analogous compounds resulted.

Reactions of Cs[SB$_9$H$_{12}$] with [(PMe$_3$)$_3$RhCl] or [(dmpe)RhCl]$_2$ yielded intractable mixtures (demonstrated by ^{31}P n.m.r. spectroscopy) of products, none of which displayed chromatographic mobility. In the case of [(dppm)RhCl]$_2$, the reaction afforded an apparently rather unstable product (mixture?); a single, yellow, mobile band was isolated by preparative t.l.c. (*Rf* 0.7, CH$_2$Cl$_2$ eluent), but was found not to contain thiaborane (by IR spectroscopy).

Preparation of 8-(dppe)-8,7-*nido*-RhSB$_9$H$_{10}$, 18

Compound **18** was synthesised by the interaction of [(dppe)RhCl]$_2$ formed *in situ* with the thiaborane precursor Cs[SB$_9$H$_{12}$]. To a suspension of [(CH$_2$=CH$_2$)$_2$RhCl]$_2$ (0.10g, 0.26mmol) in toluene (10ml) was slowly added a solution of Ph$_2$PCH$_2$CH$_2$PPh$_2$ (dppe, 0.21g, 0.52mmol) in toluene (7ml); the mixture was stirred for 22 hours then frozen to 77K. Solid Cs[SB$_9$H$_{12}$] (0.14g, 0.52mmol) was added to the frozen orange-yellow suspension, the mixture

allowed to warm to room temperature and stirred for 5 hours, during which time the solution was observed to darken. Filtration (Celite®, 1 atm) and evaporation *in vacuo* yielded the crude product as an orange powder. This was purified by preparative thin layer chromatography (Silica gel; CH_2Cl_2/*n*-hexane, 3:2; product R_f 0.4) to yield the title compound in 56% yield (0.154g, 0.29mmol). Found: 48.19 %C; 5.08 %H. Calculated for $C_{26}H_{34}B_9P_2RhS$: 48.74 %C; 5.35 %H. IR (CH_2Cl_2) ν_{BH} = 2545, ν_{CH} = 2940 (br) cm^{-1}. N.M.R. [298K, $CDCl_3$ (^1H, ^{31}P), CD_2Cl_2 (^{11}B)]: $\delta(^1H)$ 7.53-7.31 (m, 20H, P-$C_6\underline{H}_5$), 2.90-2.76 (br, m, 2H, P-C$\underline{H}_2$), 2.42-2.30 (br, m, 2H, P-C$\underline{H}_2$) p.p.m.; $\delta(^{31}P)$ 58.73 ($^1J_{RhP}$ ~ 139Hz) p.p.m. $\delta(^{11}B)$ 10.00 [br, 3B], -7.29 (2B), -11.64 (3B), -26.05 (1B) p.p.m.

Reaction of $[(CO)(PPh_3)RhCl]_2$ with $Cs[SB_9H_{12}]$. Formation of *cis*-2,3-$(CO)_2$-$\mu_{2,3}$-CO-7-Cl-2,3-$(PPh_3)_2$-2,3,1-*closo*-$Rh_2SB_9H_8$, 19

$[(CO)(PPh_3)RhCl]_2$ was formed *in situ* and then treated with the thiaborane $Cs[SB_9H_{12}]$ without isolation. $[(CO)_2RhCl]_2$ (100mg, 0.257mmol) was dissolved in degassed benzene (5ml). To this was added, dropwise over *ca.* 15 minutes, a solution of PPh_3 (134mg, 0.511mmol) in degassed benzene (5ml). The mixture was allowed to stir for a further 15 minutes, after which time the reaction was deemed complete. (During this period, a slight lightening in colour of the yellow solution was noted.) The product was not isolated, but complete conversion of the starting material was checked by solution infrared spectroscopy [I.R. (*i*-hexane) showed ν_{CO} = 2088(w), 2021(w), 2004(m), 1991(s) cm^{-1} (*cis* and *trans* products).]

The above solution of $[(CO)(PPh_3)RhCl]_2$ was frozen to 77K and solid $Cs[SB_9H_{12}]$ (141mg, 0.514mmol) was added; the mixture was allowed to warm to room temperature and stirred for *ca.* 3 hours. During the course of the reaction gas evolution (H_2) was apparent, the yellow solution became darker (and more orange) and an apparently yellow solid was deposited. The mixture was filtered and the orange filtrate evaporated *in vacuo* to yield an orange-brown solid. IR (CH_2Cl_2) spectrum of this crude product gave ν_{BH} = 2542(m, br); ν_{CO} = 2056(m), 2033(w), 1997(sh), 1984(s, br) cm^{-1}.

The above orange-brown product was dissolved in a small amount (*ca.* 5ml) of CH_2Cl_2 and applied to chromatographic plates; thin layer chromatography (Silica gel; CH_2Cl_2/*i*-hexane, 3:2) gave bands as follows:

1. brown, *Rf* 0.6, (very small amount, <1mg). IR (CH_2Cl_2): ν_{BH} = 2528(m, br); ν_{CO} = 2027(s, br), 1868(vw, br) cm^{-1}. (Not further pursued)
2. orange, *Rf* 0.5, (27mg). IR (CH_2Cl_2): ν_{BH} = 2529(m, br); ν_{CO} = 2031(s), 1863(m, br) cm^{-1}.
3. red, *Rf* 0.4, (29mg) IR (CH_2Cl_2): ν_{BH} = 2535(m, br); ν_{CO} = 2064(s), 1880(m, br) cm^{-1}.

Band 2. appeared to consist of 2 distinct (but chromatographically inseparable) components; the leading part of the band was a pink colour, whilst the remainder was orange (the pink compound seemed to develop from the orange one). This band was crystallised (slow diffusion of *i*-hexane into a CH_2Cl_2 solution at -30°C) and initially afforded a large number of red-orange *rods*, which were very unstable with respect to solvent loss upon removal from the mother liquor. Further recrystallisation (as before) of these afforded 7 red crystals of **19A**, identified by a crystallographic study **[151]** as *cis*-2,3-$(CO)_2$-$\mu_{2,3}$-CO-2,3-$(PPh_3)_2$-2,3,1-*closo*-$Rh_2SB_9H_9$; in addition, a larger number of yellow *blocks* (of **19B** - thought to be either the *trans* analogue of **19A** or a 7-substituted relative; as yet unidentified **[151]**) and a further majority of the red-orange *rods* obtained previously. The bulk of band 2. is therefore thought to be of formulation $(CO)_2(\mu\text{-}CO)(PPh_3)_2Rh_2SB_9H_9$. Combined yield of band 2.: 27mg, 0.030mmol, 5.8% based on {Rh}. Found: 49.40%C; 4.09%H. Calculated for $C_{39}H_{39}B_9O_3P_2SRh_2$: 49.16%C; 4.13%H. Infrared spectra of this band, or of the components obtained by fractional crystallisation, were always as given above, and are not fully consistent with the proposed *trans*-$(CO)_2$ formulation of the bulk of this band. However, this appears to be due to coincidence, since the ^{31}P spectrum (of the combined band) shows two doublet resonances of apparently similar intensity. N.M.R. ($CDCl_3$, 298K): $\delta(^{31}P)$ 47.9 (d, $^1J_{PRh}$ 161Hz), 23.2 (d, $^1J_{PRh}$ 107Hz) p.p.m.
Full characterisation of the above products **19A** and **19B** will be reported elsewhere **[151]**.

The new compound, *cis*-2,3-$(CO)_2$-$\mu_{2,3}$-CO-7-Cl-2,3-$(PPh_3)_2$-2,3,1-*closo*-$Rh_2SB_9H_8$, **19**, obtained as band 3. above, was fully characterised by conventional spectroscopic means; these spectra are fully consistent with the

exact structural identity of this compound established by the single crystal *X*-ray diffraction study reported later in this Chapter. Yield: 29mg, 0.029mmol, 5.7% based on {Rh}. Found: 44.30%C; 3.11%H. Calculated for $C_{39}H_{38}B_9ClO_3P_2SRh_2$: 50.62%C; 4.14%H. (Poor combustion ?) N.M.R. ($CDCl_3$, 298K): $\delta(^1H)$ 7.26-7.48 (30H, $C_6\underline{H}_5$) p.p.m. $\delta(^{31}P)$ 22.62 (d, br, $^1J_{PRh}$ 88Hz) p.p.m. $\delta(^{11}B)$ 23.94 [1B, B(7)], 11.17 (2B), 6.16 (2B), 0.91 (1B), -3.51 (2B), -35.61 (1B) p.p.m. $\delta(^1H\{^{11}B_{selective}\})$ [integral, δ_B of irradiation/p.p.m.] 4.44 [2H, 11.17], 4.27 [2H, 6.16], 2.80 [2H, -3.51], 2.48 [1H, 0.91], 0.61 [1H, -35.61] p.p.m. [Irradiation at δ_B = 23.94 p.p.m. produced no enhancement of any proton resonance, consistent with the assignment of this latter boron resonance as B(7).]

Crystallisation of band 3. by slow diffusion of *i*-hexane into a concentrated CH_2Cl_2 solution of **19** at -30°C afforded several well-formed dark red *blocks*, one of which was the subject of analysis by single crystal *X*-ray diffraction techniques.

Crystallographic Techniques

The section consists of an outline of the procedures employed in the collection and processing of reflection data for crystals of compounds **1, 2, 3, 4, 11, 12** (two crystalline forms), **18** and **19**, and of the methods used in the solution and refinement of the structures. The fractional coordinates and thermal parameters obtained from the crystallographic studies are tabulated. All data were collected on an Enraf-Nonius CAD4 diffractometer (fitted with a ULT-1 low temperature device in the case of compound **18**), using graphite-monochromated Mo *Kα X*-radiation (λ_{bar} = 0.71069Å). Crystals of diffraction quality were mounted on the diffractometer in sealed Lindemann tubes.

For each crystal, unit cell parameters and the orientation matrix for data collection were obtained from a least-squares refinement of the accurately-measured setting angles of 25 strong, high angle reflections. Data collection was by ω-2θ scans in 96 steps with ω-scan width (0.8+0.34tanθ); ω-scan speeds were in the range 0.824 - 2.356 °min^{-1}. Two standard reflections were measured every 8 *X*-ray hours to monitor any crystal decay; crystal orientation was checked by means of two control reflections which were relocated after every 500 reflections measured. Data were corrected for Lorentz and polarisation effects, and for any decay, using *CADABS* **[170]**. Scattering factors for Pt and Rh were obtained from *International Tables* **[171]**, whilst those for all other atoms were inlaid in the programs used in structure solution and refinement.

Structure solution by direct methods was performed using *SHELXS86* **[112]**, whilst that by Patterson methods employed *SHELX76* **[113]**. The location of further atoms by difference Fourier syntheses was by assignment of residual electron density peaks calculated by the structure refinement program. All refinement was by full-matrix iterative least-squares methods using *SHELX76*. Following isotropic convergence, each data set - with the exception of that for **18**.2CH_2Cl_2 - was empirically corrected for absorption using *DIFABS* **[172]**. (Maximum and minimum correction factors are denoted T_{max} and T_{min} respectively.) Thereafter, equivalent data were merged (merging *R* factor is R_{int}) prior to final (anisotropic) refinement. Molecular

geometry calculations were performed *via CALC* **[173]**, and figures were drawn using *SHELXTL PC* **[174]**.

Isotropic thermal parameters take the form

$$\exp[-8\pi^2U(\sin^2\theta)/\lambda^2]$$

For anisotropic thermal parameters U_{ij} is given by

$$U_{ij}=\exp[-2\pi^2(U_{11}a^{*2}h^2+U_{22}b^{*2}k^2+U_{33}c^{*2}l^2+2U_{23}b^*c^*kl+2U_{13}a^*c^*hl+2U_{12}\,a^*b^*hk)]$$

The equivalent isotropic thermal parameter U_{eq} is defined as

$$U_{eq} = [\Sigma_i\Sigma_jU_{ij}a_i^*a_j^*a_ia_j]/3$$

1-Ph-2-Me-1,2-*closo*-$C_2B_{10}H_{10}$, 1

Crystal Data

$C_9H_{18}B_{10}$, M_r = 234.34, monoclinic, $P2_1/n$, a = 7.3931(19), b = 24.113(5), c = 7.8245(13)Å, β = 94.100(17)°, V = 1391.3Å^3, Z = 4, D_x = 1.119Mg m^{-3}, μ = 0.049mm^{-1}, $F(000)$ = 488, T = 293(1)K. Cell parameters from 25 centred reflections, $11 \leq \theta \leq 13°$. Dimensions 0.4 x 0.2 x 0.15 mm.

Data Collection and Processing

One quadrant of data (h -8 to 8, k 0 to 28, l 0 to 9) was collected for $1 \leq \theta \leq 25°$ over 57 *X*-ray hours with no significant decay or movement. Of 2705 data measured (of which 2443 were unique), 1660 with $F \geq 2.0\sigma(F)$ were retained.

Structure Solution and Refinement

The structure was solved (C and B atoms) by automated direct methods; phenyl H atoms were located by difference Fourier syntheses and allowed positional refinement. The structure was refined by least squares on F, with methyl and cage H atoms set in idealised positions (C-H 1.08Å; B-H 1.10Å). Following application of the absorption correction (T_{max} = 1.230, T_{min} = 0.692; R_{int} = 0.0292), all non-H atoms were refined with anisotropic thermal parameters; cage, methyl and phenyl H atoms were refined with a single group thermal parameter, 0.080(4) Å^2 at convergence. A total of 191 parameters were refined. Weights were assigned according to $w^{-1} = [\sigma^2(F) + 0.003541F^2]$. R = 0.0849, wR = 0.1160, S = 1.152. Maximum shift/e.s.d. in final cycle was 0.001, and maximum and minimum residues in the final ΔF synthesis were 0.26 and -0.30 eÅ^{-3} respectively.

Table 5.1 Fractional Coordinates and Equivalent Isotropic Thermal Parameters (Å²) of Non-H Atoms for **1**

	x	y	z	Ueq
C(1)	0.2045(4)	0.61598(15)	0.8239(4)	0.0344(19)
C(2)	0.0784(5)	0.67343(16)	0.8542(4)	0.0394(22)
B(3)	0.2687(6)	0.67840(19)	0.7424(6)	0.0430(25)
B(4)	0.2771(6)	0.61638(21)	0.6226(5)	0.045(3)
B(5)	0.0915(6)	0.57424(20)	0.6735(6)	0.043(3)
B(6)	-0.0290(5)	0.61097(20)	0.8249(6)	0.0425(25)
B(7)	0.0664(7)	0.71400(21)	0.6756(6)	0.048(3)
B(8)	0.1902(7)	0.67775(21)	0.5225(6)	0.051(3)
B(9)	0.0805(7)	0.61368(23)	0.4815(6)	0.052(3)
B(10)	-0.1099(6)	0.60921(20)	0.6097(6)	0.046(3)
B(11)	-0.1182(6)	0.67175(22)	0.7265(6)	0.049(3)
B(12)	-0.0512(7)	0.67309(21)	0.5126(6)	0.049(3)
C(11)	0.3151(5)	0.59119(16)	0.9755(4)	0.0359(20)
C(12)	0.2607(5)	0.54215(18)	1.0460(5)	0.0478(24)
C(13)	0.3611(6)	0.51811(20)	1.1822(6)	0.055(3)
C(14)	0.5172(6)	0.54384(22)	1.2521(5)	0.055(3)
C(15)	0.5718(7)	0.59275(23)	1.1822(6)	0.063(3)
C(16)	0.4728(6)	0.61647(20)	1.0433(5)	0.053(3)
C(21)	0.0830(6)	0.69819(19)	1.0329(5)	0.057(3)

Table 5.2 Fractional Coordinates of H Atoms in **1**

	x	y	z
H(102)	0.155(7)	0.5244(20)	1.000(6)
H(103)	0.323(6)	0.4757(21)	1.220(6)
H(104)	0.589(6)	0.5300(20)	1.348(6)
H(105)	0.696(7)	0.6047(20)	1.218(6)
H(106)	0.513(7)	0.6483(20)	1.001(6)
H(201)	0.1541	0.73733	1.0345
H(202)	0.1522	0.67010	1.1230
H(203)	-0.0539	0.70476	1.0682
H(3)	0.39255	0.70081	0.78716
H(4)	0.40676	0.59812	0.58956
H(5)	0.09937	0.52883	0.67391
H(6)	-0.10026	0.58921	0.92430
H(7)	0.05786	0.75968	0.67710
H(8)	0.26238	0.69982	0.42481
H(9)	0.08216	0.59388	0.35563
H(10)	0.23408	0.58635	0.56876
H(11)	0.24707	0.69008	0.76160
H(12)	-0.13631	0.69212	0.40760

Table 5.3 Anisotropic Thermal Parameters (x10^3) (Å^2) for **1**

	U11	U22	U33	U23	U13	U12
C(1)	30(2)	41(2)	32(2)	01(2)	-01(1)	-03(2)
C(2)	38(2)	42(2)	37(2)	01(2)	00(2)	05(2)
B(3)	39(2)	50(3)	39(2)	10(2)	-02(2)	-11(2)
B(4)	37(2)	62(3)	34(2)	01(2)	04(2)	04(2)
B(5)	40(2)	46(3)	41(2)	-05(2)	-06(2)	-02(2)
B(6)	30(2)	53(3)	44(3)	07(2)	00(2)	-04(2)
B(7)	57(3)	42(3)	45(3)	08(2)	-05(2)	-02(2)
B(8)	52(3)	62(3)	37(2)	14(2)	01(2)	-07(3)
B(9)	53(3)	66(3)	34(2)	-07(2)	-07(2)	04(3)
B(10)	39(2)	51(3)	46(3)	07(2)	-12(2)	-07(2)
B(11)	38(2)	61(3)	46(3)	06(2)	-05(2)	12(2)
B(12)	48(3)	58(3)	39(2)	05(2)	-09(2)	02(2)
C(11)	31(2)	43(2)	33(2)	-02(2)	-01(2)	04(2)
C(12)	42(2)	48(3)	52(2)	11(2)	-10(2)	00(2)
C(13)	58(3)	52(3)	54(3)	15(2)	-05(2)	03(2)
C(14)	51(3)	71(3)	42(2)	03(2)	-06(2)	13(2)
C(15)	52(3)	82(4)	55(3)	02(3)	-19(2)	-08(3)
C(16)	47(2)	58(3)	53(3)	06(2)	-14(2)	-11(2)
C(21)	69(3)	59(3)	42(2)	-12(2)	-01(2)	13(2)

1-Ph-2-Br-1,2-*closo*-$C_2B_{10}H_{10}$, 2

Crystal Data

$C_8H_{15}B_{10}Br$, M_r = 299.21, orthorhombic, *Pbca*, a = 10.3576(30), b = 11.5431(16), c = 24.229(4)Å, V = 2896.7Å^3, Z = 8, D_x = 1.372Mg m^{-3}, μ = 2.780mm^{-1}, $F(000)$ = 1184, T = 293(1)K. Lattice parameters from 25 centred reflections in the range $12 \leq \theta \leq 13°$. Crystal dimensions 0.4 x 0.4 x 0.4 mm.

Data Collection and Processing

One octant of data was measured for $1 \leq \theta \leq 25°$ (h 0 to 12, k 0 to 13, l 0 to 28), with no significant decay or movement detected, over 59 *X*-ray hours. 2541 data were measured: all were unique, and 1671 with $F \geq 2.0\sigma(F)$ were retained for use in refinement.

Structure Solution and Refinement

The Br atom was located by Patterson synthesis and the positions of C, B and cage H atoms were obtained by difference Fourier syntheses. The structure was refined (least squares on F) with the C atoms of the phenyl ring constrained to be a regular hexagon (C-C 1.395Å) and phenyl H atoms set in idealised positions (C-H 1.08Å); cage H atoms were allowed positional refinement subject to a common B-H distance of 1.11(5)Å. An empirical absorption correction was applied following isotropic convergence (T_{max} = 1.304, T_{min} = 0.659; R_{int} = 0.0000). Thereafter, all non-H atoms were refined anisotropically; H atoms were assigned a single group thermal parameter, 0.060(5) Å^2 at convergence. Weights were assigned according to $w^{-1} = [\sigma^2(F) + 0.001023F^2]$. 192 parameters were refined to R = 0.0696, wR = 0.0729, S = 1.129. Maximum shift/e.s.d. in final cycle was 0.002, and maximum and minimum residues in the final ΔF synthesis were 0.53 (near Br) and -0.94 eÅ^{-3} respectively.

Table 5.4 Fractional Coordinates and Equivalent Isotropic Thermal Parameters (Å²) of Non-H Atoms for **2**

	x	y	z	Ueq
Br(1)	0.05573(8)	0.35618(6)	0.11907(4)	0.0670(5)
C(1)	0.1014(6)	0.0956(5)	0.12567(21)	0.030(3)
C(2)	-0.0023(6)	0.2060(5)	0.13752(24)	0.038(4)
B(3)	-0.0349(7)	0.1131(6)	0.0849(3)	0.040(4)
B(4)	0.0111(8)	-0.0252(6)	0.1087(3)	0.042(4)
B(5)	0.0798(7)	-0.0070(6)	0.1760(3)	0.044(5)
B(6)	0.0732(7)	0.1415(6)	0.1928(3)	0.043(4)
B(7)	-0.1585(8)	0.1677(8)	0.1280(3)	0.053(5)
B(8)	-0.1510(8)	0.0190(7)	0.1105(4)	0.053(5)
B(9)	-0.0824(9)	-0.0548(8)	0.1676(4)	0.061(6)
B(10)	-0.0440(8)	0.0470(8)	0.2194(3)	0.056(5)
B(11)	-0.0921(8)	0.1832(8)	0.1965(3)	0.052(5)
B(12)	-0.1860(8)	0.0612(8)	0.1805(4)	0.061(6)
C(12)	0.3367(4)	0.1410(3)	0.13320(13)	0.046(4)
C(13)	0.4586(4)	0.1547(3)	0.10956(13)	0.061(5)
C(14)	0.4741(4)	0.1438(3)	0.05260(13)	0.063(5)
C(15)	0.3677(4)	0.1193(3)	0.01928(13)	0.073(6)
C(16)	0.2458(4)	0.1056(3)	0.04292(13)	0.060(4)
C(11)	0.2303(4)	0.1165(3)	0.09988(13)	0.036(4)

Table 5.5 Fractional Coordinates of H Atoms in **2**

	x	y	z
H(12)	0.3247	0.1495	0.17729
H(13)	0.5409	0.1738	0.13536
H(14)	0.5684	0.1544	0.03430
H(15)	0.3797	0.1108	-0.02482
H(16)	0.1635	0.0865	0.01712
H(3)	-0.023	0.142	0.0434
H(4)	0.066	-0.089	0.0809
H(5)	0.175	-0.057	0.1815
H(6)	0.150	0.191	0.2171
H(7)	-0.221	0.234	0.1079
H(8)	-0.224	-0.016	0.0821
H(9)	-0.096	-0.144	0.1821
H(10)	-0.035	0.025	0.2617
H(11)	-0.119	0.263	0.2212
H(12)	-0.283	0.052	0.2009

Table 5.6 Anisotropic Thermal Parameters [x10^4 (Br), x10^3 (C, B)] (Å^2) for **2**

	U11	U22	U33	U23	U13	U12
Br(1)	0705(6)	0569(4)	0735(7)	0033(4)	-0167(5)	-0014(4)
C(1)	026(3)	053(3)	012(3)	-004(2)	-004(3)	-001(3)
C(2)	029(3)	059(3)	026(4)	001(3)	-005(3)	000(3)
B(3)	025(4)	069(4)	025(4)	-009(3)	-007(3)	-001(3)
B(4)	039(4)	054(4)	033(5)	-003(3)	007(4)	-010(3)
B(5)	044(5)	063(4)	025(4)	007(3)	009(4)	006(4)
B(6)	040(5)	069(4)	021(4)	-007(4)	-001(3)	002(4)
B(7)	031(4)	087(5)	040(6)	-005(4)	002(4)	007(4)
B(8)	038(5)	083(5)	038(6)	-015(4)	000(4)	-007(4)
B(9)	062(6)	073(5)	047(6)	-005(4)	018(5)	-015(4)
B(10)	053(6)	087(5)	026(5)	006(4)	015(4)	002(5)
B(11)	038(5)	085(5)	032(5)	-018(4)	001(4)	011(4)
B(12)	036(5)	088(6)	058(7)	-008(5)	017(4)	-001(4)
C(12)	028(4)	072(4)	038(4)	004(3)	-010(3)	001(3)
C(13)	036(5)	073(4)	075(6)	004(4)	-007(4)	-003(3)
C(14)	037(5)	077(5)	076(6)	013(4)	020(4)	-006(4)
C(15)	054(5)	121(6)	043(5)	000(4)	012(4)	-008(5)
C(16)	041(4)	106(5)	032(4)	-001(4)	012(4)	-007(4)
C(11)	031(4)	049(3)	028(3)	002(2)	003(3)	002(3)

1-Ph-2-Me_3Si-1,2-*closo*-$C_2B_{10}H_{10}$, 3

Crystal Data

$C_{11}H_{24}B_{10}Si$, M_r = 292.51, monoclinic, $P2_1/m$, a = 8.9306(23), b = 11.303(6), c = 9.1425(21)Å, β = 103.474(20)°, V = 897.5Å^3, Z = 2, D_x = 1.082Mg m^{-3}, μ = 0.111mm^{-1}, $F(000)$ = 308, T = 293(1)K. Cell parameters from 25 centred reflections with $11 \leq \theta \leq 12°$. Crystal dimensions 0.4 x 0.25 x 0.15 mm

Data Collection and Processing

One hemisphere of data was collected in the range $1 \leq \theta \leq 25°$ (h -10 to 10, k -13 to 13, l 0 to 28), over 76 *X*-ray hours with < 1% decay and no appreciable movement. In all, 3375 reflections were measured, of which 1666 were unique. 1441 reflections with $F \geq 2.0\sigma(F)$ were deemed observed.

Structure Solution and Refinement

Si, C and B atoms were located by direct methods. The structure was refined by full matrix least squares on F with methyl and phenyl H atoms, and those cage H atoms [H(9), H(12)] lying on the mirror plane, set in idealised positions (C-H 1.08Å; B-H 1.10Å). The other cage H atoms [H(3), H(4), H(7), H(8)] were allowed positional refinement subject to a common B-H distance, 1.10(3)Å at convergence. (Absorption correction factors: T_{max} = 1.203, T_{min} = 0.824; thereafter, data merged with R_{int} = 0.0129.) All non-H atoms were refined with anisotropic temperature factors; all H atoms were refined with a single group thermal parameter, 0.076(3)Å^2 at convergence. The weighting scheme $w^{-1} = [\sigma^2(F) + 0.000534F^2]$ was employed. 135 parameters were refined with final R factors R = 0.0619, wR = 0.0731 and S = 1.488. Maximum shift/e.s.d. in final cycle was 0.001, and maximum and minimum residues in the final difference Fourier synthesis were 0.32 (near Si) and -0.39 eÅ^{-3} respectively.

Table 5.7 Fractional Coordinates and Equivalent Isotropic Thermal Parameters (Å²) of Non-H Atoms for **3**

	x	y	z	Ueq
C(1)	-0.3572(4)	0.25000	-0.0840(4)	0.0335(20)
C(2)	-0.1621(4)	0.25000	-0.0631(4)	0.0307(19)
B(3)	-0.2543(3)	0.3760(3)	-0.0223(4)	0.0406(18)
B(4)	-0.4068(4)	0.3284(3)	0.0578(4)	0.0458(19)
B(7)	-0.0789(3)	0.3286(3)	0.0953(3)	0.0441(19)
B(8)	-0.2312(4)	0.3774(3)	0.1748(4)	0.0544(22)
B(9)	-0.3243(6)	0.25000	0.2263(6)	0.058(3)
B(12)	-0.1213(6)	0.25000	0.2485(5)	0.060(3)
C(11)	-0.4626(4)	0.25000	-0.2394(4)	0.0391(21)
C(12)	-0.5160(3)	0.3557(3)	-0.3102(3)	0.0573(20)
C(13)	-0.6163(4)	0.3550(4)	-0.4496(4)	0.080(3)
C(14)	-0.6660(6)	0.25000	-0.5207(6)	0.094(5)
Si(1)	-0.06586(11)	0.25000	-0.23163(11)	0.0360(6)
C(21)	0.1439(5)	0.25000	-0.1483(5)	0.068(3)
C(22)	-0.1225(4)	0.3846(3)	-0.3474(3)	0.0541(19)

Table 5.8 Fractional Coordinates of H Atoms in **3**

	x	y	z
H(102)	-0.4787	0.4389	-0.2556
H(103)	-0.6564	0.4378	-0.5038
H(104)	-0.74511	0.25000	-0.62995
H(211)	0.20515	0.25000	-0.23771
H(212)	0.17720	0.32802	-0.08065
H(221)	-0.0791	0.3789	-0.4480
H(222)	-0.0748	0.4617	-0.2836
H(223)	-0.2465	0.3914	-0.3779
H(3)	-0.268	0.451	-0.101
H(4)	-0.514	0.378	0.020
H(7)	0.021	0.383	0.088
H(8)	-0.222	0.4573	0.245
H(9)	-0.37946	0.25000	0.32249
H(12)	-0.04104	0.25000	0.36006

Table 5.9 Anisotropic Thermal Parameters [x10^4 (Si), x10^3 (C, B)] (Å^2) for **3**

	U11	U22	U33	U23	U13	U12
C(1)	029(2)	027(2)	043(2)	000	010(2)	000
C(2)	031(2)	023(2)	036(2)	000	005(1)	000
B(3)	041(2)	030(2)	048(2)	-009(1)	013(1)	-003(1)
B(4)	043(2)	043(2)	051(2)	-007(2)	019(1)	002(1)
B(7)	040(2)	051(2)	038(2)	-012(2)	008(1)	-009(2)
B(8)	056(2)	055(2)	050(2)	-022(2)	018(2)	-009(2)
B(9)	051(3)	076(4)	046(3)	000	021(2)	000
B(12)	049(3)	096(5)	032(3)	000	008(2)	000
C(11)	029(2)	043(2)	043(2)	000	008(2)	000
C(12)	046(2)	056(2)	064(2)	018(2)	000(1)	008(1)
C(13)	057(2)	105(3)	071(2)	034(2)	-002(2)	016(2)
C(14)	045(3)	176(7)	054(3)	000	000(2)	000
Si(1)	0376(6)	0347(6)	0343(6)	0000	0102(4)	0000
C(21)	039(2)	102(4)	061(3)	000	018(2)	000
C(22)	072(2)	042(2)	046(2)	008(1)	018(1)	000(1)

1-Ph-2-^{t}BuMe$_2$Si-1,2-*closo*-$C_2B_{10}H_{10}$, 4

Crystal Data

$C_{14}H_{30}B_{10}Si$, M_r = 334.58, triclinic, *P*bar1, a = 9.3854(19), b = 10.2938(26), c = 13.061(5)Å, α = 68.607(25), β = 70.281(24),γ = 64.998(17)°, V = 1039.34Å^3, Z = 2, D_x = 1.069Mg m^{-3}, μ = 0.103mm^{-1}, $F(000)$ = 356, T = 293(1)K. Cell parameters from 25 centred reflections with $7 \leq \theta \leq 12°$. Dimensions 0.35 x 0.4 x 0.45 mm.

Data Collection and Processing

Over 88 *X*-ray hours, one hemisphere of diffracted intensities was measured for $1 \leq \theta \leq 25°$ (*h* 0 to 11, *k* -13 to 13, *l* -15 to 15). No significant crystal decay or movement was detected. Of the 3895 measured data, 3650 were unique and 2708 with $F \geq 2.0\sigma(F)$ were considered observed and retained for use in solution and refinement of the structure.

Structure Solution and Refinement

Structure solution was by automated direct methods for Si, C and B atoms, and by difference Fourier syntheses for cage H atoms. The structure was refined with methyl and phenyl H atoms in idealised positions (C-H 1.08Å) and the C atoms of the phenyl ring constrained to be a regular hexagon (C-C 1.395Å). Cage H atoms were allowed positional refinement. Following an absorption correction (T_{max} = 1.122, T_{min} = 0.761) and merging of data (R_{int} = 0.0089), all non-H atoms were refined anisotropically. H atoms were assigned a single group thermal parameter, 0.094(3)Å^2 at convergence. The reflection data was weighted according to $w^{-1} = [\sigma^2(F) + 0.000609F^2]$, and a total of 260 parameters were refined. Following a final cycle with maximum shift/e.s.d. 0.001, the *R* factors were R = 0.0792 and wR = 0.0828, and S = 1.372. The maximum and minimum residues in the final ΔF map were 0.23 and -0.29 eÅ^{-3} respectively.

Table 5.10 Fractional Coordinates and Equivalent Isotropic Thermal Parameters (Å²) of Non-H Atoms for **4**

	x	y	z	Ueq
Si(1)	0.33785(13)	0.73909(12)	0.73148(10)	0.0535(8)
C(1)	0.2107(4)	0.4876(4)	0.7439(3)	0.046(3)
C(2)	0.1790(4)	0.6752(4)	0.7172(3)	0.047(3)
B(3)	0.2301(6)	0.5959(5)	0.6064(4)	0.053(3)
B(4)	0.1365(6)	0.4604(6)	0.6535(4)	0.063(4)
B(5)	0.0312(6)	0.4573(6)	0.7952(4)	0.065(4)
B(6)	0.0654(5)	0.5902(5)	0.8329(4)	0.052(3)
B(7)	0.0805(5)	0.7707(5)	0.6082(4)	0.058(4)
B(8)	0.0512(6)	0.6387(6)	0.5687(4)	0.069(4)
B(9)	-0.0753(6)	0.5542(7)	0.6853(5)	0.079(5)
B(10)	-0.1167(6)	0.6334(6)	0.7957(4)	0.070(4)
B(11)	-0.0224(5)	0.7655(5)	0.7487(4)	0.058(4)
B(12)	-0.1088(6)	0.7455(6)	0.6565(5)	0.077(5)
C(12)	0.3451(3)	0.2998(3)	0.89849(19)	0.066(3)
C(13)	0.4800(3)	0.1893(3)	0.93713(19)	0.091(5)
C(14)	0.6262(3)	0.1483(3)	0.86094(19)	0.099(5)
C(15)	0.6375(3)	0.2178(3)	0.74612(19)	0.093(5)
C(16)	0.5026(3)	0.3283(3)	0.70749(19)	0.071(4)
C(11)	0.3564(3)	0.3693(3)	0.78368(19)	0.051(3)
C(21)	0.2434(5)	0.9286(4)	0.7605(4)	0.068(4)
C(22)	0.4380(5)	0.6055(5)	0.8470(4)	0.083(4)
C(23)	0.4871(5)	0.7474(6)	0.5943(4)	0.092(4)
C(31)	0.1445(6)	1.0503(5)	0.6770(4)	0.098(5)
C(41)	0.3832(6)	0.9746(5)	0.7544(4)	0.095(5)
C(51)	0.1390(6)	0.9222(6)	0.8805(4)	0.100(5)

Table 5.11 Fractional Coordinates of H Atoms in **4**

	x	y	z
H(102)	0.2320	0.3316	0.95748
H(103)	0.4712	0.1355	1.02601
H(104)	0.7306	0.0627	0.89085
H(105)	0.7506	0.1861	0.68714
H(106)	0.5114	0.3822	0.61860
H(221)	0.4927	0.4966	0.8319
H(222)	0.3502	0.6021	0.9259
H(223)	0.5298	0.6397	0.8509
H(231)	0.5594	0.8090	0.5888
H(232)	0.4243	0.8019	0.5260
H(233)	0.5640	0.6361	0.5884
H(311)	0.0453	1.0213	0.6792
H(312)	0.2199	1.0616	0.5931
H(313)	0.0984	1.1541	0.6994
H(411)	0.4603	0.9807	0.6712
H(412)	0.4520	0.8935	0.8160
H(413)	0.3352	1.0819	0.7717
H(511)	0.0390	0.8902	0.8890
H(512)	0.0940	1.0301	0.8963
H(513)	0.2108	0.8416	0.9406
H(3)	0.355(5)	0.579(5)	0.545(3)
H(4)	0.197(5)	0.364(5)	0.619(4)
H(5)	0.036(5)	0.344(5)	0.865(4)
H(6)	0.076(5)	0.576(5)	0.911(4)
H(7)	0.107(5)	0.878(5)	0.548(3)
H(8)	0.065(5)	0.651(5)	0.474(4)
H(9)	-0.162(5)	0.514(5)	0.676(3)
H(10)	-0.227(5)	0.642(5)	0.856(4)
H(11)	-0.061(5)	0.863(5)	0.784(3)
H(12)	-0.221(5)	0.831(5)	0.632(4)

Table 5.12 Anisotropic Thermal Parameters [x10⁴ (Si), x10³ (C, B)] (Å²) for **4**

	U11	U22	U33	U23	U13	U12
Si(1)	0460(6)	0474(7)	0499(7)	-0112(5)	-0145(5)	-0172(5)
C(1)	047(2)	041(2)	032(2)	-008(2)	-004(2)	-016(2)
C(2)	042(2)	041(2)	039(2)	-010(2)	-008(2)	-014(2)
B(3)	055(3)	051(3)	035(3)	-012(2)	-009(2)	-019(2)
B(4)	068(3)	059(3)	044(3)	-015(2)	-015(2)	-028(3)
B(5)	059(3)	066(3)	050(3)	-018(3)	-001(2)	-034(3)
B(6)	047(3)	056(3)	035(3)	-017(2)	-001(2)	-020(2)
B(7)	055(3)	051(3)	048(3)	-008(2)	-022(2)	-014(2)
B(8)	064(3)	066(3)	054(3)	-021(3)	-021(3)	-019(3)
B(9)	058(3)	090(4)	069(4)	-037(3)	-012(3)	-032(3)
B(10)	044(3)	079(4)	064(3)	-032(3)	-003(2)	-023(3)
B(11)	040(2)	055(3)	061(3)	-024(2)	-013(2)	-009(2)
B(12)	056(3)	078(4)	073(4)	-030(3)	-024(3)	-014(3)
C(12)	081(3)	047(2)	040(2)	-005(2)	-018(2)	-014(2)
C(13)	115(4)	052(3)	066(3)	-002(2)	-041(3)	-008(3)
C(14)	086(4)	067(3)	098(4)	-018(3)	-037(3)	005(3)
C(15)	071(3)	076(3)	081(4)	-021(3)	-013(3)	014(3)
C(16)	057(3)	063(3)	057(3)	-017(2)	001(2)	-004(2)
C(11)	059(2)	034(2)	040(2)	-007(2)	-012(2)	-014(2)
C(21)	069(3)	049(2)	068(3)	-012(2)	-026(2)	-024(2)
C(22)	076(3)	060(3)	089(4)	-004(2)	-052(3)	-024(2)
C(23)	062(3)	113(4)	075(3)	-036(3)	004(3)	-051(3)
C(31)	104(4)	036(2)	121(5)	-001(3)	-056(3)	-017(2)
C(41)	092(4)	063(3)	105(4)	-017(3)	-038(3)	-035(3)
C(51)	082(3)	092(4)	097(4)	-058(3)	-011(3)	-021(3)

1-Ph-2-Me-3,3-$(PEt_3)_2$-3,1,2-$PtC_2B_9H_9$, 11

Crystal Data

$C_{21}H_{47}B_9P_2Pt$, M_r = 984.65, monoclinic, $P2_1/n$, a = 11.038(6), b = 16.1922(20), c = 16.381(5)Å, β = 100.95(4)°, V = 2874.4(20)Å^3, Z = 4, D_x = 1.511Mg m^{-3}, μ = 5.052mm^{-1}, $F(000)$ = 1304, T = 293(1)K. Cell parameters from 25 centred reflections with $10 \leq \theta \leq 10.5°$. Crystal dimensions 0.5 x 0.5 x 0.25 mm.

Data Collection and Processing

One quadrant of diffraction data (h -13 to 13, k 0 to 20, l 0 to 20) was collected for $1 \leq \theta \leq 26°$ over 131 X-ray hours with no significant decay or movement. Of 6064 data measured (of which 5636 were unique), 4943 with $F \geq 2.0\sigma(F)$ were retained.

Structure Solution and Refinement

The structure was solved by Patterson methods for the Pt atom and by difference Fourier syntheses for B, C and P atoms; in addition, several of the cage H atoms were located in the difference maps, but their positions did not satisfactorily refine. H atoms in hydrocarbon functions, and those bound to the cage, were set in idealised positions (C-H 1.08Å; B-H 1.10Å). Following isotropic convergence, an absorption correction was applied (T_{max} = 1.405, T_{min} = 0.732; equivalent data merged, R_{int} = 0.0812); thereafter all non-H atoms were refined with anisotropic thermal parameters; cage, methyl, ethyl and phenyl H atoms were refined with a single group thermal parameter, 0.096(4) Å^2 at convergence. In all, a total of 326 parameters were refined to R = 0.0344, wR = 0.0384, S = 0.973. Weights were assigned according to w^{-1} = $[\sigma^2(F) + 0.000393F^2]$. The maximum shift/e.s.d. in the final cycle was <0.001, and the maximum and minimum residues in the final ΔF synthesis were 0.80 and -0.75 eÅ^{-3} respectively.

Table 5.13 Fractional Coordinates and Equivalent Isotropic Thermal Parameters (Å²) of Non-H Atoms for **11**

	x	y	z	Ueq
Pt(3)	0.25081(2)	0.05795(1)	0.21772(1)	0.0310(1)
P(1)	0.45520(11)	0.07563(9)	0.27620(7)	0.0351(7)
P(2)	0.25621(12)	0.11535(10)	0.09022(7)	0.0403(7)
C(1)	0.1088(4)	0.0742(3)	0.3440(3)	0.036(3)
C(2)	0.0240(4)	0.1016(4)	0.2634(3)	0.039(3)
B(4)	0.1952(5)	-0.0143(4)	0.3240(3)	0.036(3)
B(5)	0.0645(5)	-0.0159(4)	0.3787(4)	0.043(3)
B(6)	-0.0471(5)	0.0572(5)	0.3376(4)	0.049(4)
B(7)	0.0446(5)	0.0353(4)	0.1802(3)	0.039(3)
B(8)	0.1371(6)	-0.0519(4)	0.2201(4)	0.042(3)
B(9)	0.0723(6)	-0.0917(5)	0.3020(4)	0.049(4)
B(10)	-0.0706(6)	-0.0460(5)	0.3053(4)	0.053(4)
B(11)	-0.0880(5)	0.0337(5)	0.2306(4)	0.049(4)
B(12)	-0.0242(7)	-0.0601(5)	0.2096(4)	0.052(4)
C(102)	0.2484(3)	0.19698(21)	0.37885(15)	0.044(3)
C(103)	0.3091(3)	0.25469(21)	0.43547(15)	0.051(3)
C(104)	0.2930(3)	0.25338(21)	0.51789(15)	0.055(4)
C(105)	0.2162(3)	0.19435(21)	0.54369(15)	0.063(4)
C(106)	0.1555(3)	0.13663(21)	0.48706(15)	0.050(3)
C(101)	0.1716(3)	0.13795(21)	0.40465(15)	0.037(3)
C(201)	-0.0026(5)	0.1926(4)	0.2469(3)	0.052(4)
C(111)	0.4978(5)	0.0451(4)	0.3857(3)	0.047(3)
C(112)	0.6353(5)	0.0520(5)	0.4238(3)	0.064(4)
C(121)	0.5139(5)	0.1831(4)	0.2781(3)	0.050(3)
C(122)	0.6380(5)	0.2002(4)	0.2583(4)	0.069(4)
C(131)	0.5557(5)	0.0102(4)	0.2275(3)	0.053(4)
C(132)	0.5294(7)	-0.0822(4)	0.2372(5)	0.074(5)
C(211)	0.3961(5)	0.1629(4)	0.0658(3)	0.051(3)
C(212)	0.3894(7)	0.1888(5)	-0.0254(4)	0.085(5)
C(221)	0.1379(5)	0.1916(4)	0.0521(3)	0.059(4)
C(222)	0.1625(7)	0.2778(4)	0.0894(5)	0.077(5)
C(231)	0.2189(6)	0.0338(4)	0.0129(3)	0.057(4)
C(232)	0.3160(8)	-0.0335(5)	0.0180(5)	0.080(5)

Table 5.14 Fractional Coordinates of H Atoms in **11**

	x	y	z
H(102)	0.2609	0.1980	0.3150
H(103)	0.3685	0.3004	0.4155
H(104)	0.3399	0.2981	0.5617
H(105)	0.2037	0.1933	0.6075
H(106)	0.0961	0.0909	0.5070
H(201)	-0.0636	0.2002	0.1875
H(202)	0.0830	0.2246	0.2462
H(203)	-0.0455	0.2178	0.2954
H(111)	0.4695	-0.0182	0.3908
H(112)	0.4482	0.0844	0.4214
H(113)	0.6502	0.0327	0.4880
H(114)	0.6657	0.1151	0.4203
H(115)	0.6870	0.0125	0.3897
H(121)	0.5159	0.2068	0.3400
H(122)	0.4480	0.2178	0.2341
H(123)	0.6573	0.2656	0.2621
H(124)	0.6393	0.1787	0.1961
H(125)	0.7072	0.1677	0.3020
H(131)	0.6506	0.0233	0.2551
H(132)	0.5403	0.0242	0.1619
H(133)	0.5908	-0.1181	0.2072
H(134)	0.4349	-0.0963	0.2094
H(135)	0.5452	-0.0972	0.3026
H(211)	0.4706	0.1192	0.0819
H(212)	0.4158	0.2174	0.1040
H(213)	0.4766	0.2159	-0.0317
H(214)	0.3166	0.2335	-0.0432
H(215)	0.3714	0.1353	-0.0653
H(221)	0.0515	0.1698	0.0659
H(222)	0.1304	0.1966	-0.0144
H(223)	0.0878	0.3185	0.0631
H(224)	0.2480	0.3013	0.0758
H(225)	0.1691	0.2745	0.1560
H(231)	0.2059	0.0616	-0.0481
H(232)	0.1338	0.0050	0.0214
H(233)	0.2858	-0.0788	-0.0298
H(234)	0.3297	-0.0629	0.0783
H(235)	0.4018	-0.0063	0.0088

Table 5.14 (cont.)

	x	y	z
H(4)	0.2935	-0.0244	0.3506
H(5)	0.0827	-0.0286	0.4458
H(6)	-0.1023	0.0930	0.3744
H(7)	0.0489	0.0558	0.1169
H(8)	0.1961	-0.0842	0.1832
H(9)	0.0960	-0.1567	0.3160
H(10)	-0.1482	-0.0802	0.3225
H(11)	-0.1766	0.0559	0.1950
H(12)	-0.0669	-0.1032	0.1601

Table 5.15 Anisotropic Thermal Parameters [x10^4 (Pt, P), x10^3 (C, B)] (Å^2) for **11**

	U11	U22	U33	U23	U13	U12
Pt(3)	309(1)	307(1)	302(1)	017(1)	054(1)	-025(1)
P(1)	311(6)	376(8)	353(6)	042(5)	058(5)	-012(5)
P(2)	403(7)	458(9)	332(6)	048(6)	059(5)	-020(6)
C(1)	28(2)	38(3)	41(2)	04(2)	13(2)	00(2)
C(2)	33(2)	42(3)	40(2)	08(2)	07(2)	-03(2)
B(4)	35(3)	32(3)	39(3)	07(2)	09(2)	-05(3)
B(5)	36(3)	45(4)	45(3)	07(3)	08(2)	-12(3)
B(6)	30(3)	63(5)	52(3)	10(3)	13(2)	-02(3)
B(7)	31(3)	45(4)	38(3)	06(3)	01(2)	-07(3)
B(8)	48(3)	34(3)	42(3)	-01(3)	07(2)	-09(3)
B(9)	51(4)	38(4)	53(3)	03(3)	00(3)	-13(3)
B(10)	47(3)	53(5)	55(4)	08(3)	08(3)	-15(3)
B(11)	32(3)	62(5)	51(3)	14(3)	01(2)	-13(3)
B(12)	52(4)	52(4)	47(3)	10(3)	03(3)	-14(3)
C(102)	51(3)	33(3)	48(3)	02(2)	16(2)	01(3)
C(103)	56(3)	35(3)	60(3)	-01(3)	11(3)	-04(3)
C(104)	66(4)	44(4)	51(3)	-06(3)	07(3)	-03(3)
C(105)	87(4)	59(5)	41(3)	-05(3)	17(3)	-02(4)
C(106)	59(3)	49(4)	43(3)	04(3)	19(2)	-01(3)
C(101)	34(2)	38(3)	39(2)	01(2)	10(2)	05(2)
C(201)	56(3)	43(4)	56(3)	10(3)	12(2)	13(3)
C(111)	37(3)	65(4)	37(2)	10(3)	05(2)	-03(3)
C(112)	45(3)	101(6)	44(3)	15(3)	00(2)	-04(3)
C(121)	42(3)	45(4)	60(3)	04(3)	08(2)	-03(3)
C(122)	51(3)	52(4)	101(5)	08(4)	18(3)	-11(3)
C(131)	51(3)	57(4)	50(3)	03(3)	19(2)	10(3)
C(132)	81(5)	54(5)	85(5)	00(4)	25(4)	20(4)
C(211)	46(3)	57(4)	48(3)	08(3)	14(2)	-07(3)
C(212)	80(4)	122(8)	54(4)	25(4)	26(3)	-21(5)
C(221)	50(3)	72(5)	53(3)	22(3)	03(2)	03(3)
C(222)	73(4)	51(5)	105(5)	17(4)	18(4)	00(4)
C(231)	74(4)	57(4)	37(3)	-08(3)	11(3)	-15(3)
C(232)	95(5)	71(5)	75(4)	-18(4)	35(4)	-16(4)

1-Ph-2-Me-3,3-$(PPh_3)_2$-3,1,2-$PtC_2B_9H_9$.0.5CH_2Cl_2, 12 .0.5CH_2Cl_2

Crystal Data

$C_{45}H_{47}B_9P_2Pt.0.5CH_2Cl_2$, M_r = 984.65, triclinic, *P*bar1, a = 10.264(5), b = 12.2057(28), c = 19.3403(26)Å, α = 78.301(16), β = 81.149(21), γ = 74.815(25)°, V = 2276.8Å^3, Z = 2, D_x = 1.436Mg m^{-3}, μ = 3.272mm^{-1}, $F(000)$ = 982, T = 293(1)K. Cell parameters from 25 centred reflections with $10 \leq \theta \leq 12°$. Crystal dimensions 0.3 x 0.4 x 0.3 mm.

Data Collection and Processing

One hemisphere of data (h 0 to 12, k -14 to 14, l -23 to 23) was collected for $1 \leq \theta \leq 25°$ over 202 *X*-ray hours with no significant decay or movement. Of 8494 data measured (of which 8007 were unique), 6834 with $F \geq 2.0\sigma(F)$ were retained.

Structure Solution and Refinement

The structure was solved by Patterson methods for the Pt atom and by difference Fourier syntheses for B, C, P and Cl atoms. Phenyl rings were constrained to be planar, rigid, hexagons (C-C 1.395Å); cage, methyl and phenyl H atoms were set in idealised positions (B-H 1.10Å; C-H 1.08Å). The dichloromethane solvate molecule is situated close to a crystallographic inversion centre, with 50% occupancy of the two adjacent sites. Following isotropic convergence, an absorption correction was applied (T_{max} = 1.136, T_{min} = 0.881; R_{int} = 0.0137); thereafter all non-H atoms (with the exception of those in the dichloromethane solvate molecule) were refined with anisotropic thermal parameters; cage, methyl and phenyl H atoms were refined with a single group thermal parameter, 0.100(4) Å^2 at convergence. In all, a total of 446 parameters were refined to R = 0.0420, wR = 0.0377, S = 1.100. Weights were assigned according to $w^{-1} = [\sigma^2(F) + 0.000221F^2]$. The maximum shift/e.s.d. in the final cycle was 0.002, and the maximum and minimum residues in the final ΔF synthesis were 0.74 and -1.13 eÅ^{-3} respectively.

Table 5.16 Fractional Coordinates and Equivalent Isotropic Thermal Parameters (Å²) of Non-H Atoms for **12** .0.5CH_2Cl_2

	x	y	z	Ueq
C(1)	-0.2555(6)	0.0992(5)	-0.2409(3)	0.044(4)
C(2)	-0.1878(6)	0.0947(5)	-0.3166(3)	0.042(4)
Pt(3)	-0.21742(3)	-0.14488(2)	-0.26179(1)	0.0305(1)
B(4)	-0.3727(8)	0.0111(7)	-0.2216(4)	0.050(5)
B(5)	-0.4187(9)	0.1659(7)	-0.2390(4)	0.056(5)
B(6)	-0.3000(8)	0.2226(6)	-0.3013(4)	0.051(5)
B(7)	-0.2484(7)	0.0049(6)	-0.3553(3)	0.040(4)
B(8)	-0.3995(7)	-0.0349(6)	-0.3013(4)	0.045(4)
B(9)	-0.5059(8)	0.0928(7)	-0.2794(4)	0.056(5)
B(10)	-0.4504(8)	0.2132(7)	-0.3291(4)	0.057(5)
B(11)	-0.2917(8)	0.1599(6)	-0.3770(4)	0.046(5)
B(12)	-0.4252(8)	0.0905(7)	-0.3663(4)	0.057(5)
C(12)	-0.1983(5)	0.1935(3)	-0.1494(3)	0.073(6)
C(13)	-0.1158(5)	0.1953(3)	-0.0988(3)	0.095(7)
C(14)	-0.0058(5)	0.1025(3)	-0.0830(3)	0.114(9)
C(15)	0.0217(5)	0.0080(3)	-0.1177(3)	0.116(9)
C(16)	-0.0608(5)	0.0062(3)	-0.1682(3)	0.091(7)
C(11)	-0.1708(5)	0.0990(3)	-0.1841(3)	0.056(5)
C(21)	-0.0393(6)	0.0958(5)	-0.3345(3)	0.054(4)
P(1)	-0.05174(15)	-0.25920(13)	-0.32927(7)	0.0336(9)
P(2)	-0.22868(16)	-0.27744(13)	-0.15969(8)	0.0373(9)
C(102)	0.1574(3)	-0.4571(3)	-0.28580(22)	0.052(4)
C(103)	0.2079(3)	-0.5755(3)	-0.26663(22)	0.065(5)
C(104)	0.1233(3)	-0.6503(3)	-0.26114(22)	0.065(5)
C(105)	-0.0119(3)	-0.6066(3)	-0.27481(22)	0.067(5)
C(106)	-0.0624(3)	-0.4882(3)	-0.29398(22)	0.052(4)
C(101)	0.0222(3)	-0.4134(3)	-0.29948(22)	0.038(4)
C(202)	0.1655(4)	-0.1929(3)	-0.29672(14)	0.047(4)
C(203)	0.2733(4)	-0.1391(3)	-0.31053(14)	0.062(5)
C(204)	0.3087(4)	-0.0866(3)	-0.37946(14)	0.065(5)
C(205)	0.2362(4)	-0.0879(3)	-0.43457(14)	0.063(5)
C(206)	0.1284(4)	-0.1418(3)	-0.42076(14)	0.048(4)
C(201)	0.0931(4)	-0.1942(3)	-0.35183(14)	0.038(4)
C(302)	-0.2371(4)	-0.2215(3)	-0.43038(21)	0.056(5)
C(303)	-0.2738(4)	-0.2324(3)	-0.49476(21)	0.078(6)
C(304)	-0.1780(4)	-0.2919(3)	-0.54195(21)	0.091(7)
C(305)	-0.0456(4)	-0.3407(3)	-0.52476(21)	0.079(6)
C(306)	-0.0090(4)	-0.3298(3)	-0.46038(21)	0.057(5)
C(301)	-0.1047(4)	-0.2703(3)	-0.41320(21)	0.040(4)

Table 5.16 (cont.)

	x	y	z	U_{eq}
C(402)	-0.3832(4)	-0.3706(3)	-0.22926(20)	0.056(5)
C(403)	-0.4660(4)	-0.4430(3)	-0.23293(20)	0.078(6)
C(404)	-0.4918(4)	-0.5246(3)	-0.17406(20)	0.083(7)
C(405)	-0.4348(4)	-0.5339(3)	-0.11150(20)	0.078(6)
C(406)	-0.3520(4)	-0.4615(3)	-0.10783(20)	0.064(5)
C(401)	-0.3262(4)	-0.3798(3)	-0.16670(20)	0.044(4)
C(502)	-0.4718(4)	-0.1940(4)	-0.08211(23)	0.061(5)
C(503)	-0.5555(4)	-0.1523(4)	-0.02450(23)	0.081(6)
C(504)	-0.4986(4)	-0.1385(4)	0.03323(23)	0.087(7)
C(505)	-0.3578(4)	-0.1664(4)	0.03334(23)	0.098(7)
C(506)	-0.2741(4)	-0.2081(4)	-0.02427(23)	0.073(6)
C(501)	-0.3310(4)	-0.2219(4)	-0.08199(23)	0.045(4)
C(602)	-0.0365(5)	-0.4851(4)	-0.11764(23)	0.062(5)
C(603)	0.0865(5)	-0.5481(4)	-0.09263(23)	0.082(6)
C(604)	0.1771(5)	-0.4910(4)	-0.07732(23)	0.090(7)
C(605)	0.1447(5)	-0.3709(4)	-0.08701(23)	0.091(7)
C(606)	0.0218(5)	-0.3079(4)	-0.11202(23)	0.072(6)
C(601)	-0.0688(5)	-0.3650(4)	-0.12733(23)	0.050(4)
C(1S)	-0.3697(23)	-0.5277(19)	-0.5033(12)	0.108(7)
Cl(1S)	-0.398(3)	-0.4867(24)	-0.4436(14)	0.500(15)
Cl(2S)	-0.442(3)	-0.5803(17)	-0.5427(11)	0.411(11)

Table 5.17 Fractional Coordinates of H Atoms in **12** .0.5CH_2Cl_2

	x	y	z
H(12)	-0.2834	0.2653	-0.1617
H(13)	-0.1371	0.2684	-0.0720
H(14)	0.0580	0.1039	-0.0438
H(15)	0.1068	-0.0638	-0.1054
H(16)	-0.0395	-0.0669	-0.1951
H(21)	-0.0099	0.0923	-0.3902
H(22)	0.0215	0.0222	-0.3031
H(23)	-0.0236	0.1740	-0.3228
H(102)	0.2228	-0.3992	-0.2901
H(103)	0.3125	-0.6093	-0.2560
H(104)	0.1624	-0.7420	-0.2463
H(105)	-0.0773	-0.6645	-0.2706
H(106)	-0.1670	-0.4543	-0.3046
H(202)	0.1381	-0.2335	-0.2433
H(203)	0.3293	-0.1381	-0.2679
H(204)	0.3921	-0.0449	-0.3902
H(205)	0.2637	-0.0473	-0.4879
H(206)	0.0724	-0.1428	-0.4634
H(302)	-0.3112	-0.1754	-0.3938
H(303)	-0.3762	-0.1947	-0.5081
H(304)	-0.2064	-0.3003	-0.5918
H(305)	0.0285	-0.3868	-0.5613
H(306)	0.0935	-0.3675	-0.4471
H(402)	-0.3632	-0.3073	-0.2748
H(403)	-0.5101	-0.4358	-0.2814
H(404)	-0.5559	-0.5807	-0.1769
H(405)	-0.4548	-0.5972	-0.0659
H(406)	-0.3079	-0.4687	-0.0594
H(502)	-0.5159	-0.2048	-0.1268
H(503)	-0.6645	-0.1307	-0.0246
H(504)	-0.5634	-0.1062	0.0778
H(505)	-0.3137	-0.1557	0.0780
H(506)	-0.1651	-0.2297	-0.0242
H(602)	-0.1066	-0.5293	-0.1295
H(603)	0.1115	-0.6410	-0.0851
H(604)	0.2722	-0.5398	-0.0580
H(605)	0.2149	-0.3267	-0.0752
H(606)	-0.0032	-0.2150	-0.1195

Table 5.17 (cont.)

	x	y	z
H(4)	-0.3863	-0.0477	-0.1710
H(5)	-0.4654	0.2127	-0.1939
H(6)	-0.2677	0.3020	-0.3002
H(7)	-0.1859	-0.0569	-0.3879
H(8)	-0.4255	-0.1172	-0.2995
H(9)	-0.6116	0.0876	-0.2626
H(10)	-0.5230	0.2954	-0.3485
H(11)	-0.2509	0.2002	-0.4288
H(12)	-0.4752	0.0802	-0.4109

Table 5.18 Anisotropic Thermal Parameters [x10^4 (Pt, P), x10^3 (C, B)] (Å^2) for **12**.0.5CH_2Cl_2

	U11	U22	U33	U23	U13	U12
C(1)	56(4)	32(3)	37(3)	-02(3)	01(3)	-08(3)
C(2)	41(4)	37(3)	43(3)	-04(3)	-05(3)	-13(3)
Pt(3)	292(1)	296(1)	289(1)	-048(1)	-031(1)	-065(1)
B(4)	53(5)	46(4)	40(4)	-02(3)	07(4)	-07(4)
B(5)	56(5)	40(4)	59(5)	-06(4)	09(4)	05(4)
B(6)	59(5)	32(4)	54(4)	-02(3)	00(4)	-08(4)
B(7)	38(4)	40(4)	37(4)	-04(3)	-08(3)	-06(3)
B(8)	36(4)	38(4)	53(4)	-03(3)	-08(3)	-05(3)
B(9)	38(4)	44(5)	75(5)	-07(4)	-04(4)	02(4)
B(10)	54(5)	41(4)	63(5)	00(4)	-03(4)	05(4)
B(11)	50(5)	39(4)	42(4)	-05(3)	-05(3)	-07(4)
B(12)	44(5)	58(5)	60(5)	-02(4)	-16(4)	-07(4)
C(12)	99(6)	64(5)	51(4)	-16(4)	03(4)	-37(5)
C(13)	155(10)	80(6)	50(5)	-21(4)	-06(5)	-65(7)
C(14)	162(10)	107(8)	71(6)	-11(6)	-57(6)	-59(8)
C(15)	148(10)	79(7)	116(8)	-17(6)	-78(7)	-17(6)
C(16)	115(7)	64(5)	87(6)	-24(4)	-59(6)	-02(5)
C(11)	87(5)	42(4)	35(3)	-11(3)	-10(3)	-19(4)
C(21)	50(4)	48(4)	60(4)	-09(3)	-01(3)	-23(3)
P(1)	317(8)	339(8)	317(8)	-077(6)	-043(6)	-079(7)
P(2)	382(9)	358(9)	327(8)	-042(7)	-020(7)	-079(7)
C(102)	39(4)	51(4)	59(4)	-09(3)	-12(3)	-04(3)
C(103)	58(5)	51(4)	75(5)	-20(4)	-17(4)	11(4)
C(104)	88(6)	37(4)	60(4)	-14(3)	-13(4)	06(4)
C(105)	87(6)	37(4)	69(5)	-15(3)	-04(4)	-15(4)
C(106)	55(4)	41(4)	57(4)	-14(3)	00(3)	-19(3)
C(101)	34(3)	46(4)	29(3)	-12(3)	02(2)	-02(3)
C(202)	40(4)	61(4)	35(3)	-06(3)	-05(3)	-20(3)
C(203)	51(4)	74(5)	60(4)	-07(4)	-22(3)	-27(4)
C(204)	51(4)	76(5)	66(5)	-07(4)	00(4)	-40(4)
C(205)	59(5)	75(5)	47(4)	02(4)	02(3)	-31(4)
C(206)	45(4)	52(4)	42(3)	-06(3)	-04(3)	-18(3)
C(201)	30(3)	39(3)	41(3)	-11(3)	-04(3)	-09(3)
C(302)	61(5)	54(4)	50(4)	-06(3)	-21(3)	-20(4)
C(303)	98(6)	66(5)	69(5)	-04(4)	-47(5)	-27(5)
C(304)	136(9)	93(7)	45(4)	-18(4)	-24(5)	-60(6)
C(305)	112(7)	79(6)	42(4)	-24(4)	01(4)	-35(5)
C(306)	67(5)	53(4)	45(4)	-21(3)	-02(3)	-14(4)
C(301)	44(4)	37(3)	37(3)	-08(3)	-09(3)	-15(3)

Table 5.18 (cont.)

	U11	U22	U33	U23	U13	U12
C(402)	44(4)	49(4)	71(5)	-21(4)	-05(3)	-13(3)
C(403)	56(5)	68(5)	104(6)	-26(5)	-16(5)	-15(4)
C(404)	64(5)	51(5)	128(8)	-29(5)	14(5)	-25(4)
C(405)	66(5)	43(4)	114(7)	-09(4)	11(5)	-21(4)
C(406)	75(5)	49(4)	57(4)	02(3)	05(4)	-16(4)
C(401)	37(4)	32(3)	59(4)	-17(3)	09(3)	-11(3)
C(502)	53(5)	58(4)	64(4)	-16(4)	11(4)	-17(4)
C(503)	76(6)	61(5)	94(6)	-22(5)	36(5)	-22(4)
C(504)	140(9)	52(5)	47(5)	-10(4)	39(5)	-10(5)
C(505)	151(10)	70(6)	53(5)	-24(4)	-12(6)	11(6)
C(506)	107(7)	53(5)	48(4)	-14(3)	-12(4)	00(4)
C(501)	64(4)	28(3)	35(3)	-01(3)	01(3)	-10(3)
C(602)	69(5)	56(5)	44(4)	-01(3)	-02(4)	10(4)
C(603)	83(6)	83(6)	56(5)	-02(4)	-15(4)	29(5)
C(604)	51(5)	140(9)	56(5)	02(5)	-16(4)	08(6)
C(605)	63(6)	126(8)	71(5)	03(5)	-17(4)	-26(6)
C(606)	60(5)	93(6)	54(4)	06(4)	-19(4)	-23(5)
C(601)	49(4)	64(5)	27(3)	00(3)	-06(3)	-09(4)

1-Ph-2-Me-3,3-(PPh_3)$_2$-3,1,2-$PtC_2B_9H_9$.(solvent), 12.(unknown solvent)

Crystal Data

$C_{45}H_{47}B_9P_2Pt$.(unknown solvent), M_r = 1002.25, monoclinic, $P2_1/n$, a = 10.316(13), b = 22.227(6), c = 19.996(6) Å, β = 89.86(6)°, V = 4584(6) Å^3, Z = 4, D_x = 1.452 Mg m^{-3}, μ = 3.194mm^{-1}, $F(000)$ = 2000, T = 293(1)K. Cell parameters from 25 centred reflections with $8 \leq \theta \leq 9°$. Crystal dimensions 0.2 x 0.4 x 0.25 mm. [M_r, D_x, μ and $F(000)$ calculated on the basis of "(solvent)"* being five carbon atoms of unit occupancy per asymmetric unit.]

Data Collection and Processing

A quadrant of data (h -10 to 10, k 0 to 23, l 0 to 21; $1 \leq \theta \leq 22$) was collected. Of the 5895 reflections measured over 132 X-ray hours with no significant crystal decay or movement, 5602 were unique and 4208 with $F \geq 2.0\sigma(F)$ were considered observed and retained for use in refinement.

Structure Solution and Refinement

The Pt atom was located by inspection of a Patterson map, whilst the remaining non-H atoms were found by difference Fourier syntheses. Phenyl rings were constrained to be regular planar hexagons (C—C 1.395Å); all cage, methyl and phenyl H atoms were included in fixed, calculated positions (B—H 1.10, C—H 1.08Å). Following isotropic convergence, an empirical absorption correction was applied (T_{max} = 1.119, T_{min} = 0.858); thereafter, equivalent data were merged (R_{int} = 0.0162), and all non-H atoms in the molecule of **12** were allowed to refine with anisotropic temperature factors. A total of 434 parameters were refined, to final residuals R = 0.0613, wR = 0.0652 and S = 1.244. Reflection data were weighted according to the scheme $w^{-1} = [\sigma^2(F) + 0.000669F^2]$. In the final cycle, the maximum shift/e.s.d. was <0.001, and the maximum and minimum residues in the final ΔF map were 1.08 (in the area occupied by the solvates) and 1.32 eÅ^{-3} respectively.

---

* An unidentified solvent molecule was located in the crystal lattice, and was modelled as five carbon atoms with fixed isotropic thermal parameters of 0.06Å^2. The positions and occupancies of these were allowed some refinement before these, too, were fixed. (The ultimate values of these are listed in table 5.17.) It is thought that a mixture of dichloromethane, hexane and d^6-acetone perhaps partially occupy this rather unrestricted cavity.

Table 5.19 Fractional Coordinates and Equivalent Isotropic Thermal Parameters (Å²) of Non-H Atoms for **12** .(unknown solvent)

	x	y	z	U_{eq}
C(1)	0.5411(13)	0.3084(6)	0.1294(7)	0.032(9)
C(2)	0.5145(13)	0.2617(6)	0.1857(7)	0.032(9)
Pt(3)	0.53799(5)	0.37938(3)	0.25310(3)	0.0263(3)
B(4)	0.4521(15)	0.3766(9)	0.1474(9)	0.039(10)
B(5)	0.4080(17)	0.3214(8)	0.0825(9)	0.038(11)
B(6)	0.4442(17)	0.2473(9)	0.1068(9)	0.042(12)
B(7)	0.4114(17)	0.2934(8)	0.2462(9)	0.040(11)
B(8)	0.3444(17)	0.3646(8)	0.2141(9)	0.038(11)
B(9)	0.2848(17)	0.3510(9)	0.1355(10)	0.044(12)
B(10)	0.2846(16)	0.2728(9)	0.1156(9)	0.043(12)
B(11)	0.3645(17)	0.2377(9)	0.1842(10)	0.046(12)
B(12)	0.2592(17)	0.3004(8)	0.1998(9)	0.037(11)
C(12)	0.7802(10)	0.3196(5)	0.1440(4)	0.048(11)
C(13)	0.9053(10)	0.3265(5)	0.1186(4)	0.071(14)
C(14)	0.9251(10)	0.3302(5)	0.0497(4)	0.084(16)
C(15)	0.8198(10)	0.3271(5)	0.0062(4)	0.075(15)
C(16)	0.6946(10)	0.3202(5)	0.0316(4)	0.051(12)
C(11)	0.6748(10)	0.3164(5)	0.1005(4)	0.039(10)
C(21)	0.6176(16)	0.2172(7)	0.2069(8)	0.051(11)
P(1)	0.5927(4)	0.35753(18)	0.36194(20)	0.0332(24)
P(2)	0.6467(4)	0.46949(17)	0.24080(19)	0.0312(22)
C(112)	0.6226(8)	0.4644(4)	0.4314(5)	0.040(10)
C(113)	0.6811(8)	0.5050(4)	0.4751(5)	0.050(11)
C(114)	0.8008(8)	0.4914(4)	0.5037(5)	0.069(14)
C(115)	0.8620(8)	0.4372(4)	0.4886(5)	0.074(14)
C(116)	0.8036(8)	0.3965(4)	0.4449(5)	0.060(12)
C(111)	0.6839(8)	0.4101(4)	0.4163(5)	0.030(8)
C(122)	0.3271(10)	0.3559(5)	0.3926(4)	0.045(10)
C(123)	0.2214(10)	0.3493(5)	0.4356(4)	0.062(13)
C(124)	0.2414(10)	0.3349(5)	0.5027(4)	0.072(15)
C(125)	0.3670(10)	0.3271(5)	0.5268(4)	0.070(14)
C(126)	0.4728(10)	0.3337(5)	0.4838(4)	0.050(11)
C(121)	0.4528(10)	0.3481(5)	0.4167(4)	0.042(10)
C(132)	0.8105(10)	0.2905(4)	0.3396(5)	0.047(11)
C(133)	0.8912(10)	0.2402(4)	0.3427(5)	0.070(14)
C(134)	0.8469(10)	0.1872(4)	0.3724(5)	0.094(19)
C(135)	0.7220(10)	0.1846(4)	0.3990(5)	0.084(16)
C(136)	0.6412(10)	0.2348(4)	0.3959(5)	0.065(13)
C(131)	0.6855(10)	0.2878(4)	0.3662(5)	0.043(10)

Table 5.19 (cont.)

	x	y	z	U_{eq}
C(212)	0.8931(10)	0.4281(4)	0.2589(5)	0.041(10)
C(213)	1.0199(10)	0.4283(4)	0.2830(5)	0.060(12)
C(214)	1.0619(10)	0.4749(4)	0.3243(5)	0.075(15)
C(215)	0.9771(10)	0.5214(4)	0.3415(5)	0.068(14)
C(216)	0.8504(10)	0.5212(4)	0.3173(5)	0.051(11)
C(211)	0.8083(10)	0.4745(4)	0.2761(5)	0.036(9)
C(222)	0.7862(10)	0.4833(5)	0.1186(6)	0.062(13)
C(223)	0.7989(10)	0.5029(5)	0.0526(6)	0.098(19)
C(224)	0.6965(10)	0.5328(5)	0.0216(6)	0.088(18)
C(225)	0.5814(10)	0.5430(5)	0.0565(6)	0.067(14)
C(226)	0.5687(10)	0.5234(5)	0.1225(6)	0.054(12)
C(221)	0.6711(10)	0.4936(5)	0.1535(6)	0.042(10)
C(232)	0.4434(9)	0.5221(3)	0.3117(5)	0.051(11)
C(233)	0.3751(9)	0.5704(3)	0.3389(5)	0.053(11)
C(234)	0.4208(9)	0.6290(3)	0.3302(5)	0.060(12)
C(235)	0.5348(9)	0.6392(3)	0.2943(5)	0.057(12)
C(236)	0.6031(9)	0.5908(3)	0.2670(5)	0.051(11)
C(231)	0.5574(9)	0.5322(3)	0.2758(5)	0.037(9)

Table 5.20 Fractional Coordinates, and Occupancy Parameter K, of "solvent" Atoms in **12** .(unknown solvent)

	x	y	z	K
C(1S)	0.31166	0.02237	0.35115	1.01216
C(2S)	0.41746	0.04857	0.36766	0.76383
C(3S)	0.46557	0.10117	0.33957	1.00371
C(4S)	0.21276	0.13411	0.34023	1.47133
C(5S)	0.30319	0.09329	0.31835	0.71684

Table 5.21 Fractional Coordinates of H Atoms in **12** .(unknown solvent)

	x	y	z
H(12)	0.7648	0.3167	0.1974
H(13)	0.9869	0.3289	0.1522
H(14)	1.0220	0.3356	0.0300
H(15)	0.8351	0.3300	-0.0472
H(16)	0.6130	0.3177	-0.0020
H(21A)	0.5801	0.1889	0.2464
H(21B)	0.7016	0.2413	0.2247
H(21C)	0.6447	0.1896	0.1646
H(112)	0.5300	0.4749	0.4093
H(113)	0.6336	0.5471	0.4868
H(114)	0.8460	0.5229	0.5375
H(115)	0.9547	0.4266	0.5107
H(116)	0.8511	0.3544	0.4332
H(122)	0.3116	0.3671	0.3407
H(123)	0.1241	0.3554	0.4170
H(124)	0.1595	0.3298	0.5360
H(125)	0.3825	0.3159	0.5787
H(126)	0.5701	0.3276	0.5024
H(132)	0.8447	0.3315	0.3165
H(133)	0.9880	0.2423	0.3221
H(134)	0.9095	0.1483	0.3748
H(135)	0.6877	0.1435	0.4220
H(136)	0.5444	0.2327	0.4165
H(212)	0.8606	0.3920	0.2269
H(213)	1.0855	0.3924	0.2697
H(214)	1.1600	0.4751	0.3430
H(215)	1.0097	0.5575	0.3734
H(216)	0.7847	0.5571	0.3306
H(222)	0.8656	0.4602	0.1426
H(223)	0.8881	0.4949	0.0256
H(224)	0.7063	0.5480	-0.0295
H(225)	0.5021	0.5662	0.0325
H(226)	0.4796	0.5314	0.1495
H(232)	0.4080	0.4767	0.3184
H(233)	0.2869	0.5625	0.3667
H(234)	0.3680	0.6664	0.3513
H(235)	0.5702	0.6845	0.2875
H(236)	0.6913	0.5987	0.2392

Table 5.21 (cont.)

	x	y	z
H(4)	0.49048	0.42308	0.14021
H(5)	0.42188	0.33354	0.02884
H(6)	0.47917	0.21131	0.07230
H(7)	0.42392	0.28749	0.30055
H(8)	0.31484	0.40214	0.24815
H(9)	0.20998	0.38378	0.11986
H(10)	0.20637	0.25196	0.08602
H(11)	0.34559	0.19146	0.20425
H(12)	0.16702	0.29750	0.22768

Table 5.22 Anisotropic Thermal Parameters [x10^4 (Pt), x10^3 (P, C, B)] (Å^2) for **12** .(unknown solvent)

	U11	U22	U33	U23	U13	U12
C(1)	29(8)	25(8)	41(9)	-02(7)	-02(7)	-02(7)
C(2)	25(8)	35(9)	36(9)	-01(7)	-09(7)	-08(7)
Pt(3)	258(3)	263(3)	266(3)	018(4)	001(2)	-002(4)
B(4)	22(9)	45(11)	50(11)	-10(11)	-08(8)	-06(10)
B(5)	39(11)	42(11)	32(11)	-10(9)	-01(8)	-03(9)
B(6)	39(11)	52(12)	35(11)	-13(9)	-22(9)	00(9)
B(7)	42(11)	35(11)	42(11)	-16(9)	-03(9)	-01(8)
B(8)	41(11)	39(12)	33(10)	-04(8)	-07(8)	-01(8)
B(9)	29(11)	50(12)	53(13)	-13(10)	-02(9)	-01(9)
B(10)	25(10)	63(14)	39(11)	15(10)	-03(8)	01(9)
B(11)	32(10)	43(12)	64(14)	13(10)	04(9)	-10(9)
B(12)	39(11)	36(11)	37(11)	-04(9)	-05(9)	-04(9)
C(12)	26(9)	78(13)	40(10)	-14(9)	01(8)	-07(9)
C(13)	58(13)	79(15)	76(15)	-22(12)	07(11)	-06(11)
C(14)	79(16)	79(15)	94(18)	-07(13)	44(14)	01(12)
C(15)	66(14)	120(18)	39(12)	-01(12)	32(11)	08(13)
C(16)	55(12)	53(12)	44(11)	05(9)	-08(9)	-07(9)
C(11)	41(10)	35(9)	41(10)	-08(8)	22(8)	-10(8)
C(21)	65(12)	38(10)	49(11)	-05(8)	-10(9)	18(9)
P(1)	37(2)	32(2)	30(2)	01(2)	02(2)	00(2)
P(2)	30(2)	33(2)	31(2)	-01(2)	-01(2)	01(2)
C(112)	56(10)	31(9)	34(9)	04(8)	08(8)	03(8)
C(113)	60(12)	50(11)	39(10)	-04(9)	13(9)	-06(9)
C(114)	72(14)	77(15)	56(13)	-28(11)	19(11)	-22(12)
C(115)	66(13)	78(15)	79(15)	-32(12)	-37(11)	-11(12)
C(116)	44(10)	78(15)	57(11)	-07(10)	-02(8)	11(10)
C(111)	37(8)	35(8)	19(8)	-04(7)	-07(6)	01(7)
C(122)	51(11)	53(10)	32(9)	01(8)	01(8)	01(8)
C(123)	44(11)	82(14)	60(13)	09(11)	28(10)	02(10)
C(124)	69(15)	48(12)	100(19)	-05(12)	15(13)	-14(11)
C(125)	111(18)	58(13)	39(12)	-01(10)	16(12)	-13(12)
C(126)	70(12)	41(10)	39(11)	09(8)	08(9)	-24(9)
C(121)	48(11)	31(9)	46(11)	01(8)	02(8)	-07(8)
C(132)	51(11)	50(11)	40(11)	03(9)	-06(9)	25(9)
C(133)	76(14)	80(15)	54(13)	-33(11)	-27(11)	29(13)
C(134)	140(24)	80(18)	63(15)	-05(13)	-05(14)	14(16)
C(135)	153(22)	32(12)	65(14)	39(10)	-11(14)	13(13)
C(136)	115(17)	25(10)	54(12)	07(9)	10(11)	-01(10)
C(131)	70(12)	47(11)	13(8)	-04(8)	-16(8)	11(9)

Table 5.22 (cont.)

	U11	U22	U33	U23	U13	U12
C(212)	35(9)	40(10)	48(10)	-06(8)	-05(8)	-04(8)
C(213)	51(12)	56(12)	73(13)	-26(10)	02(10)	-12(10)
C(214)	30(10)	119(19)	77(15)	23(14)	-09(10)	00(12)
C(215)	38(11)	78(14)	90(15)	-28(12)	-15(10)	-20(10)
C(216)	42(10)	71(13)	41(11)	10(9)	-03(8)	-08(9)
C(211)	37(9)	40(10)	32(9)	-08(8)	-09(7)	-09(8)
C(222)	69(13)	83(15)	34(11)	09(10)	13(9)	-02(11)
C(223)	125(22)	113(21)	55(15)	-10(14)	29(14)	-26(17)
C(224)	167(26)	49(13)	49(13)	10(11)	-16(16)	-12(15)
C(225)	107(17)	32(10)	61(14)	00(10)	-20(12)	-09(11)
C(226)	91(14)	43(11)	28(10)	05(8)	-25(9)	-15(10)
C(221)	66(12)	34(9)	27(9)	00(7)	-03(9)	-08(9)
C(232)	45(10)	44(11)	64(12)	-04(9)	00(9)	13(9)
C(233)	51(11)	39(11)	69(13)	-12(9)	-04(9)	21(9)
C(234)	75(13)	48(12)	56(11)	-25(10)	-14(9)	18(11)
C(235)	86(14)	35(11)	49(11)	03(8)	-18(9)	04(10)
C(236)	70(12)	43(10)	38(10)	00(8)	02(9)	-02(9)
C(231)	61(11)	22(8)	27(9)	-01(6)	03(8)	-06(8)

8-(dppe)-8,7-$RhSB_9H_{10}.2CH_2Cl_2$, 18.$2CH_2Cl_2$

Crystal Data

$C_{26}H_{34}B_9P_2RhS.2CH_2Cl_2$, M_r = 810.63, triclinic, *P*bar1, a = 11.1614(25), b = 11.337(6), c = 17.206(13)Å, α = 98.725(56), β = 107.306(40), γ = 111.682(39)°, V = 1845.7Å^3, Z = 2, D_x = 1.458Mg m^{-3}, μ = 0.908mm^{-1}, $F(000)$ = 820, T = 185(2)K. Cell parameters from 25 centred reflections with $8 \leq \theta \leq 10°$. Dimensions 0.4 x 0.45 x 0.4 mm.

Data Collection and Processing

The majority of one hemisphere of data (h -0 to 13, k -13 to 13, l -20 to 15) was collected in two shells ($1 \leq \theta \leq 20°$ and $20 \leq \theta \leq 25°$). No significant movement was detected over 142 *X*-ray hours; however, some slight crystal decay was noted close to the end of the second shell, at which point collection was terminated. Of 6131 data measured (of which 5771 were unique), 5364 with $F \geq 2.0\sigma(F)$ were considered observed and retained for use in refinement.

Structure Solution and Refinement

Patterson methods were used to locate the Rh atom; the positions of the remainder of the non-H atoms were determined by difference Fourier syntheses. Phenyl rings were constrained to be rigid, planar hexagons with C—C 1.395Å. All H atoms were set in fixed calculated positions (C—H 1.08Å; B—H 1.10Å). After the structure had reached isotropic convergence, an empirical absorption correction was attempted but appeared unreliable and, hence, was not incorporated. Thereafter, equivalent data were merged and all non-H atoms were allowed anisotropic refinement. All H atoms were assigned a single group thermal parameter, 0.063(4) Å^2 at convergence. A total of 359 parameters were refined, with residuals at convergence of R = 0.0528, wR = 0.0848, S = 1.618. Weights were assigned according to w^{-1} = $[\sigma^2(F) + 0.000391F^2]$. The maximum shift/e.s.d. in the final cycle was 0.001, and the maximum and minimum residues in the final ΔF synthesis were 0.83 (near Rh, S) and -1.14 eÅ^{-3} respectively.

Table 5.23 Fractional Coordinates and Equivalent Isotropic Thermal Parameters (Å²) for Non-H Atoms in **18** .2CH_2Cl_2

	x	y	z	Ueq
Rh(8)	0.10159(4)	0.23566(4)	0.18360(2)	0.0225(3)
S(7)	0.11964(15)	0.23326(14)	0.04986(9)	0.0329(9)
B(1)	0.4036(7)	0.2508(6)	0.1661(4)	0.034(4)
B(2)	0.3064(7)	0.2417(6)	0.0623(5)	0.040(5)
B(3)	0.2224(7)	0.1522(6)	0.1292(4)	0.036(4)
B(4)	0.3169(7)	0.2520(7)	0.2379(4)	0.035(4)
B(5)	0.4478(7)	0.4029(7)	0.2413(4)	0.038(5)
B(6)	0.4354(7)	0.3974(6)	0.1346(5)	0.040(5)
B(9)	0.2969(7)	0.4072(6)	0.2532(4)	0.031(4)
B(10)	0.3738(7)	0.4957(6)	0.1842(5)	0.039(5)
B(11)	0.2809(8)	0.3938(7)	0.0706(5)	0.048(5)
P(1)	-0.06066(14)	0.32101(13)	0.17119(9)	0.0268(9)
P(2)	0.06739(14)	0.20171(13)	0.30155(9)	0.0253(9)
C(1)	-0.1253(6)	0.3010(6)	0.2570(3)	0.034(4)
C(2)	-0.0118(6)	0.3051(5)	0.3363(3)	0.030(4)
C(12)	0.0528(4)	0.5403(3)	0.11858(18)	0.042(4)
C(13)	0.1266(4)	0.6749(3)	0.12856(18)	0.051(5)
C(14)	0.1709(4)	0.7690(3)	0.20602(18)	0.055(5)
C(15)	0.1414(4)	0.7285(3)	0.27350(18)	0.059(5)
C(16)	0.0676(4)	0.5938(3)	0.26352(18)	0.044(4)
C(11)	0.0233(4)	0.4997(3)	0.18605(18)	0.032(4)
C(22)	-0.2937(3)	0.3264(3)	0.05417(22)	0.036(4)
C(23)	-0.4158(3)	0.2711(3)	-0.01909(22)	0.045(5)
C(24)	-0.4603(3)	0.1445(3)	-0.07217(22)	0.048(5)
C(25)	-0.3828(3)	0.0733(3)	-0.05199(22)	0.059(5)
C(26)	-0.2607(3)	0.1286(3)	0.02127(22)	0.042(4)
C(21)	-0.2162(3)	0.2552(3)	0.07435(22)	0.028(3)
C(32)	0.2954(4)	0.3439(3)	0.45688(22)	0.036(4)
C(33)	0.4010(4)	0.3566(3)	0.53053(22)	0.048(5)
C(34)	0.4139(4)	0.2439(3)	0.54653(22)	0.054(5)
C(35)	0.3213(4)	0.1187(3)	0.48890(22)	0.060(6)
C(36)	0.2158(4)	0.1061(3)	0.41526(22)	0.045(5)
C(31)	0.2028(4)	0.2187(3)	0.39925(22)	0.031(4)
C(42)	-0.1699(4)	-0.0077(3)	0.29917(22)	0.037(4)
C(43)	-0.2717(4)	-0.1392(3)	0.26949(22)	0.047(5)
C(44)	-0.2686(4)	-0.2319(3)	0.20772(22)	0.049(5)
C(45)	-0.1637(4)	-0.1931(3)	0.17562(22)	0.043(4)
C(46)	-0.0620(4)	-0.0616(3)	0.20530(22)	0.042(4)
C(41)	-0.0651(4)	0.0311(3)	0.26707(22)	0.029(4)

Table 5.23 (cont.)

	x	y	z	U_{eq}
C(1S)	0.8552(7)	0.6712(7)	0.3824(4)	0.053(5)
Cl(1S)	0.88088(18)	0.54710(16)	0.42582(10)	0.0528(12)
Cl(2S)	0.98280(22)	0.83078(18)	0.44954(14)	0.0727(15)
C(2S)	0.5842(8)	0.2122(9)	0.3942(6)	0.079(7)
Cl(3S)	0.5329(4)	0.0492(3)	0.33622(24)	0.145(3)
Cl(4S)	0.7290(3)	0.2621(3)	0.48885(25)	0.144(3)

Table 5.24 Fractional Coordinates of Hydrogen Atoms for **18** .2CH_2Cl_2

	x	y	z
H(1)	0.47647	0.20521	0.17341
H(2)	0.31065	0.19527	0.00279
H(3)	0.16956	0.04300	0.11133
H(4)	0.32811	0.21083	0.29217
H(5)	0.54515	0.46145	0.29795
H(6)	0.52686	0.45302	0.12056
H(9)	0.29475	0.46213	0.31090
H(10)	0.41791	0.60461	0.20129
H(11)	0.26993	0.44136	0.01957
H(0)	0.27615	0.47601	0.19069
H(1A)	-0.2164	0.2068	0.2355
H(1B)	-0.1530	0.3805	0.2734
H(2A)	0.0671	0.4062	0.3683
H(2B)	-0.0585	0.2667	0.3792
H(12)	0.0186	0.4674	0.05861
H(13)	0.1495	0.7063	0.07632
H(14)	0.2280	0.8733	0.21375
H(15)	0.1756	0.8013	0.33347
H(16)	0.0447	0.5624	0.31576
H(22)	-0.2592	0.4245	0.09527
H(23)	-0.4759	0.3263	-0.03472
H(24)	-0.5549	0.1017	-0.12889
H(25)	-0.4172	-0.0247	-0.09309
H(26)	-0.2006	0.0734	0.03690
H(32)	0.2854	0.4311	0.44449
H(33)	0.4726	0.4535	0.57515
H(34)	0.4956	0.2537	0.60355
H(35)	0.3313	0.0315	0.50129
H(36)	0.1441	0.0091	0.37064
H(42)	-0.1724	0.0641	0.34699
H(43)	-0.3529	-0.1692	0.29434
H(44)	-0.3474	-0.3337	0.18474
H(45)	-0.1613	-0.2649	0.12780
H(46)	0.0192	-0.0316	0.18045
H(1S)	0.8629	0.6573	0.3209
H(2S)	0.7527	0.6632	0.3751
H(3S)	0.6113	0.2776	0.3563
H(4S)	0.4987	0.2175	0.4092

Table 5.25 Anisotropic Thermal Parameters [x10³ (Cl, C, B), x10⁴ (Rh, S, P)] (Å²) for **18** .2CH_2Cl_2

	U11	U22	U33	U23	U13	U12
Rh(8)	165(3)	204(2)	191(3)	038(2)	036(2)	038(2)
S(7)	288(8)	312(7)	232(8)	066(6)	081(7)	071(6)
B(1)	20(3)	27(3)	41(4)	04(3)	11(3)	05(3)
B(2)	34(4)	27(3)	40(4)	-01(3)	22(3)	01(3)
B(3)	30(3)	28(3)	36(4)	05(3)	13(3)	13(3)
B(4)	20(3)	42(4)	26(4)	06(3)	02(3)	11(3)
B(5)	21(3)	38(4)	35(4)	-05(3)	07(3)	03(3)
B(6)	32(4)	25(3)	41(4)	-03(3)	16(3)	-03(3)
B(9)	21(3)	27(3)	27(3)	-05(3)	04(3)	00(3)
B(10)	27(3)	25(3)	47(4)	03(3)	17(3)	03(3)
B(11)	47(4)	27(3)	54(5)	14(3)	30(4)	11(3)
P(1)	211(7)	251(7)	224(8)	058(6)	057(6)	078(6)
P(2)	201(7)	230(7)	205(7)	060(6)	044(6)	050(6)
C(1)	25(3)	41(3)	26(3)	10(3)	12(3)	15(3)
C(2)	24(3)	32(3)	20(3)	07(2)	07(2)	06(2)
C(12)	42(4)	31(3)	31(3)	12(3)	08(3)	08(3)
C(13)	49(4)	37(3)	46(4)	17(3)	14(4)	13(3)
C(14)	52(4)	32(3)	55(4)	14(3)	13(4)	10(3)
C(15)	73(5)	30(3)	45(4)	02(3)	16(4)	16(3)
C(16)	50(4)	26(3)	37(3)	06(3)	16(3)	12(3)
C(11)	24(3)	28(3)	27(3)	07(2)	07(3)	06(2)
C(22)	25(3)	33(3)	35(3)	04(3)	06(3)	10(3)
C(23)	27(3)	45(4)	43(4)	13(3)	04(3)	16(3)
C(24)	30(3)	48(4)	37(4)	01(3)	-08(3)	10(3)
C(25)	45(4)	41(4)	57(5)	-09(3)	00(4)	15(3)
C(26)	35(3)	35(3)	33(4)	-03(3)	-02(3)	17(3)
C(21)	20(3)	25(3)	24(3)	04(2)	05(2)	05(2)
C(32)	28(3)	37(3)	26(3)	06(3)	07(3)	06(3)
C(33)	35(4)	53(4)	27(4)	00(3)	00(3)	08(3)
C(34)	31(4)	76(5)	29(4)	19(4)	00(3)	15(4)
C(35)	35(4)	56(4)	63(5)	36(4)	01(4)	17(3)
C(36)	40(4)	41(3)	34(4)	15(3)	05(3)	15(3)
C(31)	20(3)	36(3)	20(3)	06(2)	01(3)	08(2)
C(42)	24(3)	36(3)	34(3)	08(3)	07(3)	07(2)
C(43)	26(3)	42(3)	50(4)	16(3)	11(3)	03(3)
C(44)	35(4)	37(3)	46(4)	14(3)	-04(3)	03(3)
C(45)	43(4)	27(3)	34(3)	06(3)	06(3)	03(3)
C(46)	44(4)	28(3)	29(3)	04(3)	05(3)	05(3)
C(41)	23(3)	23(3)	27(3)	12(2)	02(2)	07(2)

Table 5.25 (cont.)

	U11	U22	U33	U23	U13	U12
C(1S)	44(4)	45(4)	46(4)	13(3)	08(3)	16(3)
Cl(1S)	57(1)	44(1)	38(1)	11(1)	16(1)	25(1)
Cl(2S)	62(1)	43(1)	80(1)	20(1)	19(1)	12(1)
C(2S)	42(4)	88(6)	77(6)	43(5)	03(4)	27(4)
Cl(3S)	131(3)	112(2)	138(3)	17(2)	20(2)	81(2)
Cl(4S)	58(2)	119(2)	168(3)	92(2)	-44(2)	-04(2)

cis-2,3-$(CO)_2$-$\mu_{2,3}$-CO-7-Cl-2,3-$(PPh_3)_2$-2,3,1-*closo*-$Rh_2SB_9H_8$, **19**

Crystal Data

$C_{39}H_{38}B_9ClO_3P_2Rh_2S$, M_r = 987.29, triclinic, *P*bar1, a = 11.137(6), b = 13.558(7), c = 16.688(4)Å, α = 108.44(3), β = 97.66(5), γ = 110.96(5)°, V = 2139.7Å^3, Z = 2, D_x = 1.532Mg m^{-3}, μ = 0.979mm^{-1}, $F(000)$ = 988, T = 293(1)K. Cell parameters from 25 centred reflections with $11 \leq \theta \leq 11.5°$. Crystal dimensions 0.45 x 0.25 x 0.15 mm.

Data Collection and Processing

One hemisphere of data (h 0 to 13, k -16 to 16, l -19 to 19) was collected for $1 \leq \theta \leq 25$ over 228 *X*-ray hours with very little (≤ 5%) decay (for which a correction was applied) and no movement. 7953 reflections were measured; of these, 7526 were unique and 6616 with $F \geq 2.0\sigma(F)$ were retained for use in structure refinement.

Structure Solution and Refinement

The structure was solved by Patterson methods for the Rh atom and by difference Fourier syntheses for B, C, O, P, S, Cl and cage H atoms; the phenyl rings were constrained to be regular planar hexagons with C-C 1.395Å and C-H 1.08Å. The H atoms bound to the cage were allowed positional refinement. An empirical absorption correction was applied (T_{max} = 1.156, T_{min} = 0.846). Thereafter equivalent data were merged (R_{int} = 0.0137), and all non-H atoms were allowed anisotropic refinement; H atoms were included with a single, group thermal parameter, 0.0726(18) Å^2 at convergence. Reflection data were weighted prior to convergence according to $w^{-1} = [\sigma^2(F) + 0.000263F^2]$. A total of 467 parameters were refined to final residuals of R = 0.0289, wR = 0.0334, S = 1.185. The maximum shift/e.s.d. in the final cycle was 0.001, and the maximum and minimum residues in the final ΔF synthesis were 0.52 [near Rh(2)] and -0.52 eÅ^{-3} respectively.

Table 5.26 Fractional Coordinates and Equivalent Isotropic Thermal Parameters (Å²) of Non-H Atoms for **19**

	x	y	z	Ueq
S(1)	0.21970(7)	0.39986(6)	0.14516(5)	0.0383(5)
Rh(2)	0.27861(2)	0.34106(2)	0.26152(1)	0.0354(2)
Rh(3)	0.40693(2)	0.55904(2)	0.26698(1)	0.0326(2)
B(4)	0.3879(4)	0.4944(3)	0.11642(24)	0.049(3)
B(5)	0.2902(5)	0.3378(3)	0.0463(3)	0.060(3)
B(6)	0.2461(4)	0.2470(3)	0.11278(25)	0.050(3)
B(7)	0.4954(3)	0.4264(3)	0.2554(3)	0.050(3)
B(8)	0.5375(4)	0.5079(3)	0.1843(3)	0.057(3)
B(9)	0.4663(5)	0.4064(3)	0.0743(3)	0.066(3)
B(10)	0.3863(5)	0.2671(4)	0.0722(3)	0.067(3)
B(11)	0.4006(4)	0.2730(3)	0.1809(3)	0.056(3)
B(12)	0.5324(4)	0.3686(3)	0.1558(3)	0.063(3)
Cl	0.62461(9)	0.46562(9)	0.35490(7)	0.0767(8)
P(1)	0.05467(7)	0.23334(6)	0.25761(5)	0.0378(5)
P(2)	0.32333(7)	0.69969(6)	0.27698(5)	0.0322(5)
C(1)	0.3201(3)	0.50252(25)	0.35882(21)	0.0416(21)
O(1)	0.3150(3)	0.54048(20)	0.42930(15)	0.0664(20)
C(2)	0.3336(3)	0.2826(3)	0.33870(25)	0.060(3)
O(2)	0.3695(3)	0.2468(3)	0.38524(21)	0.102(3)
C(3)	0.5695(3)	0.6755(3)	0.34072(23)	0.0514(24)
O(3)	0.67182(25)	0.74520(24)	0.38327(20)	0.0782(22)
C(112)	0.07672(16)	0.32737(19)	0.43375(13)	0.0541(24)
C(113)	0.03239(16)	0.36342(19)	0.50736(13)	0.062(3)
C(114)	-0.09418(16)	0.36302(19)	0.49693(13)	0.068(3)
C(115)	-0.17643(16)	0.32658(19)	0.41288(13)	0.068(3)
C(116)	-0.13210(16)	0.29053(19)	0.33926(13)	0.0525(24)
C(111)	-0.00553(16)	0.29093(19)	0.34970(13)	0.0432(21)
C(122)	-0.09487(20)	0.28964(12)	0.14869(12)	0.0455(22)
C(123)	-0.18810(20)	0.26889(12)	0.07368(12)	0.0557(25)
C(124)	-0.25651(20)	0.15816(12)	0.00845(12)	0.066(3)
C(125)	-0.23171(20)	0.06819(12)	0.01822(12)	0.071(3)
C(126)	-0.13848(20)	0.08893(12)	0.09323(12)	0.0559(25)
C(121)	-0.07006(20)	0.19966(12)	0.15846(12)	0.0377(19)
C(132)	-0.05011(25)	0.04309(19)	0.30299(16)	0.067(3)
C(133)	-0.07648(25)	-0.06872(19)	0.29508(16)	0.093(4)
C(134)	-0.02300(25)	-0.13178(19)	0.23990(16)	0.089(4)
C(135)	0.05685(25)	-0.08304(19)	0.19263(16)	0.083(4)
C(136)	0.08322(25)	0.02877(19)	0.20054(16)	0.071(3)
C(131)	0.02974(25)	0.09183(19)	0.25572(16)	0.0497(23)

Table 5.26 (cont.)

	x	y	z	U_{eq}
C(212)	0.38766(19)	0.90109(16)	0.24563(13)	0.0491(23)
C(213)	0.46133(19)	0.98559(16)	0.21848(13)	0.060(3)
C(214)	0.56629(19)	0.97729(16)	0.18384(13)	0.065(3)
C(215)	0.59757(19)	0.88448(16)	0.17635(13)	0.064(3)
C(216)	0.52391(19)	0.79998(16)	0.20351(13)	0.0502(23)
C(211)	0.41895(19)	0.80828(16)	0.23815(13)	0.0350(18)
C(222)	0.23988(19)	0.84419(18)	0.39508(11)	0.0498(23)
C(223)	0.24905(19)	0.91820(18)	0.47810(11)	0.064(3)
C(224)	0.34145(19)	0.93553(18)	0.55215(11)	0.062(3)
C(225)	0.42469(19)	0.87885(18)	0.54319(11)	0.0552(25)
C(226)	0.41552(19)	0.80484(18)	0.46018(11)	0.0468(22)
C(221)	0.32311(19)	0.78751(18)	0.38613(11)	0.0376(19)
C(232)	0.12139(17)	0.64606(17)	0.12899(12)	0.0450(21)
C(233)	-0.01151(17)	0.60562(17)	0.08187(12)	0.0557(25)
C(234)	-0.11477(17)	0.56284(17)	0.11784(12)	0.059(3)
C(235)	-0.08513(17)	0.56050(17)	0.20093(12)	0.0544(25)
C(236)	0.04777(17)	0.60093(17)	0.24805(12)	0.0456(21)
C(231)	0.15103(17)	0.64371(17)	0.21208(12)	0.0353(19)

Table 5.27 Fractional Coordinates of H Atoms in **19**

	x	y	z
H(4)	0.366(4)	0.554(3)	0.0891(25)
H(5)	0.221(4)	0.304(3)	-0.019(3)
H(6)	0.150(4)	0.172(3)	0.0810(24)
H(8)	0.635(4)	0.584(3)	0.2120(25)
H(9)	0.512(4)	0.410(3)	0.023(3)
H(10)	0.385(4)	0.191(3)	0.0188(25)
H(11)	0.423(4)	0.212(3)	0.1976(25)
H(12)	0.626(4)	0.366(3)	0.1638(24)
H(112)	0.17471	0.32767	0.44183
H(113)	0.09607	0.39163	0.57244
H(114)	-0.12850	0.39093	0.55392
H(115)	-0.27443	0.32627	0.40480
H(116)	-0.19578	0.26232	0.27419
H(122)	-0.04190	0.37536	0.19920
H(123)	-0.20730	0.33855	0.06612
H(124)	-0.32869	0.14210	-0.04963
H(125)	-0.28468	-0.01754	-0.03229
H(126)	-0.11928	0.01927	0.10079
H(132)	-0.09152	0.09191	0.34571
H(133)	-0.13830	-0.10646	0.33167
H(134)	-0.04342	-0.21834	0.23378
H(135)	0.09825	-0.13186	0.14992
H(136)	0.14504	0.06650	0.16395
H(212)	0.30641	0.90752	0.27245
H(213)	0.43711	1.05744	0.22427
H(214)	0.62332	1.04271	0.16282
H(215)	0.67883	0.87805	0.14954
H(216)	0.54813	0.72812	0.19771
H(222)	0.16834	0.83077	0.33775
H(223)	0.18460	0.96208	0.48503
H(224)	0.34855	0.99283	0.61642
H(225)	0.49623	0.89227	0.60053
H(226)	0.47996	0.76096	0.45324
H(232)	0.20132	0.67918	0.10115
H(233)	-0.03446	0.60744	0.01755
H(234)	-0.21765	0.53153	0.08136
H(235)	-0.16506	0.52737	0.22878
H(236)	0.07072	0.59912	0.31237

Table 5.28 Anisotropic Thermal Parameters [x10^4 (Rh, P, S, Cl), x10^3 (O, C, B)] (Å^2) for **19**

	U11	U22	U33	U23	U13	U12
S(1)	385(4)	342(4)	274(4)	098(3)	074(3)	155(3)
Rh(2)	305(1)	313(1)	331(1)	145(1)	104(1)	142(1)
Rh(3)	274(1)	297(1)	290(1)	111(1)	079(1)	120(1)
B(4)	56(2)	40(2)	39(2)	20(2)	26(2)	24(2)
B(5)	81(3)	46(2)	32(2)	11(2)	23(2)	29(2)
B(6)	55(2)	37(2)	41(2)	11(2)	21(2)	21(2)
B(7)	32(2)	45(2)	60(2)	27(2)	17(2)	21(2)
B(8)	47(2)	46(2)	66(3)	29(2)	33(2)	26(2)
B(9)	76(3)	51(2)	56(3)	26(2)	45(2)	34(2)
B(10)	82(3)	45(2)	58(3)	20(2)	44(2)	37(2)
B(11)	53(2)	43(2)	61(3)	26(2)	31(2)	30(2)
B(12)	51(2)	51(2)	76(3)	30(2)	38(2)	33(2)
Cl	399(4)	750(6)	899(7)	441(6)	003(5)	248(4)
P(1)	333(4)	280(4)	383(4)	123(3)	110(3)	118(3)
P(2)	322(4)	272(3)	237(4)	068(3)	048(3)	113(3)
C(1)	33(2)	38(2)	38(2)	17(1)	09(1)	13(1)
O(1)	90(2)	48(1)	36(1)	14(1)	31(1)	22(1)
C(2)	43(2)	54(2)	64(2)	31(2)	19(2)	21(2)
O(2)	78(2)	106(2)	102(2)	78(2)	22(2)	50(2)
C(3)	37(2)	44(2)	51(2)	15(2)	07(2)	15(2)
O(3)	41(1)	67(2)	82(2)	11(2)	-03(1)	05(1)
C(112)	42(2)	54(2)	45(2)	20(2)	12(2)	15(2)
C(113)	60(2)	62(2)	37(2)	16(2)	16(2)	18(2)
C(114)	68(2)	66(2)	50(2)	27(2)	32(2)	31(2)
C(115)	57(2)	69(2)	63(2)	37(2)	33(2)	37(2)
C(116)	43(2)	50(2)	49(2)	23(2)	19(2)	22(2)
C(111)	38(2)	34(2)	43(2)	17(1)	15(1)	14(1)
C(122)	42(2)	35(2)	39(2)	08(1)	07(1)	14(1)
C(123)	56(2)	47(2)	42(2)	12(2)	05(2)	22(2)
C(124)	65(2)	60(2)	39(2)	08(2)	-06(2)	16(2)
C(125)	87(3)	43(2)	41(2)	-01(2)	-07(2)	10(2)
C(126)	60(2)	36(2)	46(2)	06(2)	06(2)	15(2)
C(121)	32(1)	30(1)	34(2)	07(1)	07(1)	09(1)
C(132)	60(2)	42(2)	78(3)	33(2)	21(2)	16(2)
C(133)	85(3)	52(2)	111(4)	51(3)	23(3)	14(2)
C(134)	77(3)	40(2)	115(4)	30(2)	-04(3)	21(2)
C(135)	77(3)	40(2)	101(3)	22(2)	12(3)	30(2)
C(136)	64(2)	46(2)	83(3)	25(2)	24(2)	32(2)
C(131)	39(2)	31(2)	60(2)	19(2)	07(2)	11(1)

Table 5.28 (cont.)

	U11	U22	U33	U23	U13	U12
C(212)	60(2)	33(2)	33(2)	09(1)	04(2)	15(2)
C(213)	79(3)	36(2)	38(2)	13(2)	-02(2)	13(2)
C(214)	72(3)	45(2)	43(2)	21(2)	01(2)	-04(2)
C(215)	55(2)	57(2)	49(2)	23(2)	15(2)	05(2)
C(216)	47(2)	41(2)	42(2)	15(2)	12(2)	11(1)
C(211)	38(2)	25(1)	23(1)	05(1)	00(1)	04(1)
C(222)	52(2)	41(2)	34(2)	05(1)	09(1)	21(2)
C(223)	69(2)	46(2)	52(2)	05(2)	23(2)	28(2)
C(224)	74(3)	46(2)	32(2)	-02(2)	15(2)	10(2)
C(225)	62(2)	46(2)	27(2)	-02(1)	02(2)	14(2)
C(226)	46(2)	40(2)	31(2)	08(1)	05(1)	10(1)
C(221)	40(2)	29(1)	27(1)	06(1)	08(1)	10(1)
C(232)	49(2)	38(2)	28(2)	02(1)	04(1)	20(1)
C(233)	56(2)	50(2)	35(2)	03(2)	-06(2)	26(2)
C(234)	42(2)	41(2)	64(2)	01(2)	-06(2)	20(2)
C(235)	37(2)	37(2)	65(2)	13(2)	08(2)	12(1)
C(236)	39(2)	34(2)	46(2)	12(1)	08(1)	13(1)
C(231)	33(1)	27(1)	31(2)	04(1)	03(1)	14(1)

Geometric calculations on both model compounds and on crystallographically-determined coordinates were performed using *CALC* **[173]**. *R. M. S. Misfit* calculations employed the program *IDEAL*, inlaid in *CALC*. The principles behind this technique, and its operation, have been outlined in Chapter 4.

Tabulated below are the 11-vertex coordinate sets [of which the pentagonal pyramidal fragments B(1, 2, 3, 4, 5, 6) were input to the above program] for the model species $[B_{11}H_{14}]^-$, **A**, $[(Ph_3P)CB_{10}H_{12}]$, **B**, $[C_2B_9H_{12}]^-$, **C**, $[B_{10}H_{14}]$, **D** and $[\{(Me_3Si)_2CH\}CB_{10}H_{10}]^-$, **E**, and for the compounds **14**, **15**, **16**, **16A**, **17**, **17A** and **18**. The lines "CELL *a b c* α β γ" are the appropriate cell parameters for the coordinates; whilst the remaining lines have the form "*Atom_Label x y z*". The coordinates of **A**, **C** and **E** have C_s symmetry, whilst those for **D** full C_{2v} symmetry; those for **A** and for **14** - **18** are the coordinates as derived from crystallographic studies, whist the others have been adjusted for molecular symmetry as necessary.

Table 5.29 Coordinates of model **A**

CELL	1	1	1	90	90 90
B1	0.6489	-0.9012	0.0000		
B2	0.5176	0.12405	1.4417		
B3	1.3646	0.7103	0.0000		
B4	0.5176	0.12405	-1.4417		
B5	-0.8794	-0.80075	-0.88675		
B6	-0.8794	-0.80075	0.88675		
B7	0.39355	1.81255	0.94775		
B8	0.39355	1.81255	-0.94775		
B9	-1.09195	0.81865	-1.52465		
B10	-2.0134	0.1909	0.0000		
B11	-1.09195	0.81865	1.52465		

Table 5.30 Coordinates of model **B**

CELL	10.211	14.661	7.962	94.45	104.47	84.76
B1	0.2579	0.2922	0.3087			
B2	0.3194	0.3937	0.4110			
B3	0.2629	0.3176	0.5303			
B4	0.3092	0.2057	0.4517			
B5	0.3990	0.2151	0.2901			
B6	0.3988	0.3295	0.2616			
B7	0.4178	0.3677	0.6224			
B8	0.3976	0.2505	0.6535			
B9	0.4846	0.1815	0.5017			
B10	0.5447	0.2712	0.3979			
C11	0.4911	0.3705	0.4553			

Table 5.31 Coordinates of model **C**

CELL	1 1	1 90	90 90
B1	0.6742	0.9060	0.0000
B2	0.5299	-0.1215	-1.4302
B3	1.3645	-0.7222	0.0000
B4	0.5299	-0.1215	1.4302
B5	-0.8726	0.8013	0.90815
B6	-0.8726	0.8013	-0.90815
C7	0.15205	-1.6607	-0.77095
C8	0.15205	-1.6607	0.77095
B9	-1.0978	-0.8759	1.41285
B10	-2.0387	-0.1838	0.0000
B11	-1.0978	-0.8759	-1.41285

Table 5.32 Coordinates of model **D**

CELL	1 1	1 90	90 90
B1	-0.0000	-1.2249	0.8896
B2	-0.0000	-1.2249	-0.8896
B3	-1.5024	-0.8529	-0.0000
B4	-0.9940	0.1158	1.4158
B5	0.9940	0.1158	1.4158
B6	1.5025	-0.8528	-0.0000
B7	-0.9940	0.1158	-1.4158
B8	-1.7949	0.8528	-0.0000
B10	1.7948	0.8528	-0.0000
B11	0.9940	0.1158	-1.4158

Table 5.33 Coordinates of model E

CELL	1 1	1 90	90 90
B1	0.0406	-1.52315	-0.8920
B2	0.0406	-1.52315	0.8920
B3	1.5044	-1.0955	0.0000
B4	0.9166	-0.04625	-1.3262
B5	-0.91145	-0.1047	-1.3372
B6	-1.4089	-1.1705	0.0000
B7	0.9166	-0.04625	1.3262
C8	1.5286	0.5867	0.0000
B9	-0.0144	1.1317	0.0000
B10	-1.6097	0.5476	0.0000
B11	-0.91145	-0.1047	1.3372

Table 5.34 Coordinates of compound **14**

CELL	14.825	10.1367	16.1193	90	90	90
B1	0.1855	0.4185	0.1886			
B2	0.2183	0.2946	0.2584			
B3	0.1054	0.3161	0.2343			
B4	0.0971	0.3572	0.1277			
B5	0.2118	0.3650	0.0872			
B6	0.2862	0.3273	0.1725			
C7	0.1559	0.1596	0.2297			
C8	0.0847	0.1989	0.1590			
PT9	0.1296	0.2076	0.0329			
B10	0.2729	0.2179	0.0903			
B11	0.2618	0.1595	0.1955			

Table 5.35 Coordinates of compound **15**

CELL	9.7813	12.312	20.519	90	99.053	90
B1	0.3386	0.3459	0.0653			
B2	0.2749	0.4476	0.1198			
B3	0.1938	0.4293	0.0372			
B4	0.1814	0.2839	0.0218			
B5	0.2909	0.2158	0.0968			
B6	0.3489	0.3266	0.1520			
C7	0.1018	0.4255	0.1010			
C8	0.0564	0.3499	0.0460			
PT9	0.0610	0.1850	0.0848			
B10	0.2165	0.2377	0.1661			
B11	0.1883	0.3717	0.1735			

Table 5.36 Coordinates of compound **16**

CELL	11.340	22.090	16.209	90	99.01	90
RH8	0.09829	0.05770	0.28062			
S7	-0.07394	-0.00090	0.29278			
B1	0.1339	-0.0849	0.3661			
B2	-0.0214	-0.0795	0.3457			
B3	0.0767	-0.0119	0.3779			
B4	0.2090	-0.0208	0.3344			
B5	0.1941	-0.0869	0.2724			
B6	0.0521	-0.1196	0.2762			
B9	0.1796	-0.0155	0.2232			
B10	0.0775	-0.0795	0.1868			
B11	-0.0633	-0.0742	0.2321			

Table 5.37 Coordinates of compound **16A**

CELL	10.271	11.401	19.426	74.86	88.51	83.51
RH8	-0.30850	0.00012	-0.20244			
S7	-0.2590	0.0932	-0.11167			
B1	-0.4668	0.2780	-0.2026			
B2	-0.3686	0.2518	-0.1268			
B3	-0.4421	0.1260	-0.1543			
B4	-0.4469	0.1636	-0.2479			
B5	-0.3693	0.2972	-0.2810			
B6	-0.3170	0.3462	-0.2072			
B9	-0.2795	0.1570	-0.2857			
B10	-0.2001	0.2793	-0.2553			
B11	-0.1979	0.2460	-0.1581			

Table 5.38 Coordinates of compound **17**

CELL	15.794	12.020	17.119	90	98.21	90
RH8	0.26094	0.00863	0.11257			
S7	0.21617	0.16548	0.03279			
B1	0.2006	-0.0246	-0.0893			
B2	0.1804	0.1179	-0.0789			
B3	0.1654	0.0118	-0.0002			
B4	0.2498	-0.0878	-0.0006			
B5	0.3131	-0.0483	-0.0736			
B6	0.2723	0.0776	-0.1176			
B9	0.3539	-0.0283	0.0275			
B10	0.3656	0.0806	-0.0484			
B11	0.2844	0.1859	-0.0500			

Table 5.39 Coordinates of compound **17A**

CELL	13.100	16.772	12.120	107.91	117.16	93.73
RH8	0.70851	0.76545	0.75472			
S7	0.88200	0.87582	0.91183			
B1	0.8801	0.7643	1.0715			
B2	0.9629	0.8543	1.0804			
B3	0.8765	0.7546	0.9216			
B4	0.7452	0.7159	0.9183			
B5	0.7462	0.7859	1.0621			
B6	0.8758	0.8701	1.1571			
B9	0.6560	0.7933	0.9048			
B10	0.7387	0.8902	1.0603			
B11	0.8745	0.9357	1.0699			

Table 5.40 Coordinates of compound **18**

CELL	11.1614	11.337	17.206	98.725	107.306	111.682
RH8	0.10159	0.23566	0.18360			
S7	0.11964	0.23326	0.04986			
B1	0.4036	0.2508	0.1661			
B2	0.3064	0.2417	0.0623			
B3	0.2224	0.1522	0.1292			
B4	0.3169	0.2520	0.2379			
B5	0.4478	0.4029	0.2413			
B6	0.4354	0.3974	0.1346			
B9	0.2969	0.4072	0.2532			
B10	0.3738	0.4957	0.1842			
B11	0.2809	0.3938	0.0706			

References

1 A. Stock, *Hydrides of Boron and Silicon*, Cornell University Press, Ithaca, New York (1933)

2 H. C. Longuet-Higgins, *J. Chim. Phys.*, 1949, **46**, 275

3 K. Hedberg & V. Schomaker, *J. Am. Chem. Soc.*, 1951, **73**, 1482

4 H. W. Smith & W. N. Lipscomb, *J. Chem. Phys.*, 1965, **43**, 1060

5 D. A. Franz & R. N. Grimes, *J. Am. Chem. Soc.*, 1970, **92**, 1438

6 P. Paetzold, J. Müller, F. Meyer, H. Hansen & L. Schneider, in Abstracts for IMEBORON VIII, Eighth International Conference on Boron Chemistry, University of Tennessee, Knoxville, Tennessee (1993)

7 H. C. Kang, Y. Do, C. B. Knobler & M. F. Hawthorne, *Inorg. Chem.*, 1988, **27**, 1716

8 J. Plešek, *Chem. Rev.*, 1992, **92**, 269

9 J. H. Morris, *Chem. In Brit.*, 1991, **27**, 331

10 H. Hatanaka (ed.), *Boron Neutron Capture Therapy for Tumours*, Nishima, Tokyo (1986)

11 S. Papetti, B. B. Schaeffer, A. P. Grey & T. L. Heying, *J. Polymer Sci., Part A*-1, 1966, **4**, 1623; H. Schroeder, *Rubber Chem. Technol.*, 1966, **39**, 1184

12 M. G. L. Mirabelli & L. G. Sneddon, *J. Am. Chem. Soc.*, 1988, **110**, 3305; W. S. Rees, Jr. & D. Seyferth, *J. Am. Ceram. Soc.*, 1988, **71**, C194

13 **(a)** T. E. Paxson & M. F. Hawthorne, *J. Am. Chem. Soc.*, 1974, **96**, 4674; **(b)** R. T. Baker, M. S. Delaney, R. E. King, III, C. B. Knobler, J. A. Long, T. B. Marder, T. E. Paxson, R. G. Teller & M. F. Hawthorne, *ibid.*, 1984, **106**, 2965; **(c)** J. A. Long, T. B. Marder, P. E. Behnken & M. F. Hawthorne, *ibid.*, 2979; **(d)** J. A. Long, T. B. Marder & M. F. Hawthorne, *ibid.*, 3004; **(e)** P. E. Behnken, J. A. Belmont, D. C. Busby, M. S. Delaney, R. E. King, III, C. W. Kreimendahl, T. B. Marder, J. J. Wilczynski & M. F. Hawthorne, *ibid.*, 3011; **(f)** J. D. Hewes, M. Thompson & M. F. Hawthorne, *Organometallics*, 1985, **4**, 13; **(g)** H. C. Kang & M. F. Hawthorne, *ibid.*, 1990, **9**, 2327

14 H. C. Longuet-Higgins & M. de V. Roberts, *Proc. Roy. Soc.*, 1955, **A230**, 110

15 M. F. Hawthorne & A. R. Pittochelli, *J. Am. Chem. Soc.*, 1960, **82**, 3228

16 W. N. Lipscomb, *Boron Hydrides*, Benjamin, NewYork (1963)

17 R. E. Williams, *Inorg. Chem.*, 1971, **10**, 210

18 R. E. Williams, *Adv. Inorg. Chem. Radiochem*, 1976, **18**, 67

19 R. W. Rudolph & W. R. Pretzer, *Inorg. Chem.*, 1972, **11**, 1974

20 R. W. Rudolph, *Acc. Chem. Res.*, 1976, **9**, 446

21 K. Wade, *Chem. In Brit.*, 1975, **11**,177

22 K. Wade, *Adv. Inorg. Chem. Radiochem*, 1976, **18**, 1

23 L. G. Sneddon, J. C. Huffman, R. O. Schaeffer & W. E. Streib, *J. Chem. Soc., Chem. Commun.*, 1972, 474; A. J. Wynd & A. J. Welch, *Acta Cryst.*, 1989, **C45**, 615

24 J. Cowie, E. J. M. Hamilton, J. C. V. Laurie & A. J. Welch, *J. Organometal. Chem.*, 1990, **394**, 1

25 D. M. P. Mingos, *Acc. Chem. Res.*, 1984, **17**, 331

26 N. N. Greenwood, in *Comprehensive Inorganic Chemistry*, J. C. Bailar, Jr., H. J. Emeléus, R. Nyholm, A. F. Trotman-Dickenson (eds.), Pergamon Press, Elmsford, New York 1973. Part I, Chapter 11, Section 5, p.855

27 R. N. Grimes, *Carboranes*, Academic Press, New York (1971)

28 T. Onak, in *Comprehensive Organometallic Chemistry*, G. Wilkinson, F. G. A. Stone & E. Abel (eds.), Pergamon Press, Elmsford, New York 1982. Part I, Chapter 5.4, p.543

29 V. I. Bregadze, *Chem. Rev.*, 1992, **92**, 209

30 B. Štíbr, *ibid.*, 225

31 J. F. Ditter, E. B. Klusmann, J. D. Oakes & R. E. Williams, *Inorg. Chem.*, 1970, **9**, 889

32 T. L. Heying, J. W. Ager, Jr., S. L. Clark, D. J. Mangold, H. L. Goldstein, M. Hillman, R. J. Polak & J. W. Szymanski, *Inorg.Chem.*, 1963, **2**, 1089

33 M. M. Fein, D. Grafstein, J. E. Paustan, J. Bobinski, B. M. Lichstein, N. Mayes, N. Schwartz & M. S. Cohen, *Inorg.Chem.*, 1963, **2**, 1115

34 M. M. Fein, J. Bobinski, N. Mayes, N. Schwartz & M. S. Cohen, *Inorg.Chem.*, 1963, **2**, 1111

35 M. F. Hawthorne, T. D. Andrews, P. M. Garrett, F. P. Olsen, M. Reintjes, F. N. Tebbe, L. F. Warren, P. A. Wegner & D. C. Young, *Inorg. Synth.*, 1968, **10**, 91

36 W. Clegg, R. Coult, M. A. Fox, W. R. Gill, J. A. H. MacBride & K. Wade, *Polyhedron*, 1993, **12**, 2711

37 R. L. Ernest, W. Quintana, R. Rosen, P. J. Carroll & L. G. Sneddon, *Organometallics*, 1987, **6**, 80

38 L. I. Zakharkin & L. S. Podovisotskaya, *Izv. Akad. Nauk S.S.S.R., Ser. Khim.*, 1964, 1464

39 L. I. Zakharkin, V. I. Bregadze & O. Yu. Okhlobystin, *J. Organomet. Chem.*, 1965, **4**, 211

40 L. I. Zakharkin & V. N. Lebedev, *Izv. Akad. Nauk S.S.S.R., Ser. Khim.*, 1972, 2337

41 Rh. Ll. Thomas & A. J. Welch (University of Edinburgh), unpublished work

42 X. Yang, C. B. Knobler & M. F. Hawthorne, *Ang. Chem. Int. Ed. Engl.*, 1991, **30**, 1507

43 B. D. Reid & A. J. Welch, *J. Organometal. Chem.*, 1992, **438**, 371

44 F. A. Gomez & M. F. Hawthorne, *J. Org. Chem.*, 1992, **57**, 1384

45 F. A. Gomez, S. E. Johnson & M. F. Hawthorne, *J. Am. Chem. Soc.*, 1991, **113**, 5915

46 L. I. Zakharkin & A. I. Kovredov, *Izv. Akad. Nauk S.S.S.R., Ser. Khim.*, 1974, 740

47 R. Coult, M. A. Fox, W. R. Gill, P. L. Herbertson, J. A. H. MacBride & K. Wade, *J. Organometal. Chem*, 1993, **462**, 19

48 G. Z. Suleimanov, V. I. Bregadze, N. A. Koval'chuk & Kh. S. Khalilov, *J. Organomet. Chem.*, 1983, **255**, C5; L. F. Rybakova, O. P. Syutkina, E. S. Petrov, R. R. Shifrina & I. P. Beletskaya, *Izv. Akad. Nauk S.S.S.R., Ser. Khim.*, 1984, 1413

49 M. F. Hawthorne, D. C. Young, P. M. Garrett, D. A. Owen, S. G. Schwerin, F. N. Tebbe & P. A. Wegner, *J. Am. Chem. Soc.*, 1968, **90**, 862

50 J. Plešek, S. Hermánek & B. Štíbr, *Inorg. Synth.*, 1983, **22**, 231

51 L. I. Zakharkin & V. N. Kalinin, *Tetrahedron Letters*, 1965, **7**, 407; M. F. Hawthorne, P. A. Wegner & R. C. Stafford, *Inorg. Chem.*, 1965, **90**, 1675

52 M. F. Hawthorne & P. A. Wegner, *J. Am. Chem. Soc.*, 1968, **90**, 896

53 P. T. Brain, J. Cowie, D. J. Donohoe, D. Hnyk, M. Bühl, D. W. H. Rankin, H. E. Robertson, B. D. Reid, D. Reed, P. v. R. Schleyer & A. J. Welch, unpublished work (manuscript in preparation)

54 Z. G. Lewis & A. J. Welch, *Acta Cryst.*, 1993, **C49**, 705

55 T.D. McGrath & A. J. Welch, *Acta Cryst.*, 1994, **C50** (paper MU1110; in press)

56 Abstracts for IMEBORON VIII, Eighth International Conference on Boron Chemistry, University of Tennessee, Knoxville, Tennessee (1993)

57 L. J. Todd, in *Comprehensive Organometallic Chemistry*, G. Wilkinson, F. G. A. Stone & E. Abel (eds.), Pergamon Press, Elmsford, New York (1982). Part I, Chapter 5.6, p.543

58 N. S. Hosmane & J. A. Maguire, *Adv. Organomet. Chem.*, 1990, **30**, 99

59 J. L. Little, J. G. Kester, J. C. Huffman & L. J. Todd, *Inorg. Chem.*, 1989, **28**, 1087

60 J. L. Little, S. S. Pao & K. K. Sugathan, *ibid.*, 1974, **13**, 1752

61 J. L. Little, *ibid.*, 1979, **18**, 1598

62 D. Seyferth, K. D. Büchner, W. S. Rees, Jr., L. Wesemann, W. M. Davis, S. S. Bukalov, L. A. Leites, H. Bock & B. Solouki, *J. Am. Chem. Soc.*, 1993, **115**, 3586

63 J. Müller, J. Runsink & P. Paetzold, *Ang. Chem. Int. Ed. Engl.*, 1991, **30**, 175

64 R. W. Rudolph & W. R. Pretzer, *Inorg. Synth.*, 1983, **22**, 226

65 W. R. Hertler, F. Klanberg & E. L. Muetterties, *Inorg. Chem.*, 1967, **6**, 1696

66 J. L. Little, G. D. Friesen & L. J. Todd, *ibid.*, 1977, **16**, 869

67 K. Nestor, X. L. R. Fontaine, N. N. Greenwood, J. D. Kennedy & M. Thornton-Pett, *J. Chem. Soc., Dalton Trans.*, 1991, 2657

68 R. N. Grimes, in *Comprehensive Organometallic Chemistry*, G. Wilkinson, F. G. A. Stone & E. Abel (eds.), Pergamon Press, Elmsford, New York (1982). Part I, Chapter 5.6, p.459

69 R. N. Grimes (ed.), *Metal Interactions With Boron Clusters*, Plenum, New York (1982)

70 J. D. Kennedy, *Prog. Inorg. Chem.*, 1984, **32**, 519; *ibid.*, 1986, **34**, 211, and references therein

71 A. K. Saxena & N. S. Hosmane, *Chem. Rev.*, 1993, **93**, 1081

72 M. Green, J. L. Spencer, F. G. A. Stone & A. J. Welch, *J. Chem. Soc., Dalton Trans.*, 1975, 179

73 S. O. Kang, P. J. Carroll & L. G. Sneddon, *Organometallics*, 1988, **7**, 772

74 M. F. Hawthorne, D. C. Young & P. A. Wegner, *J. Am. Chem. Soc.*, 1965, **87**, 1818

75 H. M. Colquhoun, T. J. Greenhough & M. G. H. Wallbridge, *Acta Cryst.*, (1974), **B34**, 2373

76 for example, M. P. Garcia, M. Green, F. G. A. Stone, R. G. Sommerville, A. J. Welch, C. E. Briant, D. N. Cox & D. M. P. Mingos, *J. Chem. Soc., Dalton Trans.*, 1985, 2343

77 (a) D. M. P. Mingos, M. I. Forsyth & A. J. Welch, *J. Chem. Soc., Chem. Commun.*, 1977, 605; **(b)** D. M. P. Mingos, M. I. Forsyth & A. J. Welch, *J. Chem. Soc., Dalton Trans.*, 1978, 1363

78 Z. G. Lewis & A. J. Welch, *Acta Cryst.*, 1993, **C49**, 715

79 H. M. Colquhoun, T. J. Greenhough & M. G. H. Wallbridge, *J. Chem. Soc., Dalton Trans.*, 1979, 619

80 G. O. Kyd, L. J. Yellowless & A. J. Welch, *J. Chem. Soc., Dalton Trans.*, submitted (paper ref. 4/02989E/DAP)

81 K. J. Adams, J. Cowie, S. G. D. Henderson, G. J. MacCormick & A. J. Welch, *J. Organomet. Chem.*, 1994, submitted

82 J. Cowie, Ph. D. Thesis, University of Edinburgh (in preparation)

83 I. T. Chizhevsky, I. A. Lobanovna, V. I. Bregadze, P. V. Petrovskii, V. A. Antonovich, A. V. Polyakov, A. I. Yanovsky & Yu. T. Struchkov, *Mendeleev Commun.*, 1991, 47

84 D. A. Brown, W. Clegg, H. M. Colquhoun, J. A. Daniels, I. A. Stephenson & K. Wade, *J. Chem. Soc., Chem. Commun.*, 1987, 889

85 F. Teixidor, A. M. Romerosa, J. Rius, C. Miravitlles, J. Casabó, C. Viñas & E Sanchez, *J. Chem. Soc., Dalton Trans.*, 1990, 525

86 F. Teixidor, C. Viñas, J. Rius, C. Miravitlles & J. Casabó, *Inorg. Chem.*, 1990, **29**, 149

87 J. Cowie, Z. G. Lewis & A. J. Welch, unpublished work

88 J. Cowie, B. D. Reid, J. M. S. Watmough & A. J. Welch, *J. Organomet. Chem.*, 1994, in press

89 Z. G. Lewis & A. J. Welch, *J. Organometal. Chem.*, 1992, **430**, C45

90 R. T. Baker, *Inorg. Chem.*, 1986, **25**, 109; R. L. Johnston & D. M. P. Mingos, *ibid.*, 3321

91 M. J. Attfield, J. A. K. Howard, A. N. de M. Jelfs, C. M. Nunn & F. G. A. Stone, *J. Chem. Soc., Dalton Trans.*, 1987, 2219

92 N. Carr, D. F. Mullica, E. L. Sappenfield & F. G. A. Stone, *Organometallics*, 1992, **11**, 3697

93 D. Grafstein & J. Dvorak, *Inorg. Chem.*, 1963, **2**, 1128

94 S. Papetti & T. L. Heying, *J. Am. Chem. Soc.*, 1964, **86**, 2295

95 R. M. Salinger & C. L. Frye, *Inorg. Chem.*, 1965, **4**, 1815

96 C. D. Beard & R. B. Moffitt, III, *U. S. Patent* ***4,111,999***. [*Chem. Abs.*, 1979, **90**, 665, Abstr. 121790z]

97 L. F. Warren, JR. & M. F. Hawthorne, *J. Am. Chem. Soc.*, 1970, **92**,1157

98 S. A. Brew, N. Carr, J. C. Jeffery, M. U. Pilotti & F. G. A. Stone, *J. Am. Chem. Soc.*, 1992, **114**, 2203

99 D. R. Baghurst, R. B. Copley, H. Fleischer, D. M. P. Mingos, G. O. Kyd, L. J. Yellowlees, A. J. Welch, T. R. Spalding & D. O'Connell, *J. Organometal. Chem.*, 1993, **447**, C14

100 W. N. Lipscomb, *Nature*, 1966, **153**, 373

101 E. L. Muetterties & W. H. Knoth, *Polyhedral Boranes*, Marcel Dekker, New York, 1968, p.70

102 S. Wu & M. Jones, Jr., *J. Am. Chem. Soc.*, 1989, **111**, 5373

103 H. S. Wong & W. N. Lipscomb, *Inorg. Chem.*, 1975, **14**, 1350

104 G. M. Edvenson & D. F. Gaines, *ibid.*, 1990, **29**, 1210

105 R. E. Enrione, F. P. de Boer & W. N. Lipscomb, *ibid.*, 1964, **3**, 1659

106 A. J. Wynd & A. J. Welch, *J. Chem. Soc., Dalton Trans.*, 1990, 2803

107 J. R. Pipal & R. N. Grimes, *Inorg. Chem.*, 1979, **18**, 257

108 J. R. Bowser, A. Bonny, J. R. Pipal & R. N. Grimes, *J. Am. Chem. Soc.*, 1979, **101**, 6229

109 for example, E. K. Nishimura, *J. Chem. Soc., Chem. Commun.*, 1978, 858; D. N. Cox, D. M. P. Mingos & R. Hoffmann, *J. Chem. Soc., Dalton Trans.*, 1981, 1788; M. E. O'Neill & K. Wade, *Inorg. Chem.*, 1982, **21**, 461

110 S. A. Macgregor, A. J. Wynd, N. Moulden, R. O. Gould, P. Taylor, L. J. Yellowlees & A. J. Welch, *J. Chem. Soc., Dalton Trans.*, 1991, 3317

111 M. F. Hawthorne, D. C. Young, P. M. Garrett, D. A. Owen, S. G. Schwerin, F. N. Tebbe & P. A. Wegner, *J. Am. Chem. Soc.*, 1968, **90**, 862

112 *SHELXS*-86. Program for crystal structure solution. G. M. Sheldrick, University of Göttingen, Germany (1986)

113 *SHELX*-76. Program for crystal structure determination. G. M. Sheldrick, University of Cambridge, England (1976)

114 The author obtained ^{11}B chemical shifts for 1-Ph-1,2-*closo*-$C_2B_{10}H_{11}$ as follows: $\delta(^{11}B)$ -1.31 (1B), -3.59 (1B), -8.13 (2B), -10.07 (4B), -11.93 (2B) p.p.m. These agree well with previously-reported values (for example, reference **[53]**).

115 K. F. Purcell & J. C. Kotz, *Inorganic Chemistry*, Saunders, Philidelphia (1977)

116 A. K. Koncharian, A. V. Nilssen, A. Pettersen, C. Rømming & L. K. Sydnes, *Acta Chem. Scand.*, 1988, **A42**, 463

117 L. I. Zakharkin, V. I. Bregadze & O. Yu. Okhlobytsin, *J. Organomet. Chem.*, 1965, **4**, 211

118 N. I. Kirillova, T. V. Klimova, Yu. T. Struchkov & V. I. Stanko, *Izv. Akad. Nauk S.S.S.R., Ser. Khim.*, 1981, 600

119 N. I. Kirillova, T. V. Klimova, Yu. T. Struchkov & V. I. Stanko, *Izv. Akad. Nauk S.S.S.R., Ser. Khim.*, 1979, 2481

120 S. V. Lindeman, I. A. Khotina, M. M. Teplyakov, Yu. T. Struchkov & V. V. Korshak, *Makromol. Chem.*, 1988, **189**, 471

121 R. R. Ryan & R. Schaeffer, *Cryst. Struct. Commun.*, 1981, **10**, 133

122 R. Kivekäs, A. Romerosa & C. Viñas, *Acta Cryst.*, 1994, **C50**, 638

123 T. J. Henly, C. B. Knobler & M. F. Hawthorne, *Organometallics*, 1992, **11**, 2313

124 L. I. Zakharkin & V. N. Kalinin, *Tetrahedron Letters*, 1965, 407

125 J. Buchanan, E. J. M. Hamilton, D. Reed & A. J. Welch, *J. Chem. Soc., Dalton Trans.*, 1990, 677

126 Extended Hückel molecular orbital calculations **[127, 128]** were performed on idealised (C_{cage}—$C_{Ph/Me}$ 1.50, C_{Ph}—C_{Ph} 1.395, C—H 1.08, C_{cage}—C_{cage} 1.650, B—C 1.7575, B—B 1.850, B—H 1.15Å for θ_{Ph} = 0 and 90°) models of the ligand [7-Ph-8-Me-7,8-*nido*-$C_2B_9H_9$]$^{2-}$.

127 ICON8. J. Howell, A. Rossi, D.Wallace, K. Haraki & R. Hoffmann, Quantum Chemistry Program Exchange, University of Indiana, 1977, no. 344

128 J. H. Ammeter, H-B. Bürgi, J. C. Thibeault & R. Hoffmann, *J. Am. Chem. Soc.*, 1982, **100**, 3686

129 C. A. Tolman, *Chem. Rev.*, 1977, **77**, 313

130 N. W. Alcock, J. G. Taylor & M. G. H. Wallbridge, *J. Chem. Soc., Dalton Trans.*, 1987, 1805

131 K. F. Shaw, B. D. Reid & A. J. Welch, *J. Organometal. Chem.*, 1994, in press (paper JOM24611)

132 K. F. Shaw, Ph.D. Thesis, University of Edinburgh, Scotland (1992)

133 C. B. Knobler, T. B. Marder, E. A. Mizusawa, R. G. Teller, J. A. Long, P. E. Behnken & M. F. Hawthorne, *J. Am. Chem. Soc.*, 1984, **106**, 2990

134 H. M. Colquhoun, T. J. Greenhough & M. G. H. Wallbridge, *J. Chem. Soc., Dalton Trans.*, 1985, 761

135 G. K. Barker, M. Green, F. G. A. Stone, A. J. Welch & W. C. Wolsey, *J. Chem. Soc., Chem. Commun.*, 1980, 627

136 G. K. Barker, M. Green, F. G. A. Stone, A. J. Welch & W. C. Wolsey, *J. Chem. Soc., Dalton Trans.*, 1983, 2063

137 G. Ferguson, M. C. Jennings, A. J. Lough, S. Coughlan, T. R. Spalding, J. D. Kennedy, X. L. R. Fontaine & B. Štibr, *J. Chem. Soc., Chem. Commun.*, 1990, 891

138 G. Ferguson, A. J. Lough, S. Coughlan & T. R. Spalding, *Acta Cryst.*, 1992, **C48**, 440

139 Appendix 1 of this ***Thesis***

140 W. Quintana & L. G. Sneddon, *Inorg. Chem.*, 1990, **29**, 3242

141 P. Lu, C. B. Knobler & M. F. Hawthorne, *Acta Cryst.*, 1984, **C40**, 1704

142 R. Brill, H Dietrich & H. Dierks, *Acta Cryst.*, 1971, **B27**, 2003

143 C. Tsai & W. E. Streib, *J. Am. Chem. Soc.*, 1966, **88**, 4513

144 S. A. Macgregor, Ph.D. Thesis, University of Edinburgh, Scotland (1991)

145 M. Murphy, T. R. Spalding, G. Ferguson & J. F. Gallagher, *Acta Cryst.*, 1992, **C48**, 638

146 C. W. Jung & M. F. Hawthorne, *J. Am. Chem. Soc.*, 1980, **102**, 3024

147 M. Brookhart & M. L. H. Green, *J. Organomet. Chem.*, 1983, **250**, 395; M. Brookhart, M. L. H. Green & L.-L. Wong, *Prog. Inorg. Chem.*, 1988, **36**, 1

148 P. Albano, M. Aresta & M. Manassero, *Inorg. Chem.*, 1980, **19**, 1069

149 S. Coughlan, T. R. Spalding, G. Ferguson, J. F. Gallagher, A. J. Lough, X. L. R. Fontaine, J. D. Kennedy & B. Štibr, *J. Chem. Soc., Dalton Trans.*, 1992, 2865

150 E. A. McNeill & F. R. Scholer, *Inorg. Chem.*, 1975, **14**, 1081

151 K. J. Adams, T. D. McGrath & A. J. Welch, unpublished work (in progress)

152 G. Ferguson, M. F. Hawthorne. B. Kaitner & F. J. Lalor, *Acta Cryst.*, 1984, **C40**, 1707

153 S. O. Kang, P. J. Carroll & L. G. Sneddon, *Inorg. Chem.*, 1989, **28**, 961

154 D. M. Schubert, C. B. Knobler, P. A. Wegner, M. F. Hawthorne, *J. Am. Chem. Soc.*, 1988, **110**, 5219

155 J. M. Jenkins & B. L. Shaw, *J. Chem. Soc.*, 1966, 770

156 G. W. Parshall, *Inorg. Synth.*, 1970, **12**, 27

157 J. C. Bailar, Jr. & H. Itatani, *Inorg. Chem.*, 1965, **4**, 1618

158 G. Cavinato & L. Toniolo, *Inorg. Chim. Acta.*, 1981, **52**, 39

159 R. G. Goel, *Inorg. Nucl. Chem. Lett.*, 1979, **15**, 437

160 J. A. McCleverty & G. Wilkinson, *Inorg. Synth.*, 1966, **8**, 211

161 D. P. Fairlie & B. Bosnich, *Organometallics*, 1988, **7**, 936

162 G. Giordiano & R. H. Crabtree, *Inorg. Synth.*, 1979, **19**,218

163 J. L. Herde, J. C. Lambert & C. V. Senoff, *ibid.*, 1974, **15**, 18

164 J. A. McCleverty & G. Wilkinson, *ibid.*, 1966, **8**, 214

165 K. Vrieze, J. P. Collman, C. T. Sears, Jr. & M. Kutoba, *ibid.*, 1968, **11**, 101

166 J. A. Labinger & J. A. Osborn, *ibid.*, 1978, **18**, 62

167 R. A. Jones, F. M. Real, G. Wilkinson, A. M. R. Galas, M. B. Hursthouse & K. M. A. Malik, *J. Chem. Soc., Dalton Trans.*, 1980, 511

168 Prepared from $[(CH_2{=}CH_2)RhCl]_2$ by an extension of the route to $[(dppe)RhCl]_2$, **[148]**

169 D. F. Steele & T. A. Stephenson, *J. Chem. Soc., Dalton Trans.*, 1972, 2161

170 *CADABS*. Program for data reduction. R. O. Gould & D. E. Smith. University of Edinburgh, Scotland (1986)

171 *International Tables for X-ray Crystallography*, Vol. 4, Kynoch Press, Birmingham (1974), p99

172 *DIFABS*. N. Walker & D. Stuart, *Acta Cryst.*, 1983 A**39**, 158

173 *CALC*. Program for crystallographic calculations. R. O. Gould & P. Taylor. University of Edinburgh, Scotland (1986)

174 *SHELXTL PC* version 4.2. G. M. Sheldrick. University of Göttingen, Germany. Seimens Analytical X-ray Instrumentation, Inc., Madison, Wisconsin, U.S.A. (1990)

Appendix 1

Crystallographic Data for [Ph_3PH][*nido*-$B_{11}H_{14}$]

This was the only identified product isolated from reaction between $Na[B_{11}H_{14}]$ **[A1]** and $[(PPh_3)HgCl_2]_2$ **[A2]** in CH_2Cl_2. Colourless *blocks* were grown by slow diffusion of *n*-hexane into a CH_2Cl_2 solution at -30°C. The general details of the crystallographic study are as given in Chapter 5.

Crystal Data

$C_{18}H_{30}B_{11}P$, Mr = 396.32, monoclinic, $P2_1/m$, a = 8.641(3), b = 13.0644(21), c = 10.945(3) Å, β = 106.861(24)°, V = 1182.5Å^3, Z = 2 (*i.e.*, 2 ion pairs), Dx = 1.113Mg m^{-3}, μ = 0.116mm^{-1}, $F(000)$ = 416 T = 293(1)K. Lattice parameters from 25 centred reflections in the range $12 < \theta < 14°$. Crystal dimensions 0.4 x 0.3 x 0.25 mm.

Data Collection and Processing

One quadrant of data was measured over 70 *X*-ray hours for $1 \leq \theta \leq 25°$ (h 0 to 10, k 0 to 15, l -13 to 13), with no significant decay or movement detected. 2334 data were measured, of which 2326 were unique, and 1513 with $F \geq 2.0\sigma(F)$ were retained for use in refinement.

Structure Solution and Refinement

The P atom was located by Patterson synthesis and the positions of C, B and cage H atoms were obtained by difference Fourier syntheses. The structure was refined (least squares on *F*) with the C atoms of the "whole" phenyl ring constrained to be a regular hexagon (C-C 1.395Å) and phenyl H atoms set in idealised positions (C-H 1.08Å). Terminal cage H atoms were allowed positional refinement subject to a common B-H distance, 1.15(3)Å at convergence, whereas the *endo* and bridging cage H atoms were not positionally refined after they had been located; the P-bound H atom was

successfully positionally refined. No absorption correction was applied. Following isotropic convergence, equivalent data were merged (R_{int} = 0.050) and all non-H atoms were refined anisotropically; H atoms were assigned a single group thermal parameter, 0.087(33)Å^2 at convergence. Weights were assigned according to $w^{-1} = [\sigma^2(F) + 0.000661F^2]$. 157 parameters were refined to R = 0.0699, wR = 0.0729, S = 1.372. Maximum shift/e.s.d. in final cycle was 0.003, and maximum and minimum residues in the final ΔF synthesis were 0.42 and -0.29 eÅ^{-3} respectively.

Structural Parameters, Atomic Coordinates, and Thermal Parameters derived from the crystallographic study are listed in tables A1 to A4. A view of the anion *nido*-[$B_{11}H_{14}$]$^-$ is shown in figure A1; the numbering scheme (also shown) is non-systematic. (The structure of the cation is unremarkable).

References

A1 V. D. Aftandillian, H. C. Miller, G. W. Parshall & E. L. Muetterties, *Inorg. Chem.*, 1962, **1**, 734

A2 R. C. Evans, F. G. Mann, H. S. Peiser & D. Purdie, *J. Chem. Soc.*, 1940, 1209

Figure A1 Perspective view of the anion in $[Ph_3PH][B_{11}H_{14}]$
(50% thermal ellipsoids; H atoms have radii of 0.1Å for clarity.
Symmetry equivalent atoms A: x, $3/_2$-y, z)

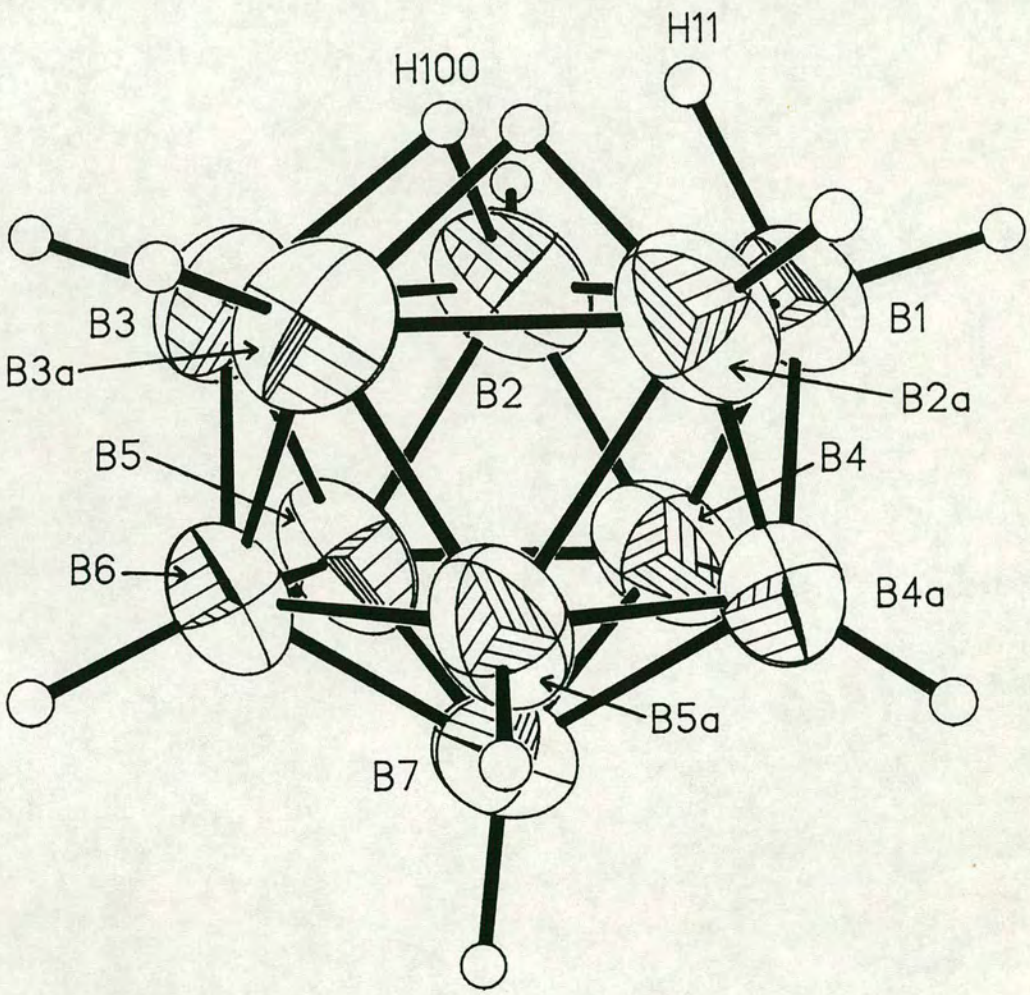

Table A1 Selected Internuclear Distances (Å) and Interbond Angles (°) for the anion in $[Ph_3PH][B_{11}H_{14}]$ (Symmetry equivalent atoms A: $x, {}^3/_2{-}y, z$)

B(1) - B(2)	1.882(8)	B(3) -B(3A)	1.902(7)
B(1) - B(4)	1.757(8)	B(4) - B(5)	1.768(8)
B(2) - B(3)	1.857(8)	B(4) - B(7)	1.755(8)
B(2) - B(4)	1.767(8)	B(4) -B(4A)	1.753(8)
B(2) - B(5)	1.778(8)	B(5) - B(6)	1.750(8)
B(3) - B(5)	1.742(7)	B(5) - B(7)	1.757(8)
B(3) - B(6)	1.758(8)	B(6) - B(7)	1.741(8)

B(2) - B(1) - B(4)	58.0(3)	B(7) - B(4) -B(4A)	60.0(3)
B(4) - B(1) -B(4A)	59.9(3)	B(2) - B(5) - B(3)	63.7(3)
B(1) - B(2) - B(4)	57.5(3)	B(2) - B(5) - B(4)	59.8(3)
B(3) - B(2) - B(5)	57.2(3)	B(3) - B(5) - B(6)	60.4(3)
B(4) - B(2) - B(5)	59.9(3)	B(4) - B(5) - B(7)	59.7(3)
B(2) - B(3) - B(5)	59.1(3)	B(6) - B(5) - B(7)	59.5(3)
B(5) - B(3) - B(6)	60.0(3)	B(3) - B(6) - B(5)	59.6(3)
B(6) - B(3) -B(3A)	57.3(3)	B(3) - B(6) -B(3A)	65.5(3)
B(1) - B(4) - B(2)	64.6(3)	B(5) - B(6) - B(7)	60.4(3)
B(1) - B(4) -B(4A)	60.1(3)	B(4) - B(7) - B(5)	60.5(3)
B(2) - B(4) - B(5)	60.4(3)	B(4) - B(7) -B(4A)	60.0(3)
B(5) - B(4) - B(7)	59.8(3)	B(5) - B(7) - B(6)	60.0(3)

Table A2 Fractional Coordinates and Equivalent Isotropic Thermal Parameters ($Å^2$) of Non-H Atoms for $[Ph_3PH][B_{11}H_{14}]$

	x	y	z	Ueq
P	-0.07944(16)	0.75000	0.70495(13)	0.0421(8)
C(12)	0.0854(3)	0.60932(18)	0.88008(18)	0.0526(24)
C(13)	0.1798(3)	0.52195(18)	0.91841(18)	0.064(3)
C(14)	0.2251(3)	0.46281(18)	0.82831(18)	0.068(3)
C(15)	0.1760(3)	0.49105(18)	0.69989(18)	0.068(3)
C(16)	0.0816(3)	0.57843(18)	0.66156(18)	0.0566(24)
C(11)	0.0363(3)	0.63757(18)	0.75165(18)	0.0433(20)
C(21)	-0.2486(6)	0.75000	0.7665(4)	0.042(3)
C(22)	-0.3164(4)	0.6580(3)	0.7864(3)	0.0526(24)
C(23)	-0.4513(5)	0.6584(3)	0.8306(4)	0.071(3)
C(24)	-0.5153(8)	0.75000	0.8513(8)	0.081(5)
B(1)	-0.8335(9)	0.75000	1.3744(7)	0.070(5)
B(2)	-0.6972(7)	0.6346(4)	1.4012(5)	0.076(4)
B(3)	-0.4836(6)	0.6772(4)	1.4380(5)	0.066(3)
B(4)	-0.7948(6)	0.6829(5)	1.2473(5)	0.080(4)
B(5)	-0.5920(6)	0.6407(4)	1.2838(5)	0.070(3)
B(6)	-0.4698(8)	0.75000	1.3065(6)	0.054(4)
B(7)	-0.6554(9)	0.75000	1.1888(7)	0.068(5)

Table A3 Fractional Coordinates of H Atoms in $[Ph_3PH][B_{11}H_{14}]$

	x	y	z
H(12)	0.0504	0.65510	0.94983
H(13)	0.2179	0.50008	1.01783
H(14)	0.2982	0.39516	0.85799
H(15)	0.2110	0.44527	0.63014
H(16)	0.0435	0.60030	0.56213
H(22)	-0.2648	0.5865	0.7678
H(23)	-0.5049	0.5874	0.8483
H(24)	-0.582	0.75000	0.878
H(1)	-0.974	0.75000	1.380
H(2)	-0.731	0.558	1.444
H(3)	-0.370	0.628	1.491
H(4)	-0.887	0.642	1.183
H(5)	-0.561	0.563	1.245
H(6)	-0.349	0.75000	1.284
H(7)	-0.649	0.75000	1.087
H(0)	-0.123	0.75000	0.569
H(11)	-0.74792	0.75000	1.49494
H(100)	-0.61465	0.69670	1.50045

Table A4 Anisotropic Thermal Parameters [x104 (P), x10^3 (C, B)] (Å^2) for $[Ph_3PH][B_{11}H_{14}]$

	U11	U22	U33	U23	U13	U12
P	400(8)	426(8)	408(8)	000	145(6)	000
C(12)	51(2)	50(2)	53(2)	00(2)	17(2)	06(2)
C(13)	51(2)	57(3)	77(3)	13(2)	20(2)	08(2)
C(14)	48(2)	45(2)	105(3)	00(2)	29(2)	04(2)
C(15)	60(3)	58(3)	84(3)	-18(2)	32(2)	06(2)
C(16)	50(2)	59(3)	58(2)	-10(2)	23(2)	03(2)
C(11)	34(2)	41(2)	51(2)	-06(2)	13(2)	-06(2)
C(21)	32(3)	43(3)	46(3)	00	08(2)	00
C(22)	41(2)	44(2)	68(2)	04(2)	16(2)	-03(2)
C(23)	49(2)	57(3)	105(3)	07(3)	33(2)	-04(2)
C(24)	46(4)	94(6)	104(5)	00	42(4)	00
B(1)	58(4)	77(5)	72(5)	00	33(4)	00
B(2)	83(4)	55(3)	90(4)	-03(3)	46(3)	-13(3)
B(3)	65(3)	52(3)	71(3)	07(3)	10(3)	09(3)
B(4)	55(3)	113(5)	70(3)	-26(3)	28(3)	-25(3)
B(5)	62(3)	60(3)	87(4)	-25(3)	41(3)	-13(3)
B(6)	47(4)	41(4)	74(4)	00	31(3)	00
B(7)	60(4)	93(6)	49(4)	00	23(4)	00

Appendix 2

Courses and Meeting Attended

"*Solving and Refining Crystal Structures*" (Postgraduate lecture course): Drs. R. O. Gould & A. J. Blake

Departmental Inorganic Meetings, Research Seminars, Symposia and Colloquia

R.S.C. Scottish Dalton Meetings

University of Strathclyde Inorganic Club (USIC) Meetings

IMEBORON VIII. Eighth International Meeting on Boron Chemistry, Knoxville, Tennessee, USA (1992)

INTRABORON XI, XII & XIII. Annual Meetings of United Kingdom Boron Chemists (1991-3)

Fourth British Crystallographic Association Intensive Course in X-ray Structural Analysis, Aston University (1992)

Appendix 3

Published Work

Certain of the results presented in this *Thesis* have been submitted for publication as follows:

Steric Effects in Heteroboranes III. Structure of 1-Ph-2-Me-1,2-*closo*-$C_2B_{10}H_{10}$, T. D. McGrath & A. J. Welch, *Acta Crystallographica, Section C* (in press)

Steric Effects in Heteroboranes IV. Structure of 1-Ph-2-Br-1,2-*closo*-$C_2B_{10}H_{10}$, T. D. McGrath & A. J. Welch, *Acta Crystallographica, Section C* (in press)

Steric Effects in Heteroboranes V. Structure of 1-Ph-2-Me_3Si-1,2-*closo*-$C_2B_{10}H_{10}$, T. D. McGrath & A. J. Welch, *Acta Crystallographica, Section C* (in press)

Steric Effects in Heteroboranes VI. Structure of 1-Ph-2-^{t}BuMe$_2$Si-1,2-*closo*-$C_2B_{10}H_{10}$, T. D. McGrath & A. J. Welch, *Acta Crystallographica, Section C* (in press)

Structure of 8-(dppe)-8,7-*nido*-$RhSB_9H_{10}.2CH_2Cl_2$, K. J. Adams, T. D. McGrath & A. J. Welch, submitted to *Acta Crystallographica, Section C*